

UNIVERSITÀ DELLA CALABRIA



UNIVERSITÀ DELLA CALABRIA

Dipartimento di Fisica

**Dottorato di Ricerca in**

Scienze e Tecnologie Fisiche, Chimiche e dei Materiali  
Convenzione Università della Calabria-Consiglio Nazionale delle Ricerche

**CICLO**

XXIX

**TITOLO TESI**

ADVANCES IN BIOCATALYTIC MEMBRANE REACTORS DEVELOPMENT

**Settore Scientifico Disciplinare CHIM/03 Chimica Generale e Inorganica**

**Coordinatore:** Ch.mo Prof. Vincenzo Carbone  
Firma Vincenzo Carbone

**Supervisore:** Dott.ssa Lidietta Giorno  
Firma Lidietta Giorno

**Tutor:** Dott.ssa Rosalinda Mazzei  
Firma Rosalinda Mazzei

**Dottorando:** Dott. Giuseppe Ranieri  
Firma Giuseppe Ranieri

# INDEX

<b>SUMMARY</b> .....	6
<b>DISSERTATION OUTLINES</b> .....	10
<b>SOMMARIO</b> .....	12
<b>CHAPTER 1</b> .....	19
<b>Membranes for biocatalytic membrane reactors</b> .....	19
1.1. Introduction.....	19
1.2. Membrane classification .....	20
1.3. Polymeric membranes.....	21
1.3.1. Phase inversion .....	23
1.4. Inorganic membranes.....	27
1.4.1. Ceramic hollow fibre membranes preparation .....	28
1.5. Effect of preparation parameters on ceramic hollow fibre membranes membrane morphology .....	33
1.5.1. The effect of suspension viscosity on the pore size distribution and fibre morphology .....	33
1.5.2. The effect of the internal coagulant flow rate on the pore size distribution and fibre morphology.....	34
1.5.3. The effect of air-gap on the pore size distribution and fibre morphology .....	34
1.5.4. The effect of calcination temperature on the pore size distribution.....	34
1.6. Membrane housing.....	35
1.7. General aspect on mass transport through membranes.....	37

<b>CHAPTER 2</b> .....	45
<b>Introduction to catalytic reactors</b> .....	45
2.1. Introduction.....	45
2.2. Batch process .....	47
2.3. Continuous process .....	48
2.4. Semi-batch process .....	49
2.5. Types of reaction.....	49
2.5.1. Homogeneous reactions .....	49
2.5.2. Heterogeneous reactions .....	49
2.6. Reactor designing.....	51
2.7. Catalytic reactor with membranes as a catalytic and separation unit .....	56
2.8. Enzyme immobilization methods .....	59
2.8.1. Physical adsorption .....	60
2.8.2 Entrapment .....	61
2.8.3. Cross-linking .....	61
2.8.4. Covalent bonding .....	62
2.9. Enzymes .....	62
2.9.1. Lipase .....	63
2.9.2. $\beta$ -glucosidase.....	65
2.10. Enzyme kinetics.....	67
2.11. Inhibition kinetics .....	73
2.11.1. Competitive inhibition.....	73
2.11.2. Mixed Inhibition.....	75
2.11.3. Uncompetitive inhibition.....	77

2.12. Summary of inhibition kinetic .....	77
<b>CHAPTER 3.....</b>	<b>87</b>
<b>Materials and methods .....</b>	<b>87</b>
3.1. Materials and chemicals.....	87
3.2. Analytical methods .....	88
3.3. Equipments and operation mode.....	92
3.3.1. Alumina hollow fiber membranes preparation.....	92
3.3.2. Stirred Tank Reactor setup.....	95
3.3.3. Surface activation of alumina membranes and enzymatic covalent immobilization .....	98
3.3.4. Pilot plant BMR with physically entrapped $\beta$ -glucosidase .....	101
3.3.5. Biocatalytic membrane reactors with immobilized biocatalysts.....	101
3.3.6. Cleaning of alumina hollow fiber membrane.....	107
3.4. Characterizations.....	108
3.4.1. Characterization of prepared inorganic membranes.....	108
3.4.2. Characterization of grafted alumina membranes surface.....	108
3.4.3. Characterization of olive leaves extracts .....	109
<b>CHAPTER 4.....</b>	<b>111</b>
<b>Alumina hollow fibre membranes preparation.....</b>	<b>111</b>
Abstract.....	111
4.1. Introduction.....	111
4.2. Characterization of prepared alumina hollow fiber membrane .....	113
4.2.1. Alumina hollow fibre membrane prepared with an internal coagulant flow rate of 5 ml/min.....	116
4.2.2. Alumina hollow fibre membrane prepared with an internal coagulant flow rate of 10 ml/min.....	118

4.2.3. Alumina hollow fibre membrane prepared with an internal coagulant flow rate of 20 ml/min .....	121
4.3. Comparison of prepared alumina hollow fibre membranes.....	124
4.4. Conclusions.....	125
<b>CHAPTER 5.....</b>	<b>129</b>
<b>Biphasic biocatalytic membrane reactor with covalently immobilized lipase .....</b>	<b>129</b>
Abstract .....	129
5.1. Introduction.....	129
5.2. Characterization of grafted alumina membranes surface.....	132
5.3. Covalent immobilization of lipase .....	135
5.4. Lipase activity measurements .....	137
5.5. Inorganic membrane regeneration .....	140
5.6. Conclusions.....	140
<b>CHAPTER 6.....</b>	<b>145</b>
<b>Monophasic biocatalytic membrane reactor .....</b>	<b>145</b>
Abstract .....	145
6.1. Introduction.....	146
6.2. Monophasic BMR with covalently immobilized $\beta$ -glucosidase.....	147
6.2.1. $\beta$ -Glucosidase activity measurements.....	147
6.2.1.1. Determination of kinetic parameters of free $\beta$ -glucosidase .....	147
6.2.2. Characterization of grafted alumina membranes surface.....	154
6.2.3. Covalent immobilization of $\beta$ -glucosidase.....	155
6.2.4. $\beta$ -glucosidase activity measurements in a monophasic biocatalytic membrane reactor.....	156
6.2.5. Monophasic biocatalytic membrane reactor with immobilized $\beta$ -glucosidase by covalent binding .....	158

6.3.2. Activity measurements of entrapped $\beta$ -glucosidase.....	163
6.4. Conclusions.....	166
<b>CHAPTER 7.....</b>	<b>169</b>
<b>Multiphasic biocatalytic membrane reactor .....</b>	<b>169</b>
Abstract.....	169
7.1. Introduction.....	170
7.2. Results and discussion .....	173
7.2.1. Selection of organic solvent .....	173
7.2.2. Study of oleuropein aglycon production/extraction in a multiphasic biocatalytic membrane reactor.....	176
7.3. Conclusions.....	180
<b>OVERALL CONCLUSIONS .....</b>	<b>182</b>

## ***SUMMARY***

In the recent years the interest about the study of membrane processes has led to the development of innovative technologies. The technological progress has allowed to extend the application of membrane processes in systems of industrial interest such as biocatalytic membrane reactors, more and more applied in food, chemical, biological, pharmaceutical, medical and environmental fields. The field of catalytic membrane reactors is an interdisciplinary research area that mainly connects the membrane material sciences with catalysis research and chemical engineering. From an engineering standpoint, the vision of process intensification through multifunctional reactors has breathed new life into research on catalytic membrane reactors, such that they may permit the elimination of process steps and hence lead to more compact and cost-efficient plants than a conventional design with separate units. In particular, catalytic membrane reactors have received increased attention over the past two decades, initially due to progress made in the field of inorganic membranes made of metal oxides, such as alumina ( $\text{Al}_2\text{O}_3$ ), Zirconia ( $\text{ZrO}_2$ ), Titania ( $\text{TiO}_2$ ) and Silica ( $\text{SiO}_2$ ). This is because conventional polymeric membranes, despite having achieved a degree of commercial success in membrane reactors (mainly in biotechnology and in other low temperature applications), have a limited thermal, chemical and mechanical stability. In particular, polymeric membrane matrix could be strongly compromised in case of contact with aggressive solvent commonly used during membrane functionalization (for covalent enzyme immobilization) and for long time operation in multiphase system. Inorganic membranes, although more expensive than polymeric ones, can withstand high temperatures, they are chemically much more stable under the often harsh environments of industrial reactors, and they are more robust. An efficient catalytic membrane system requires that the membrane material is stable for both reaction and separation and that it operates well in both modes simultaneously. Optimization of a single material for both catalytic and separative functions is challenging. In the present research work alumina membranes with a hollow fibre configuration, typical configuration of polymeric membrane, has been prepared and used for the development of both monophasic and multiphase biocatalytic membrane reactors in order to overcome the mentioned limitations due to the use of common polymeric membrane. In such a configuration, a catalyst is located in the pore of hollow fibre membranes. Reactants are fed into the catalyst zone and products have

the potential to be transported through the membrane walls and out of the reaction zone. The high surface area/volume ratio of this configuration makes the membranes both suitable for enzymatic immobilization and the catalysis in a multiphase system in which aqueous and organic phases can coexist. Besides, thanks to high chemical resistance of ceramic matrix, functionalization process for enzyme covalent immobilization can be performed by using a wide range of reagents as well as the use of strong detergents for membrane cleaning and regeneration. Biocatalytic membrane reactors with covalently immobilized enzyme are gaining increasing attention in the production of active ingredients for pharmaceutical and food industry.

In this thesis, the study was focused on the development of monophasic and multiphase biocatalytic membrane reactors. Inorganic and polymeric capillary membranes were used. Lipase and  $\beta$ -glucosidase enzymes were used as model biocatalysts for the multiphase and monophasic systems, respectively. Enzyme immobilization was carried out by covalent bond or physical entrapment. A strategy to functionalize membranes in harsh conditions while performing the enzyme covalent attachment in mild conditions was developed, which avoided or minimized the enzyme denaturation. Furthermore, the method permitted to tune the amount of functional groups on the membrane available for enzyme attachment. This is crucial in order to control the amount of immobilized enzyme on the membrane, which is among the most important parameters to optimize enzyme specific activity and reactor productivity.

Lipase is one of the most studied biocatalysts, which is active in different reactions such as hydrolysis, esterification, and transesterification, with high enantioselective properties. Lipase is an interfacial molecule with phase transfer catalytic properties, meaning it performs to the best of its abilities in an oil/water interface. Therefore, lipase was studied in a biphasic biocatalytic membrane reactor where the enzyme was covalently immobilized onto alumina hollow fibre membranes. In this system the membrane acts as a catalytic interface, separating the two phase (olive oil and aqueous phase) which remained in contact within the membrane pores. Here the reaction takes place and the fatty acids formed by hydrolysis of triglycerides are extracted in the aqueous phase.

Results showed that immobilized lipase preserved 93% of its native catalytic performance, with a specific activity of 9.5 ( $\pm 0.5$ ) U/mg. The catalytic stability was also very good, in fact, specific activity was monitored for 18 days, during which period 6 reaction cycles were performed, with constant performance. The volumetric reaction rate of this biphasic



membrane reactor, using lipase immobilized by covalent bond on alumina capillary membranes, resulted two orders of magnitude higher ( $7.2 \text{ mmol/dm}^3\text{h}$ ) compared to the biphasic system using lipase immobilized by entrapment into polymeric membrane ( $0.04 \text{ mmol/dm}^3\text{h}$ ), developed by Giorno et al [Giorno, L.; Drioli, E. Catalytic behavior of lipase free and immobilized in biphasic membrane reactor with different low water-soluble substrates. *J. Chem. Technol. Biotechnol.* 1997, 69, 11–14].

$\beta$ -glucosidase is involved in phenolic compounds production during olive oil processing in the step of olives crushing. The mechanical destruction of the two compartments containing enzyme/glucosides causes the hydrolysis of glucosides present in olives and the partition of phenolic compounds produced in olive oil or aqueous phase basing on its partition coefficient. The phenolic compounds produced in this hydrolysis, in particular oleuropein aglycon, are very important for their high antioxidant properties and in view of their potentially use in pharmaceutical and food industry. The main idea of the work presented here was to simulate the different compartments present in vegetal system, in which  $\beta$ -glucosidase action is involved, by creating a bioartificial system able to produce high added value compounds under controlled conditions. Due to their potential application in the production of antioxidant compounds present in olive oil, the enzyme/substrate studied is the biological system  $\beta$ -glucosidase/oleuropein. The development of biohybrid system for the hydrolysis of oleuropein is of high interest also because this compound is contained in waste material coming from olive oil processing and in renewable material such as leaves. In recent years, the oleuropein hydrolysis was performed by using industrial waste material in a multiphase biocatalytic membrane reactor where  $\beta$ -glucosidase was entrapped into the pores of polysulfone membranes. Since the interested molecules are stable only in organic phase, it was necessary the use of an organic solvent in order to recover the new formed products. Thus, simultaneously to the reaction, an organic solvent was used as phase extraction for the recovery of the low-water-soluble reaction products. In order to avoid the probable damaging of polymeric membrane matrix because of prolonged contact both with raw materials and organic solvent, an inorganic multiphase biocatalytic membrane reactor was developed in the present work. Here,  $\beta$ -glucosidase was covalently immobilized into the pores of alumina hollow fibre membrane in order to improve the stability of the enzyme and to avoid leaching during the reaction. Immobilized  $\beta$ -glucosidase was studied using as substrate both solution of commercial pure oleuropein and olive leaves extract. Results showed that by immobilizing about  $27.7 \text{ mg/cm}^3$  of  $\beta$ -glucosidase by covalent binding onto alumina hollow fiber membranes, a conversion degree of about  $35.7 (\pm 1)\%$  and  $33.7 (\pm 1)\%$

was obtained by using a solution of commercial pure oleuropein and olive leaves extract as feed, respectively. Immobilized  $\beta$ -glucosidase retained about 57% of the initial enzymatic activity which remained constant for more than 10 days of observation. Reactor performance was then compared with that obtained with free  $\beta$ -glucosidase in a stirred tank reactor. The conversion degree was similar for both reactors with a much higher residence time for the stirred tank reactor using free  $\beta$ -glucosidase. In fact, in such system the free enzyme converted about 33% of substrate in 300 minutes compared to the 35.7% of conversion degree obtained in 36 seconds by the immobilized enzyme in the biocatalytic membrane reactor. This was probably due to the fact that, in the continuous biocatalytic membrane reactor, competitive inhibition of glucose co-product was avoided, as reaction volume was continuously removed under convective flow. Kinetic studies carried out in stirred tank reactor with free  $\beta$ -glucosidase, demonstrated that the reaction suffers from product competitive inhibition.

On the basis of studies carried out with various membrane reactor systems, a scale-up of the  $\beta$ -glucosidase entrapped in polymeric membranes was chosen, due to its simpler immobilization procedure, in order to proof the reproducibility of the performance of biocatalytic membrane reactor on a larger scale, and the robustness of the technology for a potential industrial application. Whilst most operative condition were reproduced, so as to maintain the optimal parameters in which the best enzyme performance was obtained, the amount of immobilized enzyme was lower ( $3.5 \text{ mg/cm}^3$ ) respect to the ideal one ( $4.6 \text{ mg/cm}^3$ ), due to the fact that a lower initial enzyme concentration was used for lack of enzyme availability.

$\beta$ -glucosidase was entrapped in polysulfone asymmetric hollow fibre membranes having a membrane surface area of  $0.09 \text{ m}^2$ , about 45 time greater than the membrane surface area used in small scale. Consequently, it was necessary to adapt instrumentations, chemicals and methods to the new prototype plant biocatalytic membrane reactor. In this case, only commercial oleuropein was used to perform the hydrolysis reaction in order to monitor enzyme activity in best operating condition. Entrapped  $\beta$ -glucosidase showed a conversion degree of about 30%. The reactor was able to produce about 3.6 g/day of aglycon.

Considering the good results in terms of reactor performance, in order to further exploit the feasibility of the system, the attention was posed also on the quality of the reaction product. It is worth to recall that this reactor works in water phase under convective flow. The commercial value of aglycon is much higher if it is stabilized in organic phase, where it does not undergo conformational changes that instead occur in aqueous phase. Therefore, a

multiphase inorganic biocatalytic membrane reactor was developed in order to produce and simultaneously extract the high added value compounds deriving from oleuropein hydrolysis by the action of covalently immobilized  $\beta$ -glucosidase. In such system, membrane serves both as separation and catalytic unit where the reaction is performed by forcing oleuropein solution to pass through the enzyme-loaded membrane under convective flow, and the reaction volume (containing products and non reacted substrate) is collected from the other side of membrane. Here, the organic solvent is recirculated so that when aqueous phase appears at the membrane pore, water in oil droplets are formed and aglycon is extracted in the organic phase. In this way, bioconversion and simultaneous separation of reaction products as a function of their solubility and stability in water or in organic solvent occurs in a single operation step. Aglycon has strong antioxidant activity; it is difficult to separate from reaction mixture due its low stability and for this it is not yet available in commerce, therefore it has attracted the interest of several groups in the last decade. The present research work proposed a valid strategy to valorize industrial oil wastes and natural source, such as olive leaves, by producing and recovering oleuropein aglycon in solid form. In fact, the developed multiphase membrane reactor allowed to produce aglycon and recover about 93% of it in a non-toxic organic solvent. Therefore, the proposed multiphase biocatalytic membrane reactor can have positive perspectives for the development of a sustainable process for industrial application. In fact, aglycon production can have very strong impact both from an economic and healthy point of view. Besides, industrial wastes would be the primary source on the basis of the production process by reducing environmental pollution and disposal costs.

Finally, a method for cleaning and regeneration of the ceramic membrane is proposed in this work in order to extend their life time.

None of these membrane reactors is yet in commercial use, but they are the subject of a very intensive industrial research effort. If successfully developed, this process may change the feedstock basis of a number of industrial processes. This study, confirmed the robustness of the technology in relevant environment and produced suitable data to promote prototype demonstration.

## ***DISSERTATION OUTLINES***

The thesis is organized in two main sections. The first section covered an introduction to membranes, basic theory of catalytic reactors (with special focus on catalytic membrane reactors) and enzyme kinetics. In particular, in **Chapter 1**, types of membranes used for the development of catalytic membrane reactors and preparation methods of the membranes used in the present work were described. In **Chapter 2**, the types of catalytic reactors, their main applications and properties, and the different methods for biomolecules immobilization were summarized.

The second section covered the research activity carried out in this thesis and was organized as following:

- Description of materials, analytical methods, equipment and operation mode used during the activity research (**Chapter 3**).
- preparation and characterization of alumina hollow fibre membranes (**Chapter 4**)
- Development of biphasic biocatalytic membrane reactor by covalently immobilizing lipase onto homemade alumina hollow fiber membranes in order to improve stability and efficiency of a system commonly developed by using polymeric membrane. Studies about the impact of covalent enzyme immobilization on enzyme amount and catalytic activity were also carried out (**Chapter 5**).
- Lab-scale and scale-up development of a monophasic biocatalytic membrane reactor by using alumina and polysulfone hollow fibre membranes, respectively.  $\beta$ -glucosidase was the biocatalyst studied under different conditions, such as in its free native conformation, covalently immobilized onto prepared alumina hollow fibre membranes and entrapped into the pores of polysulfone membrane in a prototype plant. In the last case, catalytic activity of the enzyme was monitored both in presence of commercial oleuropein solution and olive leaves extract (**Chapter 6**).
- Development of multiphase inorganic biocatalytic membrane reactor in order to produce and recover the aglycon (produced from the first step of oleuropein hydrolysis by  $\beta$ -glucosidase) in one single step basing on membrane emulsification concept. In order to recover aglycon in solid form, a study of different organic solvent with specific requirements was carried out (**Chapter 7**).

## ***SOMMARIO***

Nel corso degli ultimi anni l'interesse nei confronti dello studio sui processi a membrana ha portato allo sviluppo di tecnologie innovative. Il progresso tecnologico ha permesso di ampliare l'applicazione dei processi a membrana in sistemi industriali quali reattori biocatalitici a membrana che trovano sempre di più impiego nel campo alimentare, chimico biologico, farmaceutico, medico e ambientale. Il campo dei reattori biocatalitici a membrana è un'area di ricerca interdisciplinare che connette la scienza dei materiali delle membrane sia con la ricerca nel mondo della catalisi che con l'ingegneria chimica. Da un punto di vista ingegneristico, i processi di intensificazione attraverso reattori multifunzionali, ha portato nuove speranze nella ricerca sui reattori catalitici a membrana in quanto potrebbero permettere l'eliminazione di processi a stadi e quindi portare a impianti più compatti e convenienti rispetto ad una progettazione con unità separate. In particolare, reattori catalitici a membrana hanno ricevuto maggiore attenzione nel corso degli ultimi due decenni grazie ai progressi compiuti nel campo delle membrane inorganiche fatte di ossidi metallici, come ad esempio allumina ( $\text{Al}_2\text{O}_3$ ), ossido di zirconio ( $\text{ZrO}_2$ ), Titania ( $\text{TiO}_2$ ) e silice ( $\text{SiO}_2$ ). Questo perché le convenzionali membrane polimeriche, pur avendo raggiunto un certo grado di successo commerciale in reattori a membrana (soprattutto nel campo delle biotecnologie e in altre applicazioni a bassa temperatura), hanno una limitata stabilità termica, chimica e meccanica. La matrice della membrana polimerica potrebbe essere fortemente compromessa in modo particolare nel caso di contatto con solventi aggressivi comunemente usati per la funzionalizzazione della membrana (per l'immobilizzazione covalente di enzimi) e nel caso di lunghi tempi di operazione nei sistemi multifasici. Le membrane inorganiche, sebbene più costose di quelle polimeriche, sono in grado di sopportare alte temperature, sono chimicamente molto più stabili nei drastici ambienti dei reattori industriali e sono più robuste. Un efficiente sistema catalitico a membrana richiede che il materiale della membrana sia stabile sia per le reazioni che per la separazione e che operi bene contemporaneamente con entrambe le modalità. L'ottimizzazione di un singolo materiale sia per le funzioni catalitiche che per quelle di separazione è impegnativo. Nel presente lavoro di ricerca, membrane in allumina con una configurazione a fibra cava, configurazione tipica delle membrane polimeriche, sono state preparate ed usate per lo sviluppo di reattori biocatalitici sia monofasici che multifasici in modo da oltrepassare i limiti menzionati dovuti

all'impiego delle comuni membrane polimeriche. In questa configurazione, un enzima è confinato nei pori delle membrane a fibra cava. I reagenti vengono alimentati nell'area catalitica e i prodotti hanno la possibilità di essere trasportati attraverso la membrana e allontanati dalla zona catalitica. L'elevato rapporto superficie/volume di questa configurazione rende le membrane adatte sia per l'immobilizzazione enzimatica che per la catalisi in un sistema multifasico in cui può coesistere sia una fase acquosa che una fase organica. Inoltre, grazie all'elevata resistenza chimica del materiale ceramico, i processi di funzionalizzazione e di immobilizzazione enzimatica covalente possono essere effettuate utilizzando una vasta gamma di reagenti così come forti detergenti per il lavaggio e la rigenerazione delle membrane. I reattori biocatalitici a membrana con enzimi covalentemente immobilizzati stanno guadagnando sempre maggior attenzione nella produzione di sostanze che sono alla base dell'industria farmaceutica ed alimentare.

In questa tesi, lo studio è stato focalizzato sullo sviluppo di reattori biocatalitici a membrana monofasici e bifasici. Membrane capillari inorganiche e polimeriche sono state utilizzate. Gli enzimi Lipasi e  $\beta$ -glucosidasi sono stati usati come modelli biocatalitici rispettivamente per sistemi bifasici e monofasici. L'immobilizzazione enzimatica è stata effettuata tramite legame covalente o intrappolamento fisico. È stata sviluppata una strategia per funzionalizzare le membrane in condizioni drastiche ma di condurre l'immobilizzazione enzimatica covalente in condizioni blande, evitando o minimizzando la denaturazione dell'enzima. Inoltre, il metodo ha consentito di ottimizzare la quantità di gruppi funzionali sulla membrana disponibile per l'attacco enzimatico. Questo è fondamentale per controllare la quantità di enzima immobilizzato sulla membrana, che è tra i parametri più importanti per ottimizzare l'attività specifica dell'enzima e la produttività del reattore. La lipasi è uno degli enzimi maggiormente studiati capace di catalizzare diverse reazioni quali idrolisi, esterificazione e transesterificazione con elevate proprietà enantioselettive. La lipasi è una molecola interfacciale con proprietà catalitiche di trasferimento di fase, il che significa che esplica le sue migliori prestazioni a livello di un'interfaccia olio/acqua. Perciò, la lipasi è stata studiata in un reattore biocatalitico a membrana bifasico dove l'enzima è stato immobilizzato covalentemente nelle membrane di allumina a fibra cava. In questo caso la membrana funge da interfaccia catalitica separando due fasi (olio d'oliva e fase acquosa) che rimangono in contatto all'interno dei pori della membrana. È qui che la reazione avviene e gli acidi grassi prodotti dall'idrolisi dei trigliceridi vengono estratti in fase acquosa. I risultati ottenuti hanno dimostrato che la lipasi immobilizzata ha mantenuto il 93% della sua

attività catalitica iniziale, con un'attività specifica di  $9.5 (\pm 0.5)$  U/mg. Anche la stabilità catalitica si è mantenuta bene, infatti l'attività specifica è stata monitorata per 18 giorni, periodo durante il quale sono stati eseguiti 6 cicli di reazione, con prestazioni costanti. La velocità di reazione del reattore biocatalitico a membrana, usando lipasi immobilizzata covalentemente su membrane capillari in allumina, è risultata maggiore di circa due ordini di grandezza ( $7.2 \text{ mmol/dm}^3\text{h}$ ) rispetto al sistema in cui la lipasi è stata immobilizzata tramite intrappolamento in membrane polimeriche ( $0.04 \text{ mmol/dm}^3\text{h}$ ) sviluppato da Giorno et al [Giorno, L.; Drioli, E. Catalytic behaviour of lipase free and immobilized in biphasic membrane reactor with different low water-soluble substrates. *J. Chem. Technol. Biotechnol.* 1997, 69, 11–14]. La  $\beta$ -glucosidasi è coinvolta nella produzione di composti fenolici durante i processi di lavorazione dell'olio d'oliva negli stadi di frantumazione delle olive. La distruzione meccanica dei due scomparti contenenti enzimi / glucosidi provoca l'idrolisi dei glucosidi presenti nelle olive e la partizione dei composti fenolici prodotti in olio di oliva o in fase acquosa sulla base del coefficiente di ripartizione. I composti fenolici prodotti da questa idrolisi, in particolare l'aglicone, sono molto importanti per le loro elevate proprietà antiossidanti e in vista del loro potenziale utilizzo nell'industria farmaceutica e alimentare. L'idea principale di questo lavoro è stato quello di simulare i diversi compartimenti presenti nel sistema vegetale, in cui l'azione  $\beta$ -glucosidasi è coinvolta, creando un sistema bioartificiale in grado di produrre composti ad alto valore aggiunto in condizioni controllate. Grazie alla loro potenziale applicazione nella produzione di composti antiossidanti presenti nell'olio di oliva, il sistema enzima/substrato studiato è quello biologico  $\beta$ -glucosidasi/oleuropeina. Lo sviluppo di un bioibrido sistema per l'idrolisi dell'oleuropeina è di grande interesse anche perché questo composto è contenuto nel materiale di scarto proveniente dalla produzione di olio di oliva e in materiale rinnovabile quali foglie d'ulivo. In questi ultimi anni, l'idrolisi dell'oleuropeina è stata effettuata utilizzando materiale di scarto industriale in un reattore a membrana biocatalitico multifasico dove la  $\beta$ -glucosidasi è stata intrappolata nei pori di membrane di polisulfone. Poiché le molecole di interesse sono stabili solo in fase organica, è stato necessario l'utilizzo di un solvente organico per recuperare i prodotti formati. Così, contemporaneamente alla reazione, un solvente organico viene usato come fase estraente per il recupero dei prodotti di reazione poco solubili in acqua. Al fine di evitare il probabile danneggiamento della membrana polimerica dovuto ad un prolungato contatto con materiale grezzo e solventi organici, nel presente lavoro è stato sviluppato un reattore biocatalitico a membrana con membrane inorganiche. In questo caso, la  $\beta$ -glucosidasi è stata immobilizzata mediante legame

covalente nei pori delle membrane a fibra cava in allumina per migliorare la stabilità dell'enzima e per evitare lisciviazione durante la reazione. La  $\beta$ -glucosidasi immobilizzata è stata studiata usando come substrato sia una soluzione di oleuropeina commerciale che un estratto di foglie d'ulivo. I risultati ottenuti hanno dimostrato che immobilizzando circa 27.7 mg/cm<sup>3</sup> di  $\beta$ -glucosidasi tramite legame covalente su membrane a fibra cava in allumina, una conversione del 35.7% ( $\pm 1$ ) e del 33.7% ( $\pm 1$ ) è stata ottenuta utilizzando rispettivamente una soluzione di oleuropeina commerciale pura ed estratti di foglie d'ulivo come soluzione di alimentazione. La  $\beta$ -glucosidasi immobilizzata ha mantenuto circa il 57% dell'attività enzimatica iniziale la quale è rimasta costante per più di 10 giorni di osservazione. La prestazione del reattore è stata poi comparata con quella ottenuta con la  $\beta$ -glucosidasi libera in un reattore a miscelazione completa. Il grado di conversione è risultato simile in entrambi i reattori con un tempo di residenza molto maggiore nel caso del reattore a miscelazione completa usando la  $\beta$ -glucosidasi libera. Questo probabilmente è dovuto al fatto che, nel reattore biocatalitico a membrana continuo, l'inibizione competitiva del co-prodotto glucosio è stata evitata, in quanto il volume di reazione è stato continuamente rimosso tramite flusso convettivo. Sono stati effettuati studi sulla cinetica nel reattore a miscelazione completa con la  $\beta$ -glucosidasi libera ed è stato dimostrato che la reazione subisce inibizione competitiva da parte del co-prodotto. Sulla base degli studi effettuati su vari reattori a membrana, è stato scelto di effettuare uno scale-up della  $\beta$ -glucosidasi intrappolata in membrane polimeriche, in quanto la procedura di immobilizzazione è più semplice, per testare la riproducibilità delle prestazioni del reattore biocatalitico a membrana su una scala maggiore e la solidità della tecnologia per una potenziale applicazione industriale. Nonostante siano state riprodotte la maggior parte delle condizioni operative, in modo da mantenere i parametri ottimali con le quali è stata ottenuta la migliore prestazione dell'enzima, la quantità di enzima immobilizzato utilizzata è stata inferiore (3.5 mg/cm<sup>3</sup>) rispetto a quella ideale (4,6 mg/cm<sup>3</sup>) dovuto al fatto che è stata utilizzata una minor concentrazione enzimatica iniziale per mancanza di disponibilità dell'enzima. La  $\beta$ -glucosidasi è stata intrappolata in membrane asimmetriche a fibra cava aventi una superficie di 0,09 m<sup>2</sup>, circa 45 volte più grande rispetto alla superficie di membrana utilizzata in piccola scala. Di conseguenza, è stato necessario adattare strumentazioni, prodotti chimici e metodi per il nuovo impianto pilota di reattore biocatalitico a membrana. In questo caso, è stata utilizzata solo oleuropeina commerciale per eseguire la reazione di idrolisi in modo da monitorare l'attività enzimatica nelle migliori condizioni operative. La  $\beta$ -glucosidasi immobilizzata tramite intrappolamento fisico ha mostrato un grado di conversione pari a circa il 30%. Il reattore ha prodotto circa 3.6 g/giorno di aglicone. Considerando i buoni risultati in termini di efficienza del reattore, al fine di



sfruttare ulteriormente la flessibilità del sistema, l'attenzione è stata posta anche sulla qualità del prodotto di reazione. Vale la pena ricordare che questo reattore funziona in fase acquosa sotto flusso convettivo. Il valore commerciale dell'aglicone è molto più elevato se si stabilizza in fase organica, dove non subisce modificazioni conformazionali che invece si verificano in fase acquosa. Perciò, è stato sviluppato un reattore biocatalitico a membrana multifasico per produrre e simultaneamente estrarre composti ad alto valore aggiunto derivanti dall'idrolisi dell'oleuropeina mediante l'azione della  $\beta$ -glucosidasi immobilizzata covalentemente. In questo sistema, la membrana serve sia come unità catalitica che di separazione, in cui la reazione viene condotta forzando una soluzione di oleuropeina a passare attraverso la membrana, in cui l'enzima è immobilizzato, tramite flusso convettivo, e il volume di reazione (contenente prodotti e substrato non reagito) viene raccolto dall'altro lato della membrana. Qui, un solvente organico viene fatto ricircolare in modo che, quando la fase acquosa fuoriesce dal poro, si formano gocce di acqua in olio e l'aglicone viene estratto nella fase organica. In questo modo, la conversione e la simultanea separazione dei prodotti di reazione in funzione della loro solubilità e stabilità in acqua o in solvente organico avviene in un'unica fase operativa. L'aglicone ha una forte attività antiossidante; è difficile da separare dalla miscela di reazione a causa della sua bassa stabilità e per questo non è ancora disponibile in commercio, perciò ha attratto l'interesse di diversi gruppi di ricerca nell'ultimo decennio. Il presente lavoro di ricerca ha proposto una strategia valida per la valorizzazione di scarti dell'industria olearia e da fonti naturali, quali foglie di ulivo, tramite la produzione e il recupero di aglicone in forma solida. In effetti, il reattore biocatalitico a membrana multifasico sviluppato ha permesso di produrre e recuperare circa il 93% di aglicone in un solvente organico non tossico. Pertanto, il reattore biocatalitico a membrana multifasico proposto può avere buone prospettive per lo sviluppo di un processo sostenibile per applicazioni industriali. Infatti, la produzione di aglicone può avere un notevole impatto, sia sotto il profilo economico che della salute. Oltretutto, scarti industriali sarebbero la fonte primaria alla base del processo di produzione, riducendo l'inquinamento ambientale e i costi di smaltimento. Infine, in questo lavoro è stato proposto un metodo per la pulizia e la rigenerazione delle membrane ceramiche, al fine di estendere la loro vita media. Nessuno dei reattori a membrana studiati in questo lavoro è ancora impiegato a livello commerciale, ma alcuni sono oggetto di studio in ambito industriale. Se sviluppato con successo, questo processo potrebbe modificare la fonte di materie prime di parecchi processi industriali. Questo studio, conferma la solidità della tecnologia in un ambiente rilevante e ha prodotto dati idonei per promuovere la dimostrazione del prototipo.

## ***CONTENUTO DELLA TESI***

La tesi è organizzata in due parti principali. La prima sezione copre un'introduzione alle membrane, teorie base dei reattori biocatalitici a membrana (con particolare focalizzazione su reattori catalitici a membrana) e la cinetica enzimatica. In particolare, nel **Capitolo 1** vengono descritti i tipi di membrana usati per lo sviluppo di reattori catalitici a membrana e metodi di preparazione usati nel presente lavoro. Nel **Capitolo 2**, sono descritti i tipi di reattori catalitici, le principali applicazioni e proprietà, e i diversi metodi di immobilizzazione di biomolecole.

La seconda sezione copre l'attività di ricerca svolta in questa tesi ed è organizzata come segue:

- Descrizione di materiali, metodi analitici, impianti e metodi operativi usati per lo svolgimento dell'attività di ricerca (**Capitolo 3**).
- Preparazione e caratterizzazione di membrane di allumina in configurazione di fibra cava (**Capitolo 4**).
- Sviluppo di un reattore biocatalitico a membrana bifasico con lipasi immobilizzata mediante legame covalente su membrane di allumina in configurazione di fibra cava preparate in laboratorio. L'obiettivo è quello di migliorare la stabilità e l'efficienza di un sistema tradizionalmente sviluppato con membrane polimeriche (**Capitolo 5**).
- Sviluppo di un sistema biocatalitico a membrana operante in monofase acquosa su scala laboratorio e su scala prototipale. Il primo è stato sviluppato utilizzando membrane inorganiche a fibra cava mentre il secondo è stato sviluppato utilizzando membrane polimeriche in polisulfone. L'enzima  $\beta$ -glucosidasi è stato impiegato come biocatalizzatore ed è stato studiato in varie condizioni, incluso libero in soluzione, immobilizzato con legame covalente su membrane inorganiche e intrappolato fisicamente in membrane di polisulfone su un impianto prototipale. Nell'ultimo caso, l'attività catalitica è stata monitorata sia utilizzando oleuropeina commerciale pura sia utilizzando estratto di foglie di ulivo (**Capitolo 6**).
- Sviluppo di un reattore biocatalitico a membrana multifasico allo scopo di produrre e recuperare aglicone (prodotto dal primo stadio dell'idrolisi della oleuropeina per opera della  $\beta$ -glucosidasi) in un singolo stadio, sulla base del concetto della emulsificazione a membrana. Allo scopo di recuperare l'aglicone in forma solida, lo

studio è stato condotto impiegando vari solventi organici identificando quello più appropriato (**Capitolo 7**)

# ***CHAPTER 1***

## ***Membranes for biocatalytic membrane reactors***

### ***1.1. Introduction***

Membrane technology is presently an established part of several industrial processes. Well known is its relevance in the food industry and in the manufacture of dairy products. Membranes make possible the water supply for millions of people in the world and care for the survival of the large number of people suffering from kidney disease. The chemical industry is a growing field in the application of membranes, which, however, often requires membrane materials with exceptional stability. In particular, properties and quality of membranes is crucial if used as support device in a biocatalytic membrane reactor development, where the membrane not only plays the role of a separator, but it also works as reactive system. Biocatalysis involves the enzyme-promoted transformation of a substrate into useful products. As in all other chemical processes, the separation of reactants from products and the recovery and reuse of the catalyst from the reaction mixture is an important step which significantly adds to the cost of the process. Membrane reactors constitute an attempt to integrate catalytic conversion, product separation and/or concentration, and catalyst recovery into a single operation. Most enzymatic processes currently in industrial use are carried out in batch reactors. However, batch reactors suffer from a number of well-documented limitations, such as frequent startup and shut-down procedures, the need to separate reaction products from reaction mixture and to recover the enzyme after each batch, with high labor costs [1]. By immobilizing the enzyme, it is possible to operate enzymatic processes continuously [1-3]. A complete retention of the enzyme within the system is among the most important requirement for a successful continuous operation of a membrane reactor. Upon this retention, the enzyme becomes confined to a defined region of the membrane reactor, where reaction with the substrate occurs. The immobilization of the enzyme directly onto the membrane can be achieved by chemical binding, [4-13] physical adsorption, [14,15-29] or electrostatic attraction [30-33]. In multiphase reactors the enzyme is usually found immobilized on the side of the membrane that faces the hydrophilic phase, or alternatively, inside the membrane. In certain cases (e.g., lipases), the enzyme is immobilized on the hydrophobic side of the membrane [34-37]. The products resulting from catalysis should permeate through the membrane pores, either by diffusion (induced by

concentration gradient) or convection (induced by a pressure gradient). In this way, a continuous removal of products from the reaction media is attained. In this chapter, the currently available membranes for different processes, which are suitable for the development of biocatalytic membrane reactors will be discussed. Information on different methods of membrane preparation will be given. Different materials will be compared, taking into account physical characteristics and chemical stability.

### ***1.2. Membrane classification***

The membranes can be classified according to their nature, geometry and separation regime. In particular, they can be classified into organic, inorganic and organic/inorganic hybrids. The choice of membrane type to be used in biocatalytic membrane reactor depends on parameters such as the productivity, separation selectivity, membrane life time, mechanical and chemical integrity at the operating conditions and, particularly, the cost. The discovery of new membrane materials was the key factor for increasing the application of the membrane in the catalysis field. The significant progress in this area is reflected in an increasing number of scientific publications, which have grown exponentially over the last few years, as recently shown by [38]. Generally, the membranes can be even classified into homogenous or heterogeneous, symmetric or asymmetric in structure, solid or liquid; they can possess a positive or negative charge as well as they can be neutral or bipolar. In all cases, a driving force as a gradient of pressure, concentration, etc., is applied in order to induce the permeation through the membrane. The first classification is by their nature, which distinguishes the membranes into biological and synthetic ones, which differ completely for functionality and structure. Biological membranes are extremely efficient, but present many disadvantages such as limited operating temperature (below 100 °C), limited pH range, drawbacks related to the clean-up, susceptibility to microbial attack due to their natural origin [39]. Synthetic membranes can be subdivided into organic (polymeric) and inorganic (ceramic, metal) ones. Polymeric membranes commonly operate between 100 – 300 °C [40], inorganic ones above 250 °C. Moreover, inorganic membranes show both wide tolerance to pH and high resistance to chemical degradation. In literature an overview of the commercial polymers used as membranes as well as of other polymers having high potentiality for application as a membrane material is reported [41]. However, many industrial processes involve operations at high temperatures. In this case, polymeric membranes are not useful and, therefore, inorganic ones are preferred. Table 1.1 lists some of common materials for various membrane processes.

**Tab.1.1.** Common materials for various membrane processes.

<b>Material</b>	<b>Application (s)</b>	<b>Approximate maximum working temperature (°C)</b>	<b>pH range</b>
Cellulose acetates	RO, UF, MF	50	3-7
Aromatic polyamide	RO, UF	60-80	3-11
Fluorocarbon polymers	RO, UF, MF	130-150	1-14
Polyimides	RO, UF	40	2-8
Polysulfone	UF, MF	80-100	1-13
Nylons	UF, MF	150-180	
Polycarbonate	UF, MF	60-70	
PVDF	UF	130-150	1-13
Alumina (gamma)	UF	300	5-8
Alumina (alpha)	MF	>900	0-14
Glass	RO, UF	700	1-9
Zirconia	UF, MF	400	1-14
Zirconia (hydrous)	DM (RO, UF)	80-90	4-11
Silver	MF	370	1-14
Stainless steel (316)	MF	>400	4-11

In the following section both polymeric and inorganic membranes will be discussed in more details.

### ***1.3.Polymeric membranes***

Basically, all polymers can be used as membrane material but, owing to a relevant difference in terms of their chemical and physical properties, only a limited number of them is practically utilized. In fact, the choice of a given polymer as a membrane material is not arbitrary, but based on specific properties, originating from structural factors. In the Figure 1.1 is reported a membrane classification according their morphology.

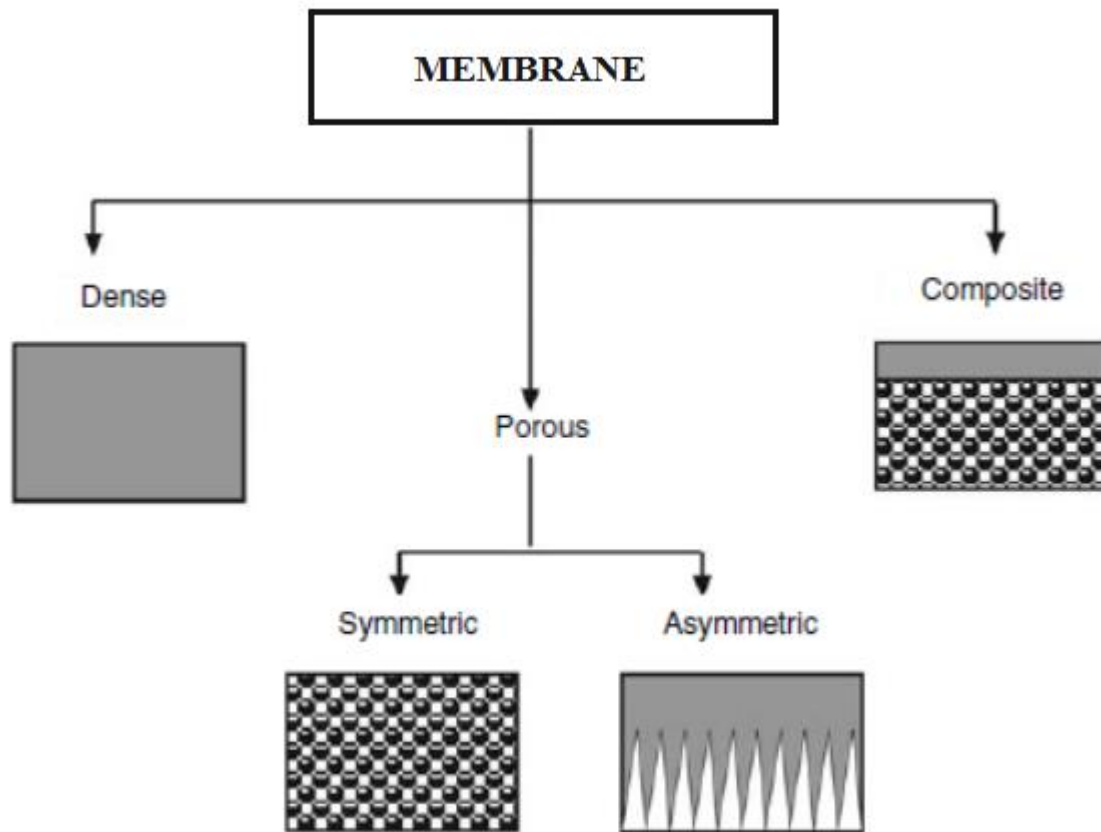


**Fig.1.1.** Membrane classification according the morphology.

The preparation method of polymeric membranes depends on the structural characteristics of the membranes suitable for specific applications. Dense homogeneous polymer membranes are usually prepared (1) from solution by solvent evaporation only or (2) by extrusion of the melted polymer. However, dense homogeneous membranes only have a practical meaning when made of highly permeable polymers such as silicone. Usually the permeant flow across the membrane is quite low, since a minimal thickness is required to give the membrane mechanical stability. Most of the presently available membranes are porous or consist of a dense top layer on a porous structure. To produce microporous symmetrical membranes, common techniques such as irradiation, stretching or template leaching can be employed. The breakthrough of the membrane technology came first in the 1960s with the development of the asymmetric porous membranes [42]. The asymmetric membranes combine high permeant flow, provided by a very thin selective top layer and a reasonable mechanical stability, resulting from the underlying porous structure. An asymmetric structure characterizes most of the presently commercially available membranes, which are now produced from a wide variety of polymers. For asymmetric

membranes, a large array of methods can be applied: interfacial polymerization, solution casting, plasma polymerization and phase-inversion. By far the most common method used in generation of asymmetric structures in membranes is the phase-inversion process. The phase inversion process is applicable to any polymers that can be dissolved in a solvent and precipitated in a continuous phase by a miscible non-solvent. It is capable of making polymeric membranes with a wide range of the pore size by varying polymer content, temperature, composition of the precipitation medium and the type of solvent. Thus, the preparation of membrane structures with controlled pore size involves several techniques with relatively simple principles, but which are quite complicated. It is not the intent of this work to get into any details of polymeric membranes preparation. Since phase inversion process is one of the most widely used technique for fabricating a wide variety of commercial membrane today, it will be discussed in the following section (1.2.1.1). For detailed information about synthesis, characteristics and application of various polymeric membranes, the readers are referred to some published work [43-48].

### ***1.3.1. Phase inversion***

Among different membrane fabrication methods, phase separation is the most common method for fabrication of hollow fiber and flat sheet asymmetric membranes. The process is realized by inducing a "thermodynamic instability" by means of a change of parameters such as:

- Temperature
- Composition
- Solubility

In this method, a homogeneous solution of polymer, solvent, non-solvent and additives is cast into a film and then converted to a solid state by immersion precipitation. Phase inversion by immersion precipitation is one of the most widely used methods for asymmetric membrane fabrication. A polymer solution is immersed in a non-solvent (coagulant) bath and solvent–non-solvent exchange will occur between the polymer solution and the non-solvent. Hydrodynamically unstable viscous fingering is a well-known phenomenon that occurs at the interface between fluids with different viscosities in the first moments of mixing and has been applied here to explain the formation of finger-like voids in ceramic



membrane precursors. When the suspension is in contact with non-solvent, a steep concentration gradient results in solvent/non-solvent exchange, a rapid increase in local viscosity and finally precipitation of the polymer phase. However, due to instabilities at the interface between the suspension and the coagulant there is a tendency for viscous fingering to occur, initiating the formation of finger-like voids. In the Figure 1.2 the initial steps during finger-like voids formation are illustrated.

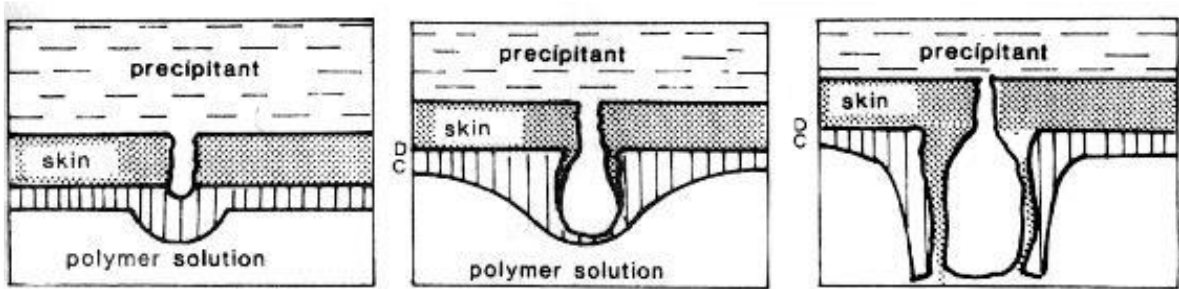


**Fig. 1.2.** Finger-like voids initiation by phase inversion process.

The relative thickness of finger-like and sponge-like regions greatly affects the properties of the membrane such as membrane mechanical strength and permeation flux and, due to the versatility of hollow fibre membranes, it is essential that fibre morphology can be controlled so that it may be tailored to a specific application. Depending on the formation conditions, a variety of different morphologies can be prepared. Thus traditionally, casting dopes are ternary polymer solutions, containing a mixture of polymer(s), solvent(s), and non-solvent. A ternary diagram is used for describing the phase separation process of a system composed of polymer/solvent/coagulant. In this diagram the equilibrium curve known as the binodal curve, divides the area of the triangle into the two following regions:

1. One-phase region: every composition of solvent/ polymer/coagulant in this region forms a homogeneous one-phase solution. It is obvious that the dope composition must lie in this region.
2. Two-phase region: every composition of solvent/polymer/coagulant in this region separates into two equilibrium rich and lean polymer phases whose compositions are given by the two ends of the tie lines.

On the other hand, the spinodal curve represents the curve where all possible fluctuations lead to phase separation. The region between the binodal and spinodal curves implies metastable compositions where phase separation by nucleation and growth takes place. As has been shown in Figure 1.3, the intersection point of these two curves is defined as the critical point (C) in the ternary-phase diagram.

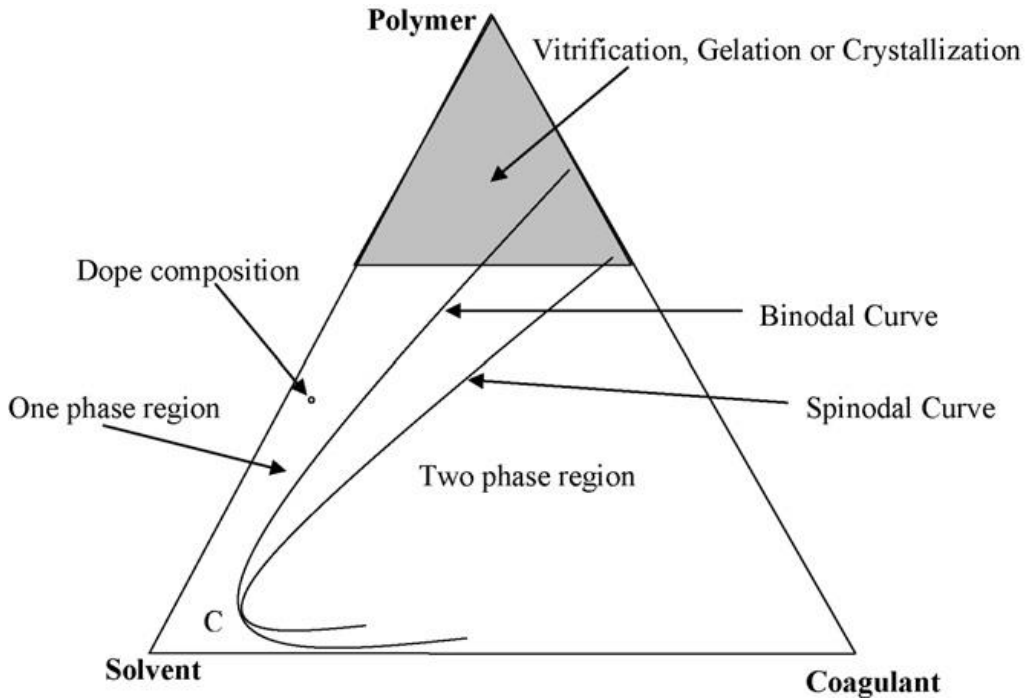


**Fig.1.3.** Ternary-phase diagram about formation of a porous system.

The morphology and properties of the membrane are strongly related to the dope position, critical point position and precipitation path. If the precipitation path crosses the binodal curve, phase separation starts with nucleation and growth of the polymeric or polymer-lean phase. Usually when the polymer concentration is low, the precipitation path crosses the equilibrium line below the critical point and nucleation of a polymer-rich phase initiates the phase separation process. But when the polymer concentration is high, the mentioned path passes through the binodal curve above the critical point. In this case, nucleation of the polymer-lean phase may occur. On the other hand at high polymer concentrations, the precipitation path bypasses the binodal curve and phenomena such as vitrification, gelation or crystallization will occur without polymer-lean phase growth. In addition to the precipitation path and the mechanism for membrane formation, the time of phase separation initiation after immersion is very important in order to predict the morphology and separation properties of the resulting membrane. If precipitation is initiated immediately

after immersion (instantaneous demixing), the resulting membranes have a porous top layer and if precipitation begins after measurable time (delayed demixing) one can expect a membrane with a dense skin layer. Therefore, the membrane formation path and the demixing process are influential parameters that can affect skin layer formation of asymmetric membranes. That is, by changing the demixing time and the precipitation path during membrane preparation one can improve the membrane morphology and separation property. Adding a non-solvent additive (NSA) to the dope solution is an effective way to change the precipitation path and the demixing behavior. It has been shown that non-solvent additives can play a very important role in determining membrane structure. Usually, the addition of a non-solvent to the membrane casting solution brings the initial composition of the dope solution nearer to the precipitation point and thus in the presence of a non-solvent additive one can expect that the binodal curve moves toward the polymer/solvent axis and the singlephase region decreases with increasing non-solvent additive concentration in the solution. Therefore, the addition of a suitable non-solvent additive into the membrane casting solution shortens the precipitation path and accelerates the coagulation process and thus membranes with thinner skin layer and more uniform structure could be obtained. Non-solvent additives should be miscible with the coagulant non-solvent additives, salts, inorganic acids, organic acids and co-solvents can be used as additives. These additives can change membrane property and morphology just like non-solvent additives. Commonly used additives can be classified into the following categories:

1. Polymer additives (PVP and PEG).
2. Low-molecular-weight chemicals including salts (LiCl), inorganic acids (acetic acid and phosphoric acid), organic acids (propionic acid).
3. Weak co-solvents (ethanol and acetone).
4. Weak non-solvents (glycerol and ethylene glycol).
5. Strong non-solvents such as water.

Thus, the addition of a NSA (non-solvent additive) into the polymer solution play an important role in the development of membranes with improved separation characteristics.

#### 1.4. Inorganic membranes

Inorganic membranes are commonly constituted by different materials as ceramic, carbon, silica, zeolite, oxides (alumina, titania, zirconia) as well as palladium, silver etc. and their alloys. They can operate at elevated temperatures. In fact, they are stable at temperatures ranging from 300 – 800 °C and in some cases (ceramic membranes) usable over 1000 °C [49]. They present also high resistance to chemical degradation. As previously said, the inorganic membranes present a high cost as main drawback. Table 1.2 sketches the most important advantages of inorganic membranes with respect to the polymeric ones.

**Tab.1.2.** Advantages of inorganic membranes with respect to the polymeric ones.

<b>Advantages of inorganic membranes</b>
Long-term stability at high temperatures
Resistance to harsh environment (chemical degradation, Ph, ETC,)
Resistance to high pressure drops
Inertness to microbiological degradation
Easy cleanability
Easy Surface activation by using a wide range of reagents

So, although inorganic membranes are more expensive than the polymeric ones, they possess advantage such as resistance towards solvents, well-defined stable pore structure (in the case of porous inorganic membranes), high mechanical stability and elevated resistance at high operating temperatures. However, currently produced inorganic membranes are usually in the form of flat discs, finite sized tubes with diameters of at least several millimeters or multi-channel monoliths and consequently have low surface area/volume ratios [50-52]. These low area/volume ratios compare unfavourably with polymeric hollow fibre modules where area/ volume ratios of several thousand are obtainable; this limits the application of current inorganic monolithic, tubular and disc membranes. This limitation is most evident in catalytic membrane reactors, where it is desirable to maximize the area of the membrane module to increase the permeation rate to remove the product species from the reaction zone [53]. Thus, one of the intent of this work was to overcome the mentioned limitations by preparing ceramic hollow fibre membranes to use as biocatalytic and separation unit in a

biocatalytic membrane reactor. Preparation method of ceramic hollow fibre membrane will be described in the following section. Experimental results obtained in this work will be presented in Chapter 4.

#### ***1.4.1. Ceramic hollow fibre membranes preparation***

Currently, a few methods have been employed for preparing inorganic hollow fibres, including dry spinning a system of inorganic material and binder [54-57], wet spinning a suitable inorganic material-containing solution and/or sols [58], depositing fibres from the gas phase on to a substrate, or pyrolyzing the polymers [59-61]. Furthermore, although some attempts have been made in fabricating a silica glass hollow fibre membranes for gas separation [62], the membrane was too fragile to be used on large industrial scales.

Recently, the well-known phase inversion method, commonly employed for spinning polymeric hollow fibre membranes, has been successfully modified to prepare the ceramic hollow fibres [63-65]. Hollow fibre membranes preparation method is a three step process including: (1) preparation of a spinning suspension; (2) spinning of ceramic hollow fibre precursors and (3) final sintering. Because of the phase inversion characteristics, the prepared ceramic hollow fibres possess an asymmetric structure, which provides a better permeability for a given thickness. An inorganic hollow fibre with an asymmetric pore structure is shown in Figure 1.4, and consists of an outer sponge-like region (Region 1), finger-like voids (Region 2), and a region close to the inner fibre surface (Region 3) which may either be occupied by a sponge-like structure or by finger-like voids, depending on the fibre preparation parameters.

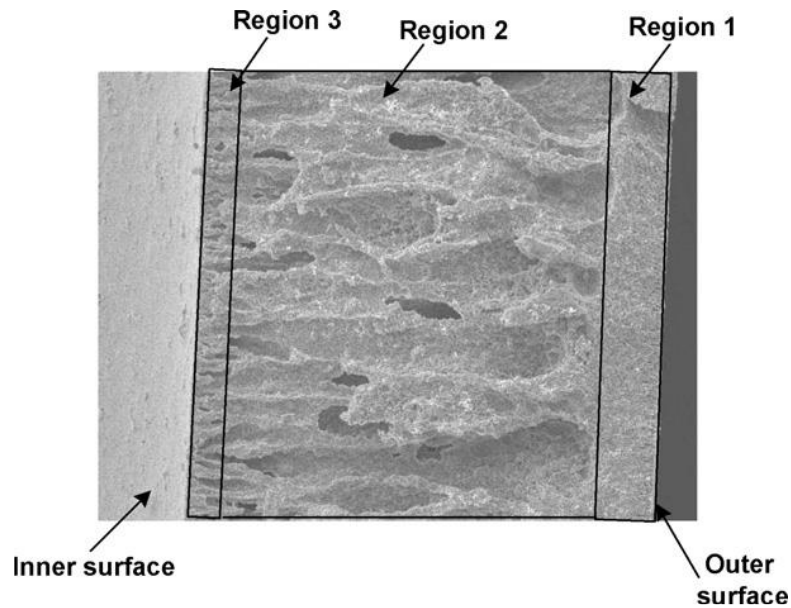


**Fig. 1.4.** Cross-sectional SEM image of an asymmetric ceramic hollow fibre consisting of finger-like voids and a sponge-like structure.

The pore size of the entrances to the finger-like voids present at the fibre surface and the finger-like void volume determine the effectiveness of the catalyst deposition process while the pore size distribution of the sponge-like region is critical in determining the efficiency of the separation process or the quality and thickness of the deposited separation layer. The sponge-like region provides the bulk of the mechanical strength (Region 1), while the finger-like voids Region (Region 2) provides to the bulk of the catalyst deposition. Preparation of ceramic membranes using the phase inversion method is a quite complex process. The choice of spinning suspension composition and adopted parameters during spinning and sintering processes strongly affects the final structure of fibres. Therefore, a detailed discussion on this preparation method is provided according to the sequence of the three steps process.

#### ***1.4.1.1. Preparation of spinning suspension***

The main components in the spinning suspension for the fabrication of hollow fibre ceramic membranes are the ceramic powder, additives and solvents. In selection of the ceramic powder, one of the most important factors is the particle size and their distribution as well as the shape of the particles. They have an effect on the porosity, pore size and pore size distribution of the final membrane product [66,67]. Additives such as deflocculants/dispersants, binders, plasticizers, anti-foaming agents, pore formers, antistatic, chelating, bactericide agents, etc. are used to give the spinning suspension the properties

required. In preparing the ceramic hollow fibre membrane using the phase inversion technique, the requirement of the organic binders is that they should not only be invertible, but also must be burned out without leaving ash and tar during the calcinations. the quantity of organic binders should be as low as possible, but without affecting the inversion capability. The solvent must dissolve the additives and binders used and must show a higher exchange rate with non-solvent (coagulants). The rates of solvent outflow and coagulant inflow have an effect on the cross sectional structures of the membrane precursor and hence the structure of the final membrane products [68]. As preparation of the spinning suspension is still in the development stage, the following few general rules are, so far, considered to be useful in preparation of a spinning suspension:

- The amount of dispersant must be maintained to ensure the stability of the suspension;
- The amount of solvent must be fixed at a minimum to maintain a homogeneous suspension;
- The ratio between organic components and ceramic powders must be as low as possible;
- The plasticizer to binder ratio must be adjusted to make the membrane precursor flexible, resistant and easy to release.

### 1.4.1.2. Spinning of inorganic hollow fibre precursors

Spinning of ceramic hollow fibre precursors can be carried out in a spinning apparatus as shown in Figure 1.5 .

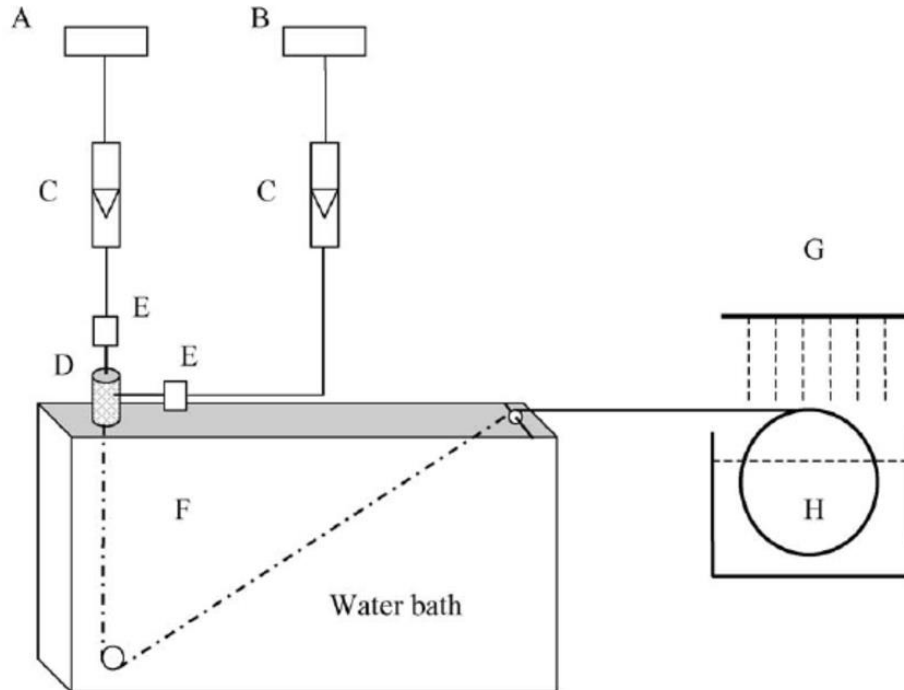


**Fig.1.5.** Spinning apparatus : **A:** Internal coagulant tank. **B:** Dope solution tank. **C:** Syringe pump. **D:** Spinneret. **E:** Filter. **F:** Coagulation bath. **G:** Water sprinkling. **H:** Fiber collecting bath.

The hollow fibre precursors are spun through a tube-in-orifice spinneret, typically with orifice diameter/inner diameter of the tube of 3.0/1.2 mm. The extrusion rate of the spinning suspension is controlled by the nitrogen pressure (or a gear pump) and adjusting valve. The non-solvent, usually water, is used at room temperature as the internal and external coagulants. The spinneret is arranged such that the nascent fibre precursor can be extruded vertically downwards into the coagulation bath. After coagulation (immersion induced phase inversion), the fibre precursor is guided through the wash bath, and then dried. Figure 1.6 shows the cross section of a typical hollow fibre precursor.



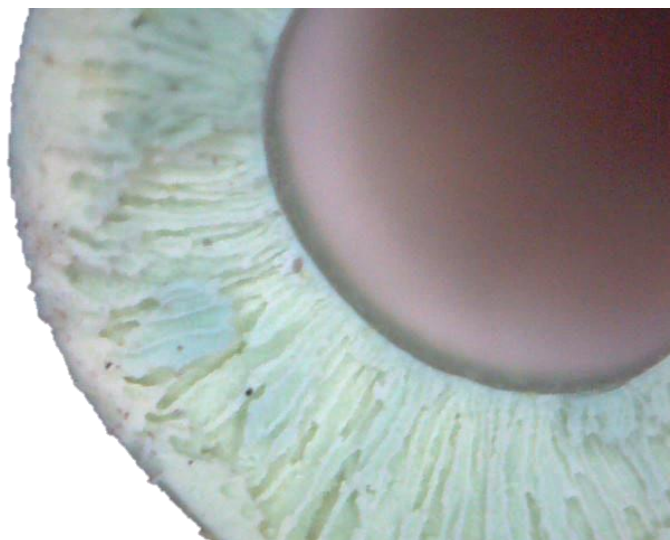


**Fig.1.6.** Cross section of a typical hollow fibre membrane precursor.

#### ***1.4.1.3. Sintering process***

Sintering might best be described as the synthetic manufacture of solid products using controlled heating of powdered raw materials. The proper application of sintering temperature results in the adhesion of the powder grains to each other without melting the material. This proper temperature is ordinarily  $2/3$  the melting point of the particular material. There are two essential methods of sintered manufacturing: solid state, and liquid phase. As its name implies, solid state sintering is the fusing, or forming of powdered material into a product without actually liquefying the material. Conversely, the liquid phase process introduces a liquid step into the process of heating the powder grains. Liquid phase sintering is generally easier and more cost-effective than solid state. However, a certain degradation of the raw material will occur that is not the case with the solid state process. The advantages of sintered products include higher purity of raw materials, the maintenance of purity through the manufacturing process, the stability of repetitive steps in manufacture, and the uniform density of the item produced. In order to impart the fibre with sufficient mechanical strength for practical applications, a minimum calcination temperature is required. It is important to determine the effect of calcination temperature on the pore size distribution. In order to facilitate the impregnation of ready-made catalyst/substrate particles of several microns in size directly into the support structure, it is critical that the entrances to the finger-like voids are present at the fibre surface and are sufficiently large while the properties of the sponge-like region change greatly during sintering, the properties of the pores formed by the entrances to the finger-like voids and the finger-like voids themselves

resist change. Densification of sponge-like regions occurs during calcination, causing a decrease in porosity. Finger-like voids are retained during calcination despite the densification of the sponge-like structure.

### ***1.5. Effect of preparation parameters on ceramic hollow fibre membranes membrane morphology***

The asymmetric structure is such that the fibre may simultaneously function either as a porous membrane and a matrix for enzyme immobilization. The effectiveness of enzyme immobilization and the quality of the separation layer depends strongly on the pore size distribution of the pores formed by the entrances to the finger-like voids and of the sponge-like region, which are affected by the calcination temperature and the fibre preparation parameters [69]. The effect of the calcination temperature and preparation parameters on the pore size distribution and fibre morphology will be discussed in more details in the following sections (1.1.2.3, 1.1.2.4, 1.1.2.5, 1.1.2.6).

#### ***1.5.1. The effect of suspension viscosity on the pore size distribution and fibre morphology***

The relative ratios of the finger like void and sponge-like regions in asymmetric hollow fibres, i.e. the thickness of the sponge-like region of the fibre can be varied by adding a non-solvent additive to the spinning suspension. This greatly affects not only the initial suspension viscosity but also the rate at which the viscosity increases during the phase inversion process. Considering fibres prepared from suspensions containing water as a non-solvent additive, the effect of water addition to the spinning suspension is a reduction in length of finger like voids and an increase in the thickness of the sponge like region of the fibre. Addition of water to the spinning suspension first result in a reduction in size of the pores formed by entrances to the finger like voids and then in the formation of a sponge like region at the inner surface of the fibre. Thus, increasing the mechanical strength of an asymmetric support by introducing a non-solvent additive into the spinning suspension is an unsuitable method when preparing support structure for catalyst impregnation, due the unfavorable pore size reduction and elimination of the entrances to the finger-like voids present at the inner fibre surface.

### ***1.5.2. The effect of the internal coagulant flow rate on the pore size distribution and fibre morphology***

The progressive decrease of the internal coagulant flow rate leads an increase in the thickness of the sponge like region. At lowest internal coagulant flow rate (3 ml/min) the driving force for the formation of finger like voids is insufficient to overcome the viscosity of the suspension film and the internal coagulant. Consequently, viscous fingering is not initiated at this interface but instead initiated within the suspension film where the viscosity is lower and a sponge like region is formed at the inner fibre surface (Region 3), rendering the fibre unsuitable for catalyst impregnation. Therefore, increasing the mechanical strength of the asymmetric support by reducing the internal coagulant flow rate is an unsuitable method when preparing support structures for catalyst impregnation, due the unfavorable pore size reduction and elimination of the entrances to the finger-like voids present at the inner fibre surface.

### ***1.5.3. The effect of air-gap on the pore size distribution and fibre morphology***

A reduction of air gap gives rise to an increase in the thickness of the sponge like region. The thickness of the sponge like region and the mechanical strength of the fibre can be controlled by varying the air gap only if the internal coagulant flow rate is sufficient to prevent the formation of isolated voids and generate an acceptable pore size of the entrances to the finger-like voids. In all three cases, the pore size of the entrances to the finger-like voids is dramatically reduced or even eliminated altogether and the appearance of isolated voids within the sponge-like structure of the fibre is observed, which cause an undesired reduction in mechanical strength.

### ***1.5.4. The effect of calcination temperature on the pore size distribution***

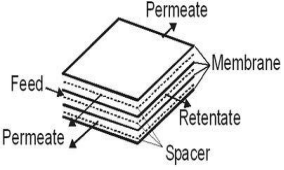
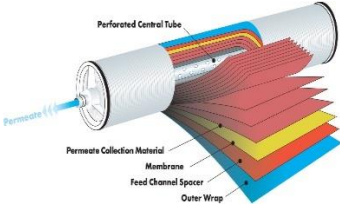
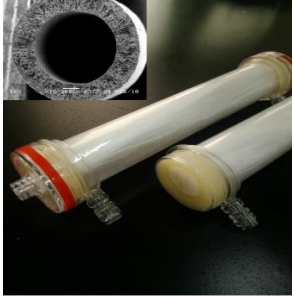
In order to impart the fibre with sufficient mechanical strength for practical applications, a calcination process is required. As calcination temperature is a critical factor in determining the mechanical strength of the hollow fibre membrane or membrane support and a minimum calcination temperature is often required, it is important to determine the effect of calcination temperature on the pore size distribution. It has been shown that an increase in calcination temperature leads to an increase in the mechanical strength of the fibre but this is accompanied by an unwanted increase in the mean pore size of the sponge-like region as well as a decrease in porosity [69]. However, the entrances to fingerlike voids that are present


at the fibre surface remain open during the calcination process and resist densification, a crucial property that allows for enzyme location within the finger-like voids.

### ***1.6. Membrane housing***

Concerning the applications of both organic and inorganic membranes, several configurations are conventionally used for the membrane housing. Generally, a modular configuration (parallel, in series and so on) may be combined for producing the desired effect. Membrane housing provides support and protection against operating pressures. Plate-and-frame, spiral wound, tubular and hollow fiber systems are the most common membrane housing configurations. The advantages and disadvantages of the different membrane elements are listed in Table 1.3.

**Tab.1.3.** Advantages and disadvantages of different kind of membrane housing.

Figure	Membrane module	Advantages	Disadvantages
	<p>Flat sheet/Plate and frame</p>	<ul style="list-style-type: none"> <li>✓ Moderate membrane surface/volume ratio.</li> <li>✓ Well-developed equipment.</li> <li>✓ Easy membrane replacement.</li> </ul>	<ul style="list-style-type: none"> <li>✗ Susceptible to plugging at flow stagnation points.</li> <li>✗ Difficult to clean.</li> <li>✗ Expensive.</li> </ul>
	<p>Spiral wound</p>	<ul style="list-style-type: none"> <li>✓ Compact.</li> <li>✓ Good membrane surface/volume ratio.</li> <li>✓ Minimum energy consumption.</li> <li>✓ Low capital/operating cost.</li> </ul>	<ul style="list-style-type: none"> <li>✗ Not suitable for very viscous fluid.</li> <li>✗ Difficult to clean.</li> <li>✗ Faulty membrane-change whole module.</li> </ul>
	<p>Hollow fibre</p>	<ul style="list-style-type: none"> <li>✓ Compact.</li> <li>✓ Excellent membrane surface/volume ratio.</li> <li>✓ Low energy consumption.</li> </ul>	<ul style="list-style-type: none"> <li>✗ Susceptible to end-face fouling.</li> <li>✗ Susceptible to plugging by particulates.</li> </ul>

			<ul style="list-style-type: none"> <li>× Single fibre damage-replace entire module.</li> </ul>
	Tubular	<ul style="list-style-type: none"> <li>✓ Easy to clean.</li> <li>✓ Feed stream with particulate matter can be put through membrane.</li> <li>✓ Good hydrodynamic control.</li> <li>✓ Individual tubes can be replaced.</li> </ul>	<ul style="list-style-type: none"> <li>× Relative high volume required for unit membrane area.</li> <li>× High energy consumption.</li> <li>× Relatively expensive.</li> </ul>

### ***1.7. General aspect on mass transport through membranes***

The mass transport between two homogeneous systems through a membrane may be the result of diffusion, convection or migration depending on the driving forces and the structure of the membrane. A mass transport process is referred to as diffusion when individual components permeate a matrix independent of each other by random movement under the driving force of a chemical potential gradient. The permeation rate in a diffusion process depends on the magnitude of the driving force, i.e. the chemical potential gradient of the diffusing component and on its diffusion coefficient which is determined by friction between the diffusing component and other components in a mixture. A mass transport process is referred to as convection when bulk flow occurs under the driving force of a hydrostatic pressure difference relative to a matrix which acts as a frame of reference. The flow velocity depends on the hydrostatic pressure difference and hydrodynamic permeability of the matrix which is determined by the friction between the solution and the matrix. A mass transport is referred to as migration when charged components move through a matrix under the driving

force of an electrical potential difference. The migration rate depends on the electrical potential gradient and the mobility of the components in the matrix. The mobility of a component is directly related to its diffusion coefficient and is determined by the friction between the migrating component and other components in a mixture. In membrane processes all three forms of mass transport can contribute to the overall flux. Generally, however, one transport form is dominant while the others contribute to a lesser extent to the overall mass flux. In micro- and ultrafiltration convection of a bulk solution is the dominant form of transport while diffusion is generally insignificant. In reverse osmosis matter is transported through the membrane mainly by diffusion of individual molecules through a more or less homogeneous membrane matrix, but convection can become significant with high flux membranes. In electrodialysis migration of ions in an electric field is the dominant form of transport, but under certain process conditions diffusion and convection can also become relevant. The mass transport through membranes can be described by various mathematical relations. Most of them are semi-empirical, postulating membrane models, such as Fick's law, Hagen-Poiseuille's law and Ohm's law, which are reported below

Fick's law:

$$J = -D \Delta C / \Delta x$$

where J is the diffusion flux, D is the diffusion coefficient, C the concentration of species and x the distance.

Hagen-Poiseuille's law:

$$F = \Delta P \pi r^4 / 8 \eta L$$

where F is the flux,  $\Delta P$  is the pressure difference between the two ends of the tube, r is the radius of pipe,  $\eta$  is the dynamic viscosity and L is the length of pipe.

Ohm's law:

$$V = I \cdot R$$

where V is the electromotive force, I is the current and R is the resistance.

## References

1. Cheryan, M. and Mehaia, M. A. Membrane bioreactors. In: Membrane Separations in Biotechnology (MacGregor, W. C., ed.). Marcel Dekker, New York, 1986, pp.255-302
2. Siebel, M. A. Batch reactors. In: Bioreactor Design and Product Yield. Butterworth-Heinemann, Great Britain, 1992, pp.103-112.
3. Cheryan, M. Ultrafiltration applications. In: Ultrafiltration Handbook. Technomic Publishing Company, Lancaster, PA, 1986, pp. 231-350.
4. Nakajima, M., Watanabe, A., Jimbo, N., Nishizawa, K. and Nakao, S. Forced-flow bioreactor for sucrose inversion using ceramic membrane activated by silanization. *Biotechnol. Bioeng.* 1989, 33. 856-861.
5. Lozano, P., Manjón, A., Iborra, J. L., Canovas, M. and Romojaro, F. Kinetic and operational study of a cross-flow reactor with immobilized pectolytic enzymes. *Enzyme Microb. Technol.* 1990, 12. 499-505.
6. Harrington, T. J., Gainer, J. L. and Kirwan, D. J. Ceramic membrane microfilter as an immobilized enzyme reactor. *Enzyme Microb. Technol.* 1992, 14, 813-818.
7. Hausser, A. G., Goldberg, B. S. and Mertens, J. L. An immobilized two-enzyme system (fungal  $\alpha$ -amylase/glucoamylase) and its use in the continuous production of high conversion maltose-containing syrups. *Biotechnol. Bioeng.* 1983, 25, 525-539.
8. Nakajima, M., Nishizawa, K. and Nabetani, H. A forced flow membrane enzyme reactor for sucrose inversion using molasses. *Bioproc. Eng.* 1993, 9, 31-35.
9. G. Bayramoglu, M. Yilmaz and M. Y. Arica, *Food Chem.*, 2004, 84, 591–599.
10. Ricca E, Calabro` V, Curcio S, et al. (2010). Fructose production by inulinase covalently immobilized on sepabeads in batch and fluidized bed bioreactor. *Int J Mol Sci*, 11, 1180–9.
11. N. Vasileva, T. Godjevargova, V. Konsulov, A. Simeonova and S. Turmanova, *J. Appl. Polym. Sci.*, 2006, 101, 4334–4340.
12. A. De Maio, M. M. El-Masry, M. Portaccio, N. Diano, S. Di Martino, A. Mattei, U. Bencivenga and D. G. Mita, *J. Mol. Catal. B: Enzym.*, 2003, 21, 239–252.
13. K. Gabrovska and T. Godjevargova, *J. Mol. Catal. B: Enzym.*, 2009, 60, 69–75.



14. Garcia, H. Malcata, F. X., Hill, C. G. and Amundson, C. H. Use of *Candida rugosa* Lipase immobilized in a spirai wound membrane reactor for the hydrolysis of milkfat. *Enzyme Microb. Technol.* 1992, 14, 535-545.
15. Habulin, M. and Knez, Z. Enzymatic synthesis of *n*-butyl oleate in a hollow fiber membrane reactor. *J Membrane Sci.* 1991, 61, 315-324
16. Malcata, F. X., Hill, C. G. and Amundson, C. H. Use of a lipase immobilized in a membrane reactor to hydrolyze the glycerides of butteroil. *Biotechnol. Bioeng.* 1991, 38, 853-868.
17. Hoq, M. M., Yamane, T. and Shimizu, S. Continuous hydrolysis of olive oil by lipase in microporous hydrophobic membrane bioreac- tor. *J. Am. Oil Chem. Soc.* 1985, 62, 1016-1021.
18. Hoq, M. M., Koike, M., Yamane, T. and Shimizu, S. Continuous hydrolysis of olive oil by lipase in microporous hydrophobic hollow fiber bioreactor. *Agric. Bio/. Chem.* 1985, 49, 3171-3178.
19. .Hoq, M. M., Tagami, H., Yamane, T. and Shimizu, S. Some character- istics of continuous glyceride synthesis by lipase in a microporous hy- drophobic membrane bioreactor. *Agric Biol Chem.* 1985, 49, 335-342.
20. Prazeres, D. M. F., Garcia, F. A. P. and Cabrai, J. M. S. Batch and continuous lipolysis/product separation in a reversed micellar mem- brane bioreactor. In: *Biocatalysis in Non-Conventional Media* (Tramper, J., Vermue, M. H., Beeftink, H. H. and Stockar, U. eds.). Elsevier, Amsterdam, 1992, pp. 713-718.
21. Prazeres, D. M. F., Garcia, F. A. P. and Cabrai, J. M. S. Continuous lipolysis in a reversed micellar membrane bioreactor. *Bioproc. Eng.* 1994, 10, 21-27 1994, 10, 21 27.
22. Cheng HN, Richard AG. (2010). *Green polymer chemistry: Biocatalysis and biomaterials* (ACS Symposium Serie #1043). Northamptonshire, Great Britain: Oxford University Press.
23. Wang Z-G, Wang J-Q, Xu Z-K. (2006). Immobilization of lipase from *Candida rugosa* on electrospun polysulfone nanofibrous membranes by adsorption. *J Mol Catal B Enzym*, 42, 45–51.
24. .Ebrahimi M, Placido L, Engel L, et al. (2010). A novel ceramic membrane reactor system for the continous enzymatic synthesis of oligosaccharides. *Desalination*, 250, 1105–8.

25. S. P. Beier, A. D. Enevoldsen, G. M. Kontogeorgis, E. B. Hansen and G. Jonsson, *Langmuir*, 2007, 23, 9341–9351.
26. G. Delcheva, G. Dobrev and I. Pishtiyski, *J. Mol. Catal. B: Enzym.*, 2008, 54, 109–115.
27. G. Bayramoglu, A. U. . Metin, B. Altintas and M. Y. ArIca, *Bioresour. Technol.*, 2010, 101, 6881–6887.
28. H.-T. Deng, J.-J. Wang, Z.-Y. Liu and M. Ma, *J. Appl. Polym. Sci.*, 2010, 115, 1168–1175.
29. H. Adikane and D. Thakar, *Appl. Biochem. Biotechnol.*, 2010, 160, 1130–1145.
30. Furusaki, S. and Asai, N. *Enzyme immobilization by the coulomb force. Biotechnol. Bioeng.* 1983, 25, 2209-2219.
31. Furusaki, S., Nozawa, T. and Nomura, S. *Membrane enzyme reactor with simultaneous separation using electrophoresis. Bioproc. Eng.* 1990, 5, 73-78.
32. Lingtian Wu, Shanshan Wu, Zheng Xu, Yibin Qiu, Sha Li, Hong Xu, *Modified nanoporous titanium dioxide as a novel carrier for enzyme immobilization, Biosensors and Bioelectronics, Volume 80, 15 June 2016, Pages 59–66.*
33. A. Vinu, V. Murugesan and M. Hartmann, *J. Phys. Chem. B*, 2004, 108, 7323.
34. Van der Padt, A., Edema, M. J., Sewalt, J. J. W. and Van't Riet, K. *Enzymatic acylglycerol synthesis in a membrane bioreactor.1 Am. Oil Chem. Soc.* 1990, 67, 347-352.
35. Van der Padt, A., Sewalt, J. J. W., Agoston, S. M. I. and Van't Riet, K. *Candida rugosa lipase stability during acylglycerol synthesis. Enzyme Microb. Technol.* 1992, 14, 805-812.
36. Janssen, A. E. M., Klabbers, C., Franssen, M. C. R. and Van't Riet, K. *Enzymatic synthesis of carbohydrate esters in 2-pyrrolidone. En- zyme Microb. Technol.* 1991, 13, 565-572.
37. Pronk, M., Boswinkel, G. and Van't Riet, K. *Parameters influencing hydrolysis kinetics of lipase in a hydrophilic membrane bioreactor. Enzyme Microb. Technol.* 1992, 14, 214-220.
38. E.E. McLeary, J.C. Jansen, F. Kapteijn, *Zeolite based films, membranes and membrane reactors: Progress and prospects, Microp. & Mes. Mat.*, 90, 198–220 (2006).

39. Y. Xia, Y. Lu, K. Kamata, B. Gates, Y. Yin, *Macroporous materials containing threedimensionally periodic structures*, *Chemistry of Nanostructured Materials* (Ed.: Yang, P.), *World Scientific* 69–100 (2003).
40. *Catalytica®*, *Catalytic membrane reactors: concepts and applications*, *Catalytica Study N. 4187 MR*, (1988).
41. S.S. Ozdemir, M.G. Buonomenna, E. Drioli, *Catalytic polymeric membranes: next term Preparation and application*, *Appl. Catal. A: Gen.*, 307, 167–183 (2006).
42. Loeb, S. Sourirajan, *Sea water demineralization by means of an osmotic membrane*. *Advances in Chemistry Series 38* (1962), 117.
43. Strathmann H., Giorno L., Drioli E., *An Introduction to Membrane Science and Technology* ( *Institute on Membrane Technology, CNR-ITM, Italy*).
44. Belfort, G. (Ed.), 1984, *Synthetic Membrane Processes* (Academic Press, Orlando, USA).
45. Lloyd, D.R. (Ed.), 1985, *Material Science of Synthetic Membranes* (ACS Symposium Ser. 269, American Chemical Society, Washington, D.C., USA).
46. Baker, R.W., E.L. Cussler, W. Eykamp, W.J. Koros, R.L. Riley and H. Strathmann, 1991, *Membrane Separation System – Recent Developments and Future Directions* (Noyes Data Corp., New Jersey, USA).
47. Baker, R. W. 2000. *Membrane Technology*. *Kirk-Othmer Encyclopedia of Chemical Technology*.
48. Ivo F. J. Vankelecom, *Polymeric Membranes in Catalytic Reactors*, *Chem. Rev.* 2002, 102, 3779-3810.
49. Van Veen, M. Bracht, E. Hamoen, P.T. Alderliesten, *Feasibility of the application of porous inorganic gas separation membranes in some large-scale chemical processes* *Fundamentals of inorganic membrane science and technology*, edited A.J. Burggraaf, L. Cot, Elsevier, 14, 641–681 (1996).
50. G. Saracco, G.F. Versteeg, W.P.M. van Swaaij, *Current hurdles to the success of high-temperature membrane reactors*, *J. Membrane Sci.* 95 (1994) 105.
51. H.P. Hsieh, *Inorganic membrane reactors*, *AICHE Symp. Ser., No. 268* (85) (1989) 53.
52. H.P. Hsieh. *General characteristics of inorganic membranes*, in: Ramesh R. Bhave (Ed.), *Book of Inorganic Membranes Synthesis, Characteristics and Applications*, 1991, pp. 65–93.

53. J.N. Armor, *Applications of catalytic inorganic membrane reactors to refinery products*, *J. Membrane Sci.* 147 (1998) 217.
54. R.A. Terpstra, J.P.G.M. Van Eijk, F.K. Feenstra, *Method for the Production of Ceramic Hollow Fibres*, USpatent 5,707,584, 1998.
55. J. Smid, C.G. Avci, V. Guñay, R.A. Terpstra, J.P.G.M. Van Eijk, *Preparation and characterisation of microporous ceramic hollow fibre membranes*, *J. Membrane Sci.* 112 (1996) 85.
56. H.W. Brinkman, J.P.G.M. Van Eijk, H.A. Meinema, R.A. Terpstra, *Innovative hollow fiber ceramic membranes*, *Am. Ceram. Soc. Bull.* (1999) 51.
57. R.A. Terpstra, J.P.G.M. Van Eijk, J.C.T. van der Heijde, *Alternative way of producing silicon nitride ceramics for membrane application*, *Key Eng. Mater.* 132–136 (1997) 1770.
58. K.H. Lee, Y.M. Kim, *Asymmetric hollow inorganic membranes*, *Key Eng. Mater.* 61 and 62 (1991) 17.
59. J.E. Koresh, A. Sofer, *Molecular sieve carbon permselective membrane, Part I. Presentation of a new device for gas mixture separation*, *Sep. Sci. Technol.* 18 (1983) 723.
60. J.E. Koresh, A. Sofer, *Mechanism of permeation through molecular-sieve carbon membrane*, *J. Chem. Soc., Faraday Trans.* 82 (1986) 2057.
61. V.M. Linkov, R.D. Sanderson, E.P. Jacobs, *Highly asymmetrical carbon membranes*, *Proc. 34th IUPAC Symp. Macromolecules* 7 (1992) 56.
62. Way, J.D. and Roberts, D.L., *Hollow fibre membranes for gas separations. Separation Science and Technology*, 27 (1): 29-41 (1992).
63. X. Tan, S. Liu, K. Li, *Preparation and characterization of inorganic hollow fibre membranes*, *J. Membrane Sci.* 188 (2001) 87.
64. J. Luyten, A. Buekenhoudt, W. Adriansens, J. Coymans, H. Weyten, F. Servaes, R. Leysen, *Preparation of LaSrCoFeO<sub>3-x</sub> membranes*, *J. Membrane Sci.* 135 (2000) 637.
65. S. Liu, X. Tan, K. Li, R. Hughes, *Preparation and characterization of SrCe<sub>0.95</sub>Yb<sub>0.05</sub>O<sub>2.975</sub> hollow fiber membranes*, *J. Membrane Sci.* 193 (2001) 249.
66. Hsieh, H. P., *Inorganic Membrane for Separation and Reaction*. (1996) Amsterdam, the Netherlands: Elsevier Science B.V., p. 23-86.
67. JeonghwanKim, BartVanderBruggen, *The use of nanoparticles in polymeric and ceramic membrane structures: Review, of manufacturing procedures and*

- performance improvement for water treatment, Environmental Pollution 158 (2010) 2335-2349.*
68. *Tan, X.Y., Liu, S.M. and Li, K., Preparation and characterization of inorganic hollow fibre membranes, Journal of Membrane Science, 188 (1): 87-95 (2001).*
69. *Benjamin F.K. Kingsbury, Zhentao Wu, K. Li, A morphological study of ceramic hollow fibre membranes: A perspective on multifunctional catalytic membrane reactors, Catalysis Today 156 (2010) 306–315.*

## ***CHAPTER 2***

### ***Introduction to catalytic reactors***

#### ***2.1. Introduction***

There are distinct types of reactors intended to face extremely varied operating conditions, both in terms of the nature of the chemical species involved (reactants and products of the reaction) and of the physical conditions under which they operate. In general, a chemical reactor needs to be able to carry out at least three functions: provide the necessary residence time for the reactants to complete the chemical reaction; allow the heat exchange necessary; place the phases into intimate contact to facilitate the reaction. Reactors are designed based on features like mode of operation or types of phases present or the geometry of reactors. They are thus called:

- Batch or Continuous depending on the mode of operation.
- Homogeneous or Heterogeneous depending upon the phases present.

They may also be classified as:

- Stirred Tank Reactor,
- Tubular Reactor,
- Packed Bed Reactor,
- Fluidized Bed Reactor,

depending upon the flow pattern and manner in which the phases make contact with each other. A detailed comparison of various chemical reactors is reported in Table 2.1.

**Tab.2.1.** Comparison of chemical reactors.

Type of reactor	Principle of working	Advantages	Limitations	Area of application
<b>Batch reactor</b>	All reactants are added at the commencement and the product withdrawn at the completion of the reaction. They are conducted in tanks attached with impellers, gas, bubbles or pumps	<ol style="list-style-type: none"> <li>1. Suitable for small scale production</li> <li>2. suitable for processes where a range of different products or grades is to be produced in the same equipment</li> <li>3. Suitable for reaction requiring long reaction times</li> <li>4. Suitable for reaction with superior selectivity</li> </ol>	<p>× Not suitable for large batch size</p> <p>× It is a closed system in which once the reactants are added in the reactor, they will come out as product only after the completion of the reaction</p>	Batch processes are used in chemical (inks, dyes, polymers) and food industry
<b>Continuous Stirred Tank Reactor (CSTR)</b>	One or more fluid reagents are introduced into a tank reactor equipped with an impeller while the reactor effluent is recovered. A stepped up concentration gradient exists	<p>✓ Highly flexible device</p> <p>✓ By products may be removed in between the reaction</p> <p>✓ It is economically beneficial to operate several CSTRs in series or in parallel</p>	<p>× More complex and expensive than tubular units</p> <p>× All calculations performed with CSTRs assume perfect mixing</p> <p>× At steady state, the flow rate</p>	Chemical industry especially involving liquid/gas reactions

		<ul style="list-style-type: none"> <li>✓ Reaction can be carried out in horizontal as well as vertical reactors</li> </ul>	<ul style="list-style-type: none"> <li>in must equal the flow rate out, otherwise the tank will overflow or go empty</li> </ul>	
<b>Plug Flow Reactor (PFR)</b>	<p>One or more fluid reagents are pumped through a pipe or tube. These are characterized by continuous gradients of concentration in the direction of flow</p>	<ul style="list-style-type: none"> <li>✓ Higher efficiency than a continuous stirred tank reactor of the same volume</li> <li>✓ PFRs may have several pipes or tubes in parallel</li> <li>✓ Both horizontal and vertical operation are common</li> <li>✓ They can be jacketed</li> <li>✓ Reagents may be introduced at locations even other than inlet</li> </ul>	<ul style="list-style-type: none"> <li>× Not economical for small batches</li> </ul>	<p>The tubular reactor is specially suited to cases needing considerable heat transfer, where high pressures and very high or very low temperatures occur</p>

More details of batch and continuous reactors will be presented in the following paragraph.

## **2.2. Batch process**

Batch process is a process in which all the reactants are added together at the beginning of the process and products removed at the termination of the reaction is called a batch process. In this process, all the reagents are added at the commencement and no addition or withdrawal is made while the reaction is progressing (Figure 2.1).



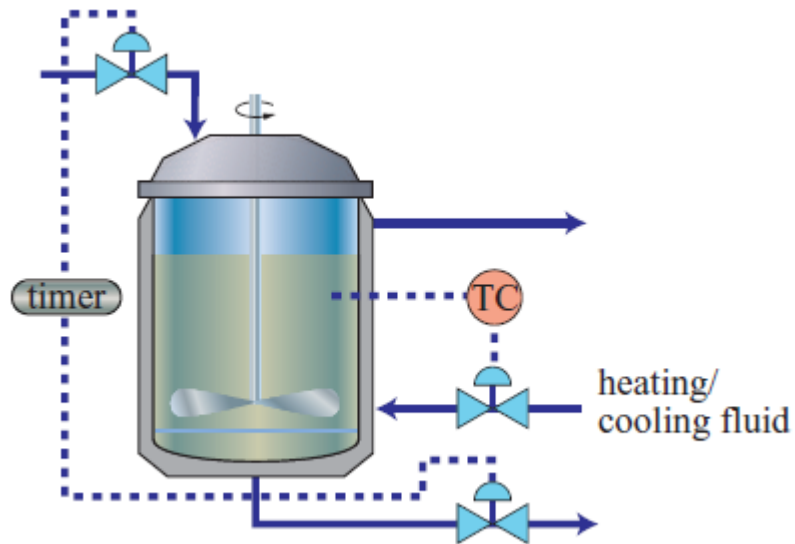


**Fig. 2.1.** Schematic representation of a batch process.

Batch processes are suitable for small production and for processes where a range of different products or grades is to be produced in the same equipment.

### 2.3. *Continuous process*

Continuous process is a process in which the reactants are fed to the reactor and the products or byproducts are withdrawn in between while the reaction is still progressing (Figure 2.2).

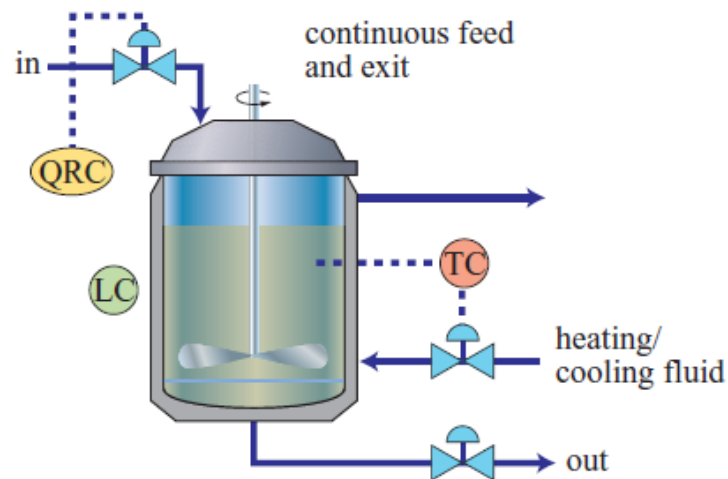


**Fig. 2.2.** Schematic representation of a continuous process.

Continuous production will normally give lower production costs as compared to batch production, but it faces the limitation of lacking the flexibility of batch production. Continuous reactors are usually preferred for large scale production.

#### ***2.4. Semi-batch process***

Process that do not fit in the definition of batch or a semi-batch reactor is operated with both continuous and batch inputs and outputs and are often referred to as semi continuous or semi-batch. In such semi-batch reactors, some of the reactants may be added or some of the products withdrawn as the reaction proceeds. A semi-continuous process can also be one which is interrupted periodically for some specific purpose, for example, for the regeneration of catalyst, or for removal of gas for example, a fermentor is loaded with a batch, which constantly produces carbon dioxide, which has to be removed continuously. Another example is chlorination of a liquid.

#### ***2.5. Types of reaction***

To classify a reactor, the number of phases in the reactor itself, whether or not there are agitation systems and the mode of operation (continuous reactor, semi-continuous or discontinuous) need to be taken into consideration.

##### ***2.5.1. Homogeneous reactions***

As far as phases are concerned, the most simple reactors are homogeneous reactors, where a single gaseous or liquid phase is usually stirred to avoid the presence of stagnant zones. The reaction can be operated in discontinuous mode, by loading the reactants mixture into the reactor and waiting until the process is completed, or in continuous mode, by making a stream containing the reactants flow into the reactor and extracting another stream containing the reaction products. Typical examples of homogeneous reactors are those for thermal cracking and for polymerization in solution.

##### ***2.5.2. Heterogeneous reactions***

In a heterogeneous reaction two or more phases exist and the overriding problems in the reactor design is to promote mass transfer between the phases.

The possible combination of phases are :

1) *Liquid-Liquid*: Liquid reactions of industrial importance are fairly numerous. Such reactions can be carried out in any kind of equipment that is suitable for physical extraction, including mixer-settlers and towers of various kinds, for example empty or packed, still or agitated, etc. Mechanically agitated tanks are favoured because the interfacial area can be made large as much as 100 times that of spray towers. When agitation is sufficient to produce a homogeneous dispersion and the rate varies with further increase of agitation, mass-transfer rates are likely to be significant.

2) *Liquid-Solid*: The solid may be a reactant or catalyst. For example, platinum acts as a catalyst in the hydrogenation of oils. In the design of reactors for liquids in the presence of granular catalysts, account must be taken of heat transfer, pressure drop and contacting of the phases and sometimes provision for periodic or continuous regeneration of deteriorated catalyst. Several different kinds of vessel configurations for continuous processing are in commercial use. Most solid catalytic processes employ fixed beds. Although fluidized beds have the merit of nearly uniform temperature and can be designed for continuous regeneration, they cost more and more, difficult to operate, require extensive provisions for dust recovery, and suffer from back mixing.

3) *Liquid-Solid Gas*: In reactions involving gas, liquid and solid phases, the solid phase is generally a porous catalyst. For example, gasoline cracking using zeolite catalysts. It may be in a fixed bed or it may be suspended in fluid mixture. In general, the reaction occurs either in the liquid phase or at the liquid / solid interface. In trickle bed reactors both phases usually flow down, the liquid as a film over the packing. In flooded reactors, the gas and liquid flow upward through a fixed bed, the slurry reactors keep the solids in suspension mechanically; the overflow may be a clear liquid or a slurry, and the gas disengages from the vessel. In fluidized bed reactors a stable bed of solids is maintained in the vessel and only the fluid phases flow through, except for entrained very fine particles.

4) *Solid-Solid*: Many reactions of solids are industrially feasible only at elevated temperatures which are often obtained by contact with combustion gases, particularly when the reaction is done on a large scale. A product of reaction also is often a gas that must diffuse away from a remaining solid, sometimes through a solid product. Thus thermal and mass-transfer resistances are major factors in the performance of solid reactions.

5) *Gas-Solid*: In some reactions, the solid either takes part in the reaction or act as a catalyst. Examples of solid /gas reactions include combustion of solid fuels, atmospheric corrosion, manufacture of hydrogen by action of steam on iron, chlorination of ores of uranium, titanium, zirconium and aluminum, conversion of ferrous oxide to magnetic ferric oxide in contact with reducing atmosphere of CO in combustion gases.

6) *Gas-Liquid*: in certain processes, liquid may either take part in the reaction or act as catalyst. Gas/liquid reaction processes are generally employed by the industry either for the purpose of gas purification or the removal of relatively small amounts of impurities such as CO<sub>2</sub>, CO, SO<sub>2</sub>, H<sub>2</sub>S, NO and others from air, natural gas, hydrogen for ammonia, synthesis, etc. This type of reaction is also utilized in the manufacture of pure products such as sulphuric acid, nitric acid, nitrates, phosphates, adipic acid, etc. or processes like hydrogenation, halogenation oxidation, nitration, alkylation, etc. Bio-chemical processes such as fermentation oxidation of studies sludges, production of proteins etc. are also examples of gas/liquid reactions.

## ***2.6. Reactor designing***

Chemical reactors are vessels designed to contain chemical reactions. The design of a chemical reactor deals with multiple aspects of chemical engineering including mathematical modeling. A model of a reaction process is a set of data and equation that is believed to represent the performance of a specific vessel configuration (mixed, plug flow, laminar, dispersed, etc.). The equations used in mathematical modeling include the stoichiometric relations, rate equations, heat and material balances and auxiliary relations such as those of mass transfer, pressure variation, residence time distribution, etc. Reactor design is today realized by means of appropriate mathematical models, based on mass, energy and momentum conservation equations, intended to simulate reactor behavior. The analytical formulations that make the description of the main reactor performances and features possible must thus take into consideration not only the kinetics features of the chemical reactions but also all the fluid dynamics aspects which influence the transport and distribution of the reactants inside the reactor itself. Reactor working conditions, when chemical and transport phenomena are both important, are called macrokinetics. Such a description is generally very complex; thus, the reactors are often analyzed first in ideal conditions where the fluid dynamic aspects are described in simple terms and where their behavior is only dependent on chemical reactions. An important principle to taking into

account in the reactor design is the mass balance. Mass is a conservative entity, hence given a control volume  $V$  the sum of mass flows entering the system will equal the sum exiting minus (plus) the consumed (generated) or accumulated fractions:

$$\left\{ \begin{array}{c} \text{rate of} \\ \text{mass} \\ \text{in} \end{array} \right\} - \left\{ \begin{array}{c} \text{rate of} \\ \text{mass} \\ \text{out} \end{array} \right\} + \left\{ \begin{array}{c} \text{rate of} \\ \text{mass} \\ \text{generated} \end{array} \right\} - \left\{ \begin{array}{c} \text{rate of} \\ \text{mass} \\ \text{consumed} \end{array} \right\} = \left\{ \begin{array}{c} \text{rate of} \\ \text{mass} \\ \text{accumulated} \end{array} \right\} \quad (2.1)$$

shortly:

$$\mathbf{IN - OUT + PROD - CONS = ACC}$$

(2.2)

Equation 2 represents the key point in mass transfer: analogously to the force balance in statics, the mass balance allows us to quantify and verify mass flows in our system. In the following paragraphs, this fundamental balance will be applied and described to some ideal systems.

A batch reactor, as its name states, is a non-continuous and perfectly mixed closed vessel where a reaction takes place. Figure 2.3 shows a schematic drawing of it.



**Fig. 2.3.** Schematic drawing of batch reactor.

Given its volume  $V$ , and the initial internal concentration  $C_0$ , the total mass will be  $M = V \cdot C_0$ . In the unit time, the concentration will be able to change only in virtue of a chemical reaction. The mass balance (2) quantifies this change:

$$\text{IN} - \text{OUT} + \text{PROD} - \text{CONS} = \text{ACC.}$$

In this case:

$$Q \cdot c_{in} - Q \cdot c_{out} \pm \int_V r dV = \frac{dm}{dt} \quad (2.3)$$

where  $r$  is the rate of generation (+) or depletion (-). Since the assumption of no flow in or out of the reactor volume ( $Q = 0$ ), and constant reactor volume  $V$ ,

$$\frac{dm}{dt} = \frac{d(c \cdot V)}{dt} = V \cdot \frac{dc}{dt} = V \cdot r \quad (2.4)$$

where  $c = c(t)$  is the concentration at any time inside the reactor  $V$ . Then,

$$\frac{dc}{dt} = r \quad (2.5)$$

The differential equation 2.5 is the characteristic equation of a batch reactor.

Equation 2.5 offers a relationship between reaction rate and time variant concentration. Thus, reaction rate can be calculated from the linear section of the curve  $C$  vs  $t$ . In the Figure 2.4 is represented the corresponding concentration profile of substrate and product in a batch reactor.

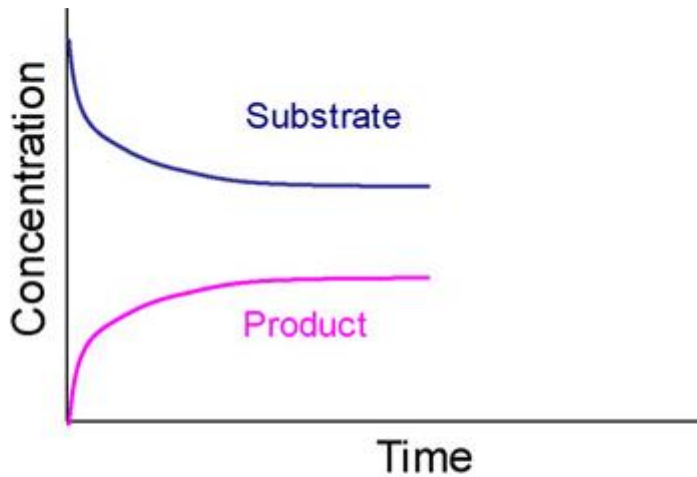


**Fig. 2.4.** Concentration profile of substrate and product in a batch reactor.

A Continuous-Stirred Tank Reactor (CSTR) is a well-mixed vessel that operates at steady-state ( $Q_{in} = Q_{out} = Q$ ). The main assumption in this case is that the concentration of the incoming fluid will become instantaneously equal to the outgoing upon entering the vessel. Figure 2.5 explains visually this concept.

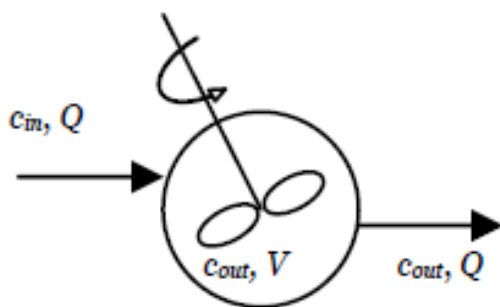


**Fig. 2.5.** Schematic drawing of continuous-stirred tank reactor.

A CSTR differs from a batch only in the fact that it is not closed. Thus, the mass flows in and out of the reactor in eq. 2.2 will not cancel:

$$\frac{dm}{dt} = Q \cdot (c_{in} - c_{out}) + \int_V r \cdot dV = 0 . \tag{2.6}$$

The mass balance in 2.6 equals to 0 thanks to the steady state hypothesis (=no accumulation). Solving,

$$C_{in} - C_{out} + \theta_H \cdot r = 0 \quad (2.7)$$

where  $\theta_H = V/Q =$  average hydraulic residence time.

Thus, reaction rate in a continuous stirred tank reactor can be derived from following equation:

$$r = \frac{Q (C_{in} - C_{out})}{V} \quad (2.8)$$

In all the continuous reactors, and thus also for the CSTR, the residence time (or contact time) is defined as the ratio between the reaction volume and the feed volumetric flow rate and it represents the average residence time of the reactants within the reactor. It is important to note that the volumetric flow rate for the leaving stream can be different from that of the feed if, as a result of the effect of the chemical reactions, a change in the number of moles, and consequently of the fluid molar density, occurs. Eq. 2.7 represents the characteristic equation for a CSTR. In the Figure 2.6 is illustrated the concentration profile of substrate and product in a continuous stirred tank reactor.

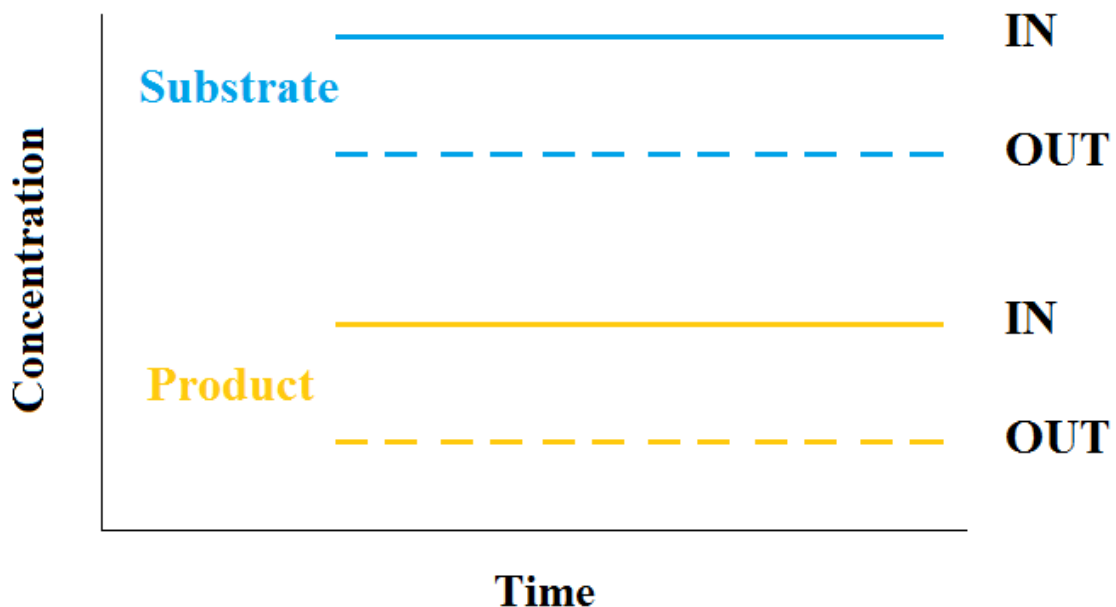


**Fig. 2.6.** Concentration profile of substrate and product in a continuous stirred tank reactor.



## ***2.7. Catalytic reactor with membranes as a catalytic and separation unit***

The basic concept of membrane reactors is based on the separation of enzyme and products (or substrates) by a semipermeable membrane that creates a selective barrier. Permeable solutes can be separated from the reaction mixture by the action of a driving force (chemical potential, pressure, electric field) that is present across the membrane. Membranes can also be used in a reactor exclusively as a matrix for immobilization of the enzyme, without any separation intentions [1-8]. In recent years, the functions of the membrane have been extended with the systematic use of these reactors in two-phase bioconversions. Here, the membrane acts as a support for the interface between two distinct liquid phases. The membrane not only separates the phases, but also provides interfacial contact area and, together with the enzyme, acts as an interfacial catalyst [9-12]. A complete retention of the enzyme within the system is among the most important requirements for a successful continuous operation of a membrane reactor. Upon this retention, the enzyme becomes confined to a defined region of the membrane reactor, where reaction with the substrate occurs. The enzyme is usually present in two forms: soluble or insolubilized at the surface, or inside the pores or membrane matrix. If the enzyme is in the free form, the immobilization is achieved by confining the enzyme to one side of the membrane. The products resulting from catalysis should permeate through the membrane pores, either by convection (usually induced by a pressure gradient) or diffusion (induced by concentration gradient). In Figure 2.7 is reported a schematic representation of two examples of biocatalytic membrane reactors with different transport mechanisms, in particular convective mass transfer in an ultrafiltration membrane (2.7 a) and diffusion mass transfer in a biphasic catalytic reactor (2.7 b).

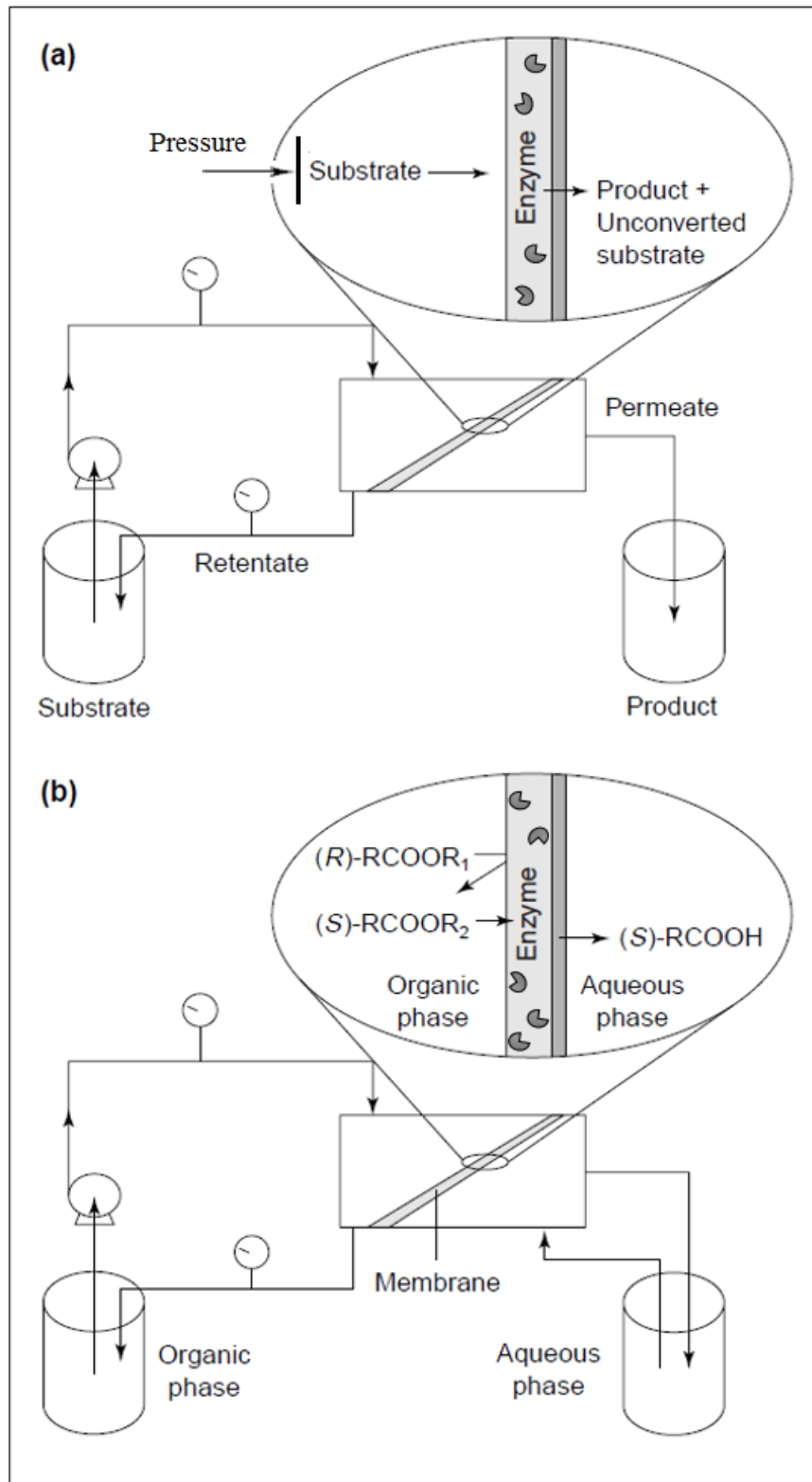


**Fig. 2.7.** Schematic representation of mechanisms mass transfer by convection (a) and diffusion (b).

In this way a continuous removal of products from the reaction media is attained. This permeation of products in membrane reactors has always been regarded as an essential requirement in this kind of reactor and is traditionally part of the membrane reactor concept. However, in the case of low-solubility precipitating products, complete rejection of solid products might turn out to be an unexpected advantage of these reactors. In such a case, the product of interest is recovered behind the membrane and remains in the reactor during the course of operation. Ultrafiltration (UF) membranes, due to the range of pore size distribution displayed (1-100 nm or NMWCO 500-100,000 Daltons), are most adequate for the retention of the majority of enzymes (10,000-100,000 Daltons), modified or native. These membranes are usually classified according to nominal molecular weight cutoff (NMWCO), which is defined as the molecular weight of a macrosolute capable of being rejected at 90% under well-defined filtration conditions [13]. The selection of a membrane to be used in enzymatic membrane reactors should take into account the size of the enzyme, substrate(s), and product(s) as well as the chemical nature of the species in solution and of the membrane itself. An important parameter to be used in this selection is the solute rejection coefficient, which should be zero for the products to facilitate permeation, and should be one for the enzyme to insure a complete retention of the catalyst inside the reaction system. The selectivity of a membrane toward a solute is normally associated with a discrimination according to size: molecules smaller than the micropores are not retained. Apart from this effect, a steric exclusion process may be present for those molecules with sizes inferior but close to the dimensions of the pores [14]. However, the chemical nature of the membrane can interfere with solute permeation due to nonspecific interactions (electrostatic, hydrophobic, and hydrophilic) which lead to the formation of a second layer (gel layer) that decreases the permeation (concentration polarization phenomena). This is especially true when chemical reaction and membrane separation occur simultaneously. The majority of commercially available UF membranes are asymmetric, i.e., the pore size varies continuously in one direction. The surface of these membranes is formed by an ultrathin layer that lies upon a sublayer of higher porosity. Due to their unique structure, these membranes are less susceptible to clogging, allow higher permeate flow rates, and are easier to clean [15,16]. The materials most often used in the manufacture of UF membranes are synthetic polymers and certain ceramic materials (Table 1) [17,19]. Ceramic membranes, compared with polymeric membranes are generally more resistant to high temperatures and chemicals, and mechanically stronger under pressure. Particular attention should be paid to the selection of the membrane material for a particular enzymatic process, since it can

significantly affect enzyme stability [20-23]. This choice is usually made by trial and error and is based on characteristics such as morphology, porosity, pore size distribution, molecular weight cutoff, chemical resistance, temperature, pH and pressure tolerance, and price [13,15]. UF membranes are usually assembled and associated in a module with a determined geometry offering distinct flow zones for the feed and permeate streams [24] (Table 1). The modules can be combined and integrated with pumps, valves, and tanks in numerous ways, thus forming a membrane reactor.

## ***2.8. Enzyme immobilization methods***

One of the most important roles of enzymes as natural biocatalysts is their capacity to enhance the rate of virtually all chemical reactions within a cell. Enzymes increase the rates of chemical reactions without themselves being permanently altered or consumed by the reactions. They also increase the reaction rates without changing the equilibrium between the reactants and the products [25]. The majority of enzymes are fairly unstable and industrial application is often hampered by a lack of long-term operational stability and the technically challenging recovery process and reuse of the enzyme [26,27]. In order to make enzyme utilization in biotechnological processes more favorable, different methods for cost reduction have been put into practice and, immobilization is one of them. The term ‘immobilized enzymes’ refers to ‘enzymes confined or localized in a certain defined region of space with retention of their catalytic activities, and which can be used repeatedly and continuously’ [28]. Immobilization provides an easy separation of the enzyme from the product [27,29,30] hence protein contamination of the product is minimized. Apart from easy separation of the enzyme from the reaction mixture, enzyme immobilization also remarkably reduces the cost of enzyme and the enzymatic products. Insolubilization of the enzyme by attachment to a matrix also imparts several added benefits such as (1) rapid arrest of the reaction by removal of the enzyme from the reaction solution and (2) improvement of enzyme stability against temperature, solvents, pH, contaminants and impurities [31,27,30-32]. It also helps for efficient recovery and reuse of expensive enzymes [27,32,33]. The immobilization methods exploit the fact that proteins have amino acids with different features, [27,34] whereby functional groups in side chains of these amino acids can be involved in binding to the support through various types of linkages and interactions. The enzymes can be attached by interactions ranging from reversible physical adsorption, ionic linkages and affinity binding, to the irreversible but stable covalent bonds. Basically, immobilization methods can be divided into two general classes namely, the chemical and

physical methods. Physical methods are characterized by weaker interactions such as hydrogen bonds, hydrophobic interactions, van der Waals forces, affinity binding, ionic binding of the enzyme with the support material, or mechanical confinement of enzyme within the support [34,35]. In the chemical method, formation of covalent bonds achieved through ether, thio-ether, amide or carbamate bonds [34] between the enzyme and support material are involved [36]. There are four principal techniques for immobilization of enzymes namely, adsorption, entrapment, covalent and cross-linking (Figure 2.8).

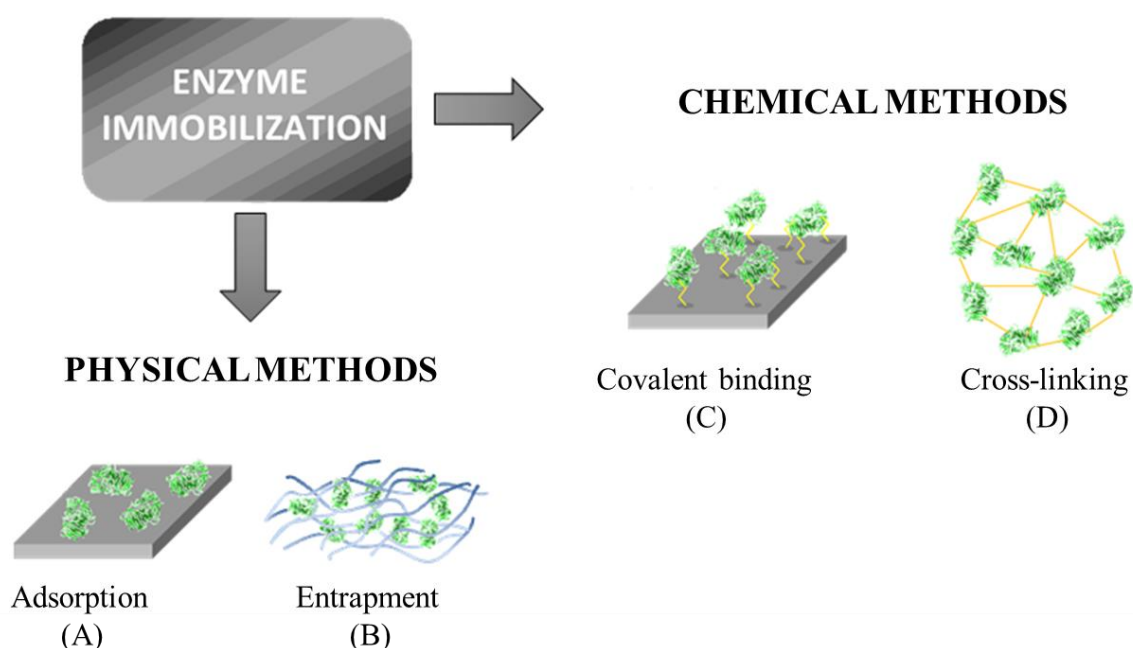


**Fig.2.8.** Schematics of the most common enzyme immobilization techniques: (A) physical adsorption, (B) entrapment, (C) covalent binding and cross-linking (D).

### 2.8.1. Physical adsorption

The physical adsorption method can be defined as one of the straightforward methods of reversible immobilization that involve the enzymes being physically adsorbed or attached onto the support material. Adsorption can occur through weak non-specific forces such as van der Waals, hydrophobic interactions and hydrogen bonds [37-40], whereas in ionic bonding the enzymes are bound through salt linkages. The reversibly immobilized enzymes can be removed from the support under gentle conditions, a method highly attractive as when

the enzymatic activity has decayed, the support can be regenerated and reloaded with fresh enzyme. The technique of physical adsorption is quite simple and may have a higher commercial potential due to its simplicity, low cost and retaining high enzyme activity [41] as well as a relatively chemical-free enzyme binding [42]. In most cases, the biocatalyst activity is not affected. However, this method has few disadvantages for instance, quite liable to changes under certain conditions such as pH, temperature and ionic strength of the buffer [31,40,44,45]. Physical bonding is generally too weak to keep the enzyme fixed to the carrier and is prone to leaching of the enzyme [46,47]. Enzyme leaching can be further enhanced when subjected to industrial conditions of high reactant and product concentrations and high ionic strength [27] thereby, potential contamination of the substrate.

### ***2.8.2 Entrapment***

Entrapment is defined as a method of enzyme immobilization where enzymes are entrapped in a support or inside of fibres that allows the substrate and products to pass through but retains the enzyme [33,35]. Entrapment is also described as physical restriction of enzyme within a confined space or network [48]. Typically, entrapment can improve mechanical stability and minimize enzyme leaching [49] and the enzyme does not chemically interact with the matrix support; therefore, denaturation is usually avoided. Disadvantages of this immobilization technique include possibility of enzyme leakage [27] which can occur when the pores of the support matrix are too large, deactivation during immobilization, low loading capacity and abrasion of support material during usage.

### ***2.8.3. Cross-linking***

Cross-linking is another method of enzyme immobilization that does not require a support to prevent enzyme loss into the substrate solution [50-53,30,59]. Technically, cross-linking is performed by formation of intermolecular cross-linkages between the enzyme molecules by means of bi- or multifunctional reagents. The most commonly used cross-linking reagent is glutaraldehyde as it is economical and easily obtainable in large quantities [27,56,57]. It has been used for decades for cross-linking proteins via reaction of the free amino groups of lysine residues, on the surface of neighboring enzyme molecules, with oligomers or polymers of glutaraldehyde resulting from inter- and intramolecular aldol condensations. Cross-linking can involve both Schiff's base formation and Michael-type 1,4 addition to  $\alpha$ ,  $\beta$ -unsaturated aldehyde moieties, and the exact mode of cross-linking is pH dependent [58,59].

#### **2.8.4. Covalent bonding**

Covalent bonding is one of the most widely used methods for irreversible enzyme immobilization. The functional group that takes part in the binding of the enzyme usually involves binding via the side chains of lysine ( $\epsilon$ -amino group), cysteine (thiol group) and aspartic and glutamic acids (carboxylic group [43,61], imidazole and phenolic groups which are not essential for the catalytic activity of enzyme) [60]. Activity of the covalent bonded enzyme depends on the size and shape of carrier material, nature of the coupling method, composition of the carrier material and specific conditions during coupling [60]. For the covalent attachment between enzyme and support, the direction of the enzyme binding is a crucial factor that determines its stability. It has been reported that the highest enzyme activity level is achieved when the active centre amino acids is not involved in the binding with the support. The coupling with the support can be done in two ways, depending on active groups present in the molecule that is to be immobilized. The reactive functional groups can be added to the support without modifications, or the support matrix is modified to generate activated groups. In both cases, it is anticipated that the electrophilic groups generated on the support will react with strong nucleophiles on the protein. Covalent bonds provide powerful link between the enzyme and its carrier matrix, allow its reuse more often than with other available immobilization methods [27,62] and prevent enzyme release into the reaction environment [43,37,38,60]. The method also increases half-life and thermal stability of enzymes when coupled with different supports like mesoporous silica, chitosan, etc. [63]. The conferred stability comes from unlimited covalent binding between the enzyme and support.

#### **2.9. Enzymes**

Enzymes are the most proficient catalysts, offering much more competitive processes compared to chemical catalysts. Applications of enzymes and whole cell biocatalysis for producing diverse types of chemical and biological substances have become a proven technology in chemical and pharmaceutical industries because enzyme-based processes usually lead to a reduction in the process time, number of reaction steps, and amount of waste [64].

Lipase from *Candida Rugosa* and  $\beta$ -glucosidase from Almond are the enzymes that have been used in this research for the development of biocatalytic membrane reactors. Additional background information about these two enzymes are provided below.

### 2.9.1. Lipase

Lipases (triacylglycerol acylhydrolases EC 3.1.1.3) are a class of hydrolase which catalyze the hydrolysis of triglycerides to glycerol and free fatty acids over an oil– water interface. In addition, lipases catalyze the hydrolysis and transesterification of other esters as well as the synthesis of esters and exhibit enantioselective properties. The ability of lipases to perform very specific chemical transformation (biotransformation) has made them increasingly popular in the food, detergent, cosmetic, organic synthesis, and pharmaceutical industries [65-68]. Lipases are produced by animals, plants, and microorganisms. Microbial lipases have gained special industrial attention due to their stability, selectivity, and broad substrate specificity [69,70]. Their broad synthetic potential is largely due to the fact that lipases, in contrast to most other enzymes, accept a wide range of substrates, are quite stable in non-aqueous organic solvents, and thus, depending on the solvent system used, can be applied to hydrolysis reactions or ester synthesis (Figure 2.9).

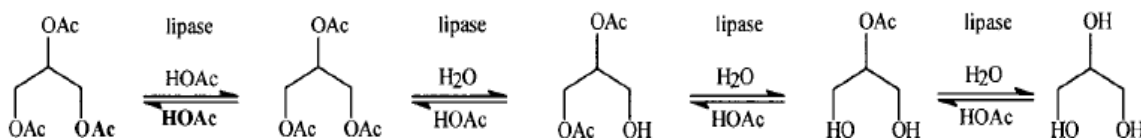


**Fig. 2.9.** Hydrolysis and ester synthesis with lipases.

In addition, lipases can accommodate a wide range of substrates other than triglycerides such as aliphatic, alicyclic, bicyclic, and aromatic esters and even esters based on organometallic sandwich compounds. With respect to racemic esters or substrates with several hydroxyl groups, lipases react with high enantio- and regioselectivity [71,72]. In 1958 Sarda and Desnuelle defined lipases in kinetic terms, based on the phenomenon of interfacial activation [73]. It amounts to the fact that the activity of lipases is low on monomeric substrates but strongly enhanced once an aggregated “supersubstrate” (such as an emulsion or a micellar solution for instance) is formed above its saturation limit. This property is quite different from that of the usual esterases acting on water-soluble carboxylic ester molecules, and for a long time lipases were considered as a special category of esterases which are highly efficient at hydrolyzing molecules aggregated in water. All of lipases are members of the “ $\alpha/\beta$ -hydrolase fold” family with a common architecture composed of a specific sequence of  $\alpha$ -helices and  $\beta$ -strands [74,75,76,77,80,81-86]. They hydrolyze ester bonds by means of



a “catalytic triad”, composed of a nucleophilic serine residue activated by a hydrogen bond in relay with histidine and aspartate or glutamate (Figure 2.10).

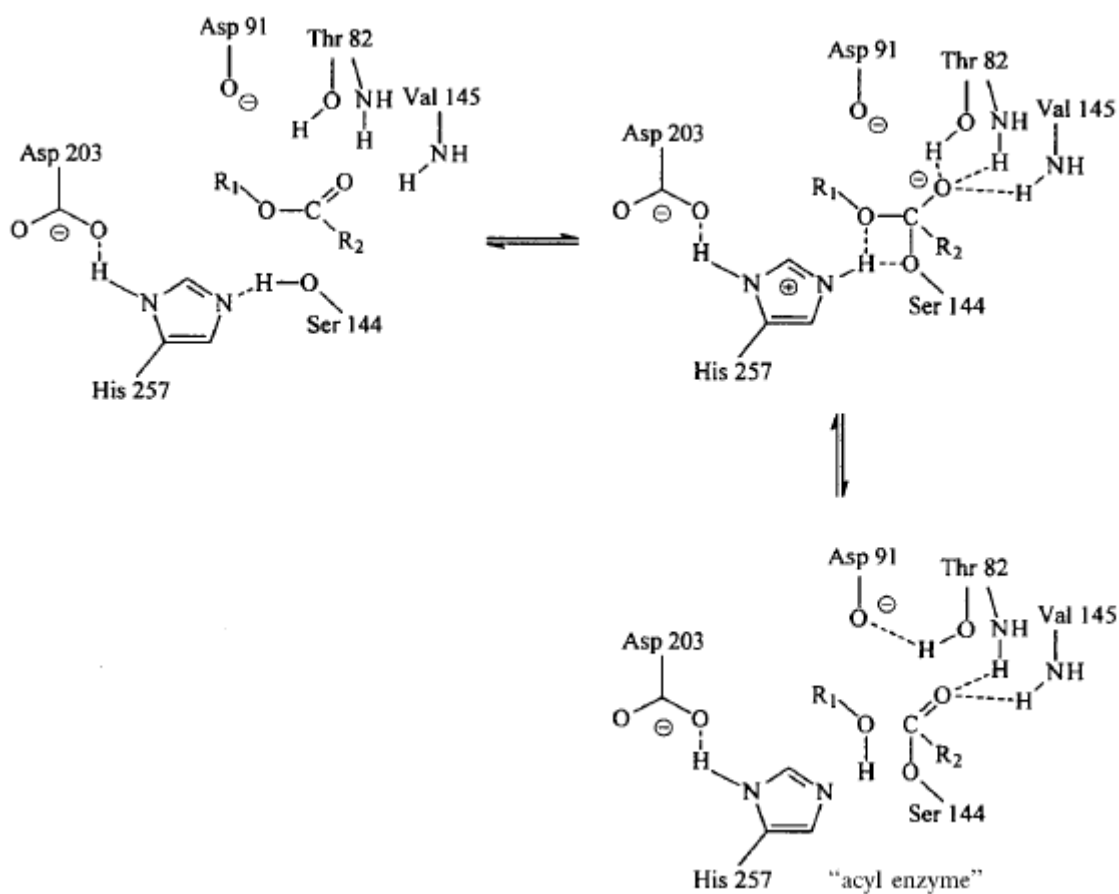


**Fig. 2.10.** Catalytic mechanism of lipases based on a “catalytic triad” of serine (nucleophile), histidine, and aspartate or glutamate (connected through a hydrogen bond).

A unique structural feature common to most lipases is a lid or flap composed of an amphiphilic  $\alpha$ -helix peptide sequence, which in its closed conformation (i.e., in the absence of an interphase or organic solvent) prevents access of the substrate to the catalytic triad. After the lid has opened, a large hydrophobic surface is created to which the hydrophobic supersubstrate (usually the oil drop) binds. Interfacial activation of lipase occurs when lid undergoes a conformational rearrangement due to the contact with a lipid/water interface, rendering the active site accessible to the substrate. In the Figure 2.11 the three-dimensional structures of lipase both in open and closed form is depicted.

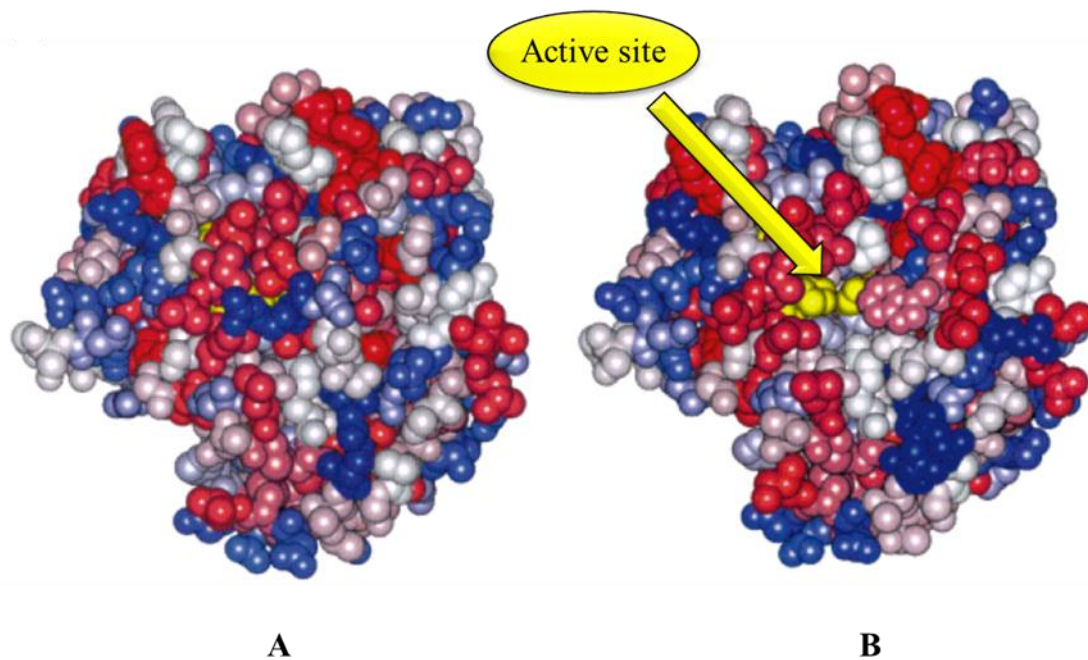


**Fig. 2.11.** Structure of lipase in closed (A) and open form (B).

The fact that lipases are activated by, and act at, interfaces probably makes them the perfect biocatalyst to use in membrane reactors, and particularly in multiphase membrane reactors, which promote interracial contact between enzymes and substrate. Since in the recent years lipase have gained enormous popularity thanks its properties and versatility for different applications, in this work a lab-scale multiphase biocatalytic membrane reactor was developed by immobilizing the enzyme into alumina hollow fibre membranes in order to improve important aspects of the reactor such as reusability of the enzyme for long time operations.

### 2.9.2. *$\beta$ -glucosidase*

$\beta$ -Glucosidases constitute a major group among glycosylhydrolase enzymes. The enzyme  $\beta$ -glucosidase is ubiquitous and occurs in all the living kingdoms starting from bacteria to highly evolved mammals and performs varied functions in these organisms. In bacteria and fungi,  $\beta$ -glucosidases are mainly a part of the cellulase enzyme system and are responsible for the hydrolysis of short chain oligosaccharides and cellobiose into glucose in a rate-limiting step. In insects and plants,  $\beta$ -glucosidase is involved in the release of cyanides from cyano-glucoside precursors. This is a part of a defense mechanism displayed in these systems [87]. Additionally, its functions in plants include the hydrolysis of phytohormone precursors, pigment metabolism, seed development, and biomass conversion. In humans, membrane-

bound lysosomal acid  $\beta$ -glucosidase is implicated in Gaucher's disease as the cells deficient in this enzyme are unable to hydrolyze glycosylceramides. The enzyme  $\beta$ -glucosidase catalyzes the hydrolysis of glycosidic linkages formed between the hemiacetal-OH group of a cyclic aldose or glucose and the -OH group of another compound viz., sugar, amino-alcohol, aryl-alcohol or primary, secondary, or tertiary alcohols. Little is known about the interaction of  $\beta$ -glucosidases with their substrates, especially with respect to the aglycon moiety, which forms the basis of tremendous diversity in terms of substrate range and is responsible for subtle differences in substrate specificity. Candidates for hydrolytic attack by  $\beta$ -glucosidases are flavanoids and isoflavanoid glucosides. These are phenolic and phytoestrogen glucosides that occur naturally in fruits, vegetables, tea, red wine, and soybeans. The aglycon moiety, released as a result of hydrolytic activity of  $\beta$ -glucosidases, has potent biological activity, with several uses in the field of medicine as antitumor agents, in general biomedical research, and in the food industry. In a recent application of the hydrolytic activity of  $\beta$ -glucosidase, the bioconversion of oleuropein, that causes bitterness in unripe olives, was performed in a bioreactor using immobilized  $\beta$ -glucosidase [88,89]. The aglycon moiety released due to cleavage is a pharmacologically active compound useful in the prevention of coronary heart disease and cancer. Oleuropein (1, Fig. 1) is a phenolic compound which accumulates in olive (*Olea europea*) fruits and leaves [90]. Chemical hydrolysis of oleuropein (1) produces the aglycon (2), glucose (3), hydroxytyrosol (4) and elenolic acid (5) as represented in Figure 2.12 .

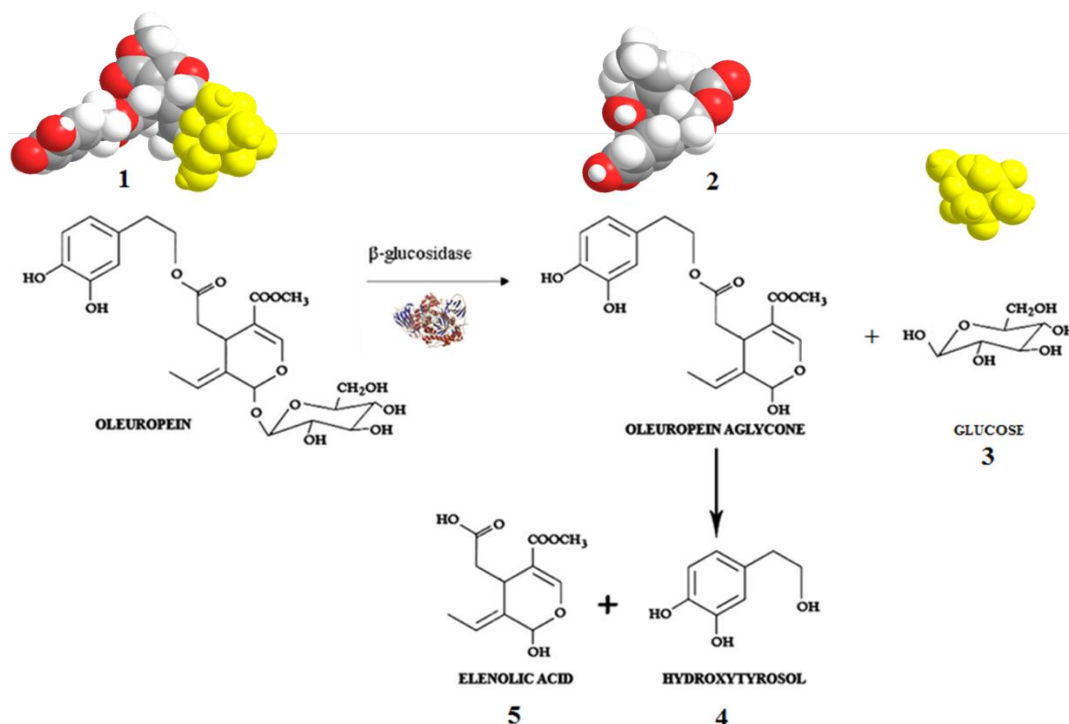


**Fig. 2.12.** Chemical hydrolysis of oleuropein.

On the contrary, enzymatic hydrolysis by  $\beta$ -glucosidase gives rise to glucose and aglycon [91]. In addition, the chemical hydrolysis of oleuropein, however, must be carried out under severe physico-chemical conditions as described in the literature [90,91] and is associated with low yields [91]. Side products other than glucose and aglycon are also present, thus reducing process selectivity. On the contrary, enzymatic hydrolysis of oleuropein occurs under mild conditions with complete conversion into glucose and aglycon, the most interesting compound for its strong antioxidant activity [92]. Possible technological and biotechnological developments of the hydrolysis reaction deserve specific consideration. Glucose is of obvious appeal, mainly in view of alimentary applications.

### **2.10. Enzyme kinetics**

The primary function of enzymes is to enhance rates of reactions. For many enzymes, the rate of catalysis  $V_0$ , which is defined as the number of moles of product formed per second, varies with the substrate concentration  $[S]$  in a manner shown in Figure 2.13.

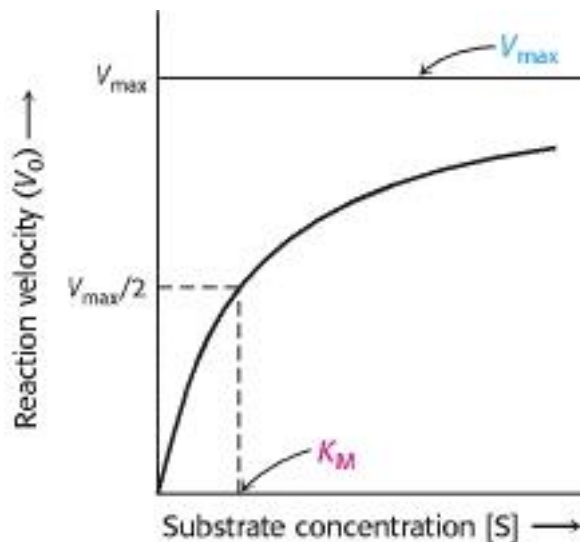
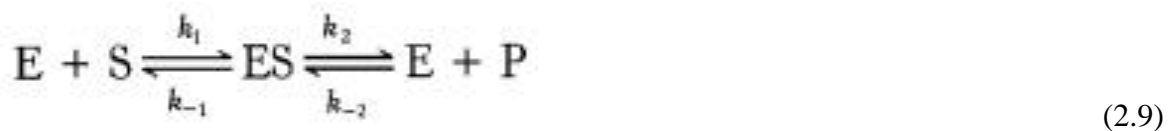


**Fig. 2.13.** A plot of the reaction velocity ( $V_0$ ) as a function of the substrate concentration  $[S]$  for an enzyme that obeys Michaelis-Menten kinetics shows that the maximal velocity ( $V_{\max}$ ) is approached asymptotically.

The Michaelis constant ( $K_M$ ) is the substrate concentration yielding a velocity of  $V_{\max}/2$ . The rate of catalysis rises linearly as substrate concentration increases and then begins to level off and approach a maximum at higher substrate concentrations. In order to accurately interpret this graph, it need to consider the following pathway which resumes an enzyme (E) that catalyzes the substrate (S) to product (P):



The extent of product formation is determined as a function of time for a series of substrate concentrations (Figure 2.14).

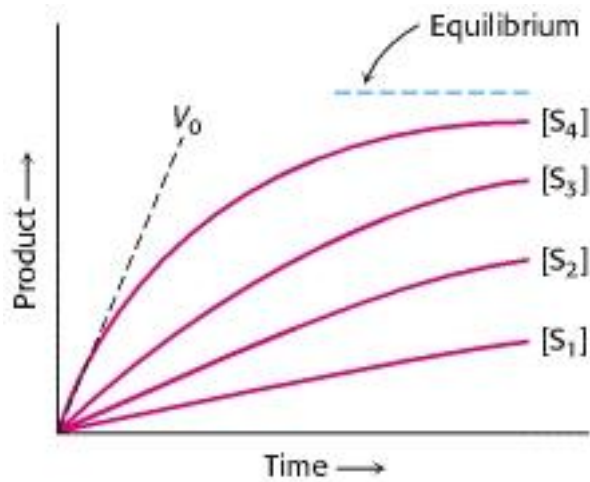


**Fig. 2.14** Determining initial velocity. The amount of product formed at different substrate concentrations is plotted as a function of time.

The initial velocity ( $V_0$ ) for each substrate concentration is determined from the slope of the curve at the beginning of a reaction, when the reverse reaction is insignificant. As expected, in each case, the amount of product formed increases with time, although eventually a time is reached when there is no net change in the concentration of S or P. The enzyme is still actively converting substrate into product and vice versa, but the reaction equilibrium has been attained. Figure 2.15(A) illustrates the changes in concentration observed in all of the reaction participants with time until equilibrium has been reached.

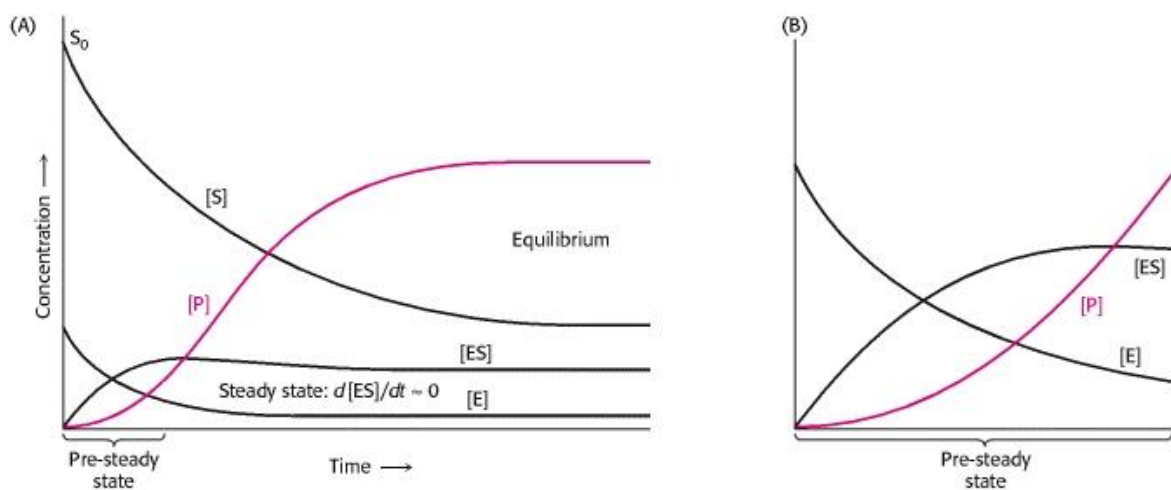


**Fig. 2.15.** Changes in the Concentration of Reaction Participants of an Enzyme-Catalyzed Reaction with Time. Concentration changes under (A) steady-state conditions, and (B) the pre-steady-state conditions.

Enzyme kinetics are more easily approached if it is ignore the back reaction. We define  $V_0$  as the rate of increase in product with time when  $[P]$  is low; that is, at times close to zero (hence,  $V_0$ ) (Figure 2.15 B). Thus, for the graph in Figure 2.13,  $V_0$  is determined for each substrate concentration by measuring the rate of product formation at early times before P accumulates (Figure 2.14). By considering the graph shown in Figure 2.13, at a fixed concentration of enzyme,  $V_0$  is almost linearly proportional to  $[S]$  when  $[S]$  is small but is nearly independent of  $[S]$  when  $[S]$  is large. In 1913, Leonor Michaelis and Maud Menten proposed a simple model to account for these kinetic characteristics. The critical feature in their treatment is that a specific ES complex is a necessary intermediate in catalysis. The model proposed, which is the simplest one that accounts for the kinetic properties of many enzymes, is



An enzyme E combines with substrate S to form an ES complex, with a rate constant  $k_1$ . The ES complex has two possible fates. It can dissociate to E and S, with a rate constant  $k_{-1}$ , or it can proceed to form product P, with a rate constant  $k_2$ . Again, it assumes that almost none of the product reverts to the initial substrate, a condition that holds in the initial stage of a reaction before the concentration of product is appreciable. In order to derive an expression that relates the rate of catalysis to the concentrations of substrate and enzyme and the rates of the individual steps, the starting point is that the catalytic rate is equal to the product of the concentration of the ES complex and  $k_2$ .

$$V_0 = k_2[ES] \quad (2.11)$$

The rates of formation and breakdown of ES are given by:

$$\text{Rate of formation of ES} = k_1[E][S] \quad (2.12)$$

$$\text{Rate of breakdown of ES} = (k_{-1} + k_2)[ES] \quad (2.13)$$

To simplify matters, it is considered the steady-state assumption. In a steady state, the concentrations of intermediates, in this case [ES], stay the same even if the concentrations of starting materials and products are changing. This occurs when the rates of formation and breakdown of the ES complex are equal. Setting the right-hand sides of equations 2.12 and 2.13 equal gives:

$$k_1[E][S] = (k_{-1} + k_2)[ES] \quad (2.14)$$

By rearranging equation 2.14:

$$[E][S]/[ES] = (k_{-1} + k_2)/k_1 \quad (2.15)$$

Equation 2.15 can be simplified by defining a new constant,  $K_M$ , called the Michaelis constant:

$$K_M = \frac{k_{-1} + k_2}{k_1} \quad (2.16)$$

Note that  $K_M$  has the units of concentration.  $K_M$  is an important characteristic of enzyme-substrate interactions and is independent of enzyme and substrate concentrations.

Inserting equation 2.16 into equation 14 and solving for [ES] yields

$$[ES] = \frac{[E][S]}{K_M} \quad (2.17)$$

The concentration of uncombined substrate [S] is very nearly equal to the total substrate concentration, provided that the concentration of enzyme is much lower than that of substrate. The concentration of uncombined enzyme [E] is equal to the total enzyme concentration  $[E]_T$  minus the concentration of the ES complex.

$$[E] = [E]_T - [ES] \quad (2.18)$$



Substituting this expression for [E] in equation 2.17 gives

$$[\text{ES}] = \frac{([\text{E}]_{\text{T}} - [\text{ES}])[\text{S}]}{K_{\text{M}}} \quad (2.19)$$

Solving equation 2.19 for [ES] gives

$$[\text{ES}] = \frac{[\text{E}]_{\text{T}}[\text{S}]/K_{\text{M}}}{1 + [\text{S}]/K_{\text{M}}} \quad (2.20)$$

or

$$[\text{ES}] = [\text{E}]_{\text{T}} \frac{[\text{S}]}{[\text{S}] + K_{\text{M}}} \quad (2.21)$$

By substituting this expression for [ES] into equation 2.11, we obtain

$$V_0 = k_2 [\text{E}]_{\text{T}} \frac{[\text{S}]}{[\text{S}] + K_{\text{M}}} \quad (2.22)$$

The maximal rate,  $V_{\text{max}}$ , is attained when the catalytic sites on the enzyme are saturated with substrate, that is when  $[\text{ES}] = [\text{E}]_{\text{T}}$ . Thus,

$$V_{\text{max}} = k_2 [\text{E}]_{\text{T}} \quad (2.23)$$

Substituting equation 2.23 into equation 2.22 yields the Michaelis-Menten equation:

$$V_0 = V_{\text{max}} \frac{[\text{S}]}{[\text{S}] + K_{\text{M}}} \quad (2.24)$$

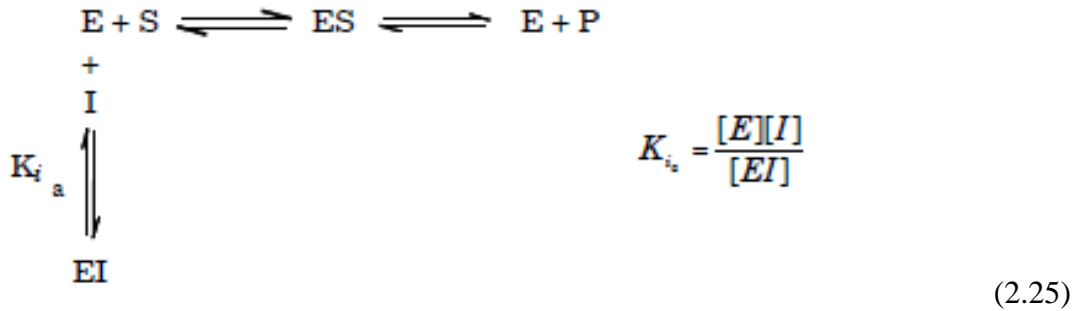
This equation accounts for the kinetic data given in Figure 2.13. At very low substrate concentration, when  $[S]$  is much less than  $K_M$ ,  $V_0 = (V_{\max}/K_M) [S]$ ; that is, the rate is directly proportional to the substrate concentration. At high substrate concentration, when  $[S]$  is much greater than  $K_M$ ,  $V_0 = V_{\max}$ ; that is, the rate is maximal, independent of substrate concentration. The meaning of  $K_M$  is evident from equation 23. When  $[S] = K_M$ , then  $V_0 = V_{\max}/2$ . Thus,  $K_M$  is equal to the substrate concentration at which the reaction rate is half its maximal value.  $K_M$  is an important characteristic of an enzyme-catalyzed reaction and is significant for its biological function.

### ***2.11. Inhibition kinetics***

Structure-based enzyme mechanism studies are extremely useful for understanding the mechanism used by an inhibitor. However, for many proteins, structural information is not available. In addition, even if structural information is available for the enzyme, information may not be available for the inhibitor/enzyme complex. Finally, enzyme-inhibitor binding affinity is very difficult to measure using the structural information alone. In many cases, therefore, full understanding of the inhibition of a given enzyme requires performing kinetic analyses of the system. Kinetic studies will yield information regarding the mechanism; however, kinetics cannot prove a given mechanism. Kinetic studies can only either refute the proposed mechanism, or provide supporting evidence for it.

#### ***2.11.1. Competitive inhibition***

In one common type of inhibition, the inhibitor acts as though it competes with the substrate for binding to the enzyme. This is called competitive inhibition: kinetically, the enzyme behaves as though the binding of the substrate and inhibitor are mutually exclusive. This adds an additional term to the reaction scheme that we have already discussed (shown below). Note that the  $K_i$  (the equilibrium dissociation constant for the inhibitor) is an equilibrium constant (i.e. a ratio of rate constants). The  $K_i$  can be expressed as a function of the inhibitor concentration, free enzyme concentration, and enzyme-inhibitor complex concentration as shown in the equation below:



This reaction scheme requires the addition of a new term to the possible states of the enzyme:

$$[E]_{\text{total}} = [E]_{\text{free}} + [ES] + [EI] \tag{2.26}$$

Taking the additional term in the reaction into account results in a modification to the Michaelis-Menten equation 2.24 :

$$v = \frac{V_{\text{max}}[S]}{K_m \left( 1 + \frac{[I]}{K_i} \right) + [S]}$$

(2.27)

This additional term also appears in the slope of the Lineweaver-Burk equation:

$$\frac{1}{v} = \left( 1 + \frac{[I]}{K_i} \right) \frac{K_m}{V_{\text{max}}} \frac{1}{[S]} + \frac{1}{V_{\text{max}}}$$

$$y = m x + b$$

(2.28)

The usual method of determining the  $K_i$  is to perform  $K_m$  determinations at several different inhibitor concentrations. In competitive inhibition, the apparent  $K_m$  increases as a result of the inhibitor. The effect of the inhibitor is to raise the concentration of substrate required for a given velocity. In contrast, the apparent  $V_{\text{max}}$  is unaffected by a competitive inhibitor. This is because once substrate binds, the reaction proceeds normally, and therefore  $V_{\text{max}}$  depends only on the maximum possible ES complex concentration (and on the  $k_{\text{cat}}$ , but  $k_{\text{cat}}$  is unaffected by a competitive inhibitor), and the maximum ES concentration depends only on the total amount of enzyme present. Each line in the Lineweaver-Burk plot (Figure 2.16) corresponds to a set of data obtained at a single inhibitor concentration. The fact that the

$V_{\max}$  does not change is immediately obvious, because the lines all intersect at the same point on the y-axis.

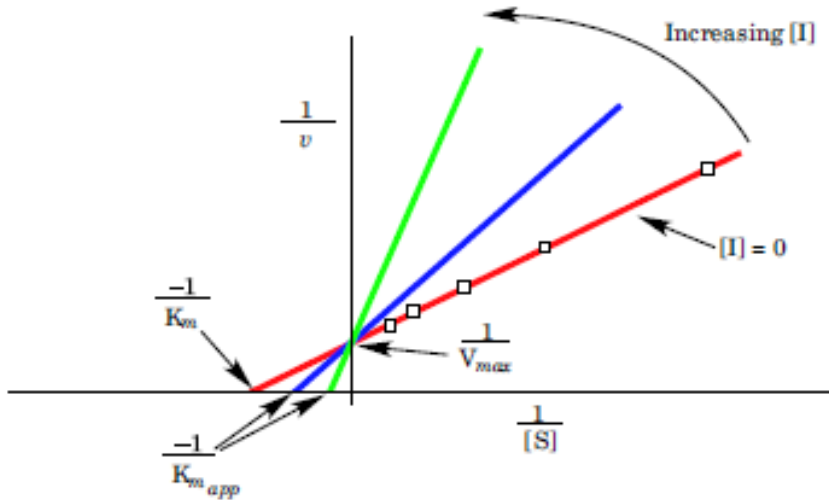
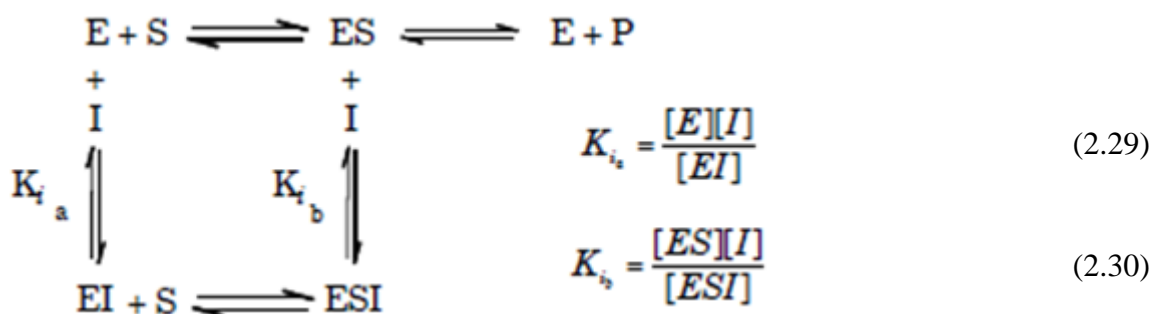


**Fig. 2.16.** Lineweaver-Burk plot of competitive inhibition.

Note that, in competitive inhibition the true values of the  $K_m$  and  $V_{\max}$  do not change. The enzyme either binds the inhibitor, and does nothing, or binds the substrate and behaves normally. The measured values of  $K_m$  in the presence of the inhibitor are altered, and are called the apparent  $K_m$ . The apparent  $K_m$  varies depending on the inhibitor concentration involved.

### 2.11.2. Mixed Inhibition

The other major type of inhibition occurs when the inhibitor is capable of binding to both the free enzyme and to the enzyme-substrate complex. This adds an additional term to the reaction scheme. Note that the dissociation constant for binding the free enzyme may differ from the dissociation constant for binding the ES complex.



$$K_{i_a} = \frac{[E][I]}{[EI]} \quad (2.29)$$

$$K_{i_b} = \frac{[ES][I]}{[ESI]} \quad (2.30)$$

The result of the inhibitor binding is a somewhat different alteration to the Michaelis-Menten equation.

$$v = \frac{V_{max}[S]}{K_m \left(1 + \frac{[I]}{K_{i_e}}\right) + [S] \left(1 + \frac{[I]}{K_{i_s}}\right)} \quad (2.31)$$

This results in an altered Lineweaver-Burk equation. The representation of plot is shown in Figure 2.17.

$$\frac{1}{v} = \left(1 + \frac{[I]}{K_{i_e}}\right) \frac{K_m}{V_{max}} \frac{1}{[S]} + \frac{\left(1 + \frac{[I]}{K_{i_s}}\right)}{V_{max}} \quad (2.32)$$

$$y = m x + b$$

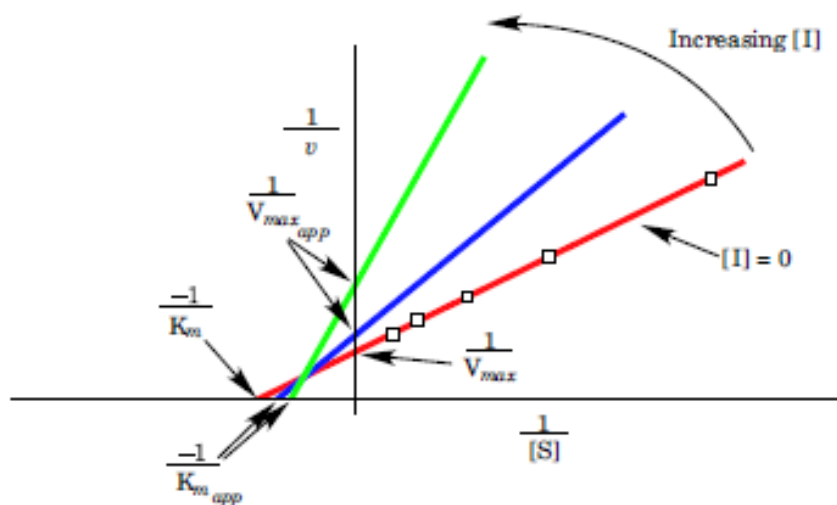


**Fig. 2.17.** Lineweaver-Burk plot of mixed inhibition.

In the case of mixed inhibition, the apparent  $V_{max}$  changes, because the inhibitor is capable of preventing catalysis regardless of whether the substrate is bound to the enzyme. With mixed inhibitors, the change in apparent  $K_m$  varies, depending on the relative values of  $K_{i_a}$  (the  $K_i$  for binding to the free enzyme) and  $K_{i_b}$  (the  $K_i$  for binding to the ES complex). Note that, depending on the relative values of the  $K_i$ , the apparent  $K_m$  may decrease. In the special case where the two  $K_i$  values are equal, the apparent  $K_m$  will be unchanged. This special case

is called non-competitive inhibition. In noncompetitive inhibition, all of the lines of a Lineweaver-Burk plot intersect at the same point on the x-axis.

### 2.11.3. Uncompetitive inhibition

One more special case for inhibitor kinetics is occasionally observed, primarily with multisubstrate enzymes. This final type of inhibition, which is really another special case for mixed inhibition, occurs when the inhibitor only binds to the ES complex. For this type of inhibition, the altered Michaelis-Menten and Lineweaver-Burk equations are:

$$v = \frac{V_{max}[S]}{K_m + [S] \left(1 + \frac{[I]}{K_i}\right)}$$

$$\frac{1}{v} = \frac{K_m}{V_{max}} \frac{1}{[S]} + \frac{\left(1 + \frac{[I]}{K_i}\right)}{V_{max}} \quad (2.33)$$

$$y = m x + b$$

Uncompetitive inhibition results in parallel lines on a Lineweaver-Burk plot (Figure 2.18):

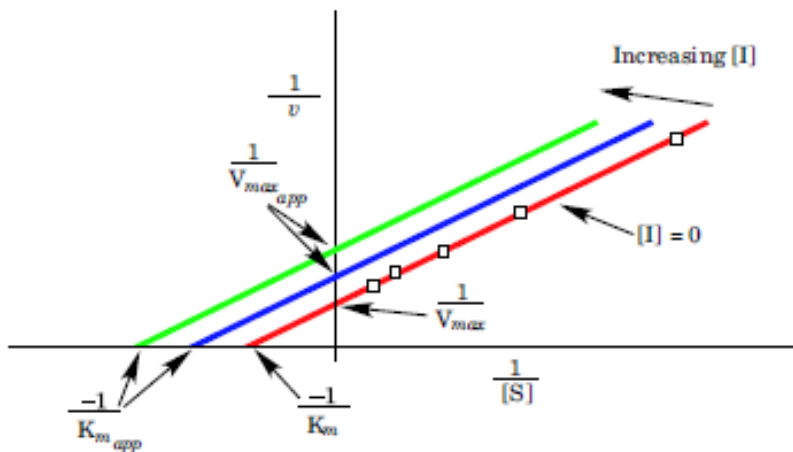


**Fig. 2.18.** Lineweaver-Burk plot of uncompetitive inhibition.

### 2.12. Summary of inhibition kinetic

The binding of molecules to enzymes may alter the activity of the enzyme. If this alteration is a decrease in activity, the compound is called an inhibitor. Inhibitors that bind only the

free enzyme are called competitive inhibitors. Competitive inhibitors increase the apparent  $K_m$  of the enzyme, but have no effect on the  $V_{max}$ . Inhibitors that bind to both the free enzyme and the ES complex are called mixed inhibitors. In the special case where the inhibitor has the same affinity for the free enzyme and the ES complex (non-competitive inhibition), the inhibitor has no effect on apparent  $K_m$ . Most mixed inhibitors, however, alter the apparent  $K_m$  (either increasing or decreasing the value). All mixed inhibitors decrease the apparent  $V_{max}$ . In the Table 2.2, the different types of inhibition are summarized.

**Table 2.2.** Summary of types of inhibition.

Type of Inhibition	$K_{m_{app}}$	$V_{max_{app}}$
None	$K_m$	$V_{max}$
<b>Competitive</b> (Inhibitor only binds to free enzyme)	$K_m \left( 1 + \frac{[I]}{K_{i_2}} \right)$	$V_{max}$
<b>Mixed</b> (Inhibitor binds E and ES)	$K_m \frac{\left( 1 + \frac{[I]}{K_{i_1}} \right)}{\left( 1 + \frac{[I]}{K_{i_2}} \right)}$	$\frac{V_{max}}{\left( 1 + \frac{[I]}{K_{i_2}} \right)}$
<b>Non-competitive</b> (Inhibitor binds E and ES with equal affinity)	$K_m$	$\frac{V_{max}}{\left( 1 + \frac{[I]}{K_{i_2}} \right)}$
<b>Uncompetitive</b> (Inhibitor only binds to ES complex)	$\frac{K_m}{\left( 1 + \frac{[I]}{K_{i_2}} \right)}$	$\frac{V_{max}}{\left( 1 + \frac{[I]}{K_{i_2}} \right)}$

## References

1. Furusaki, S. and Asai, N. Enzyme immobilization by the coulomb force. *Biotechnol. Bioeng.* 1983, 25, 220-2219.
2. E. Magnan, I. Catarino, D. Paolucci-Jeanjean, L. Preziosi-Belloy, M.P. Belleville, Immobilization of lipase on a ceramic membrane: activity and stability, *Journal of Membrane Science* Volume 241, Issue 1, 15 September 2004, Pages 161–166.
3. Furusaki, S., Nozawa, T. and Nomura, S. Membrane enzyme reactor with simultaneous separation using electrophoresis. *Bioproc. Eng.* 1990, 5, 73-78.
4. Brindle, K., Stephenson, T., 1996. The application of membrane biological reactors for the treatment of wastewaters. *Biotechnol. Bioeng.* 49, 601-610.
5. Bakken, A.P., Hill, C. G. and Amundson, C. H. Hydrolysis of lactose in skim milk by immobilized 13-galactosidase (*Bacillus circulans*), *Biotechnol. Bioeng.* 1992, 39, 408-417.
6. Prazeres, D.M.F., Cabral, J.M.S., 2001. Enzymatic membrane reactors. In: Cabral, J.M.S., Mota, M., Tramper, J. (Eds.), *Multiphase Bioreactor Design*. Taylor & Francis, London, pp. 135-180.
7. Garcia, H. Malcata, E X., Hill, C. G. and Amundson, C. H. Use of *Candida rugosa* Lipase immobilized in a spiral wound membrane reactor for the hydrolysis of milkfat. *Enzyme Microb. Technol.* 1992, 14, 535-545
8. C. López, I. Mielgo, M.T. Moreira, G. Feijoo, J.M. Lema, Enzymatic membrane reactors for biodegradation of recalcitrant compounds. Application to dye decolourisation, *Journal of Biotechnology* 99 (2002) 249-257.
9. Matson, S. L. and Quinn, J. A., *Membrane reactors in bioprocessing*. *Ann. NYAcad. Sci.* 1986, 469, 152-165.
10. Bouwer ST, Cuperus FP, Derksen JTP, The performance of enzyme-membrane reactors with immobilized lipase. *Enzyme Microb. Technol.* 1997, 21, 291–6.
11. Lopez, J. L., Wald, S. A., Matson, S. L. and Quinn, J. A. Multiphase membrane reactor for separating stereoisomers. *Ann. NYAcad. Sci.* 1990, 613, 155-166.
12. Wei Sing Long, Azlina Kamaruddin, Subhash Bhatia, Chiral resolution of racemic ibuprofen ester in an enzymatic membrane reactor, *Journal of Membrane Science* Volume 247, Issues 1–2, 1 February 2005, Pages 185–200.



13. Hildebrandt, J. R. *Membranes for bioprocessing: Design considerations*. In: *Chromatographic and Membrane Processes in Biotechnology* (Costa, C. A. and Cabral, J. S., eds.). Kluwer Academic Publishers, The Netherlands, 1991, pp. 363-378
14. Meireles, M., Aimar, E and Sanchez, V. *Les techniques à membranes: Micro et ultrafiltration*. *Le Technoscope de Biofutur* 1992, 111, cahier 52
15. Leuchtenberger, W., Karrenbauer, M. and Plöcker, U. *Scale-up of an enzyme membrane reactor process for the manufacture of L-enantiomeric compounds*. *Ann. NY Acad. Sci.* 1984, 434, 78-86
16. Nakajima, M., Shoji, T. and Nabetani, H. *Protease hydrolysis of water soluble fish proteins using a free enzyme membrane reactor*. *Proc. Biochem.* 1992, 27, 155-160
17. Prazeres, D. M. E, Garcia, E A. E and Cabral, J. M. S. *An ultrafiltration membrane reactor for the lipolysis of olive oil in reversed micellar media*. *Biotechnol. Bioeng.* 1993, 41, 761-770
18. Santos, J. A. L., Mateus, M. and Cabral, J. M. S. *Pressure driven membrane processes*. In: *Chromatographic and Membrane Processes in Biotechnology* (Costa, C. A. and Cabral, J. S., eds.). Kluwer Academic Publishers, The Netherlands, 1991, pp. 177-205
19. Datta, S., Christena, L.R. & Rajaram, Y.R.S. *3 Biotech* (2013) 3: 1.
20. Nakajima, M., Shoji, T. and Nabetani, H. *Protease hydrolysis of water soluble fish proteins using a free enzyme membrane reactor*. *Proc. Biochem.* 1992, 27, 155-160
21. Joey N. Talbert, Julie M. Goddard, *Enzymes on material surfaces, Colloids and Surfaces B: Biointerfaces*, Volume 93, 1 May 2012, Pages 8–19.
22. Alfani, E, Cantarella, L., Galifuoco, and Cantarella, M. *Membrane reactors for the investigation of product inhibition of enzyme activity*. *J. Membrane Sci.* 1990, 52, 339-350.
23. S. Rejikumar, S. Devi, *Hydrolysis of lactose and milk whey using a fixedbed reactor containing beta-galactosidase covalently bound onto chitosan and cross-linked poly(vinyl alcohol)*, *Int. J. Food Sci. Technol.* 36 (2001) 91–98.
24. Hildebrandt, J. R. *Scale-up and optimization of membrane processes*. In: *Chromatographic and Membrane Processes in Biotechnology* (Costa, C. A. and Cabral, J. S., eds.). Kluwer Academic Publishers, The Netherlands, 1991, pp. 415-428.
25. Cooper GM. *The chemistry of cells: the central role of enzymes as biological catalysts*. In: Cooper GM, editor. *The cell: a molecular approach*. 2nd ed. Sunderland (MA): Sinauer Associates; 2000. p. 145-146.

26. Krajewska B. *Chitin and its derivative as supports for immobilization of enzymes. Enzyme Microb Technol.* 2004;35:26-39.
27. Sheldon RA. *Cross-linked enzyme aggregates (CLEAs): stable and recyclable biocatalysts. Biochem Soc.* 2007;35 (6):1583-1587.
28. Tosa T, Mori T, Fuse N, Chibata I. *Studies on continuous enzyme reactions. I. Screening of carriers for preparation of water-insoluble aminoacylase. Enzymologia.* 1966;31: 214-224.
29. Asuri P, Karajanagi SS, Sellitto E, Kim DY, Kane RS, Dordick JS. *Water-soluble carbon nanotube-enzyme conjugates as functional biocatalytic formulations. Biotechnol Bioeng.* 2006;95(5):804-811.
30. Saifuddin N, Raziah AZ, Junizah AR. *Carbon nanotubes: a review on structure and their interaction with proteins. J Chem.* 2013; 2013:676815.
31. Guisan JM. *Immobilization of enzymes as the 21st century begins. In: Guisan JM, editor. Immobilization of enzymes and cells. 2nd ed. New Jersey (NJ): Humana Press Inc.; 2006. p. 1-13.*
32. Tian X, Anming W, Lifeng H, Haifeng L, Zhenming C, Qiuyan W, Xiaopu Y. *Recent advance in the support and technology used in enzyme immobilization. Afr J Biotechnol.* 2009;8(19):4724-4733.
33. Aehle W. *Enzymes in industry. 3rd ed. Weinheim: Wiley- VCH; 2007.*
34. Brena BM, Batista-Viera F. *Immobilization of enzymes. In: Guisan JM, editor. Immobilization of enzymes and cells. 2nd ed. New Jersey (NJ): Humana Press Inc.; 2006. p. 123-124.*
35. Costa SA, Azevedo HS, Reis RL. *Enzyme immobilization in biodegradable polymers for biomedical applications. In: Reis RL, Roman JS, editors. Biodegradable systems in tissue engineering and regenerative medicine. London: CRC Press LLC; 2005. p. 109-112.*
36. Chiou SH, Wu WT. *Immobilization of Candida rugose lipase on chitosan with activation of the hydroxyl groups. Biomaterials.* 2004;25:197-204.
37. Flickinger MC, Drew SW. *Fermentation, biocatalysis and bioseparation. In: Flickinger MC, editor. Encyclopedia of bioprocess technology. Vol. 1. 1st ed. New York (NY): Wiley; 1999.*
38. Samanta D, Sarkar A. (2011). *Immobilization of bio-macromolecules on self-assembled monolayers: methods and sensor applications. Chem Soc Rev, 40, 2567–92.*

39. Jegannathan KR, Abang S, Poncelet D, Chan ES, Ravindra P. *Production of biodiesel using immobilized lipase - a critical review. Crit Rev Biotechnol.* 2008;28:253-264.
40. Kumar N. *Studies of glucose oxidase immobilized carbon nanotube-polyaniline composites [MSc thesis]. Patiala (India): Thapar University; July 2009.*
41. Huang L, Cheng ZM. *Immobilization of lipase on chemically modified bimodal ceramic foams for olive oil hydrolysis. Chem Eng J.* 2008;144:103-109.
42. Chronopoulou L, Kamel G, Sparago C, Bordi F, Lupi S. *Structure-activity relationships of Candida rugosa lipase immobilised on polylactic acid nanoparticles. Soft Matter.* 2011;7:2653-2662.
43. Bucur B, Danet AF, Marty JL. *Versatile method of cholinesterase immobilisation via affinity bonds using concanavalin A applied to the construction of a screen-printed biosensor. Biosens Bioelectron.* 2004;20:217-225.
44. Pryakhin AN, Chukhrai ES, Poltorak OM. *Glucose 6- phosphate dehydrogenase immobilized by adsorption on silica gel solid supports. Vest Moskov Univ Ser 2 Khim.* 1977;18(1):125.
45. Deng H-T, Xu Z-K, Liu Z-M, et al. (2004). *Adsorption immobilization of Candida rugosa lipases on polypropylene hollow fiber microfiltration membranes modified by hydrophobic polypeptides. Enzyme Microb Technol,* 35, 437–43.
46. Kumakura M, Kaetsu I. *Immobilization of cellulase using porous polymer matrix. J Appl Polym Sci.* 2003;29 (9):2713-2718.
47. Won K, Kim S, Kim KJ, Park HW, Moon SJ. *Optimization of lipase entrapment in Calcium alginate gel beads. Process Biochem.* 2005;40:2149-2154.
48. Shen Q, Yang R, Hua X, Ye F, Zhang W, Zhao W. *Gelatin- templated biomimetic calcification for b-galactosidase immobilization. Process Biochem.* 2011;46:1565-1571.
49. Wang A, Wang H, Zhu S, Zhou C, Du Z, Shen S. *An efficient immobilizing technique of penicillin acylase with combining mesocellular silicafoams support and p-benzoquinone cross linker. Bioprocess Biosyst Eng.* 2008;31 (5):509-517.
50. Subramanian A, Kennel SJ, Oden PI, Jacobson KB, Woodward J, Doktycz MJ. *Comparison of techniques for enzyme immobilisation on silicon supports - effect of cross-linker chain length on enzyme activity. Enzyme Microb Technol.* 1999;24(1):26-34.
51. Berezhetsky AL, Sosovska OF, Durrieu C, Chovelon JM, Dzyadevych SV, Tran-Minh C. *Alkaline phosphatase conductometric biosensor for heavy-metal ions determination. ITBM-RBM* 2008;29:136–40.

52. Shi Y, Jin F, Wu Y, Yan F, Yu X, Quan Y. Improvement of immobilized cells through permeabilizing and crosslinking. *Chin J Biotechnol.* 1997;13(1):111-113.
53. Zhang Z, Xia S, Leonard D, Jaffrezic-Renault N, Zhang J, Bessueille F, et al. A novel nitrite biosensor based on conductometric electrode modified with cytochrome c reductase composite membrane. *Biosens Bioelectron* 2009;24:1574–9.
54. Honda T, Miyazaki M, Nakamura H, Maeda H. Immobilization of enzymes on microchannel surface through cross-linking polymerization. *AICHE Spring National Meeting*; 2006 Apr 23-27; Orlando, FL.
55. Gorecka E, Jastrzebska M. Immobilization techniques and biopolymer carriers. *Biotechnol Food Sci.* 2011;75:65-86.
56. Hanefield U, Gardossi L, Magner E. Understanding enzyme immobilisation. *Chem Soc Rev.* 2008;38:453-468.
57. Sheldon RA. Characteristic features and biotechnological applications of cross-linked enzyme aggregates (CLEAs). *Appl Microbiol Biotechnol.* 2011;92:467-477.
58. Migneault I, Dartiquenave C, Bertrand MJ, Waldron KC. Glutaraldehyde: behaviour in aqueous solution, reaction with proteins, and application to enzyme crosslinking. *Biotechniques.* 2004;37(5):790-802.
59. Obzturk B. Immobilization of lipase from *Candida rugosa* on hydrophobic and hydrophilic supports [MSc dissertation]. Izmir (Turkey): Izmir Institute of Technology; 2001. p. 40.
60. Singh BD. Biotechnology expanding horizons-*amylase immobilization on the silica nanoparticles for cleaning performance towards starch soils in laundry detergents.* *J Mol Catal B.* 2009;74:1-5.
61. Ovsejevi K, Manta C, Battista-Viera F. Reversible covalent immobilization of enzymes via disulphide bonds. *Methods Mol Biol.* 2013;1051:89-116.
62. Ispas C, Sokolov I, Andreescu S. Enzyme-functionalized mesoporous silica for bioanalytical applications. *Anal. Bioanal Chem.* 2009;393:543-554.
63. Bing Z, Rui Z, Yazhen W, Congcong L, Jingtao W, Jindun L. Chitosan-halloysite hybrid nanotubes: horseradish peroxidase immobilization and applications in phenol removal. *Chem Eng J.* 2013;214:304-309.
64. Wohlgemuth R. Biocatalysis—key to sustainable industrial chemistry. *Curr Opin Biotechnol* 2010;21:713–24.

65. Park, H., Lee, K., Chi, Y., & Jeong, S. (2005). Effects of methanol on the catalytic properties of porcine pancreatic lipase. *Journal of Microbiology and Biotechnology*, 15(2), 296–301.
66. Gupta, N., Shai, V., & Gupta, R. (2007). Alkaline lipase from a novel strain *Burkholderia multivorans*: Statistical medium optimization and production in a bioreactor. *Process Biochemistry*, 42(2), 518–526. doi:10.1016/j.procbio.2006.10.006.
67. Grbavcic, S. Z., Dimitrijevic-Brankovic, S. I., Bezbradica, D. I., Siler-Marinkovic, S. S., & Knezevic, Z. D. (2007). Effect of fermentation conditions on lipase production by *Candida utilis*. *Journal of the Serbian Chemical Society*, 72(8–9), 757–765. doi:10.2298/JSC0709757G
68. Franken, L.P.G., Marcon, N.S., Treichel, H., Oliveira, D., Freire, D.M. G., Dariva, C. et al. (2009). Effect of treatment with compressed propane on lipases hydrolytic activity. *Food and Bioprocess Technology*. doi:10.1007/s11947-008-0087-5.
69. Dutra, J. C. V., Terzi, S. C., Bevilaqua, J. V., Damaso, M. C. T., Couri, S., Langone, M. A. P., et al. (2008). Lipase production in solidstate fermentation monitoring biomass growth of *Aspergillus niger* using digital image processing. *Applied Biochemistry and Biotechnology*, 147, 63–75. doi:10.1007/s12010-007-8068-0.
70. Griebeler, N., Polloni, A.E., Remonato, D., Arbter, F., Vardanega, R., Cechet, J.L. et al. (2009). Isolation and screening of lipaseproducing fungi with hydrolytic activity. *Food and Bioprocess Technology*. doi:10.1007/s11947-008-0176-5.
71. C.-S. Chen, C. J. Sih, *Angew. Chem.* 1989, 101, 711 ± 724; *Angew. Chem. Int. Ed. Engl.* 1989, 28, 695 ± 708.
72. Pauliina Virsu, Arto Liljeblad, Anu Kanerva, Liisa T. Kanerva, Preparation of the enantiomers of 1-phenylethan-1,2-diol. Regio- and enantioselectivity of acylase I and *Candida antarctica* lipases A and B, *Tetrahedron: Asymmetry*, Volume 12, Issue 17, 28 September 2001, Pages 2447–2455.
73. L. Sarda, P. Desnuelle, *Biochim. Biophys. Acta* 1958, 30, 513 ± 521.
74. F. K. Winkler, A. Darcy, W. Hunziker, *Nature* 1990, 343, 771 ± 774.
75. James R. Mead · Scott A. Irvine · Dipak P. Ramji, Lipoprotein lipase: structure, function, regulation, and role in disease, *J Mol Med* (2002) 80:753–769.
76. L. Brady, A. M. Brzozowski, Z. S. Derewenda, E. Dodson, G. Dodson, S. Tolley, J. P. Turkenburg, L. Christiansen, B. Huge-Jensen, L. Norskov, L. Thim, U. Menge, *Nature* 1990, 343, 767 ± 770.

77. Jurgen Pleiss, Markus Fischer, Marcus Peiker, Claudia Thiele, Rolf D. Schmid, *Lipase engineering database Understanding and exploiting sequence–structure–function relationships*, *Journal of Molecular Catalysis B: Enzymatic* 10 2000. 491–508
78. M. E. M. Noble, A. Cleasby, L. N. Johnson, L. G. J. Frenken, M. R. Egmond, *FEBS Lett.* 1993, 331, 123 ± 128.
79. Howard Wong and Michael C. Schotz, *The lipase gene family*, *The Journal of Lipid Research*, July 2002, 43, 993-999.
80. J. Uppenberg, M. T. Patkar, S. Hansen, A. Jones, *Structure* 1994, 2, 293.
81. P. Grochulski, Y. Li, J. D. Schrag, F. Bouthillier, P. Smith, D. Harrison, B. Rubin, M. Cygler, *J. Biol. Chem.* 1993, 268, 12843 ± 12 847.
82. J. D. Schrag, M. Cygler, *J. Mol. Biol.* 1993, 230, 575.
83. U. Derewenda, L. Swenson, R. Green, Y. Wei, G. G. Dodson, S. Yamaguchi, M. J. Haas, Z. S. Derewenda, *Nat. Struct. Biol.* 1994, 1, 36 ± 47.
84. C. Martinez, P. de Geuss, M. Lauwereys, G. Matthyssens, C. Cambilleau, *Nature* 1992, 356, 615 ± 618.
85. J. D. Schrag, Y. Li, M. Cygler, D. Lang, T. Burgdorf, H. J. Hecht, R. D. Schmid, L. C. Strickland, S. B. Larson, J. Day, A. Mc Pherson, *Structure* 1997, 5, 187 ± 202.
86. D. L. Ollis, E. Cheah, M. Cygler, B. Dijkstra, F. Frolow, S. Franken, M. Harel, S. J. Remington, I. Silman, *Protein Eng.* 1992, 5, 197 ± 211.
87. Esen, A. 1993.  $\beta$ -glucosidases: overview, in  *$\beta$ -Glucosidases: Biochemistry and Molecular Biology*, Esen, A., Ed., American Chemical Society, Washington, DC, 1–14
88. Briante, R., Cara, F.L., Febbraio, F., Barone, R., Piccialli, G., Carolla, R., Mainolfi, P., Napoli, L.D., Patumi, M., Fontanazza, G., and Nucci, R. 2000. Hydrolysis of oleuropein by recombinant  $\beta$ -glycosidase from hyperthermophilic archeon *Sulfolobus solfataricus* immobilized on chitosan matrix. *J. Biotechnol.* 77: 275–286.
89. R. Mazzei, L. Giorno, E. Piacentini, S. Mazzuca, E. Drioli, *Kinetic study of a biocatalytic membrane reactor containing immobilized  $\beta$ -glucosidase for the hydrolysis of oleuropein*, *Journal of Membrane Science* 339 (2009) 215–223.
90. Panizzi, L. M., Scarpati, M. L., and Oriente, E. G., (1960), *Gazz. Chim. Ital.* 90, 1449 1485
91. Walter, W. M. Jr., Fleming, H. P., and Etchells, J. L. (1973), *Appl. Microbiol.* 26, 773-776.

92. M.H. Gordon, F. Paiva-Martins, F. Almeida, *Antioxidant activity of hydroxytyrosol acetate compared with that of other olive oil polyphenols*, *J. Agric. Food Chem.* 49 (2001) 2480–2485

## CHAPTER 3

### *Materials and methods*

#### *3.1. Materials and chemicals*

Reagents have been used as purchased without further purification. Aluminium oxide powders 1  $\mu\text{m}$  (alpha, 99.9% metal basis, surface area 6–8  $\text{m}^2/\text{g}$ ), 0.3  $\mu\text{m}$  (gamma–alpha, 99.9% metal basis, surface area 15  $\text{m}^2/\text{g}$ ), 0.05  $\mu\text{m}$  (gamma–alpha, 99.5% metal basis, surface area 32–40  $\text{m}^2/\text{g}$ ) and 0.01  $\mu\text{m}$  (gamma–alpha, 99.98% metal basis, surface area 100  $\text{m}^2/\text{g}$ ) were purchased from Alfa Aesar (a Johnson Matthey company, London, UK) and were used as supplied. Polyethersulfone (Radal A300, Ameco Performance, Houston, FL, USA), N-methyl-2-pyrrolidone (HPLC grade, Rathbone, London, UK) and Arlacel P135 (Polyethyleneglycol 30-dipolyhydroxystearate, Uniqema, Paterson, NJ, USA) were used as binder, solvent and additive, respectively. Tap water and de-ionized water were used as the external and internal coagulants, respectively. Hydrogen peroxide solution (30% wt from Sigma-Aldrich, Milan, Italy) and Sulfuric acid 96% (purchased from VWR, UK) were used for the preparation of piranha solution. Absolute Ethanol (purchased from VWR), (3-Aminopropyl) triethoxysilane 99% (APTES) and Glutaraldehyde solution (both purchased from Sigma-Aldrich) were used for the functionalization process of the alumina membrane. Ninhydrin and Glycine (purchased from Sigma-Aldrich) were used respectively as reagent and standard for the ninhydrin test and to build calibration line respectively, in the characterization of functionalized membranes. Sodium dihydrogen phosphate anhydrous ( $\text{NaH}_2\text{PO}_4$ ) and disodium hydrogen phosphate anhydrous ( $\text{Na}_2\text{HPO}_4$ ) (purchased from Sigma-Aldrich) were used to prepare phosphate buffer solution at pH 6.5.  $\beta$ -glucosidase from Almond (chromatographically purified lyophilized powder, 10-30 U/mg, Cod G4511, one unit will liberate 1.0  $\mu\text{mole}$  of glucose from salicin per min at pH 5.0 at 37  $^\circ\text{C}$ ) and glucose were obtained from Sigma–Aldrich. Oleuropein was purchased from Extrasynthese (France). Olive leaves extract was kindly provided by the “Olive Growing and Olive Product Industry Research Centre” (CRA-OLI). Alumina hollow fiber membranes were prepared at the Department of Chemical Engineering of Imperial College of London. ROMICON® 1” hollow fiber cartridge was purchased from Koch Membrane System. Centrifugal concentrators Vivaspin 2 (Sartorius Stedim) were used to separate the  $\beta$ -glucosidase from reaction mixture of the stirred tank reactor. Olive leaves extract used to feed the biocatalytic



membrane reactor was produced from olive leaves belonging to different cultivar and collected in the period July-October 2015. Olive leaves extract was pre-treated by ultrafiltration through 30 kDa hollow fiber membranes in order to remove suspended impurities. Ethyl acetate (purchased from Sigma-Aldrich) was used as organic solvent for the extraction of reaction product. Acetonitrile and o-phosphoric acid for HPLC mobile phase preparation were purchased from VWR and Sigma–Aldrich, respectively.

### 3.2. Analytical methods

“BCA assay kit” was used to evaluate protein concentration. The principle of the bicinchoninic acid (BCA) assay is a procedure which consists in the formation of a  $\text{Cu}^{2+}$  protein complex under alkaline conditions, followed by reduction of the  $\text{Cu}^{2+}$  to  $\text{Cu}^{1+}$ . The amount of reduction is proportional to the protein present. It has been shown that cysteine, cystine, tryptophan, tyrosine, and the peptide bond are able to reduce  $\text{Cu}^{2+}$  to  $\text{Cu}^{1+}$ . BCA forms a purple-blue complex with  $\text{Cu}^{1+}$  in alkaline environments, thus providing a basis to monitor the reduction of alkaline  $\text{Cu}^{2+}$  by proteins. A schematic representation of the process is reported in Figure 3.1

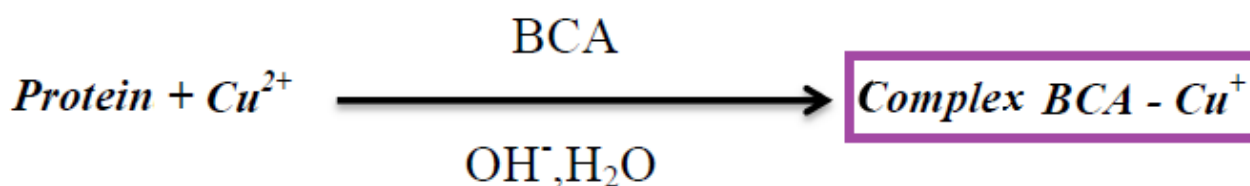


**Fig. 3.1.** Schematic representation of BCA assay

This water-soluble complex exhibits a strong absorbance at 562 nm that is nearly linear with increasing protein concentrations over a broad working range (20-2000 $\mu\text{g}/\text{mL}$ ). Protein concentrations is determined and reported with reference to standards of a common protein such as bovine serum albumin (BSA). A series of dilutions of known concentration are prepared from the protein and assayed alongside the unknown(s) before the concentration of each unknown is determined based on the standard curve. In the Figure 3.2 a calibration plot of BSA in a range of concentration from 0 to 1 mg/ml is reported .

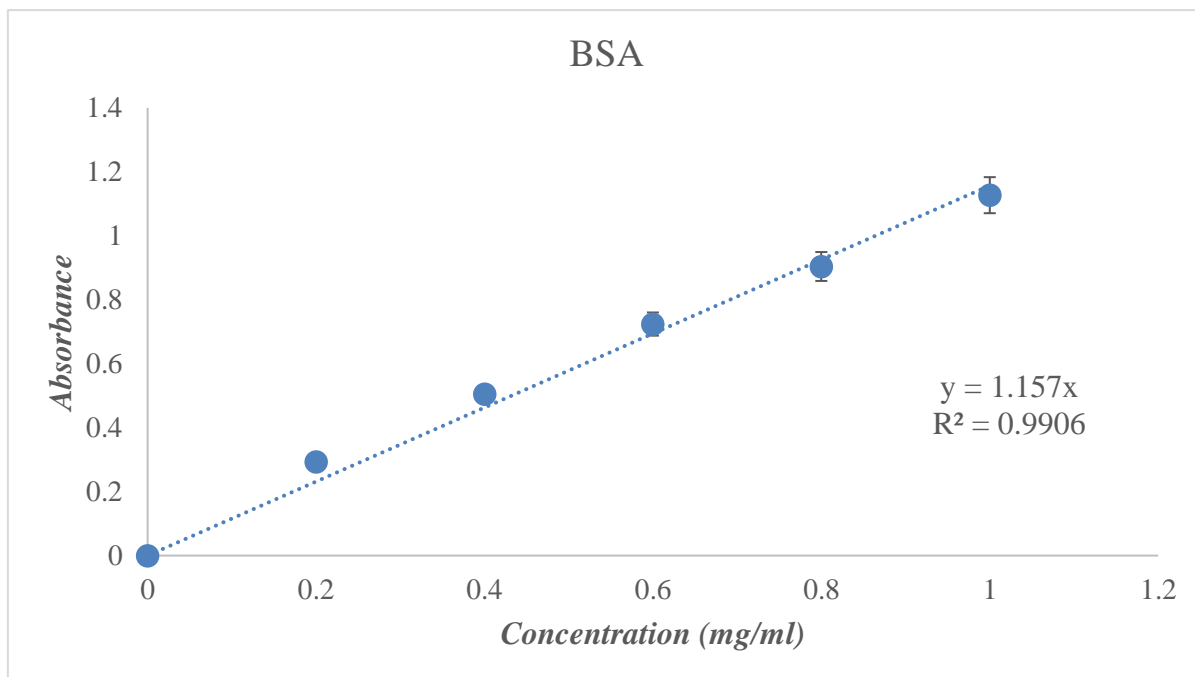


**Fig. 3.2.** Calibration plot of BSA.

It is possible to derive the unknown protein concentration of the sample by considering the relation between absorbance and concentration in Lambert-Beer's law:

$$A = \mathcal{E} \cdot C \cdot l \quad (3.1)$$

where  $A$  is the absorbance,  $\mathcal{E}$  is the extinction coefficient,  $C$  is the protein concentration and  $l$  is the length of the light path.

By knowing the value of  $\mathcal{E}$  (derived from the slope of the calibration plot), the protein concentration can be calculated by solving equation 3.1 as:

$$C = A / \mathcal{E} \cdot l \quad (3.2)$$

“Glucose (HK) assay kit” (Sigma-Aldrich) was used to evaluate glucose concentration. Figure 3.3 reports a schematic representation of glucose assay principle.

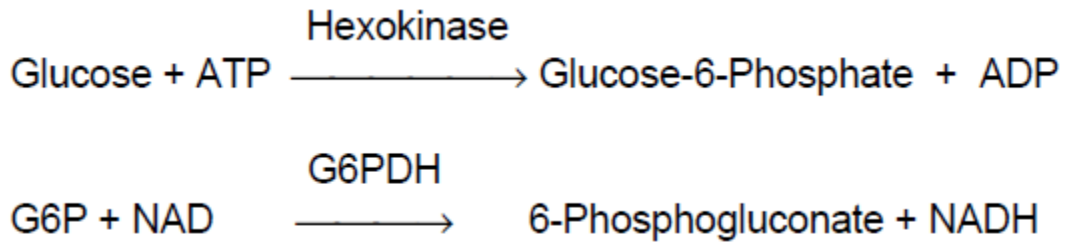


**Fig. 3.3.** Schematic representation of glucose assay principle.

Glucose is phosphorylated by adenosine triphosphate (ATP) in the reaction catalyzed by hexokinase. Glucose- 6-phosphate (G6P) is then oxidized to 6-phosphogluconate in the presence of oxidized nicotinamide adenine dinucleotide (NAD) in a reaction catalyzed by glucose-6-phosphate dehydrogenase (G6PDH). During this oxidation, an equimolar amount of NAD is reduced to NADH. The consequent increase in absorbance at 340 nm is directly proportional to glucose concentration.

Calculations:

The total blank must take into account the contribution to the absorbance of the sample and the glucose assay reagent. In the following table (Tab. 3.1) calculation for the determination of glucose concentration is reported.

**Tab. 3.1.** Calculation for the determination of glucose concentration.

$$A_{\text{Total Blank}} = A_{\text{Sample Blank}} + A_{\text{Reagent Blank}}$$

$$\text{mg glucose/ml} = \frac{(\Delta A) (TV) (\text{Glucose Molecular Weight}) (F)}{(\epsilon)(d)(SV)(\text{Conversion Factor for } \mu\text{g to mg})}$$

$$\text{mg glucose/ml} = \frac{(\Delta A) (TV) (180.2) (F)}{(6.22) (1) (SV) (1,000)}$$

$$\text{mg glucose/ml} = \frac{(\Delta A) (TV) (F) (0.029)}{(SV)}$$

$$\Delta A = A_{\text{Test}} - A_{\text{Total Blank}}$$

$$TV = \text{Total Assay Volume (ml)}$$

$$SV = \text{Sample Volume (ml)}$$

$$\text{Glucose MW} = 180.2 \text{ g/mole or equivalently } 180.2 \mu\text{g}/\mu\text{moles}$$

$$F = \text{Dilution Factor from Sample Preparation}$$

$$\epsilon = \text{Millimolar Extinction Coefficient for NADH at 340 nm } \text{Millimolar}^{-1} \text{ cm}^{-1} \text{ or equivalently (ml}/\mu\text{moles)(1/cm)}$$

$$d = \text{Light path (cm)} = 1 \text{ cm}$$

$$1,000 = \text{Conversion Factor for } \mu\text{g to mg}$$

Oleuropein concentration was measured by HPLC with an adapted method from the one described by Ranalli et al. [1]. A reverse silica Adsorbosphere XL C18 column, 250–4.6 mm, 5  $\mu\text{m}$  (Grace) was used. The mobile phase was a mixture of acetonitrile/water (21:79) acidified with o-phosphoric acid (up to pH 3). The flow rate and pressure were 1.2 ml/min and 145 ( $\pm 4$ ) bar, respectively. The volume of sample injection was 5  $\mu\text{l}$ . The oleuropein was detected at 280 nm wavelength. Figure 3.4 report an example of standard oleuropein chromatogram.

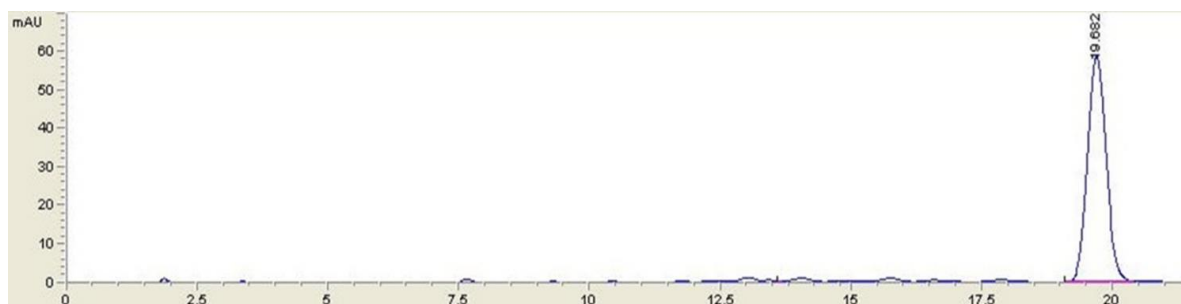


**Fig. 3.4.** Chromatogram of pure oleuropein used as standard.

### ***3.3. Equipments and operation mode***

#### ***3.3.1. Alumina hollow fiber membranes preparation***

Alumina hollow fiber membranes were prepared by a combined phase inversion and sintering technique [2]. Briefly, dispersant (Arlacel P135 1.3 wt %) was dissolved in NMP/water solutions and then aluminum oxide powders (58.7 wt %) at a ratio of 1:2:7 (0.01  $\mu\text{m}$ :0.05  $\mu\text{m}$ :1  $\mu\text{m}$ ) were added to the mixture. The dispersion was rolled/milled with 20 mm agate milling balls for 48 h. Milling was continued for a further 48 h after the addition of polyethersulfone (6.1 wt %). The suspension was then transferred to a gas tight reservoir and degassed under vacuum until no bubbles could be seen at the surface. Two stainless steel syringes (Harvard 200 mL) are placed on the top of the system where the spinning suspension and internal coagulant were loaded respectively. After degassing, the suspension was transferred to the stainless steel syringe and was extruded through a tube-in-orifice spinneret (ID 1.2 mm, OD 3.0 mm) connected to the syringes into a 120 L coagulation bath containing water (a non-solvent for the polymer) with an air-gap of 15 cm. The extrusion rate of the spinning suspension and the internal coagulant were accurately controlled and monitored by two individual Harvard PHD 22/2000 Hpsi syringe pumps, ensuring the uniformity of the prepared precursor fibers. A schematic representation of the plant used for the preparation of membrane precursors is reported in Figure 3.5.

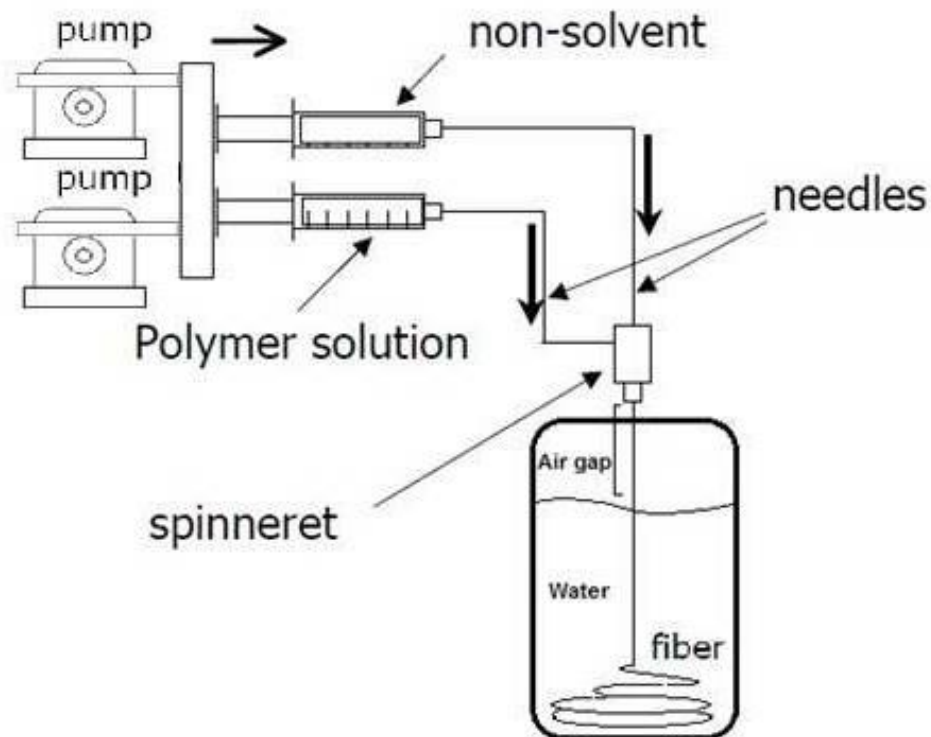


**Fig.3.5.** Schematic representation of the plant used for the preparation of membrane precursors.

Deionized water was used as the internal coagulant and 5, 10 and 20 mL/min were used as the extrusion flow rate. The extrusion rate of the spinning suspension was 7 mL/min. The fiber precursors were left in the external coagulation bath overnight to allow for completion of phase inversion. They were then immersed in an excess of tap water which was replaced periodically over a period of 48 h in order to remove traces of NMP. In the table 3.2 are resumed materials used during hollow fibre membrane precursors.

**Table 3.2** Materials used during hollow fibre membrane precursors.

Materials	
Powder	Al <sub>2</sub> O <sub>3</sub> - Aluminium Oxide 1 µm (alpha 99.9% metal basis, surface area 6-8 m <sup>2</sup> /g)
Binder	PESf - Polyethersulfone
Solvent	DMSO -Dimethyl Sulfoxide
Additive	Arlacel P135
External Coagulant	Tap Water
Internal Coagulant	De-ionized Water

Finally, the fiber precursors were calcined in air in a CARBOLITE furnace to yield ceramic hollow fiber membranes. The temperature was increased from room temperature to 600 °C at a rate of 2 °C/min and held for 2 h, then to the target temperature of 1350 °C at a rate of 5 °C/min and held for 4 h. The temperature was then reduced to room temperature at a rate of 3 °C/min. In the Figure 3.6 is reported a schematic representation of the steps during sintering process.

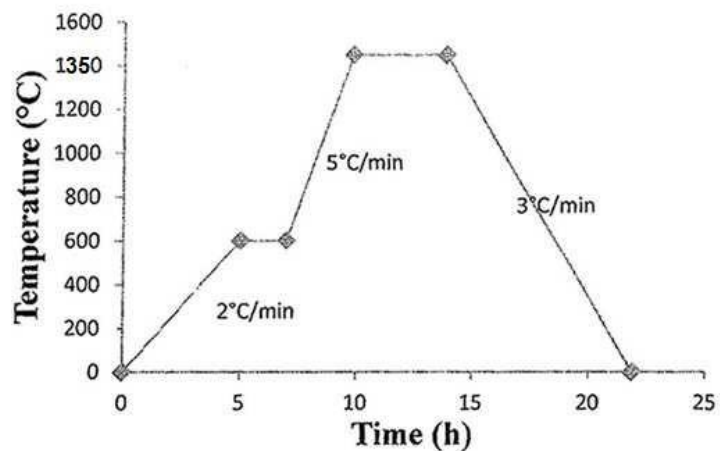


**Fig. 3.6.** Steps during sintering process.

In Table 3.3 are summarized the parameters used for membrane preparation.

**Table 3.3.** Operative conditions used for membranes preparation.

Sample n°	Internal coagulant flow rate	Polymer:powder ratio	Air gap	Spinning suspension flow rate	Sintering temperature
1	5 ml/min	1:10	150 mm	7 ml/min	1350 °C
2	10 ml/min				
3	20 ml/min				

The Figure 3.7 shows a schematic representation of the steps involved during hollow fibre membrane preparation process.

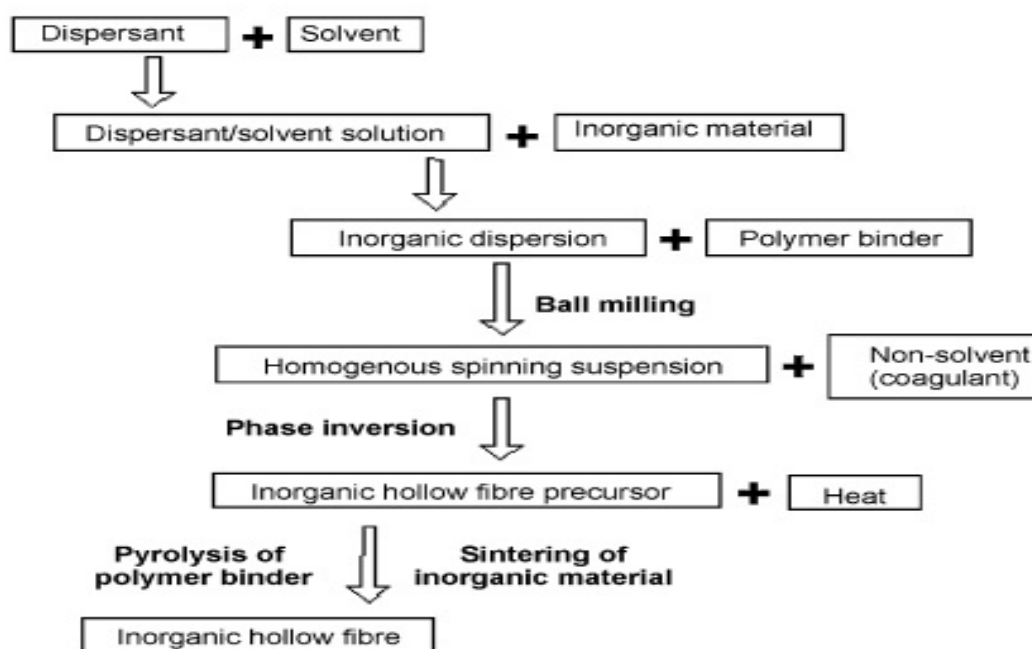


**Fig 3.7.** Schematic representation of the steps involved during hollow fibre membranes preparation process.

### 3.3.2. Stirred Tank Reactor setup

Activity measurements of both lipase and  $\beta$ -glucosidase in its native conformation were carried out in a stirred tank reactor. Operative conditions used to perform the reaction with



each enzyme, will be singularly described in detail in the following paragraphs. Equipment of a stirred tank reactor is depicted in the Figure 38.

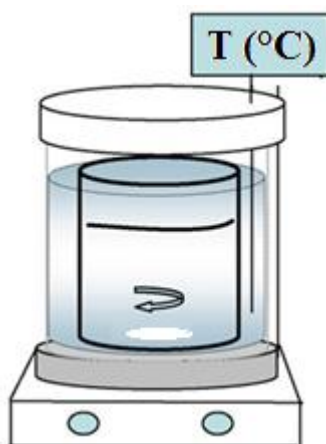


**Fig. 3.8** Equipment for stirred tank reactor.

### ***3.3.2.1 Stirred tank reactor with free lipase***

The reaction of triglycerides hydrolysis with free lipase took place in a tank of 50 mL of total reaction containing 21 mL of total reaction mixture which consisted of 19 mL of phosphate buffer 50 mM, 1 mL of olive oil and 1 mL of enzymatic solution 0.8 g/L (so that the final enzyme concentration in the aqueous phase was 0,04 g/L). The mixture was stirred at 300 rpm by a magnetic stirrer to disperse the two immiscible phases (olive oil and water) and create an oil-water reaction interface. The reaction tank was kept at 30 °C in a thermostatic bath. The reaction was monitored by measuring the extracted fatty acids into the aqueous phase produced during tryglycerides hydrolysis. The specific activity is expressed as U/mg enzyme. One unit (U) is defined as 1  $\mu$ mol of fatty acid produced per minute. A Mettler DL25 automatic titrator was used to determine the fatty acids extracted into the aqueous phase titrating with NaOH (20 mM) (being the moles of fatty acids equivalent to the moles of titrating phase). The specific activity was calculated as the slope in the straight line of the micromoles of reaction products versus time and then normalized by the mass of enzyme.

### ***3.3.2.2. Stirred tank reactor with free $\beta$ -glucosidase***

Oleuropein hydrolysis reaction was carried out in a tank of 50 mL containing 25 ml total volume of reaction mixture composed by 23.5 ml of substrate solution and 1.5 ml of  $\beta$ -glucosidase solution. Both enzymatic and oleuropein solutions were prepared by dissolving

their respective lyophilized powders in phosphate buffer pH 6.5. Concentration of  $\beta$ -glucosidase solution was 0.008 mg/ml. In some experiments, glucose was added in the initial reaction mixture in order to monitor its effect as enzyme inhibitor. Both oleuropein (substrate) and glucose (inhibitor) concentrations were varied from 0.63 mM to 2.50 mM and from 0 mM to 2.50 mM, respectively, in order to determine kinetic parameters of the free enzyme and the type of inhibition. Whereupon, free  $\beta$ -glucosidase activity measurements were evaluated also in presence of olive leaves extract. The experiments of inhibition were carried out by using pure oleuropein (substrate) solutions with a concentration of 0.63, 1.25, 2.5 mM in which glucose (inhibitor) concentration was varied from 0 to 2.5 mM, as reported in table 3.4.  $\beta$ -glucosidase concentration was kept constant during the studies (0.008 g/l).

**Tab. 3.4.** Solutions used during the experiments in a STR for the evaluation of kinetic parameters of  $\beta$ -glucosidase.

Oleuropein concentration (mM)	Glucose concentration (mM)
0.63	0
	1.25
	2.50
1.25	0
	1.25
	2.50
2.50	0
	1.25
	2.50

Samples of reaction mixture were taken each 30 seconds for a total time of 6 minutes in order to evaluate the initial reaction rate. The enzyme contained in each sample was denaturated by thermal shock by immersing the sample in boiling water for 30 seconds and then in ice. Whereupon, the deactivated enzyme was separated from reaction mixture through centrifugal concentrators Vivaspin 2. Performance of native  $\beta$ -glucosidase was evaluated by considering initial reaction rate and conversion degree.

### 3.3.3. Surface activation of alumina membranes and enzymatic covalent immobilization

The equipment used to perform the surface activation of the membranes and the enzymatic immobilization is depicted in Figure 3.9.

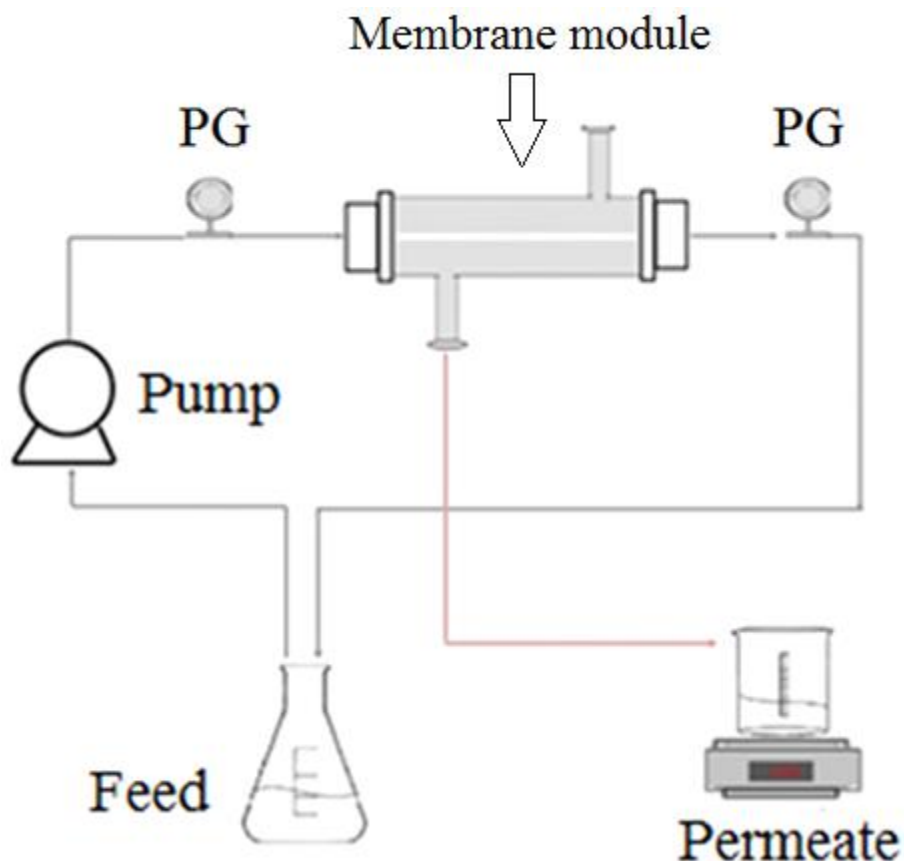


**Fig. 3.9.** Equipment for surface activation of alumina membranes and enzymatic covalent immobilization.

The plant includes hollow fiber membranes assembled in Pyrex module 100 mm long containing two alumina hollow fibre membranes with internal and external diameter of 0.9 mm and 1.8 mm, respectively. The membranes have asymmetric structure with a thin sponge-like layer on the shell side and a finger-like voids layer on the lumen side. The membrane surface area was  $10.9 (\pm 0.7) \text{ cm}^2$ , while the membrane void volume, which represents the membrane reactor volume, was  $0.18 (\pm 0.03) \text{ cm}^3$ . It was calculated as the volume of evaporated water from calibrated pieces of wet membrane by thermal balance. Briefly, calibrated pieces of dry alumina fibre were soaked in water and the weighed by a

thermal balance after the water excess was gently removed. The fibre piece was left in the thermal balance at 100 °C in order to permit the water evaporation. Water evaporation was monitored by the decreasing of mass registered by the balance until no mass variation was detected. The operation was repeated several times. Membrane void volume was calculated as the average of the evaporated water volumes (obtained from density) which was detected in a total of 10 cycle operations. In addition to the module, the system is constituted by a peristaltic pump (P) to feed the reagent solutions (either the solution for surface activation or the one for enzyme covalent attachment) to the lumen side of the membranes, pressure gauges (PG) to measure inlet and outlet pressure and a beaker to collect retentate and permeate solution (Figure 3.9). Prior that alumina hollow fibre membranes were assembled into the glass module, some of them were immersed in freshly prepared piranha solution (30% H<sub>2</sub>O<sub>2</sub> and 96% H<sub>2</sub>SO<sub>4</sub> 1:3 v/v) for 15 min in order to increase density of hydroxyle groups on the membrane surface, as reported by Nesrine Aissaoui et al. [3]. Membranes used for the hydroxylation process, were then thoroughly washed in ultrapure (UP) water and dried under nitrogen gas flow. Whereupon, both hydroxylated alumina fibers (Hydr-Al) and non-hydroxylated ones (Al) were assembled in a glass module, as reported in Figure 3.9. In order to activate the surface with silanol groups, Hydr-Al and Al membranes were reacted with a fresh ethanol solution of APTES (5% APTES, 5% water and 90% pure ethanol) for 2 h at room temperature [4] with an axial velocity of 0.033 m/s and a transmembrane pressure (TMP) of 0.05 bar. Fibers were then rinsed several times with deionized water. Silanized fibers were then treated with two Glutaraldehyde solution (5% and 10% v/v) for 2 h at room temperature with an axial velocity of 0.033 m/s and a transmembrane pressure of 0.05 bar. Fibers were then rinsed several times with deionized water in the same conditions of axial velocity and pressure. Covalent binding occurs through formation of a Schiff base between aldehydic terminal group of glutaraldehyde and amino group of silane. Non-hydroxylated alumina fibers functionalized with APTES and 5% or 10% GA will be referred in the text as Al APTES-GA5% and Al-APTES-GA10%, respectively. Al-Hydr-APTES-GA5% and Al-Hydr-APTES-GA10% will be used respectively to refer the hydroxylated fibers functionalized with APTES and 5% or 10% GA. The chemical functionalized membranes were then used for enzyme immobilization. Phosphate buffer pH 7 was used to prepare the enzymatic solution. The initial lipase concentration was 0.8 g/L as estimated by BCA protein assay. In the case of  $\beta$ -glucosidase, covalent immobilization process was optimized by investigating the effect of the initial concentration of enzymatic solution on the immobilized enzyme amount. Different concentrations of  $\beta$ -glucosidase solutions were used (0.05, 0.1,

0.2 and 0.4 mg/ml) taking into account only Al-APTES-GA10% functionalized membranes for the investigation. The choice to use only Al-APTES-GA10% for the study of the  $\beta$ -glucosidase immobilization was made after the valuation of the results obtained from the study with lipase and will be discussed later in chapter 5. The optimal enzyme concentration was determined on the basis of the reaction rate and conversion degree shown by the different amounts of immobilized enzyme. The immobilization was carried out by feeding enzymatic solution into the membrane, at room temperature, along the lumen circuit with an axial velocity of 0.033 m/s and a transmembrane pressure of 0.05 bar for 16 h. The enzyme solution was forced to pass through the membrane porous wall. Membranes were then rinsed with phosphate buffer pH 6.5 until any trace of the enzyme was detected by monitoring the absorbance (280 nm) of the collected solution. In order to confirm that enzymatic immobilization is only due to the covalent immobilization, blank experiments were carried out to be sure that any interaction between enzyme and native membrane materials was occurring. This process was carried out by ultrafiltering enzyme solution through native membrane, applying a pressure of 0.2 bar. Each step of the immobilization process is illustrated in Figure 3.10.

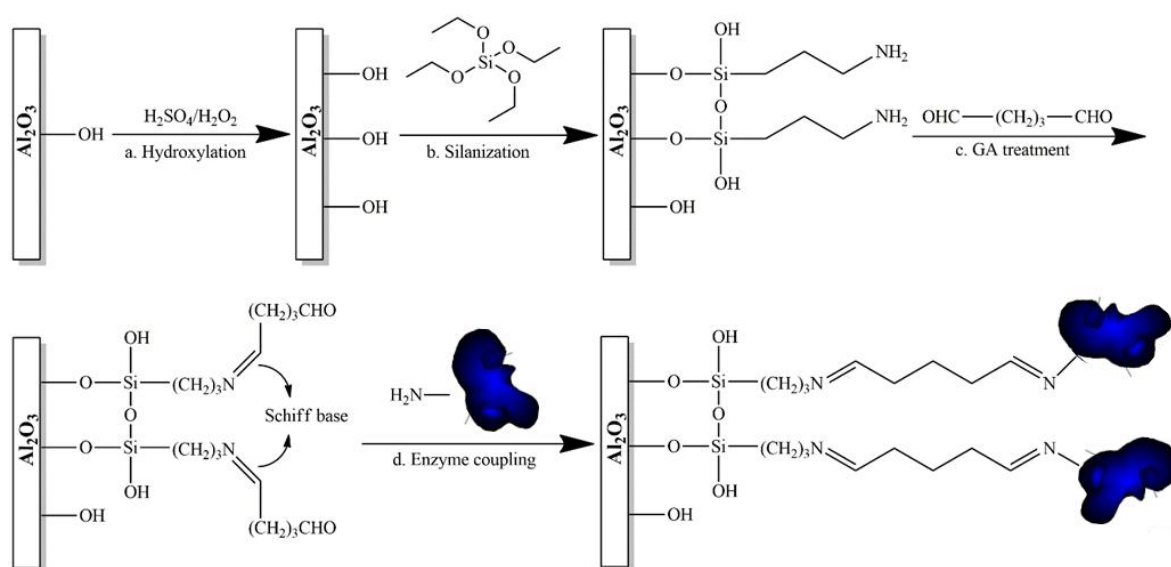


**Fig.3.10.** Stages involved during immobilization process: (a) Hydroxylation process by immersing inorganic hollow fiber membranes in a piranha solution; (b) Silanization process by treating membranes with APTES solution; (c) Cross-linker binding between glutaraldehyde and amino-group of silane by forming Schiff base; (d) Enzyme covalent binding on the inorganic hollow fiber membranes.

In order to evaluate the quantity of immobilized enzyme on the membrane, the protein concentration in the initial, final, and washing solutions was measured by BCA test. The amount of immobilized protein was determined by mass balance according to the following equation:

$$C_i V_i = C_f V_f + C_{ws} V_{ws} + m \quad (3.3)$$

where  $m$  indicates the immobilized protein mass in the membrane,  $C$  and  $V$  represent the concentration and volume, respectively; the subscripts  $i$ ,  $f$  and  $ws$  indicate the initial, final, and washing solutions, respectively. The immobilized mass was then normalized by the membrane void volume to estimate the immobilized enzyme amount related to membrane volume, which represents the biocatalytic membrane reactor volume, as mentioned earlier.

### ***3.3.4. Pilot plant BMR with physically entrapped $\beta$ -glucosidase***

A similar scheme was used to immobilize the enzyme by entrapment. Here the size of the membrane module was 0.09 m<sup>2</sup>. The membranes are asymmetric polysulfone hollow fibres with a molecular weight cut off of 30 kDa. Characterization of PS membranes was performed by measuring the pure water permeability. A preliminary study to evaluate protein and oleuropein adsorption on the membrane surface was carried out. Pure oleuropein solution or olive leaves extract were ultrafiltered through the polymeric membrane in order to evaluate adsorption effect on membrane permeability. Enzymatic immobilization of  $\beta$ -glucosidase by physical entrapment was performed ultrafiltering a 0.25 mg/ml enzymatic solution from shell to lumen side and the enzyme remained entrapped due to its larger size compared to the thin membrane layer. The system was then rinsed several times with phosphate buffer solution 50 mM pH 6.5 in order to remove non stably entrapped enzyme and excess enzymatic solution. Performance of immobilized enzyme was evaluated by oleuropein hydrolysis reaction.

### ***3.3.5. Biocatalytic membrane reactors with covalently immobilized biocatalysts***

After the enzymes were immobilized onto hollow fibre membranes, hydrolysis reactions with lipase or  $\beta$ -glucosidase were carried out in appropriate biocatalytic membrane reactors. Each type of biocatalytic membrane reactor in which lipase and  $\beta$ -glucosidase worked, will be described in detail in the following paragraphs.

### 3.3.5.1. Biphase biocatalytic membrane reactor with immobilized lipase

The biphasic system is constituted by an organic/enzyme-loaded membrane/aqueous system. The membrane served as support for the enzyme and as contactor between the two immiscible phases. Dispersion of one phase into another was avoided by using appropriate transmembrane pressure. The biphasic biocatalytic membrane reactor with immobilized lipase is depicted in the Figure 3.11.

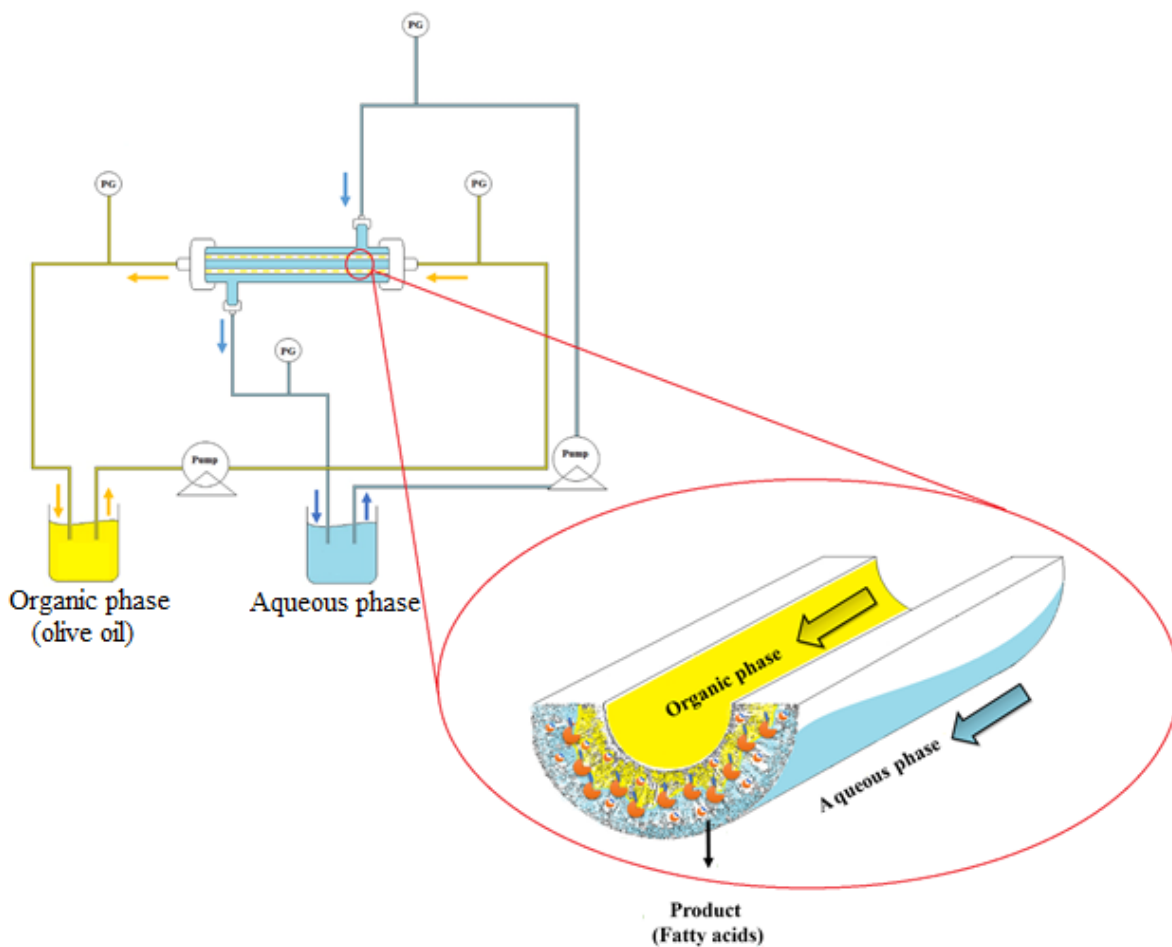


**Fig. 3.11.** Schematic representation of biphasic biocatalytic membrane reactor with immobilized lipase.

The lumen circuit was recirculated with olive oil while aqueous phase was recirculated along the shell side, both with an axial flow rate of 300 mL/min. The organic phase pressure was maintained at 0.6 bar and the aqueous phase pressure was maintained at 0.35 bar; therefore, a transmembrane pressure of 0.25 bar was applied from the organic phase to the aqueous phase, to prevent the aqueous phase passing through the membrane into the organic phase. The system was kept at constant temperature (30 °C) by submerging the module and the

tanks containing the two phases in thermostatic baths. The membrane acted as a catalytic interface, separating the two phases which remained in contact within the membrane pores. The enzyme reaction took place within the membrane phase and the fatty acids formed by the hydrolysis of triglycerides were extracted in the aqueous phase by diffusion. The reaction was monitored by titration of the produced fatty acids extracted in the aqueous phase with NaOH (20 mM) as previously reported for the batch system. The performance of the membrane reactor was expressed as “observed specific activity” on the basis of fatty acids present in the bulk aqueous phase, measured in terms of units expressed as U/mg enzyme. One unit is defined as 1 mol of fatty acid produced per minute. The fatty acids present in the bulk depend on both reaction and transport properties. Therefore, the observed specific activity approaches the intrinsic specific activity when mass transfer is negligible and the system works in reaction limited regime.

#### ***3.3.5.2. Monophasic biocatalytic membrane reactors with immobilized $\beta$ -glucosidase***

Monophasic biocatalytic membrane reactor was developed both through entrapment and covalent binding of  $\beta$ -glucosidase into the pores of polysulfone and alumina hollow fibre membranes, respectively. A schematic representation of monophasic biocatalytic membrane reactor with immobilized  $\beta$ -glucosidase is illustrated in the Figure 3.12.



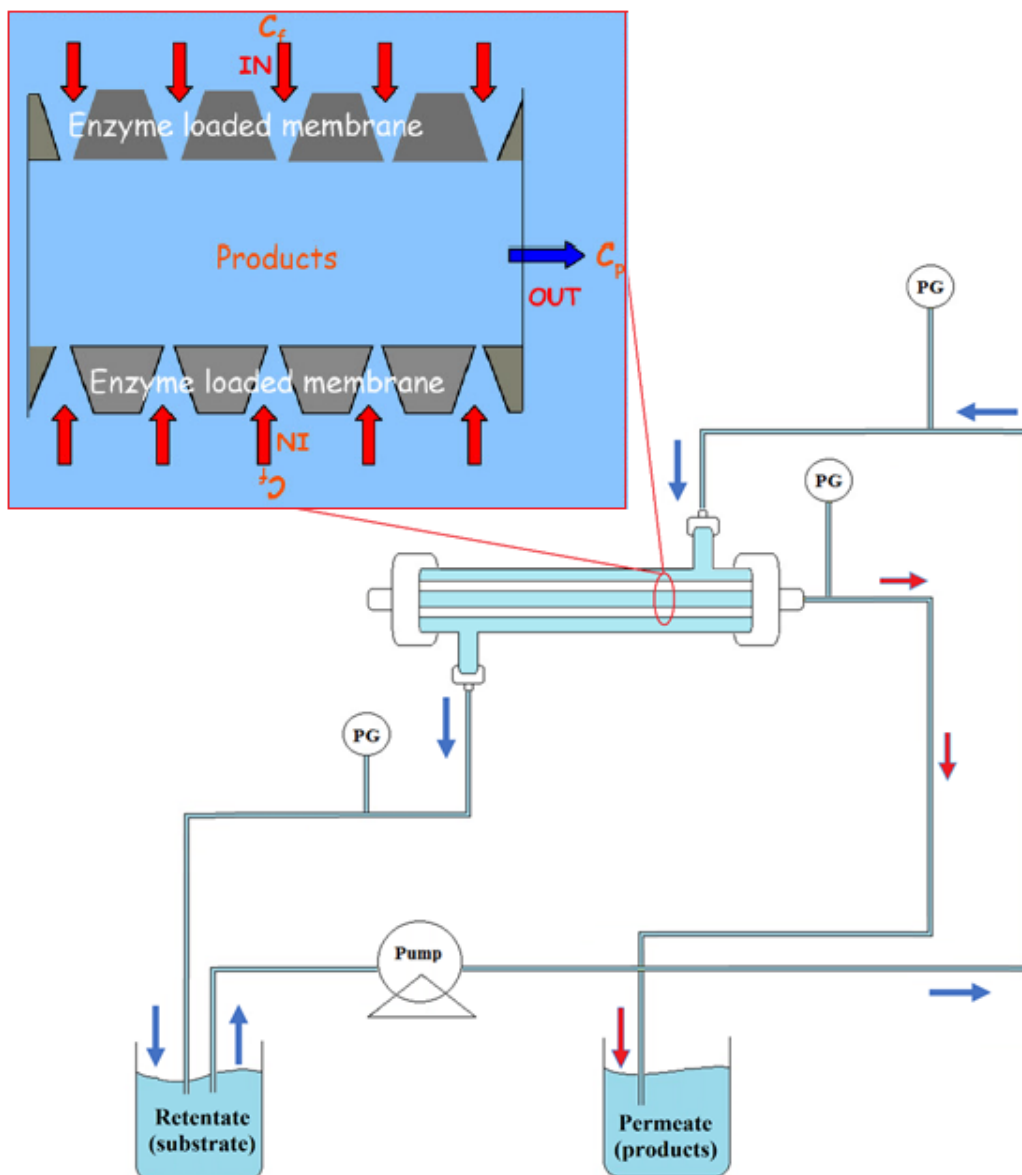


**Fig. 3.12.** Schematic representation of monophasic BMR with immobilized  $\beta$ -glucosidase.

The system was kept at 25 °C by submerging the module and the tank containing the substrate solution in thermostatic baths. The system was fed with a 2.5 mM oleuropein solution from shell to lumen side. The oleuropein solution was transported by convective flow through the membrane pores, from shell to lumen side. Here, the substrate met the immobilized biocatalyst and hydrolysis reaction occurred. In such system, it is assumed that at the steady state each pore of the membrane works like a continuous stirred tank reactor, therefore the overall membrane is a high throughput of microreactors in parallel, where the total reactor volume is the membrane voids volume.

Aglycon, glucose (products of reaction) and unreacted oleuropein were then recovered in the lumen circuit of the system. Both commercial oleuropein solution and olive leaves extract (aqueous phase) were used as substrate to perform the reaction. A graduate cylinder was used to collect the permeate containing the products of the reaction. The volume of permeate was monitored as a function of time and different samples were collected in order to evaluate reaction rate and conversion degree of immobilized enzyme. Operative conditions used to perform the hydrolysis reaction of oleuropein in a pilot plant polymeric biocatalytic membrane reactor and lab scale ceramic biocatalytic membrane reactor were reported in the table 3.5. Operative conditions of the pilot plant were set basing on the optimized operative conditions studied from Mazzei et al [5] in small scale system. Instead, the effect of the operative conditions set in the lab scale prototype were investigated in this work.

Table 3.5 Operative conditions used to perform the hydrolysis reaction of oleuropein in a pilot plant polymeric biocatalytic membrane reactor and lab scale ceramic biocatalytic membrane reactor.

	<b>Prototype plant polysulfone biocatalytic membrane reactor with entrapped <math>\beta</math>-glucosidase</b>	<b>Lab-scale alumina biocatalytic membrane reactor with covalently immobilized <math>\beta</math>-glucosidase</b>
<b>Temperature (<math>^{\circ}</math>C)</b>	25	25
<b>Oleuropein concentration (mM)</b>	2.5	2.5
<b>Axial velocity (m/sec)</b>	$2.3^{-3}$	$4.2^{-3}$
<b>Pressure (bar)</b>	0.03	0.3
<b>Permeate flow rate (ml/min)</b>	10.2	0.3
<b>Residence time (sec)</b>	112	36

In order to confirm that changes in substrate and product concentration were only due to the biocatalyst action and no interference with the membrane materials was occurring, blank

experiments were carried out, where no enzyme or deactivated enzyme was present in the membrane.

### ***3.3.5.3. Multiphasic biocatalytic membrane reactor with covalently immobilized $\beta$ -glucosidase onto alumina membranes***

Set up and operative conditions of the previously described lab-scale system were maintained for the development of a multiphase biocatalytic membrane reactor. Here  $\beta$ -glucosidase is covalently immobilized into the pores of alumina hollow fibre membranes. Initially, the system worked as a monophasic biocatalytic membrane reactor (see previous paragraph). Thus, oleuropein solution was forced to pass through the pores of membrane by a convective mass transport. Here oleuropein hydrolysis took place and both reaction products and unconverted oleuropein were collected in the permeate. Permeate flow rate was monitored during the reaction and samples of permeate and retentate were taken as a function of time and analyzed through HPLC in order to determine reaction rate and conversion degree of immobilized  $\beta$ -glucosidase. When the system reached steady state, ethyl acetate (organic phase) was recirculated with an axial velocity of  $4.2 \cdot 10^{-3}$  m/s into the lumen side of membranes. The water phase continued to pass through the membrane being collected into the organic phase. Since the two phases are immiscible, water-in-oil droplets are here formed. In this way, the droplets were continuously removed from the lumen. The formed emulsion was collected in a glass cylinder where the two phase easily separated after few seconds (the separation time can be tune by acting on the droplet size, which are influenced by axial velocity). Samples of aqueous phase were taken and analyzed in order to determine the oleuropein amount decrease. A schematic representation multiphasic biocatalytic membrane reactor with covalently immobilized  $\beta$ -glucosidase is illustrated in the Figure 3.13.

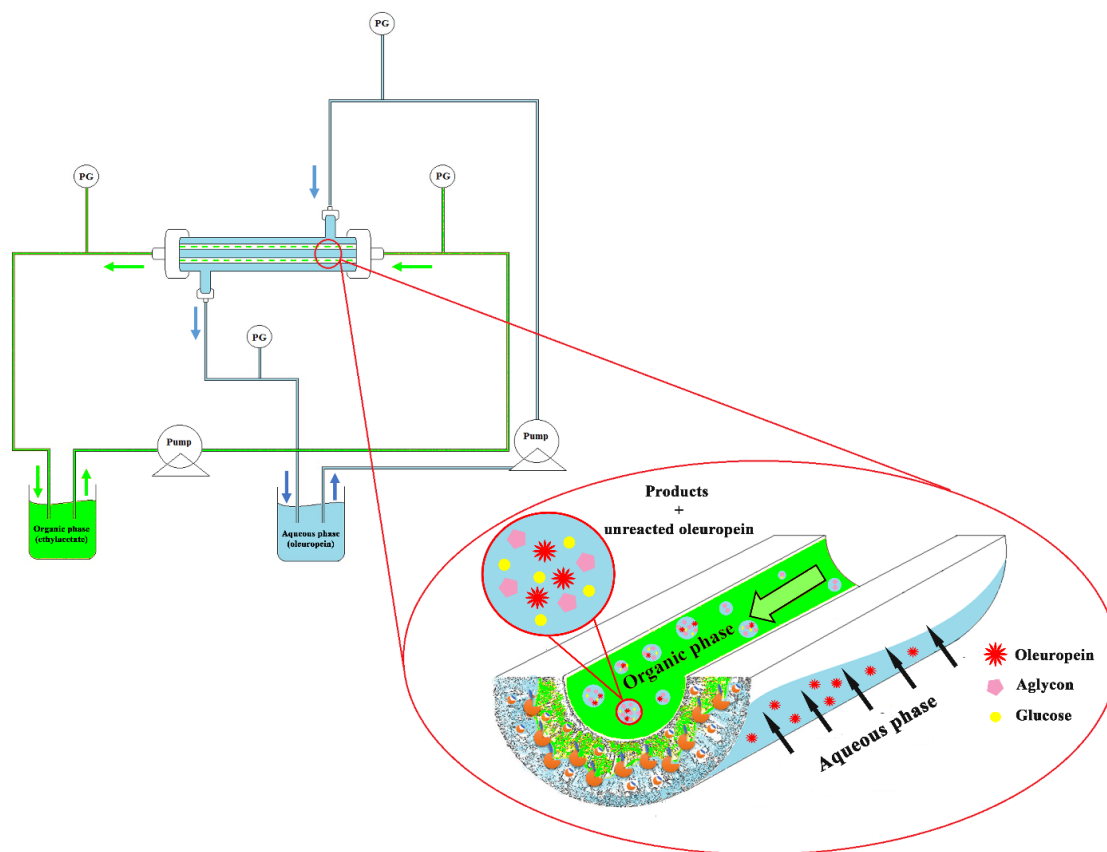


**Fig. 3.13.** Schematic representation of multiphasic BMR with immobilized  $\beta$ -glucosidase

Samples of ethyl acetate containing oleuropein aglycon extracted during the hydrolysis reaction were collected in a glass tube and cured in a heater at 80 °C until evaporation of the organic solvent. Residue remaining after the evaporation of ethyl acetate was dissolved in 50 mM phosphate buffer pH 6.5 and again analyzed by HPLC in order to confirm the amount of oleuropein aglycon extracted into the organic phase.

### **3.3.6. Cleaning of alumina hollow fiber membrane**

Thanks the high chemical and temperature resistance of the inorganic membranes, it was possible to apply a cleaning procedure by using a strong basic detergent in order to regenerate native properties of the membranes. Membranes were cleaned using a detergent solution obtained with 20 wt % of NaOH, 2.5 wt % of NaOCl and 77.5 wt % of water. 2% (v/v) of this prepared solution was pressed through the membrane with a transmembrane pressure of 0.4 bar and a temperature of 80 °C for 1 h. Membranes were then rinsed several time with deionized water until the pH of the washing waters was unaltered. Ultrapure water permeability tests were used to monitor the recovered native properties.

### 3.4. Characterizations

#### 3.4.1. Characterization of prepared inorganic membranes

SEM characterization was conducted for sintered fibers which were flexed at ambient temperature until a fracture occurred prior to being mounted on an SEM slide. Samples were gold coated under vacuum for 3 min at 20 mA (EMITECH Model K550) and SEM images at varying magnifications were collected (JEOL JSM-5610 LV). Water permeability of the fibers was determined by ultrafiltration of 15 MW pure water at different TMP.

#### 3.4.2. Characterization of grafted alumina membranes surface

A rapid and sensitive method for the qualitative and quantitative determination of free amino groups created on the alumina surface has been developed. The method developed is a modification of Kaiser's method [6-8]. The technique involves the reaction of the amine with ninhydrin; under carefully controlled conditions Ruhemann's purple dye anion is formed. Steps involved in the assay is represented in Figure 3.14.

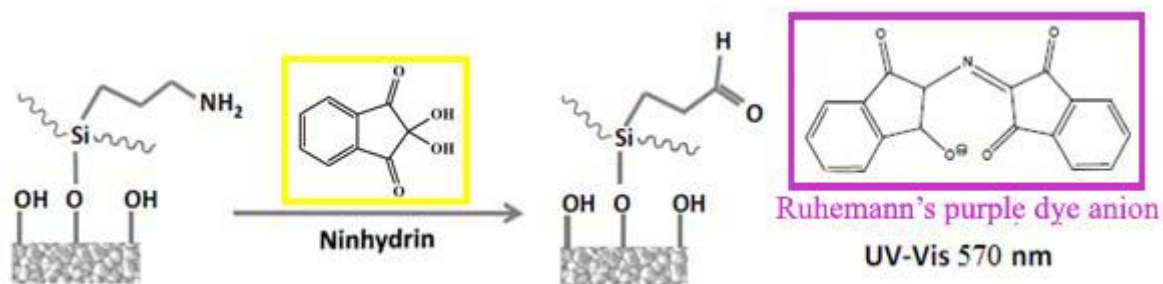


**Fig. 3.14.** Reaction between ninhydrin and amino-groups with formation of Ruhemann's purple dye anion.

Briefly, small pieces of functionalized alumina membranes with APTES (3.5 cm) were introduced in the tubes together with 1 mL of the ninhydrin solution and absolute ethanol up to a total volume of 6 mL. The mixtures were heated at 100 °C for 5 min and then cooled down in a cool water bath [9]. Blank experiments were performed also by using virgin alumina hollow fiber membranes in order to check that no interference occurs with the membrane matrix and to confirm that the purple color is only due to the presence of amino groups. Ninhydrin tests were subsequently repeated after the treatment with glutaraldehyde of silanized alumina fibers in order to confirm that the cross-linker binding occurred by covering the free amino groups on the surface by producing a colorless solution. Different

solutions of known concentration of glycine were used to establish a slope of the linear curve between absorbance and concentration necessary for the quantification measurement of the amino groups. In order to study the effect of the immobilization strategy on the membrane behaviour, ultrapure (UP) water permeability was evaluated after treatment with GA and finally after the enzyme was covalently immobilized.

### 3.4.3. Characterization of olive leaves extracts

Olive leaves extracts belonging to three different cultivar were analyzed in order to establish the oleuropein concentration. In the table 3.6 are indicated both cultivars and harvesting period of olive leaves used for the extraction.

**Tab. 3.6.** Cultivar and harvesting period of olive leaves used for the extraction process.

<b>CULTIVAR</b>	<b>HARVESTING</b>
Ottobratica	July 2014
Sinopolese	July 2014
Ciciariello	July 2014

Due to the high viscosity of olive leaves extracts and the presence of some impurities, a preliminary treatment before performing the hydrolysis reaction was necessary in order to avoid the fouling of the membranes. Thus, olive leaves extracts were diluted with 50 mM phosphate buffer pH 6.5 and then ultrafiltered. Samples of the permeate were taken and analyzed by HPLC according the method previously described. Clear solution obtained from ultrafiltration process was appropriately adjusted in pH (6.5) and oleuropein concentration (2.5 mM). Collected solution was then used to carry out the hydrolysis reaction by immobilized  $\beta$ -glucosidase into a monophasic biocatalytic membrane reactor.

## References

1. A. Ranalli, S. Contento, L. Lucera, M. Di Febo, D. Marchigiani, V. Di Fonzo, *Factors affecting the contents of irinoids oleuropein in olive leaves (Olea europaea L.)*, *J. Agric. Food Chem.* 54 (2006) 434–440.
2. Kingsbury, B.F.K.; Li, K. *A morphological study of ceramic hollow fibre membranes.* *J. Membr. Sci.* 2009, 328, 134–140.
3. Aissaoui, N.; Landoulsi, J.; Bergaoui, L.; Boujday, S.; Lambert, J.-F. *Catalytic activity and thermostability of enzymes immobilized on silanized surface: Influence of the crosslinking agent.* *Enzym. Microb. Technol.* 2013, 52, 336–343.
4. Wang, Z.-H.; Jin, G. *Covalent immobilization of proteins for the biosensor based on imaging ellipsometry.* *J. Immunol. Methods* 2004, 285, 237–243.
5. R. Mazzei, L. Giorno, E. Piacentini, S. Mazzuca, E. Drioli, *Kinetic study of a biocatalytic membrane reactor containing immobilized  $\beta$ -glucosidase for the hydrolysis of oleuropein*, *Journal of Membrane Science* 339 (2009) 215–223.
6. Barbosa, O.; Ortiz, C.; Berenguer-Murcia, Á.; Torres, R.; Rodrigues, R.C.; Fernandez-Lafuente, R. *Glutaraldehyde in bio-catalysts design: A useful crosslinker and a versatile tool in enzyme immobilization.* *RSC Adv.* 2014, 4
7. Kaiser, E.; Colescott, R.L.; Bossinger, C.D.; Cook, P.I. *Color test for detection of free terminal amino groups in the solid-phase synthesis of peptides.* *Anal. Biochem.* 1970, 34, 595–598
8. Sarin, V.K.; Kent, S.B.H.; Tam, J.P.; Merrifield, R.B. *Quantitative monitoring of solid-phase peptide synthesis by the ninhydrin reaction.* *Anal. Biochem.* 1981, 117, 147–157
9. Poli, E.; Chaleix, V.; Damia, C.; Hjezi, Z.; Champion, E.; Sol, V. *Efficient quantification of primary amine functions grafted onto apatite ceramics by using two UV-Vis spectrophotometric methods.* *Anal. Methods* 2014, 6, 9622–9627

## **CHAPTER 4**

### ***Alumina hollow fibre membranes preparation***

#### ***Abstract***

A very challenging objective of recent research in the membrane technology is the development and processing of ceramic hollow fibre membranes which are especially attractive due to their excellent chemical, thermal and mechanical properties compared to polymeric membranes. Asymmetric alumina hollow fibre membranes have been prepared in this work by using a combined phase inversion and sintering technique for use in multifunctional catalytic membrane reactor. A sequence of spinning suspension preparation, extrusion process and sintering were carried out during the fabrication of alumina fibres membranes. Preparation parameters, such as suspension viscosity, air-gap, internal coagulant flow rate and sintering temperature, strongly affect the final morphology of the fibres where finger-like and sponge-like structures can be observed. In this work, the effect of the internal coagulant flow rate on the membrane morphology was studied. All the preparation parameters were kept constant during the study except the internal coagulant flow rate which was varied from 5, 10 and 20 ml/min. Ratio between finger-like voids and sponge layer resulting in the final fibre structures was determined through scanning electron microscopy (SEM) analysis. Ultrapure water characterization was also carried out in order to determine the permeability of the prepared hollow fibre membranes with different morphologies.

#### ***4.1. Introduction***

In the last decades, membrane catalysis has attracted considerable interest in the field of membrane technology (1-10). Different studies have been made and significant progresses were obtained in the fields of food industries, fine chemical synthesis or even for environmental purpose. Despite good results obtained in the different fields of application where membranes are already serving as important tools, membrane technology could propose new potential solutions in the near future. Therefore, optimizing processes and supplying membranes for chemical applications is a challenge for membrane scientists today. One of the fields requiring innovation in membrane science and technology is represented by biocatalytic membrane reactor. The use of biocatalytic membrane reactor in



the chemical industry, wastewater treatment and many other processes could be a potential strategy able to valorize industrial wastes and to ensure a sustainable industrial growth. [11]. Most of the time the reactions are carried out in a classical batch reactor at controlled pH and temperature. At the end of the reaction the enzyme is inactivated and the final products are recovered. Despite the use of such reactors is quite simple also in large scale, this type of bioreactor presents several disadvantages. By considering the industrial practice as the main use of the reactors, it is supposed to be necessary to treat huge quantities of raw material which could result in low productivity, high operating costs, loss of catalytic activity due to inactivation and great variability of the quality of the products. Therefore, the idea of immobilizing enzymes on specific devices appeared as an interesting alternative to overcome some of these inconveniences. By immobilizing the enzyme, it is possible to operate enzymatic processes continuously with all the attendant advantages, such as better process control, higher productivity, more uniform products, and the integration of a purification step in a single unit [12-16]. Enzyme immobilization has been accomplished by chemical and physical attachment to solid surfaces [17-20]. The advantages of using a membrane as solid support were first pointed out by Rony [21]. Since that time, a number of membrane reactor configurations have been suggested, with the membrane offering additional services, such as product separation, phase separation, etc. The main requirements that must be considered to develop a biocatalytic membrane reactor (BMR) are the low costs, high selectivity, high stability under reaction conditions, non-toxicity, green properties and the possibility to recover and reuse the biocatalyst [22]. In addition, a highly uniform and stable nanostructured porous matrix is needed; in fact the non-homogeneity of the membrane does not permit a uniform enzyme distribution during chemical immobilization or maintain a uniform and constant residence time during the biocatalytic reaction. Therefore, the choice of membrane type to be used in BMR on the basis of nature and configuration, it could strongly affect the final parameters of the system in terms of selectivity, life time, mechanical and chemical integrity at the operating conditions, and the cost. For this reasons, in the present work both polymeric and ceramic asymmetric hollow fiber membranes were used to develop biocatalytic membrane reactors. Asymmetric hollow fiber configuration offers a high surface area/volume ratio, after counting in the surface area of the self-organized micro-channels, which promotes an increased loading of the enzyme (while preventing its inhibition due to high concentration) and a higher oil/water interfacial surface preferred in a multiphasic system. Different biocatalytic membrane reactors were developed by immobilizing different biocatalysts into different hollow fibre membranes for the production

of active pharmacologically compounds from natural sources. In particular,  $\beta$ -glucosidase from Almond was immobilized by covalent binding into alumina hollow fibre membrane and by physical entrapment into the pores of polysulfone (PS) hollow fibre membranes on a pilot plant prototype.  $\beta$ -glucosidase was used to hydrolyze oleuropein, the major phenolic compound in the olive fruit and leaves.

In addition, biocatalytic membrane reactor with covalently immobilized lipase was developed and studied in this work. Lipase is one of the most studied biocatalysts, which is active in different reactions such as hydrolysis, esterification, and transesterification, with high enantioselective properties [23,24]. Lipase is an interfacial molecule with phase transfer catalytic properties, meaning it performs to the best of its abilities in an oil/water interface [25,26]. The need to use organic solvents to perform the reaction of immobilized enzyme could be a problem for polymeric membrane reactors in a long term operation. Prolonged contact time with an organic solvent might swell the polymeric material, reducing the performance of the biocatalytic reactor in terms of stability. The use of inorganic membranes in a multiphase membrane reactor may overcome these limitations. In the literature, there is insufficient information about the catalytic performance of lipase and  $\beta$ -glucosidase covalently immobilized in inorganic membranes. Thus, in the present work, biocatalytic membrane reactors were developed by immobilizing lipase and  $\beta$ -glucosidase on “home-made” alumina hollow fiber membranes through covalent binding. Alumina hollow fibre membranes were prepared according to the method described by Benjamin et al. [27] and described in the previous chapter. The fabricating method was modified in order to obtain an asymmetric structure with finger-like supporting layers functioning as high throughput microreactors in series. Phase inversion has been widely adopted for the production of polymeric hollow fibre membranes [27], and has been further developed to fabricate ceramic counterparts after modifying the suspension compositions and incorporating an additional sintering process. In the following paragraphs results obtained from inorganic membrane preparation will be discussed.

#### ***4.2. Characterization of prepared alumina hollow fiber membrane***

Instrumental and operative conditions used to prepare alumina hollow fiber membranes were described in the previous chapter (chapter 3).

Alumina hollow fiber membranes were prepared by a combined phase inversion and sintering technique [27]. Briefly, the prepared spinning suspension and internal coagulant (Deionized water) were loaded in two stainless steel syringes and then spinning suspension was extruded through a tube-in-orifice spinneret (ID 1.2 mm, OD 3.0 mm) connected to the syringes into a 120 L coagulation bath containing water (a non-solvent for the polymer) with an air-gap of 15 cm. A schematic representation of the plant used for the preparation of membrane precursors is reported in Figure 4.1.

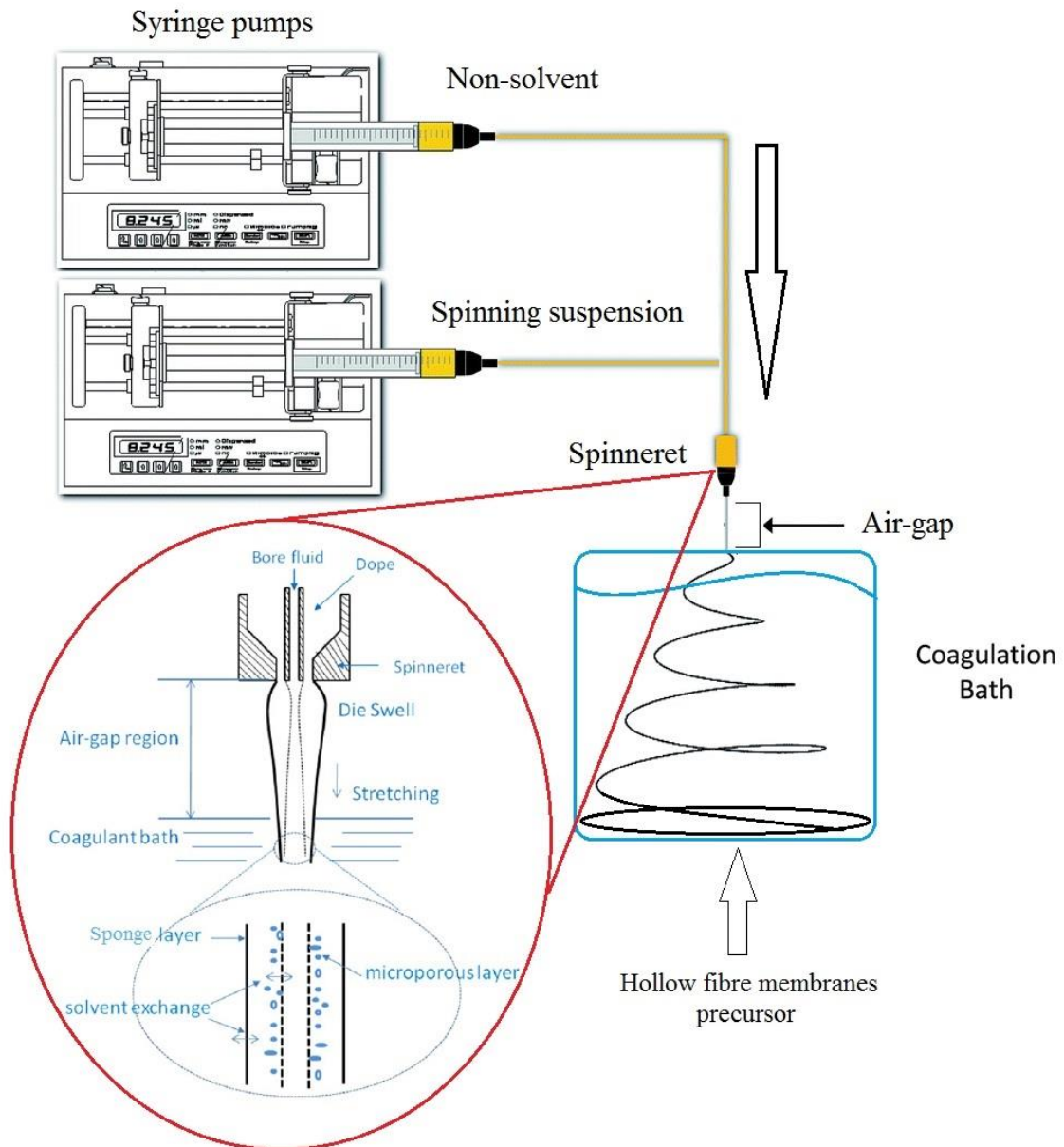
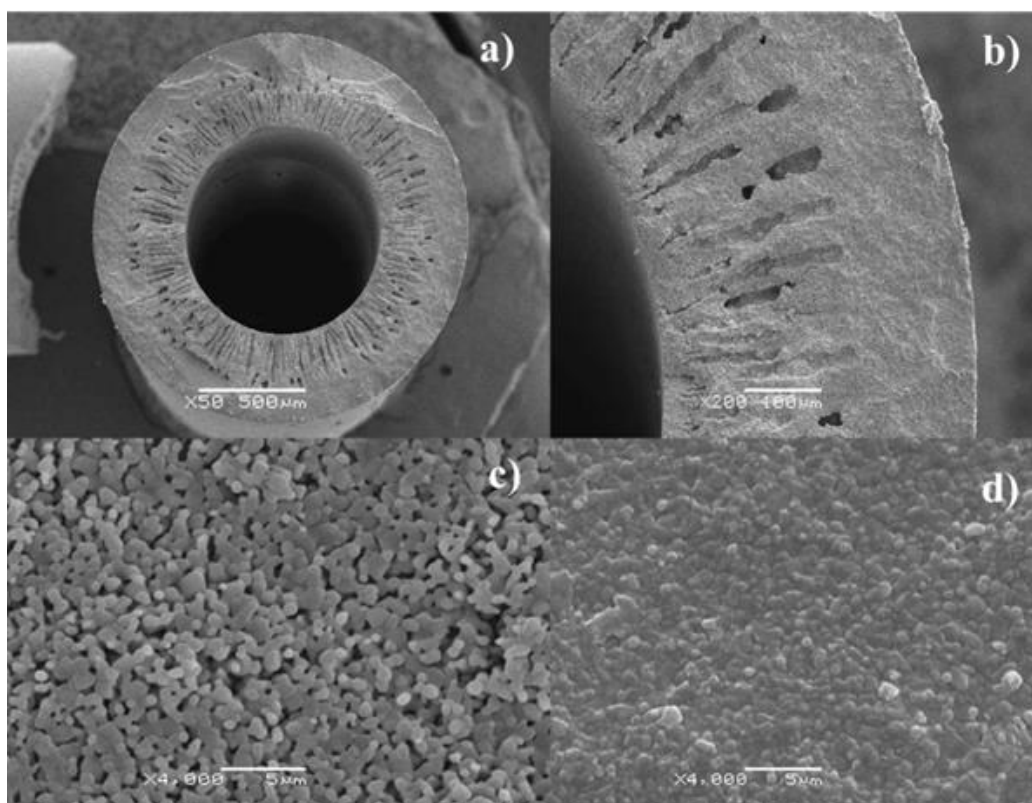


**Fig. 4.1.** Schematic representation of the plant used for the preparation of membrane precursors.

The formation of finger-like voids at the lumen surface is initiated by instabilities at the interface between the non-solvent and the suspension. Finger-like void growth then proceeds as a result of non-solvent influx into the suspension, similar to the viscous fingering phenomenon. Because of the high concentration of non-solvent at the interface, polymer precipitation instantaneous results in a rapid, large increase in the viscosity of the suspension in this region. Consequently, the suspension viscosity exceeds the critical value at which further morphological change may take place and the size of the entrances to the finger-like voids is determined at this point. Non-solvent influx through these entrances into the suspension results in finger-like void growth. However, the polymer precipitation rate within the suspension is lower than that at the interface with non-solvent due to the less availability of non-solvent in this region. As a result, the suspension viscosity remains below the critical value, thus longer finger-like void growth may proceed, giving rise to the characteristic finger-like shape. Finger-like void growth cannot proceed above a critical suspension viscosity and consequently growth is halted when this value is exceeded. Exposure of the outer fiber surface to the atmosphere can cause an increase in viscosity in this region due to simultaneous solvent evaporation and non-solvent condensation from the surrounding atmosphere. For fibers prepared in this work, the critical suspension viscosity is exceeded in the outer region of the fiber before immersion in non-solvent takes place. Consequently, finger-like void growth is not observed at the outer fiber surface and a sponge-like structure is formed. The extrusion rate of the internal coagulant (deionized water) used in the present work were 5, 10 and 20 mL/min in order to study the influence on the membrane morphology. On the contrary, the spinning suspension flow rate was maintained at 7 mL/min. Finally, the fiber precursors were calcined in air in a CARBOLITE furnace to yield ceramic hollow fiber membranes. In this section, the results of the fabrication and characterization of alumina hollow fibre membranes are presented. Membranes were prepared using various internal coagulant flow rates, which affected the length of the finger-like voids as well as the membrane porosity. The other preparation parameters, such as suspension viscosity and flow rate, airgap and calcination temperature were kept constant. Hollow fibre membranes obtained was observed by a scanning electron microscope (SEM) and values of membrane thickness, outer and inner diameter, length of finger-like voids and sponge-like regions were determined by a reading image software (ImageJ).

#### 4.2.1. Alumina hollow fibre membrane prepared with an internal coagulant flow rate of 5 ml/min

This membrane was prepared by using an internal coagulant flow rate of 5 ml/min, the lowest extrusion rate respect to the others. In the Figure 4.2 are reported SEM images of the cross section (Figure 4.2 a), magnification of membrane thickness (Figure 4.2 b), inner (Figure 4.2 c) and outer (Figure 4.2 d) surface of the membrane prepared with mentioned parameters. Table 4.1 reports characteristics of the obtained fibres.



**Tab. 4.1.** Characteristics of fibres obtained with an internal coagulant flow rate of 5 ml/min

<b>Inner diameter</b>	0,92 mm
<b>Outer diameter</b>	1,8 mm
<b>Total thickness</b>	0,42 mm

<b>Finger length</b>	0,25 mm
<b>Sponge region</b>	0,17 mm
<b>Thickness finger like voids percentage</b>	~ 50%

**Fig. 4.2.** SEM images of the cross section (a), magnification of membrane thickness (b), inner (c) and outer (d) surface of the membrane prepared with an internal coagulant flow rate of 5 ml/min.

The mechanical resistance of this fibre membranes should be the highest respect to the others due to a formation of a larger sponge-like region (0.17 mm) because of the lowest internal coagulant flow rate employed. On the other side, it is expected that a larger sponge-like structure in the thickness of the membrane causes a reduction of permeability. From the Figure 4.2 b it is evident that almost half of the membrane thickness consists in a sponge like structure. In the following Figures the behavior of flux as a function of time for different transmembrane pressure (Figure 4.3) and ultrapure water permeability of the studied membrane (Figure 4.4), respectively, are reported.

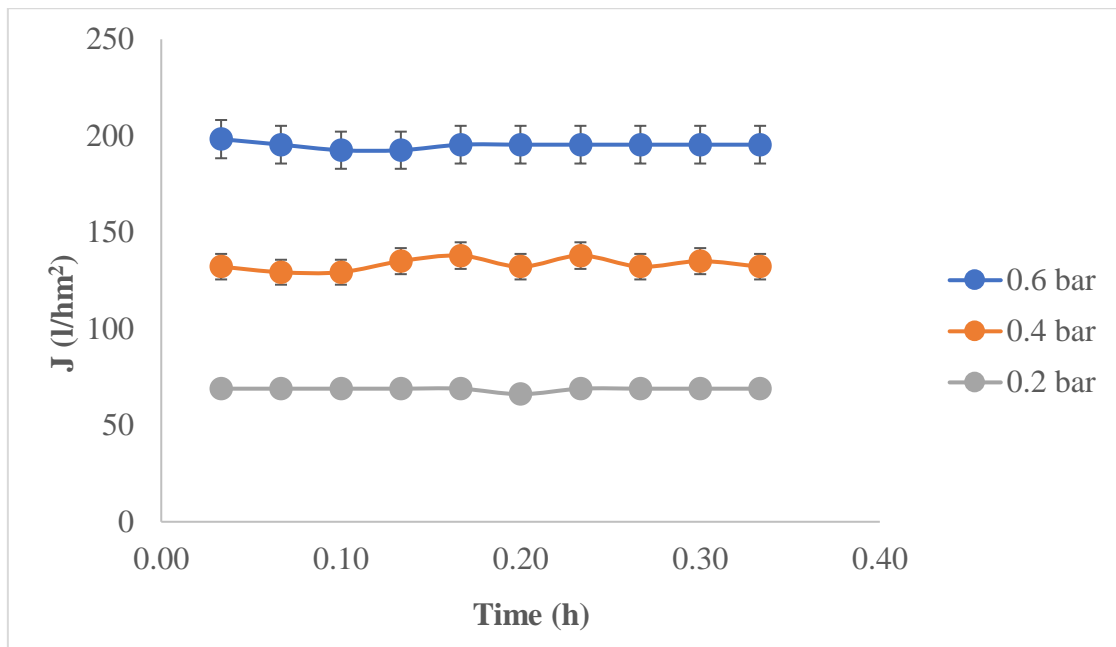


**Fig. 4.3.** Flux as a function of time for different transmembrane pressure of membrane prepared with an internal coagulant flow rate of 5 ml/min.

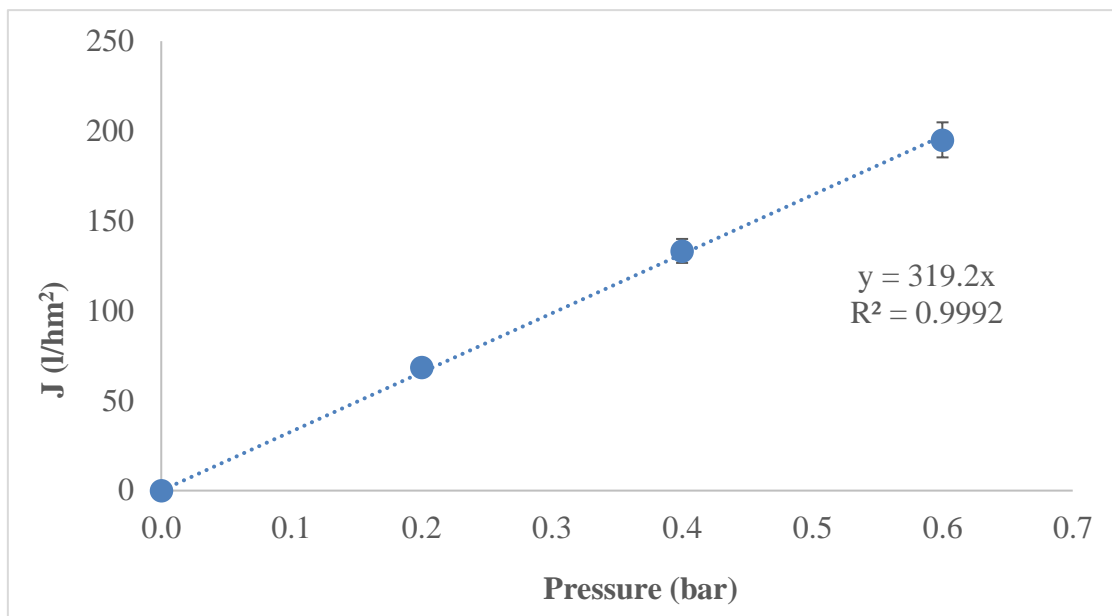


**Fig. 4.4.** Ultrapure water permeability of membrane prepared with an internal coagulant flow rate of 5 ml/min.

#### ***4.2.2. Alumina hollow fibre membrane prepared with an internal coagulant flow rate of 10 ml/min***

In this case the internal coagulant flow rate was increased to 10 ml/ml. In the Figure 4.5 and in the Table 4.2 are reported the characteristics of the prepared membrane.

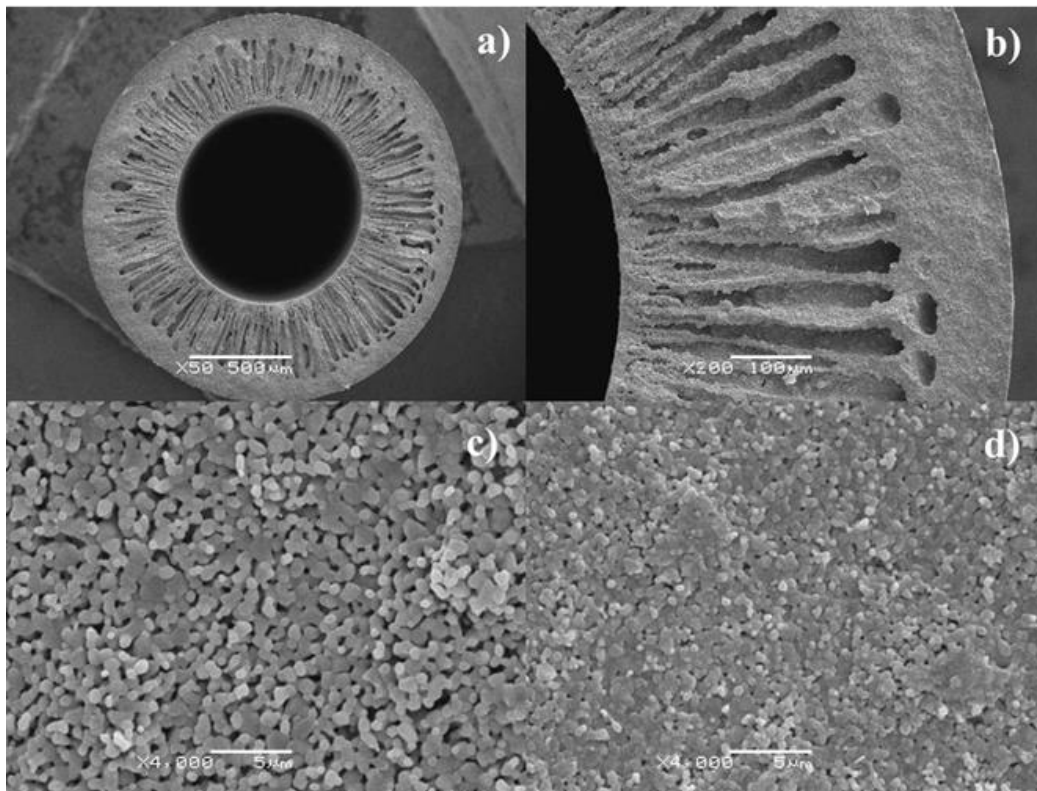


**Fig. 4.5.** SEM images of the cross section (a), magnification of membrane thickness (b), inner (c) and outer (d) surface of the membrane prepared with an internal coagulant flow rate of 10 ml/min.

**Tab. 4.2.** Characteristics of fibres obtained with an internal coagulant flow rate of 10 ml/min

<b>Inner diameter</b>	0,91 mm
<b>Outer diameter</b>	1,85 mm
<b>Total thickness</b>	0,48 mm
<b>Finger length</b>	0,36 mm
<b>Sponge region</b>	0,12 mm
<b>Thickness finger like voids percentage</b>	~ 80 %

Due to the increase of the internal coagulant flow rate, here the finger-like voids region increases up to about the 80% of the total thickness of the membrane structure, as evident



from SEM image (Figure 4.5 b). In the following Figures the flux as a function of time for different transmembrane pressures (Figures 4.6) and ultrapure water permeability of the studied membrane (Figures 4.7), respectively, are illustrated.

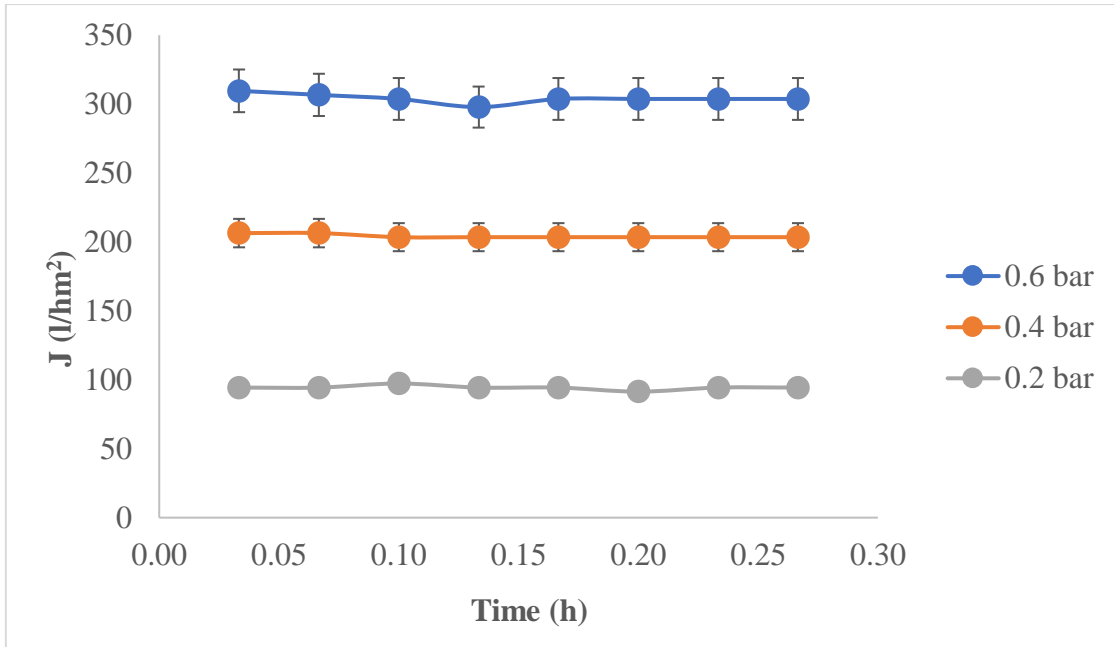


**Fig. 4.6.** Flux as a function of time at different transmembrane pressures of membrane prepared with an internal coagulant flow rate of 10 ml/min.

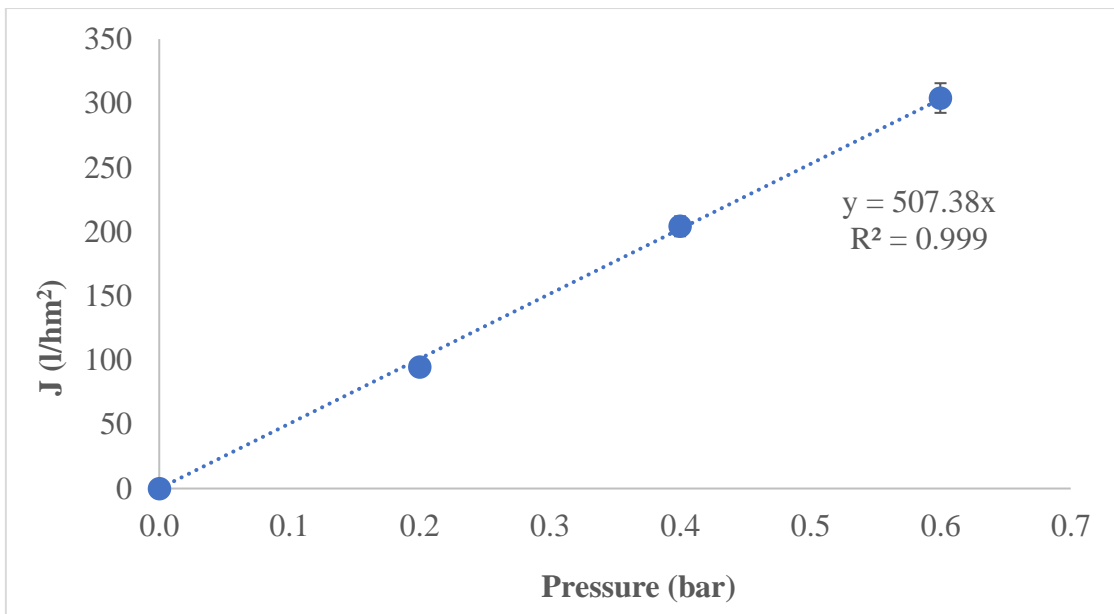


**Fig. 4.7.** Ultrapure water permeability of membrane prepared with an internal coagulant flow rate of 10 ml/min.

It is clear that an internal coagulant flow rate of 10 ml/min promoted the formation of a larger finger-like voids region respect to the previous membrane. The confirmation of a thinner sponge layer in this fibre respect to the previous one is given also by the increase of ultrapure water permeability from previous 319( $\pm$ 19) to 507( $\pm$ 51) L/hm<sup>2</sup>bar.

#### ***4.2.3. Alumina hollow fibre membrane prepared with an internal coagulant flow rate of 20 ml/min***

The last type of hollow fibre membrane was prepared by using the highest internal coagulant flow rate respect to the previous ones. The internal coagulant flow rate was set to 20 ml/ml and in this case finger-like voids were grown for almost the total thickness of membrane structure (about 90%), as shown in Figure 4.8 a and 4.8 b.

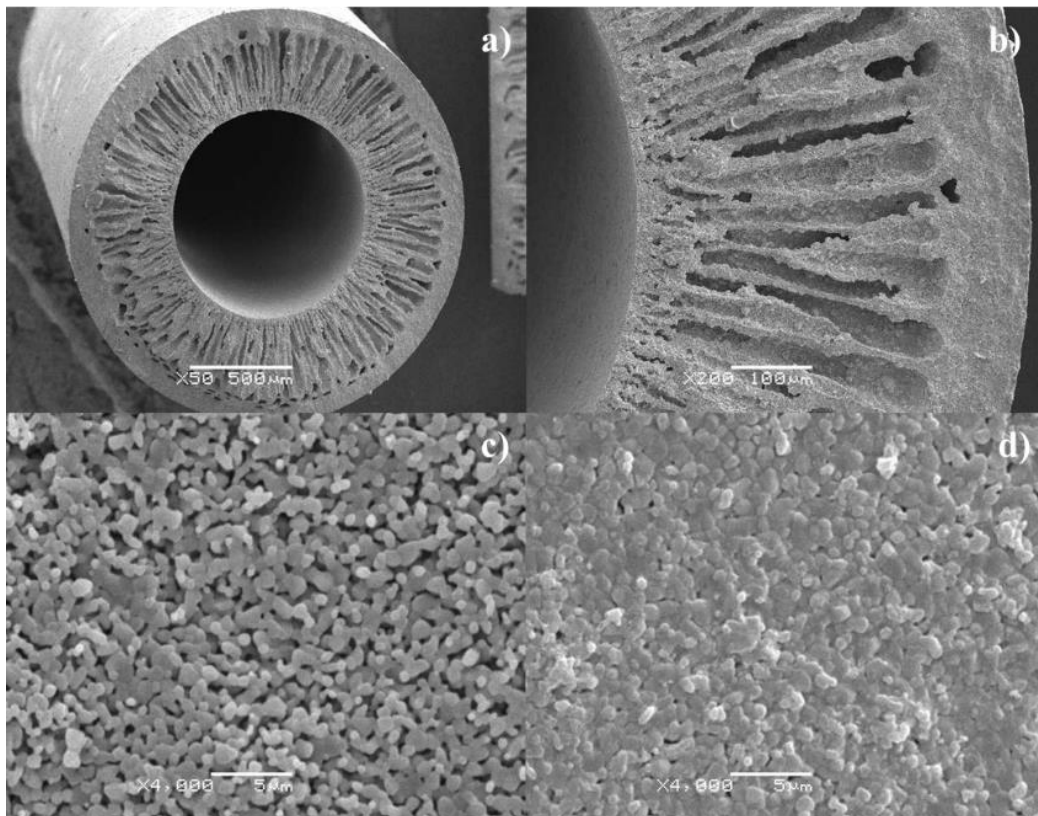


**Fig. 4.8.** SEM images of the cross section (a), magnification of membrane thickness (b), inner (c) and outer (d) surface of the membrane prepared with an internal coagulant flow rate of 20 ml/min.

**Tab.4.3.** Characteristics of fibres obtained with an internal coagulant flow rate of 20 ml/min

<b>Inner diameter</b>	0,94 mm
<b>Outer diameter</b>	1,93 mm
<b>Total thickness</b>	0,48 mm
<b>Finger length</b>	0,38 mm
<b>Sponge region</b>	0,1 mm
<b>Thickness finger like voids percentage</b>	~ 85-90 %

Since this is the hollow fibre membranes with the thinnest sponge like region respect to the others, it is expected a low mechanical resistance, thus a weaker structure. The ultrapure water permeability Figure 4.10 is significantly higher than the previous ones due to the lower resistance which water meets during the passage through the membrane because of a very thin sponge layer. In the Figure 4.9 is also reported the flux at different transmembrane pressure.

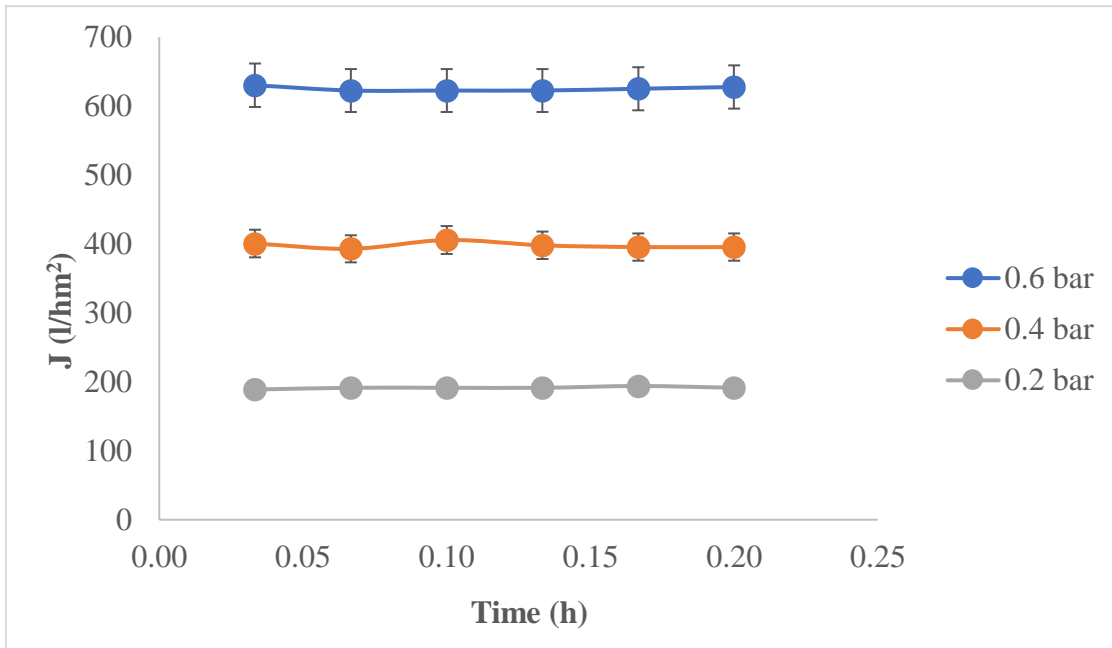


**Fig. 4.9.** Flux at different transmembrane pressure of membrane prepared with an internal coagulant flow rate of 20 ml/min.

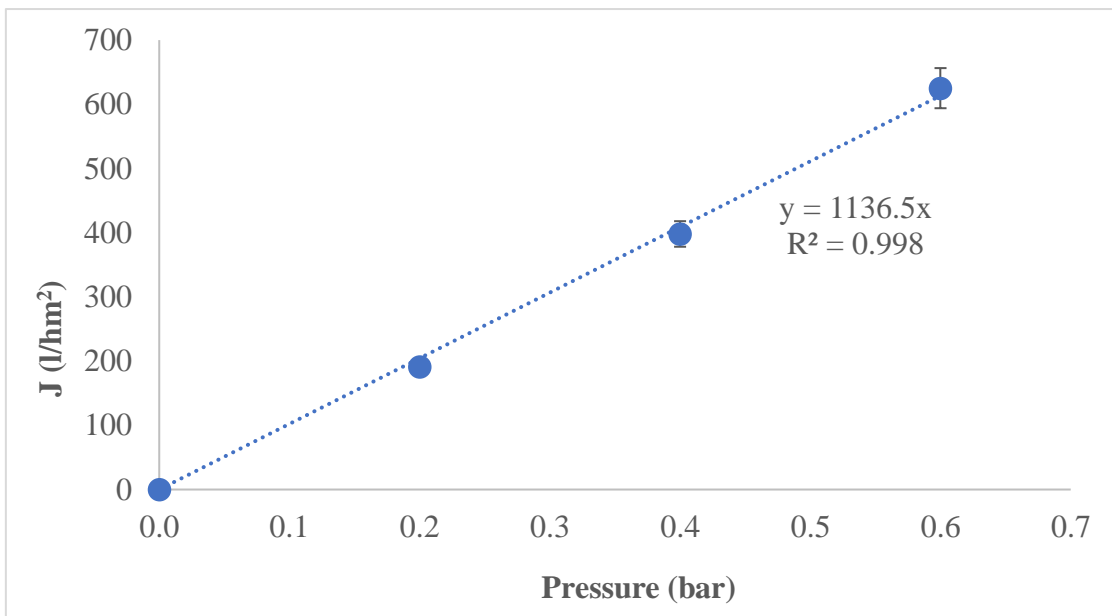


**Fig. 4.10.** Ultrapure water permeability of membrane prepared with an internal coagulant flow rate of 20 ml/min.

### 4.3. Comparison of prepared alumina hollow fibre membranes

The fibers showed uniform wall thickness along the fiber length. The outer diameter (OD) and internal diameter (ID) of the fibers were  $1830\ \mu\text{m}$  ( $\pm 0.08$ ) and  $920\ \mu\text{m}$  ( $\pm 0.01$ ), respectively. The hollow fibers possess a unique asymmetric structure composed of relatively long finger-like voids and a thin sponge-like layer.

SEM images clearly confirm the progressive increase in the thickness of the finger-like region as the internal coagulant flow rate increases. Accordingly, ultrapure water permeability increases with the same trend. In the Figure 4.11 it is represented the linear relationship between ultrapure water permeability and internal coagulant flow rate increase for the different membrane morphology obtained.

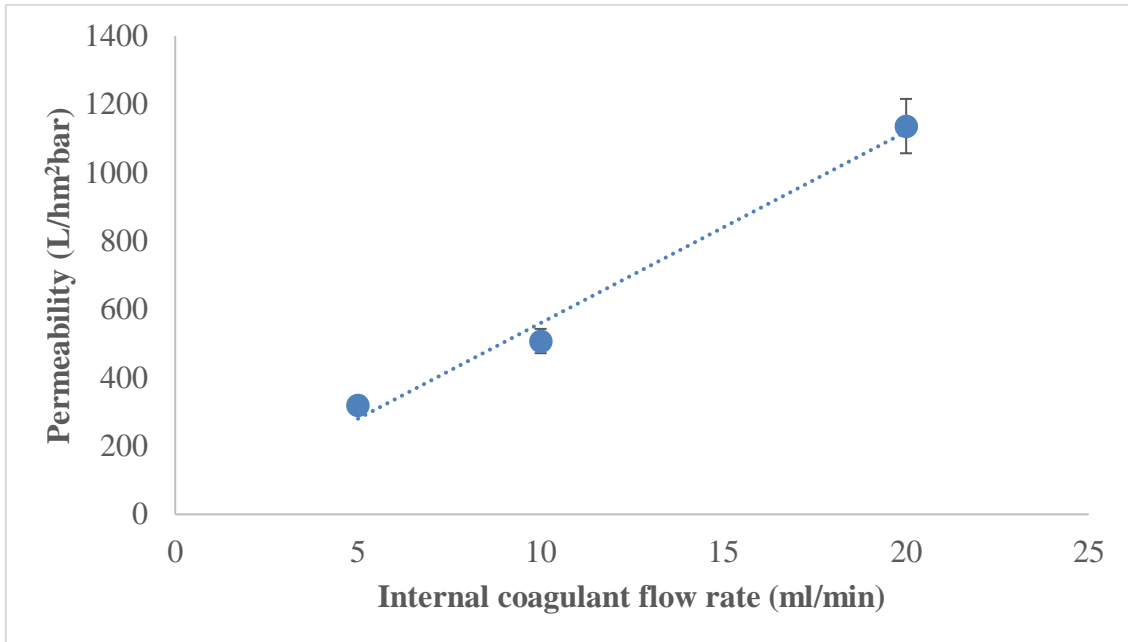


**Fig 4.11.** Behavior of ultrapure water permeability of the different membrane morphology obtained at different flow rate of internal coagulant.

By considering that packing of the sponge layer is equal in all three cases because they are prepared with same spinning suspension, same air-gap and same calcination temperature, it can be deduced that the porosity of the membranes depends only on the thickness of the sponge-like region, thus from the internal coagulant flow rate with which they are prepared. A major porosity lead to a lower mechanical resistance of the membrane fibres. So, in the course of this work, three different morphologies of fibers were prepared which can be adapted to various applications according to their characteristics:

- the membrane prepared with an internal coagulant flow rate of 5 ml/min, is the membrane with the greater mechanical strength and lower permeability due to a ratio of about 50: 50 between "finger-like voids" and "sponge like region";
- the membrane prepared with an internal coagulant flow rate of 10 ml/min, is the membrane with intermediate characteristics between the first and the last one prepared. it had good ultrapure water permeability and a good mechanical resistance;
- the last membrane, prepared with an internal coagulant flow rate of 20 ml/min, is the most fragile membrane but with the highest permeability.

The alumina hollow fibre membrane with intermediate properties was selected for the development of the biocatalytic membrane reactor due to the high surface area/volume ratio for enzyme loading as well as a good mechanical strength. Membrane void volume of pieces of prepared membrane was calculated and results are reported in Table (4.4) (the methods to measure void volume of biocatalytic membrane reactors developed with the prepared hollow fibre membranes was already described in Chapter 3).

**Table 4.4.** Membrane void volumes of the prepared fibres.

<b>Internal coagulant flow rate (ml/min)</b>	<b>Finger-like voids in fibre cross section (%)</b>	<b>Fibre length (cm)</b>	<b>Membrane void volume (cm<sup>3</sup>)</b>
<b>5</b>	<b>50</b>	9.3	0.08
<b>10</b>	<b>80</b>	9.3	0.09
<b>20</b>	<b>90</b>	9.3	0.12

#### **4.4. Conclusions**

In this study alumina hollow fibre membranes were prepared and characterized. By using various internal coagulant flow rates (5, 10, 20 mL/min) different lengths of finger-like voids were obtained in the structure of asymmetric fibres (50%, 80% and 90% of the fiber cross-section, respectively). Accordingly, ultrapure water permeability confirms the progressive increase in the thickness of the finger-like region, from 319 ( $\pm 19$ ) L/hm<sup>2</sup>bar to 1136 ( $\pm 186$ ) L/hm<sup>2</sup>bar and an intermediate value of 507( $\pm 5$ ) L/hm<sup>2</sup>bar. Due to the high surface

area/volume ratio for enzyme loading as well as a good mechanical strength, hollow fibre membrane with intermediate properties was selected for the development of the biocatalytic membrane reactor.

## References

1. J.N. Armor, *Catalysis with permselective inorganic membranes*, *J. Membrane Sci.*, 147, 217–233 (1998).
2. Mackay R, Sammells AF. US patent 09/905651. 2002.
3. Y.S. Lin, *Microporous and dense inorganic membranes: current status and prospective*, *Sep. Purif. Tech.*, 25, 39–55 (2001).
4. G.Q. Lu, J.C. Diniz de Costa, M. Duke, S. Giessler, R. Socolow, R.H. Williams, T. Kreutz, *Inorganic membranes for hydrogen production and purification: A critical review and perspective*, *J. Coll. Interface Sci.*, 314, 589–603 (2007).
5. E.E. McLeary, J.C. Jansen, F. Kapteijn, *Zeolite based films, membranes and membrane reactors: Progress and prospects*, *Microp. & Mes. Mat.*, 90, 198–220 (2006).
6. M.J.G. Sanchez, T.T. Tsotsis, *Catalytic membranes and membrane reactors*, 1. Edition – April 2002, Wiley-VCH Eds.
7. G. Saracco, V. Specchia, *Catalytic inorganic membrane reactors: present experience and future opportunities*, *Catal. Rev. Sci. Eng.*, 36, 305–384 (1994).
8. Mendes D, Mendes A, Madeira LM, Iulianelli A, Sousa JM, Basile A. *Asia-Pac J Chem Eng* 2010;5(1):111–137.
9. J. Shu, B.P.A. Grandjean A. Vanneste, S. Kaliaguine, *Catalytic palladium-based membrane reactors: a review*, *Can. J. Chem. Eng.*, 89, 1036–1060 (1991).
10. Babita K, Sridhar S, Raghavan KV. *Int J Hydrogen Energy* 2011;36(11):6671–6688.
11. Char pentier J.C. *Ind Eng Chem Res* , 2007, 46( 11) : 3465
12. Cheryan, M. and Mehaia, M. A. *Membrane bioreactors*. In: *Membrane Separations in Biotechnology* (MacGregor, W. C., ed.)
13. Marcel Dekker, New York, 1986, pp.255-302 2 Siebel, M. A. *Batch reactors*. In: *Bioreactor Design and Product Yield*.
14. Uwe T. Bornscheuer, *Immobilizing Enzymes: How to Create More Suitable Biocatalysts*, *Angew. Chem. Int. Ed.* 2003, 42, 3336 – 3337
15. Butterworth-Heinemann, Great Britain, 1992, pp. 103- 112 3 Cheryan, M. *Ultrafiltration applications*. In: *Ultrafiltration Handbook*. Technomic Publishing Company, Lancaster, PA, 1986, pp. 231-350 1,3.



16. G. FernKndez-Lafuente, M. Terreni, C. Mateo, A. Bastida, R. FernKndez-Lafuente, P. Dalmasas, J. Huguet, J. M. Guisan, *Enzyme Microb. Technol.* 2001, 28, 389 – 396.
17. Gekas, V. C. *Artificial membranes as carriers for the immobilization of biocatalysts.* *Enzyme Microb. Technol.* 1986, 8, 450-460 5.
18. Persson M, Wehtje E, Adlercreut P (2000) *Immobilisation of lipases by adsorption and deposition: high protein loading gives lower water activity optimum.* *Biotechnol Lett* 22:1571–1575
19. Gerhartz, W. *General production methods.* In: *Enzymes" in Industo,,: Production and Applications.* VCH VerlagsgeseUschaft, Weinheim, 1990, pp. 33-74 4,5
20. Fu J, Reinhold J, Woodbury NW (2011) *Peptide-modified surfaces for enzyme immobilization.* *PLoS ONE.*
21. Rony, P. R. *Hollow fiber enzyme reactors.* *J. Am. Chem. Soc.* 1972, 94, 8247-8248 6
22. Hill C L. *Nature*, 1999, 401( 6752) : 436
23. Giorno, L.; Molinari, R.; Natoli, M.; Drioli, E. *Hydrolysis and regioselective transesterification catalyzed by immobilized lipases in membrane bioreactors.* *J. Membr. Sci.* 1997, 125, 177–187.
24. Karl-Erich Jaeger , Thorsten Eggert, *Lipases for biotechnology, Current Opinion in Biotechnology, Volume 13, Issue 4, 1 August 2002, Pages 390–397.*
25. Prazeres, D.M.F.; Cabral, J.M.S. *Enzymatic membrane bioreactors and their applications.* *Enzym. Microb.Technol.* 1994, 16, 738–750.
26. Maruyama, T., Nakajima, M., Uchikawa, S. et al. *J Amer Oil Chem Soc* (2000) 77: 1121. doi:10.1007/s11746-000-0176-4.
27. Kingsbury, B.F.K.; Li, K. *A morphological study of ceramic hollow fibre membranes.* *J. Membr. Sci.* 2009,328, 134–140.

## CHAPTER 5

### *Biphasic biocatalytic membrane reactor with covalently immobilized lipase*

#### *Abstract*

Biocatalytic membrane reactors (BMR) combining reaction and separation within the same unit have many advantages over conventional reactor designs. Ceramic membranes are an attractive alternative to polymeric membranes in membrane biotechnology due to their high chemical, thermal and mechanical resistance. Another important use is their potential application in a biphasic membrane system, where support solvent resistance is highly needed. In this chapter, the use of asymmetric ceramic hollow fibre membranes in a two-separate-phase biocatalytic membrane reactor will be described. The asymmetric ceramic hollow fibre membranes prepared as described in the previous chapter, were used as support for lipase covalent immobilization in order to develop a two-separate-phase biocatalytic membrane reactor. A functionalization method was proposed in order to increase the density of the reactive hydroxyl groups on the surface of ceramic membranes, which were then amino-activated and treated with a cross-linker. The performance and the stability of the immobilized lipase were investigated as a function of the amount of the immobilized biocatalyst. Results showed that it is possible to immobilize lipase on a ceramic membrane without altering its catalytic performance (initial residual specific activity 93%), which remains constant after 6 reaction cycles.

Part of this work has been published:

G. Ranieri, R. Mazzei, Z. Wu, K. Li and L. Giorno, “*Use of a Ceramic Membrane to Improve the Performance of Two-Separate-Phase Biocatalytic Membrane Reactor*”, *Molecules* 2016, 21, 345; doi:10.3390/molecules21030345

#### **5.1. Introduction**

In the last decade inorganic membranes have attracted considerable interest in the field of membrane technology. The excellent properties of inorganic membranes in terms of chemical, mechanical and thermal resistance make them suitable materials to develop innovative devices, promoting new research from production to their application. The versatility of these membranes has allowed their use in various applications such as

hydrogen production and separation [1-3], propane dehydrogenation [4], filtration for corrosive fluids [5] and for the development of high temperature reactors [6], membrane contactors [7], biosensors [8] and biocatalytic membrane reactors [9,10]. The present study explored the suitability of inorganic hollow fibers to improve the performance of a biocatalytic membrane reactor (BMR), often developed by using polymeric membranes mainly due to their lower costs. On the other hand, inorganic membranes are more resistant to organic solvents [11] and therefore they might be more suitable for biocatalytic membranes operating in a biphasic system. Recent works [12,13] reported very good performance from polymeric and hybrid membranes with regard to organic solvents, even though some problems still remain to be solved such as polymer plasticization, swelling and clustering [13]. For BMR development a highly uniform and stable nanostructured porous matrix is needed; in fact, the non-homogeneity of the membrane does not permit a good enzyme distribution during chemical immobilization or maintain a constant residence time during the biocatalytic reaction. For this reason we used ceramic membranes to develop the BMR. Asymmetric hollow fiber configuration offers a high surface area/volume ratio, after counting in the surface area of the self-organized micro-channels, which promotes an increased loading of the enzyme and a higher oil/water interfacial surface preferred in a biphasic system. Many studies have been carried out on BMRs by employing different kinds of polymeric membranes and biocatalysts [14], with limited studies available on BMRs using inorganic support, summarized in Table 1.

<b>Immobilized protein</b>	<b>Catalyzed reaction</b>	<b>Inorganic material support</b>	<b>Reference</b>
<b>Candida antarctica lipase B</b>	Hydrolysis of p-nitrophenyl palmitate	Alumina	10
<b>Rat hepatic microsomal CYP2E1</b>	Para-nitrophenol hydroxylation	Alumina	15
<b>Alliinase</b>	Conversion of alliin in alliin	Alumina	16
<b>Glucose-6-phosphate dehydrogenase</b>	Oxidation of Glucose-6 phosphate (G6P)	Alumina Silica	17 18
<b>Laccase</b>	Oxidation of 2,2'-azino-bis-(3 ethylbenzothiazoline-6-sulfonic acid)	Titania	19
<b>Urease</b>	Urea hydroxylation	Alumina	20
<b>Glutathione transferase</b>	Glutathione conjugation to 1-chloro-2,4-dinitrobenzene	Alumina	21

One of the most studied biocatalysts is lipase, which is active in different reactions such as hydrolysis, esterification, and transesterification, with high enantioselective properties [22,23]. Lipase is an interfacial molecule with phase transfer catalytic properties, meaning it performs to the best of its abilities in an oil/water interface [24,25]. Besides, most lipase substrates have low water solubility, so the reaction is conventionally performed in a multiphase membrane reactor where the membrane acts not only as a support for the enzyme, but also as a separation-and-contacting unit between the two immiscible phases. This configuration permits the continuous removal of the selected product, via extraction, from the reaction microenvironment, thus promoting reaction yield to a higher level. The need to use organic solvents to perform the reaction of immobilized enzyme could be a problem for polymeric membrane reactors in a long-term operation. Prolonged contact time with an organic solvent might swell the polymeric material, reducing the performance of the biocatalytic reactor in terms of stability. The use of inorganic membranes in a multiphase membrane reactor may overcome these limitations. Furthermore, inorganic membranes are easy to regenerate and reuse for subsequent enzyme immobilization, after long term use and enzyme deactivation. So far, there is insufficient information about the catalytic performance of lipase immobilized in inorganic membranes. In the present work, a biocatalytic membrane reactor was developed by immobilizing lipase from *Candida rugosa* on “home-made” alumina hollow fiber membranes through covalent binding. Lipase from *Candida rugosa* was immobilized using (3-aminopropyl) triethoxysilane (APTES)—glutaraldehyde (GA) modification approach. Since the effect of APTES concentration on the immobilization process has already been studied by Miletić et al. [24], in this study the silanization process was performed with a constant concentration of APTES, addressing the effects of hydroxylation and GA concentration on enzyme immobilization. The influence of immobilized lipase amount on the specific activity and biocatalytic reactor performance was also studied. The catalytic activity was evaluated in a two-separate-phase biocatalytic membrane reactor (TSP-BMR).

## ***5.2. Characterization of grafted alumina membranes surface***

Prior to enzyme immobilization, as explained in Materials and Methods section, blank experiments were carried out on native membranes to evaluate the exclusive enzyme covalent binding. No adsorbed or entrapped enzyme was detected. In addition, on the same native membranes, no color variation of ninhydrin solution was observed, which confirmed that there is no interference between the matrix and ninhydrin assay. Performing the assay

on membrane functionalized with APTES (Al-APTES), a variation of ninhydrin solution from yellow to purple was detected. As expected, after cross-linking of Al-APTES with glutaraldehyde a colorless solution was obtained by carrying out the assay on Al-APTES-GA, because no more exposed amino-groups on the membrane surface were presents, being quenched by GA. Figure 5.1 summarizes the steps of ninhydrin test.

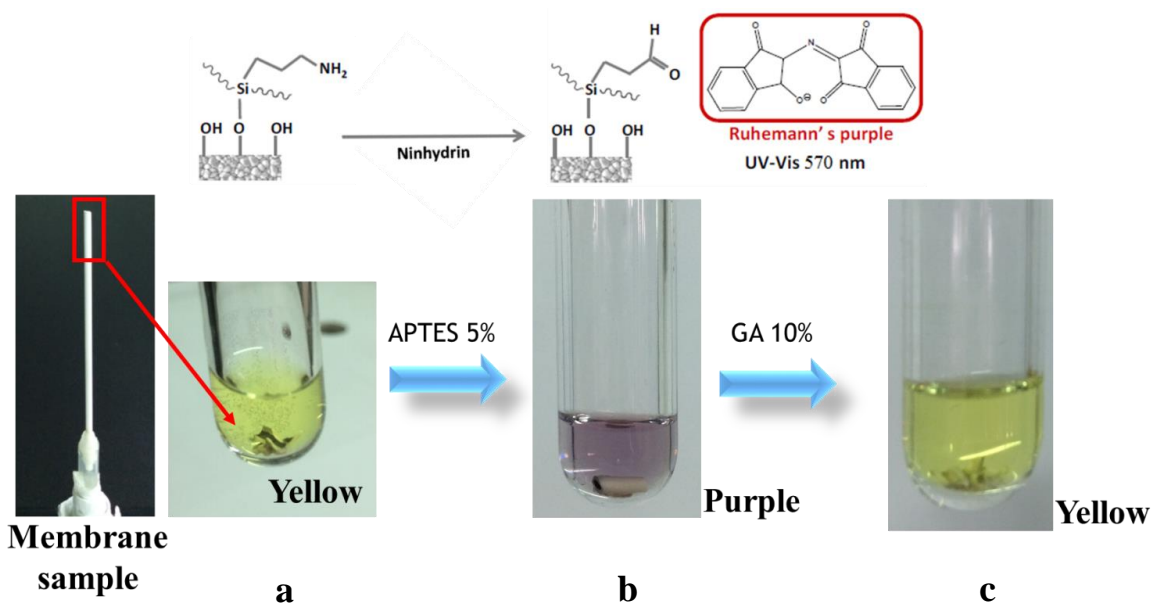


**Fig. 5.1.** Ninhydrin test on the native membranes (a), after functionalization with 5% APTES (b) and after the treatment with the crosslinking reagent GA (c).

The correlation coefficient between absorbance and concentration resulting from calibration plot of glycine was 310.95, as reported in Figure 5.2.

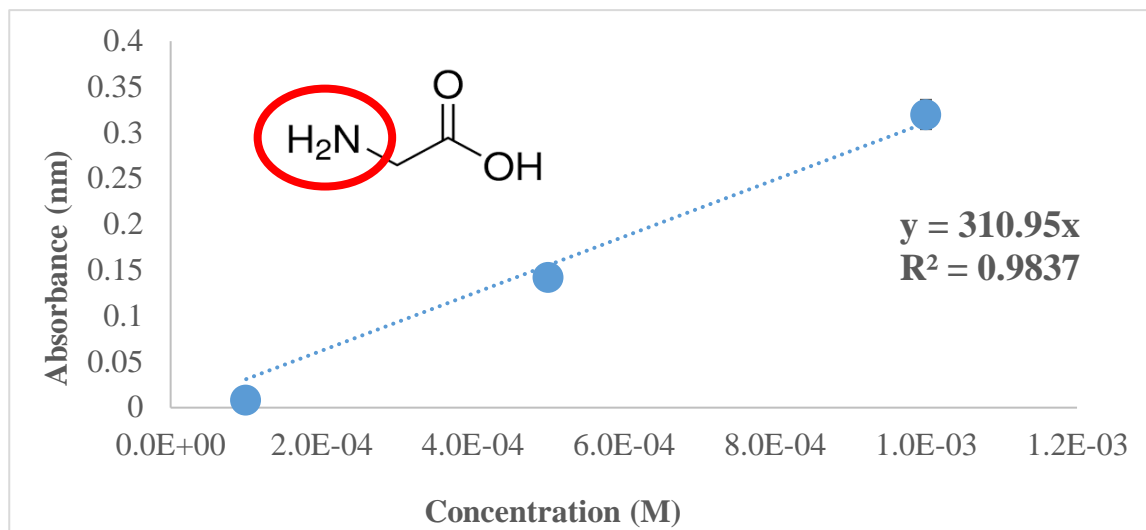


**Fig. 5.2.** Calibration plot of glycine.

Finally, the amount of the amino groups per unit surface generated after the functionalization process was calculated equal to  $1.26^{-3}$  ( $\pm 1.56^{-4}$ ) mmol/cm<sup>2</sup>. The effect of the functionalization on water permeability was investigated. Compared to the initial permeability value of native membranes, permeability decreased by about 26% after the silanization process and by about 35% after the treatment with glutaraldehyde. Figure 5.3 shows the decrease of ultrapure water permeability as confirmation of the presence of new components bearing functional groups. Reduction of permeability is a further confirmation of the occurred functionalization.

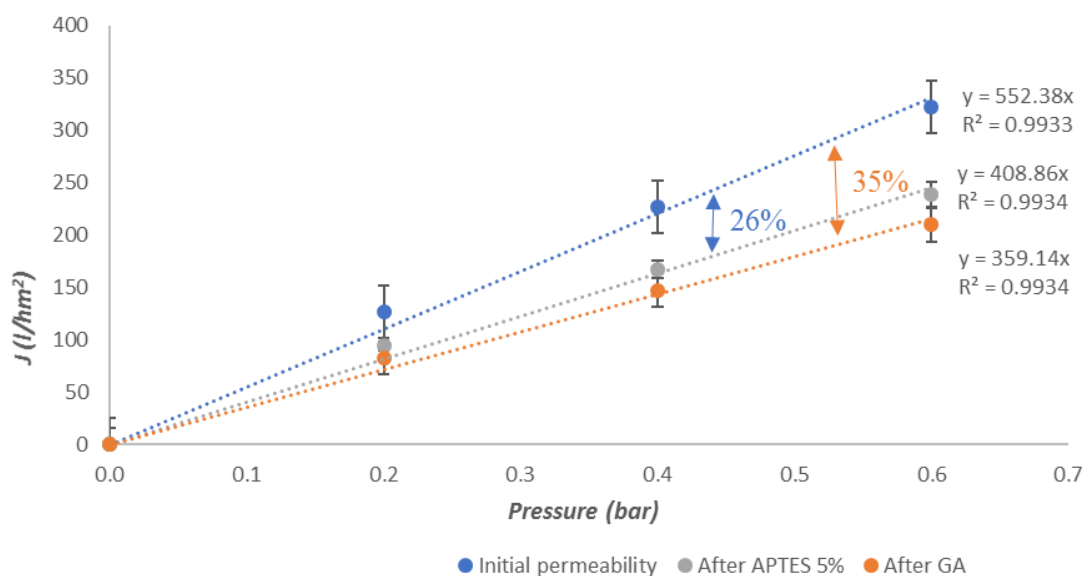


**Fig. 5.3.** Decrease of ultrapure water permeability after functionalization steps

### 5.3. Covalent immobilization of lipase

Lipase immobilization was carried out as described in the “Materials and Methods” section. A further permeability reduction of about 88% was detected (compared to the initial one), confirming the presence of the covalently bonded enzyme on the membrane. In addition, the flux monitored during the immobilization process decreases considerably because of the occlusion of the membrane pores by enzymatic presence, as shown in Figure 5.4.

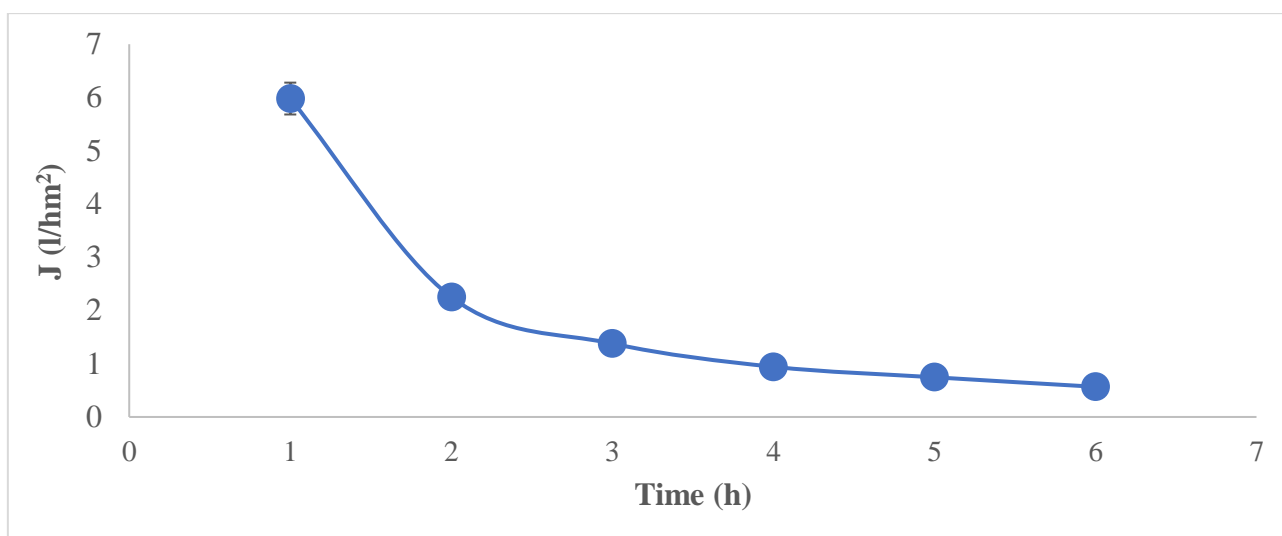


**Fig. 5.4.** Flux of membranes during enzyme immobilization by covalent binding.

The results achieved, in terms of immobilized lipase amount, by performing hydroxylation process on membrane and by varying GA concentration are shown in Figure 5.5.



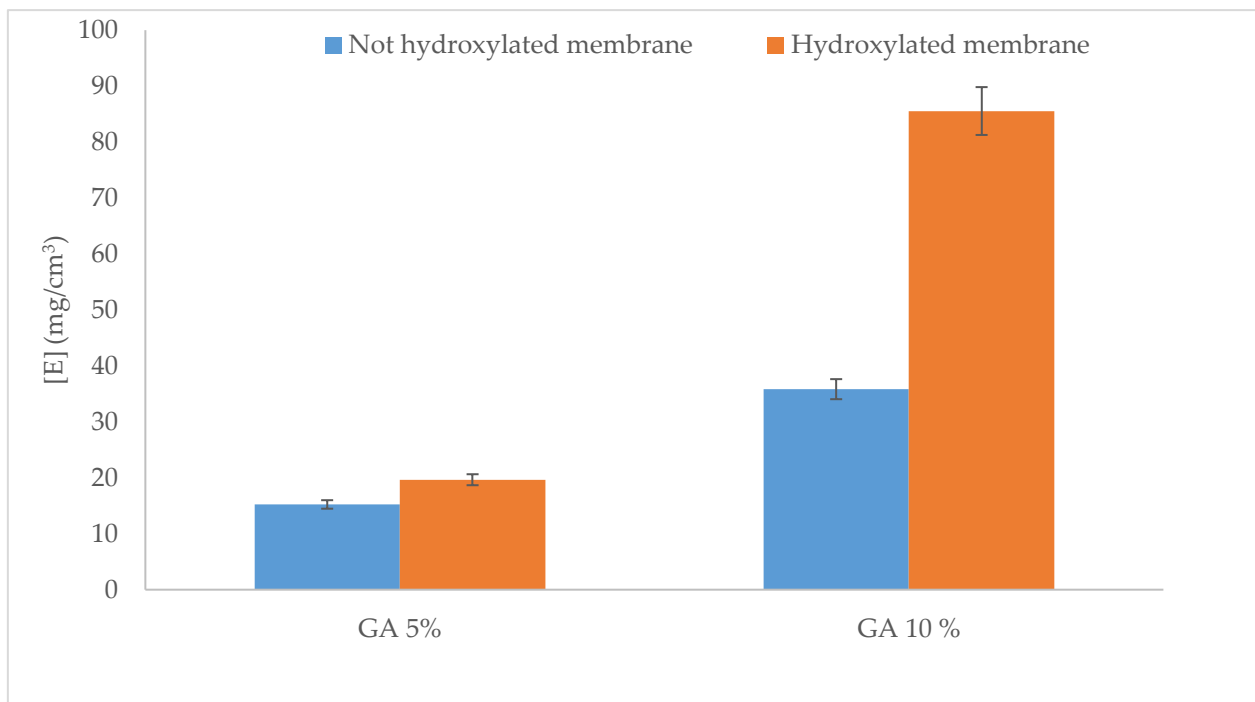


**Figure 5.5.** Immobilized enzyme amount depending on hydroxylation and GA concentration.

Immobilized enzyme concentration increased to about 58% by increasing the GA concentration when the fibers are non-hydroxylated. The situation is different in the case of hydroxylated fibers where the amount of immobilized enzyme increased to about 80.7%. By comparing non-hydroxylated fibers and the hydroxylated ones at the same GA concentration, it can be noticed a slight increase of 14.6% of immobilized enzyme amount by using 5% GA concentration. On the other hand, a significant increase of about 60.5% of immobilized amount occurred between non-hydroxylated fibres and hydroxylated fibres by performing the covalent immobilization with 10% GA concentration. During hydroxylation process the density of hydroxyl groups on the membrane should increase, consequently more silanol molecules should react. Therefore, more amino-groups should be exposed on the hydroxylated fibers in contrast to the non-hydroxylated ones. Probably, by using 5% GA concentration, amino-groups formed on the surface are not completely quenched. A further functionalization of amino-groups may occur by using 10% GA concentration with a final higher amount of immobilized enzyme. An additional effect that could cause higher enzyme immobilization is given by the formation of GA multilayer on membrane due to the GA polymerization [27, 28]. This additional layer can cause enzyme immobilization by covalent

attachment on available aldehyde groups, as well as retention by unspecific interactions as observed in the literature in the case of highly activated glutaraldehyde supports [29].

#### 5.4. Lipase activity measurements

Performance of free and immobilized lipase was tested in a multiphase stirred tank reactor (STR) and in a two-separate-phase biocatalytic membrane reactor (TSP-BMR), respectively. The schematic and operation mode of STR and TSP-BMR were presented in chapter 3, Fig. 3.8 and Fig. 3. 11, respectively.

The specific activity of free lipase was 10.2 ( $\pm 1$ ) U/mg. Observed specific activity of immobilized lipase was evaluated in order to compare the performance with the free one. Specific activities obtained from biocatalytic membrane reactors with different immobilized enzyme amounts were also investigated. Figure 5.6 presents the behavior of the observed catalytic activity and observed specific activity as a function of immobilized enzyme amount. Immobilization strategy is also highlighted.

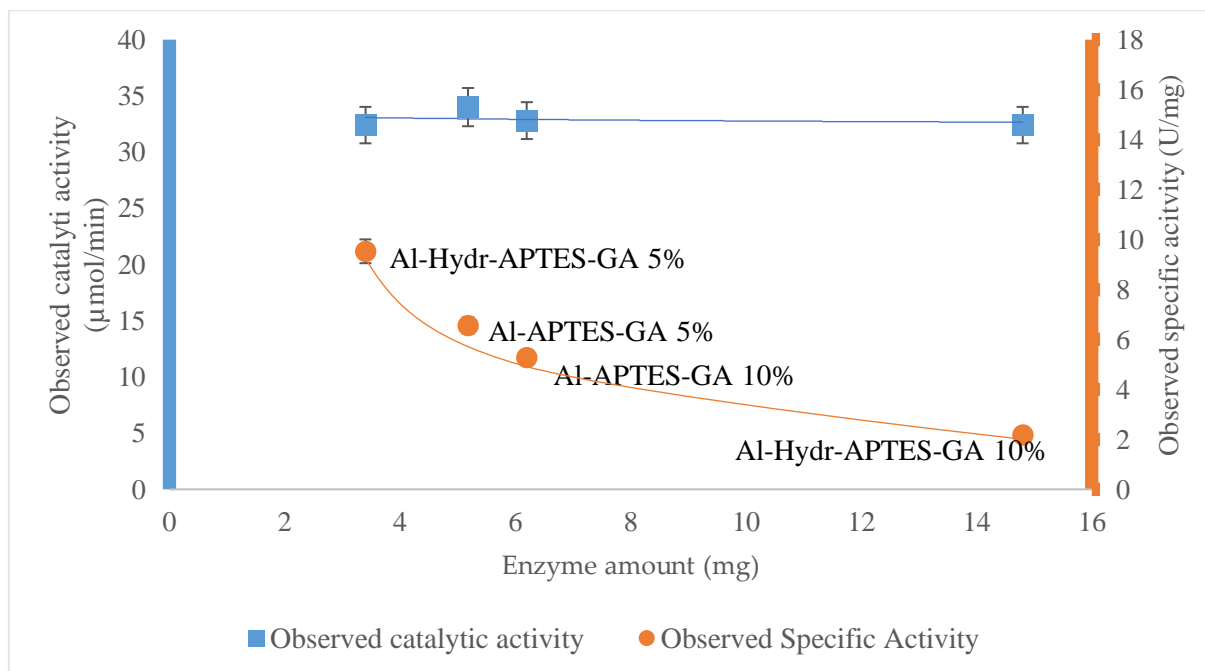


**Figure 5.6.** Trend of observed specific activity depending on immobilized enzyme amount.

Results show that observed catalytic activity is constant whilst observed specific activity decreases with increase of enzyme amount. This means that the same amount of immobilized

lipase works at the interface and the enzyme immobilized in excess not contributing to the reaction, negatively affects the observed specific activity, since the value is normalized by the total immobilized enzyme mass. Crowding phenomena, mass transport and interfacial properties contribute to the overall observed effect. Indeed, the best results in terms of observed specific activity, were achieved in the case of the lower amount of immobilized lipase, i.e., in the case of Al-Hydr-APTES-GA 5% where the enzyme retains an observed specific activity of about 93% compared to the free one ( $10.2 \pm 1$  U/mg). Therefore, a lower enzyme amount was not investigated since the observed specific activity ( $9.5 \pm 0.5$  U/mg) was similar to the one of the free enzyme. In the case of Al-Hydr-APTES-GA 10%, the highest immobilized enzyme amount causes a considerably decay of observed specific activity while Al-APTES-GA 5% and Al-APTES-GA 10% retain an observed specific activity about 65% and 52%, respectively. Besides, the observed specific activity of the immobilized lipase does not undergo significant variations after 6 cycles of measurements, for a total time of about 18 days (Figure 5.7). After each reaction cycle any permeability change was observed.

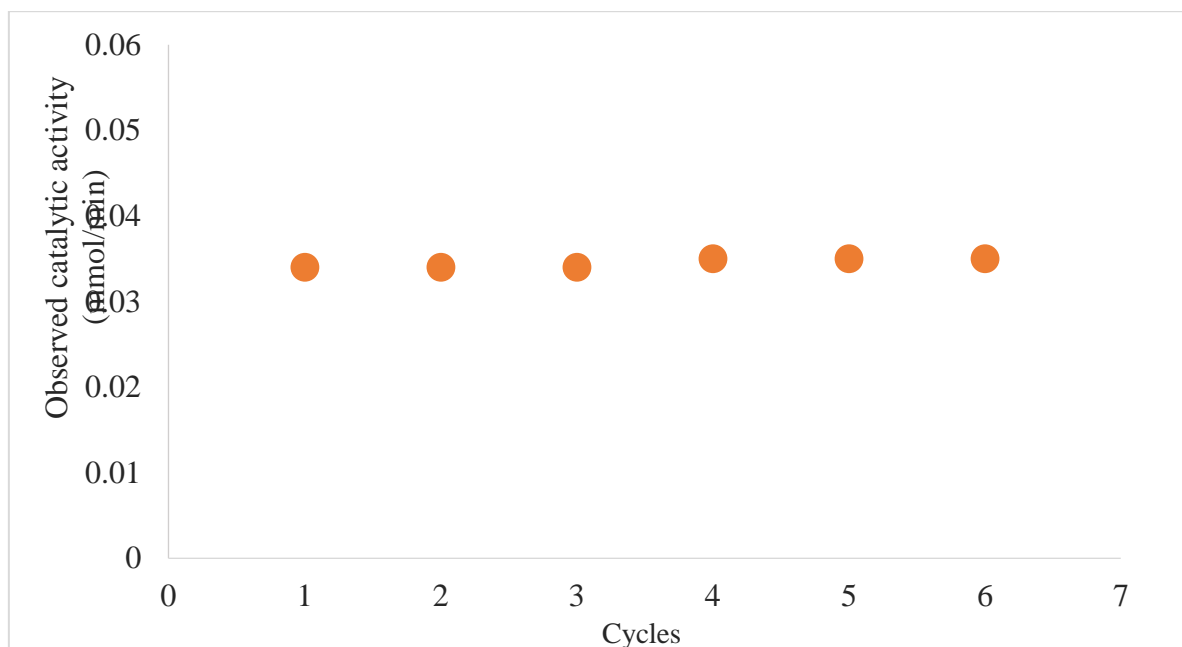


**Figure 5.7.** Observed catalytic activity of immobilized lipase after different reaction cycles carried out for about 18 days.

The behavior confirms that the amount of immobilized biocatalyst is a key parameter to be optimized in biocatalytic membrane reactor development since higher amount of enzyme does not implies better performance of the reactor system. By comparing results obtained in this work with a previous study about lipase from *Candida rugosa*, where the TSP-BMR was developed by immobilizing the enzyme onto polymeric membranes through physical entrapment [30], it is possible to confirm that better performance of the immobilized lipase was detected. In that case, about 0.044 mg of lipase from *Candida rugosa* was immobilized onto asymmetric polyamide hollow fiber membranes and the reaction was performed recirculating 200 mL of organic phase (olive oil) with an axial flow rate of 80 mL/min along the shell side and 600 mL of aqueous phase (50 mM phosphate buffer pH 8.00) with an axial flow rate of 400 mL/min along the lumen side. Volumetric reaction rate of free and immobilized lipase from *Candida rugosa* resulting from the two studies are reported in Table 5.1.

**Table 5.1.** Volumetric reaction rate resulting from the study about lipase immobilized with different approaches onto different matrices.

	Volumetric reaction rate (mmol/dm <sup>3</sup> h)	
	Free lipase	Immobilized lipase
<b>In a previous work with Polyamide membranes [30]</b>	6.95 (± 0.61)	0.044 (± 0.008)
<b>In the present work with Alumina membranes</b>	12.4 (± 0.62)	7.2 (± 0.36)

Native lipase from *Candida Rugosa* previously studied in a STR from Giorno et al. [30] has a lower activity respect from the native lipase examined in the present study, probably due to lower purity of the enzymatic powder. Independently from a lower volumetric reaction rate, a decrease of about 99% occurred after the immobilization of lipase onto polymeric membranes by physical entrapment, as reported in Table 6. On the other hand, volumetric reaction rate of lipase from *Candida rugosa* studied in this work decreases only about 34% after covalent immobilization onto alumina membranes. Despite of the covalent attachment of the enzyme on the inorganic support, which in most cases causes a decrease of the enzymatic performance due to modifications of the native conformation of protein, as

reported in literature [14], the enzyme preserved better performance than in the polyamide membrane, where it was immobilized by physical entrapment.

### 5.5. Inorganic membrane regeneration

The suitability of inorganic membranes for TSP-BMR development was also demonstrated after enzyme removal by cleaning procedure. In fact, the initial membrane permeability ( $507 \pm 51$  L/hm<sup>2</sup>bar) was completely restored ( $527 \pm 68.5$  L/hm<sup>2</sup>bar). In Figure 5.7 membrane pure water permeability before and after the experiments are compared.

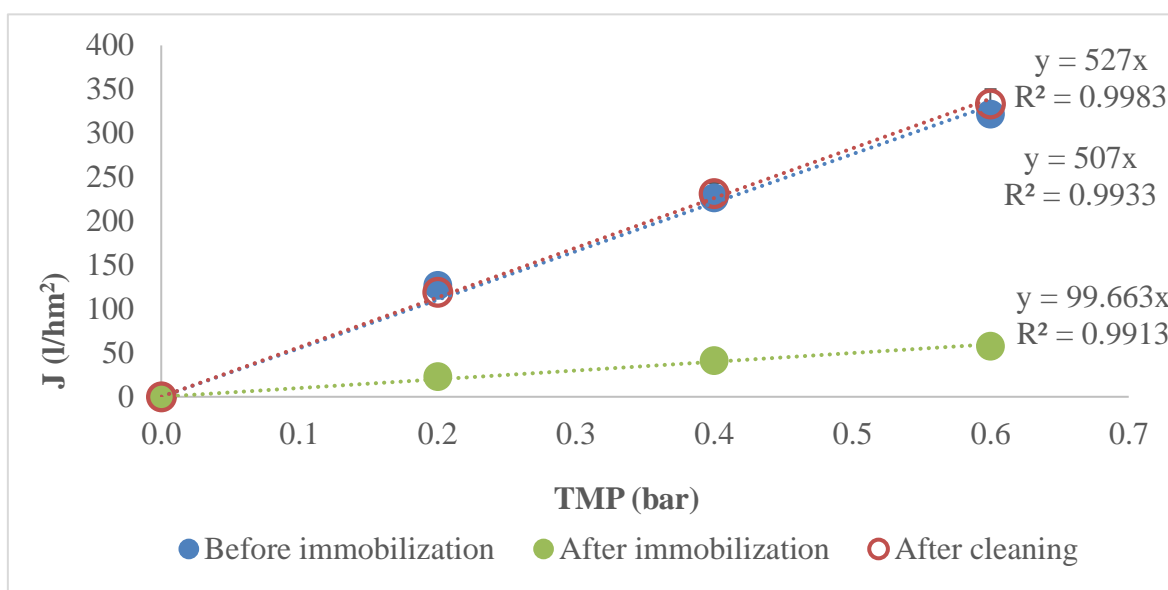


**Fig. 5.7.** Comparison of membrane pure water permeability before and after cleaning process.

Therefore, this procedure allows the reuse of the fibers for enzyme immobilization in case of biomolecule denaturation during industrial processes.

### 5.6. Conclusions

In this chapter, the suitability of alumina hollow fiber membranes to improve the performance of a two-separate-phase biocatalytic membrane reactor was demonstrated. An appropriated method in order to immobilize lipase from *Candida rugosa* by covalent binding on alumina membrane was identified. Results confirmed that a higher immobilized enzyme amount does not correspond to a higher observed specific activity and that it is a parameter to be optimized. The best results, in terms of observed specific activity, were obtained by

performing the immobilization process through hydroxylation of alumina membranes followed by a 5% glutaraldehyde treatment (Al-Hydr-APTES-GA 5%) in which immobilized lipase retains about 93% of the observed specific activity. In the mentioned conditions, it is possible to carry out olive oil hydrolysis without any significant variation of enzymatic specific activity for about 6 reaction cycles with a running period of about 18 days.

## References

1. Lu, G.Q.; Diniz da Costa, J.C.; Duke, M.; Giessler, S.; Socolow, R.; Williams, R.H.; Kreutz, T. *Inorganic membranes for hydrogen production and purification: A critical review and perspective. J. Colloid Interface Sci.* 2007, 314, 589–603.
2. Armor, J.N. *Applications of catalytic inorganic membrane reactors to refinery products. J. Membr. Sci.* 1998, 147, 217–233.
3. Ing.Steffen Wielanda, Ing.Thomas Melina, Ing.A. Lamm, *Membrane reactors for hydrogen production, Chemical Engineering Science, Volume 57, Issue 9, May 2002, Pages 1571–1576.*
4. Gbenedio, E.; Wu, Z.; Hatim, I.; Kingsbury, B.F.K.; Li, K. *A multifunctional Pd/alumina hollow fibre membrane reactor for propane dehydrogenation. Catal. Today* 2010, 156, 93–99.
5. Weber, R.; Chmiel, H.; Mavrov, V. *Characteristics and application of new ceramic nanofiltration membranes. Desalination* 2003, 157, 113–125. [CrossRef]
6. Neomagus, H.W.J.; Saracco, G.; Wessel, H.F.; Versteeg, G. *The catalytic combustion of natural gas in a membrane reactor with separate feed of reactants. Chem. Eng. J.* 2000, 77, 165–177.
7. Koonaphapdeelert, S.; Li, K. *The development of ceramic hollow fibre membranes for a membrane contactor. Desalination* 2006, 200, 581–583.
8. Wang, Z.-H.; Jin, G. *Covalent immobilization of proteins for the biosensor based on imaging ellipsometry. J. Immunol. Methods* 2004, 285, 237–243.
9. Magnan, E. *Immobilization of lipase on a ceramic membrane: Activity and stability. J. Membr. Sci.* 2004, 241, 161–166.
10. Lozano, P. *Active membranes coated with immobilized Candida antarctica lipase B: Preparation and application for continuous butyl butyrate synthesis in organic media. J. Membr. Sci.* 2002, 201, 55–64.
11. Van Gestel, T. *Corrosion properties of alumina and titania NF membranes. J. Membr. Sci.* 2003, 214, 21–29.
12. Wessely, L.; Samhaber, W.M. *Separation Performance of Polymer Membranes for Organic Solvent Mixtures. Chem. Eng. Trans.* 2013, 32, 1815–1890.
13. Penha, F.M.; Razzadori, K.; Proner, M.C.; Zanatta, V.; Zin, G.; Tondo, D.W.; de Oliveira, J.V.; Petrus, J.C.C.; di Luccio, M. *Influence of different solvent and time*

- of pre-treatment on commercial polymeric ultrafiltration membranes applied to non-aqueous solvent permeation. Eur. Polym. J.* 2015, 66, 492–501.
14. Jochems, P.; Satyawali, Y.; Diels, L.; Dejonghe, W. *Enzyme immobilization on/in polymeric membranes: Status, challenges and perspectives in biocatalytic membrane reactors (BMRs). Green Chem.* 2011, 13, 1609.
  15. Tanvir, S.; Morandat, S.; Frederic, N.; Adenier, H.; Pulvin, S. *Activity of immobilised rat hepatic microsomal CYP2E1 using alumina membrane as a support. New Biotechnol.* 2009, 26, 222–228.
  16. Milka, P.; Krest, I.; Keusgen, M. *Immobilization of alliinase on porous aluminum oxide. Biotechnol. Bioeng.* 2000, 69, 344–348.
  17. Tanvir, S.; Pantigny, J.; Boulnois, P.; Pulvin, S. *Covalent immobilization of recombinant human cytochrome CYP2E1 and glucose-6-phosphate dehydrogenase in alumina membrane for drug screening applications. J. Membr. Sci.* 2009, 329, 85–90.
  18. Aissaoui, N.; Landoulsi, J.; Bergaoui, L.; Boujday, S.; Lambert, J.-F. *Catalytic activity and thermostability of enzymes immobilized on silanized surface: Influence of the crosslinking agent. Enzym. Microb. Technol.* 2013, 52, 336–343.
  19. Hou, J.; Dong, G.; Ye, Y.; Chen, V. *Laccase immobilization on titania nanoparticles and titania-functionalized membranes. J. Membr. Sci.* 2014, 452, 229–240.
  20. Yang, Z.; Si, S.; Dai, H.; Zhang, C. *Piezoelectric urea biosensor based on immobilization of urease onto nanoporous alumina membranes. Biosens. Bioelectron.* 2007, 22, 3283–3287.
  21. Kjellander, M.; Mazari, A.M.A.; Boman, M.; Mannervik, B.; Johansson, G. *Glutathione transferases immobilized on nanoporous alumina: Flow system kinetics, screening, and stability. Anal. Biochem.* 2014, 446, 59–63.
  22. Giorno, L.; Molinari, R.; Natoli, M.; Drioli, E. *Hydrolysis and regioselective transesterification catalyzed by immobilized lipases in membrane bioreactors. J. Membr. Sci.* 1997, 125, 177–187.
  23. Karl-Erich Jaeger, Thorsten Eggert, *Lipases for biotechnology, Current Opinion in Biotechnology, Volume 13, Issue 4, 1 August 2002, Pages 390–397.*
  24. Prazeres, D.M.F.; Cabral, J.M.S. *Enzymatic membrane bioreactors and their applications. Enzym. Microb. Technol.* 1994, 16, 738–750.
  25. Maruyama, T., Nakajima, M., Uchikawa, S. et al. *J Amer Oil Chem Soc* (2000) 77: 1121. doi:10.1007/s11746-000-0176-4



26. Miletić, N.; Fahriansyah; Nguyen, L.-T.T.; Loos, K. *Formation, topography and reactivity of Candida antarctica lipase B immobilized on silicon surface. Biocatal. Biotransform.* 2010, 28, 357–369.
27. Monsan, P. *Optimization of glutaraldehyde activation of a support for enzyme immobilization. J. Mol. Catal.* 1978, 3, 371–384.
28. Migneault, I.; Dartiguenave, C.; Bertrand, M.J.; Waldron, K.C. *Glutaraldehyde: Behavior in aqueous solution, reaction with proteins, and application to enzyme crosslinking. Biotechniques* 2004, 37, 790–802.
29. Barbosa, O.; Ortiz, C.; Berenguer-Murcia, Á.; Torres, R.; Rodrigues, R.C.; Fernandez-Lafuente, R. *Glutaraldehyde in bio-catalysts design: A useful crosslinker and a versatile tool in enzyme immobilization. RSC Adv.* 2014, 4.
30. Giorno, L.; Drioli, E. *Catalytic behaviour of lipase free and immobilized in biphasic membrane reactor with different low water-soluble substrates. J. Chem. Technol. Biotechnol.* 1997, 69, 11–14.

## **CHAPTER 6**

### ***Monophasic biocatalytic membrane reactor***

#### ***Abstract***

Monophasic aqueous biocatalytic membrane reactor was developed using  $\beta$ -glucosidase from Almond immobilized by covalent binding into inorganic hollow fibre or by entrapment in polymeric hollow fibre membranes. The enzymatic hydrolysis of oleuropein was studied. Oleuropein is a phenolic compound known for its different pharmacological effects, but different studies showed that the biotransformation produces aglycon species which have more marked effects than oleuropein. In a previous work, biocatalytic membrane reactor (BMR) was realized entrapping the enzyme into the pores of polymeric membranes. In the present work, the study was advanced by both using inorganic lab-made membranes and developing a prototype of the BMR using commercial polymeric membrane. Therefore, the enzyme was covalently immobilized on ceramic membrane in order to avoid enzyme leaching, improve the enzyme distribution within the membrane and consequently improve reactor performance. Ceramic membranes do not possess reactive groups for direct coupling of enzyme and the activation of hydroxy, amino, amide, and carboxy was needed. Therefore, fibres were treated with a 5% solution of silanization reagent ((3-aminopropyl) triethoxysilane, APTES) and then with a 10% solution of cross-linker reagent (glutaraldehyde). Covalent immobilization process was optimized by investigating the effect of the initial protein concentration on the immobilized enzyme amount. Commercial oleuropein and natural feed were used as substrate to perform the reaction. Natural feed consists in olive leaves extracts belonging to different cultivar collected in different periods. Before performing the reaction in the BMR, olive leaves extracts were characterized in order to determine the amount of oleuropein. Results showed that same performance of the system was obtained by feeding either pure oleuropein or extract from olive leaves, demonstrating that the presence of the other polyphenols do not alter the catalytic performance of the immobilized enzyme. In addition, a prototype-scale implementation of the biocatalytic membrane reactor by using commercial polymeric membranes was carried out. A conversion degree of 30% was achieved with a maximum immobilized enzyme amount of 3.5 mg/cm<sup>3</sup>.

## **6.1. Introduction**

For centuries plants have provided useful active ingredients. In the last century, the use of natural medicine has expanded and many researches have been performed on active components of herbs. These components are known as plant secondary metabolites [1] and possess higher antioxidative, antimicrobial, antiviral and anti-inflammatory properties [2-4]. Free radical scavenging properties of these metabolites can be explained by their high antioxidant activities. Phytochemicals in fruits and vegetables act synergistically and additively to provide potential health benefits against chronic diseases by inhibiting the harmful effects of free radicals [2,4-7]. The traditional Mediterranean diet is characterized by high consumption of foods of plant origin, relatively low consumption of red meat, and high consumption of olive oil, which in several studies has been reported to have physiologically active polyphenols [8,9]. Also olive leaves are rich in polyphenols, especially in oleuropein, rutin, verbacoside, apigenin-7-glucoside and luteolin-7-glucoside [10,11]. The concentration of polyphenolic compounds in olive leaves changes depending on the quality, origin and variety [12] of the plant material. Oleuropein is the most abundant polyphenol in olive fruits and leaves, which has been used in a number of medical treatments [10]. In particular, it was demonstrated that the aglycon, produced by oleuropein hydrolysis, has potential application as an antimicrobial agent in some fairly common diseases of olive trees [5] and also for its strong active antioxidant property [6-10]. Despite the reported importance of the oleuropein aglycon biological properties, this molecule is commercially unavailable. Chromatographic purification methods for oleuropein aglycon recovery can only be used for laboratory applications. Currently, enzymatic procedures for oleuropein aglycon production on productive scale are not available. In this chapter the study aimed to investigate the performance of immobilized  $\beta$ -glucosidase from Almond in a monophasic biocatalytic membrane reactor for the production and isolation of oleuropein aglycon. The influence of the glucose, the co-product of the isomer of oleuropein aglycon, was studied in batch system to investigate the presence of a potential inhibition phenomena on the enzyme. The biocatalyst performance was then studied both when it is covalently immobilized into inorganic membranes and entrapped into polymeric membrane. In this last case the system was also implemented on a pilot prototype scale. The effect of the amount of immobilized biocatalyst on the conversion was also investigated. Then, hydrolysis reaction was performed feeding the system with both a solution of commercial oleuropein and olive leaves extract containing oleuropein.

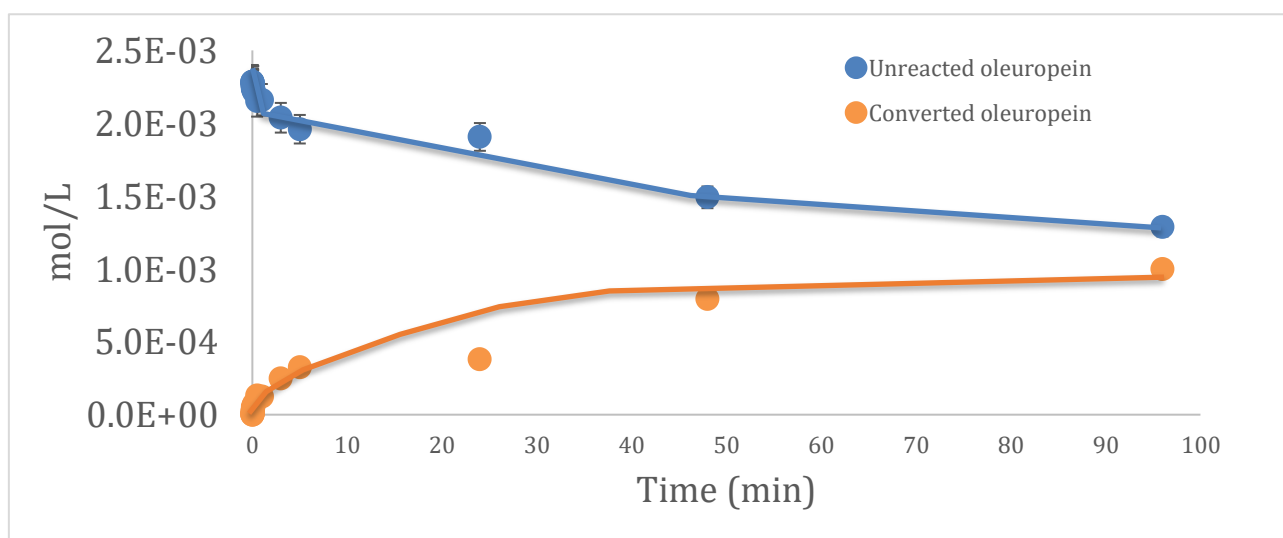
## 6.2. Monophasic BMR with covalently immobilized $\beta$ -glucosidase

In this section the study was focused on the performance of immobilized  $\beta$ -glucosidase in a monophasic biocatalytic membrane reactor. Studies about kinetic parameters of the free  $\beta$ -glucosidase in a stirred tank reactor were carried out in order to better define enzymatic profile and to determine the type of inhibition in case of product accumulation.

### 6.2.1. $\beta$ -Glucosidase activity measurements

#### 6.2.1.1. Determination of kinetic parameters of free $\beta$ -glucosidase

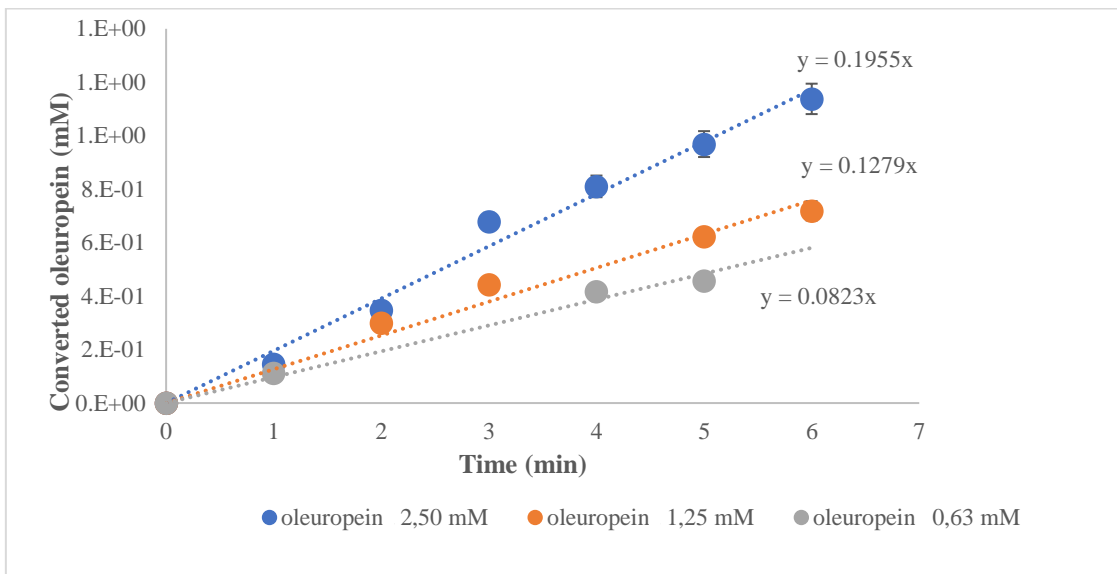
Before immobilizing  $\beta$ -glucosidase on the membrane, the enzyme was tested in a stirred tank reactor (STR) in order to investigate the performance in its native conformation, through determination of kinetics parameters by using operative conditions described in the previous chapter. Figure 6.1 shows an example of reaction trend in a STR with corresponding concentration profile of substrate (●) and product (●).



**Fig. 6.1.** Typical concentration profile of oleuropein decrease and product formation in a STR.

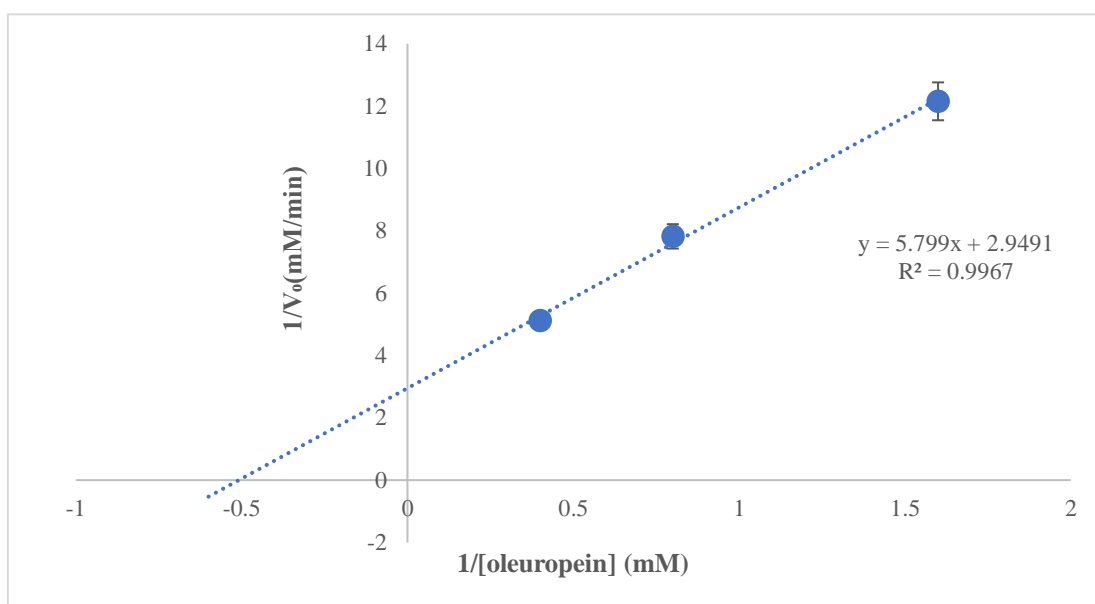
Since the standard of oleuropein hydrolysis product (aglycon) is not commercially available, the product profile in the Figure above is referred to as "converted oleuropein", which is stoichiometric to the formed aglycon and glucose. The stoichiometry of the reaction was cross-checked by measuring the glucose concentration.

In Figure 6.2 results of typical runs at various substrate concentration is represented. Here only the initial linear reaction time is considered since it is the part relevant for the initial reaction rate evaluation ( $V_r$ ). From the slope of each straight-line during the first minutes of hydrolysis reaction it is possible to calculate the value of initial reaction rate, that is  $8.23 \cdot 10^{-2}$ ,  $1.28 \cdot 10^{-1}$ ,  $1.95 \cdot 10^{-1}$  mM/min when the initial substrate used is 0.63, 1.25 and 2.50 mM, respectively. In agreement with the enzyme kinetic, it is clear that an increase of substrate concentration implies an increase of initial reaction rate.



**Fig. 6.2.** Example of concentration of converted oleuropein as a function of time by increasing initial substrate concentration.

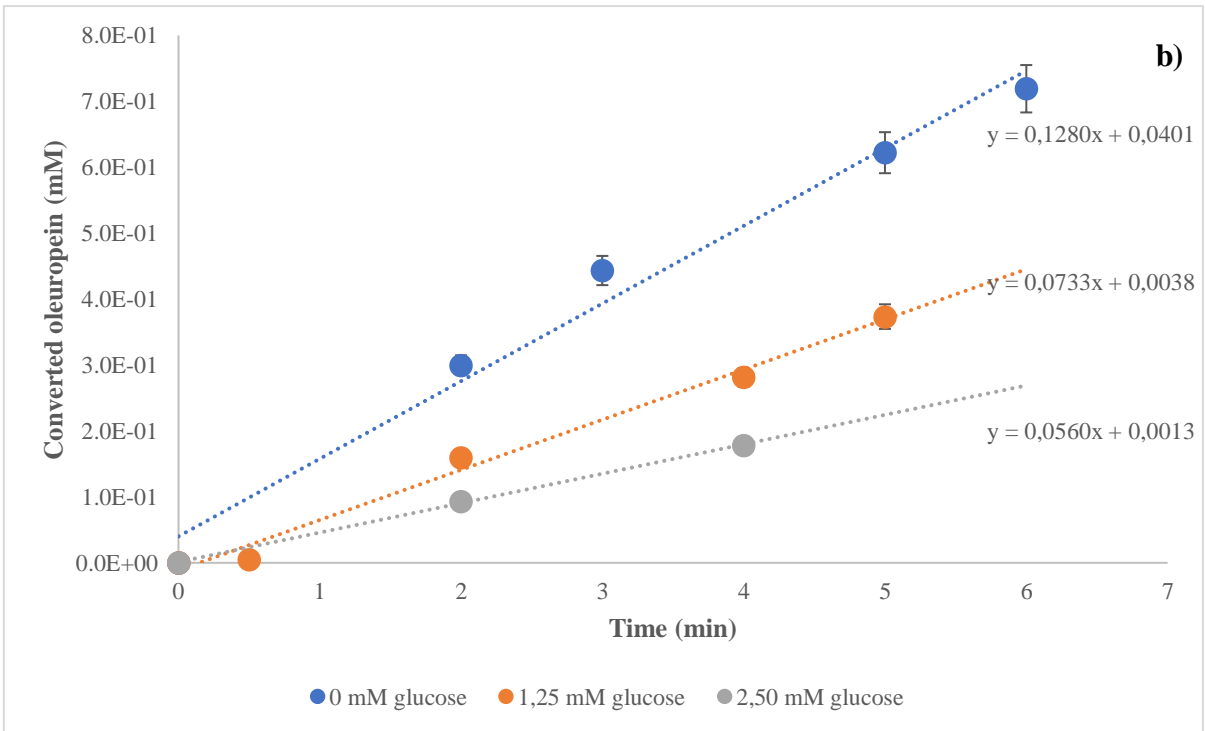
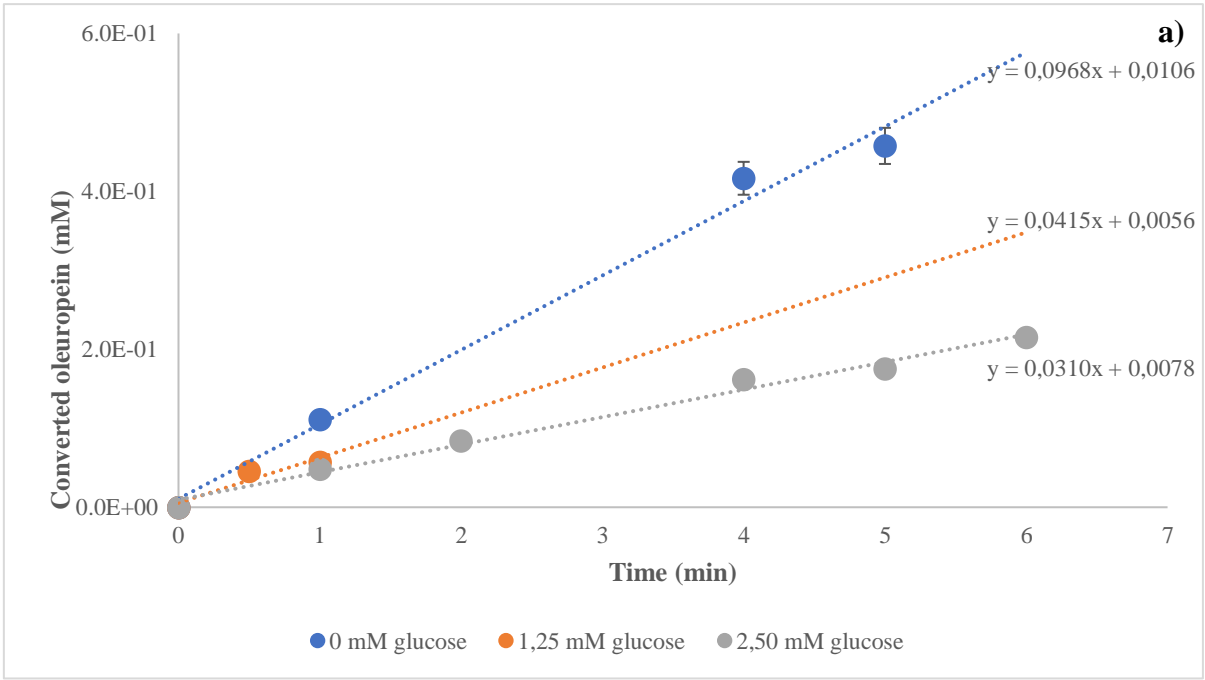
Initial reaction rates achieved from experiments and oleuropein concentrations are related in the Lineweaver–Burk graph illustrated in Fig. 6.3, where values of  $K_m$  (1.97 mM) and  $V_{max}$  (0.34 mM/min) were calculated ( $\frac{1}{V_0} = \frac{K_m}{V_{max}} \frac{1}{[S]} + \frac{1}{V_{max}}$ ).



**Fig. 6.3.**  $K_m$  and  $V_{max}$  calculation from Lineweaver–Burk graph.

#### 6.2.1.2 Study of inhibition by product

Operative conditions used in order to determine the type of inhibition and  $K_i$  of  $\beta$ -glucosidase were described in the Table 3.4 of Chapter 3. Results obtained from experiments were represented in the following Figures (Fig 6.3a,6.3b,6.3c) in terms of concentration of converted substrate (equivalent to obtained product) as a function of different concentrations of initial oleuropein and initial glucose.



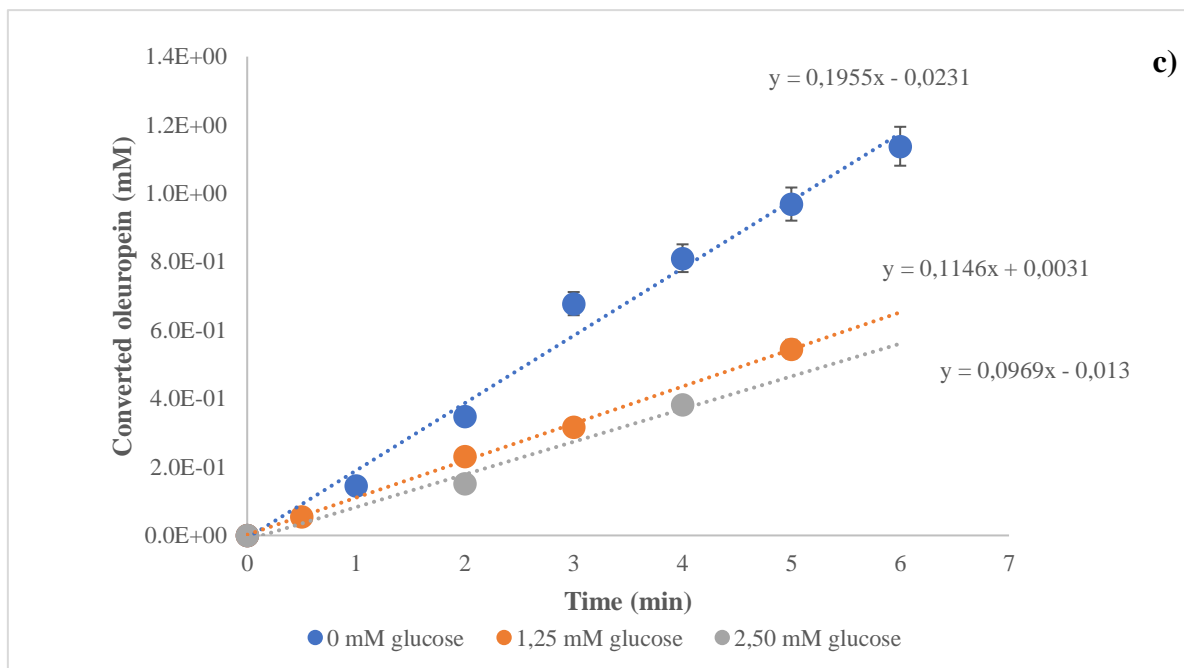


**Fig. 6.3.** Converted oleuropein versus time using different oleuropein initial concentration: 0.63 mM (a), 1.25 mM (b) and 2.5 mM (c) and by varying glucose concentration.

As expected, the reaction rate decreases by increasing glucose concentration and it is higher in absence of inhibitor. In the Figure 6.4 the results about reaction rate of  $\beta$ -glucosidase as a function of different initial oleuropein and glucose concentrations are summarized.

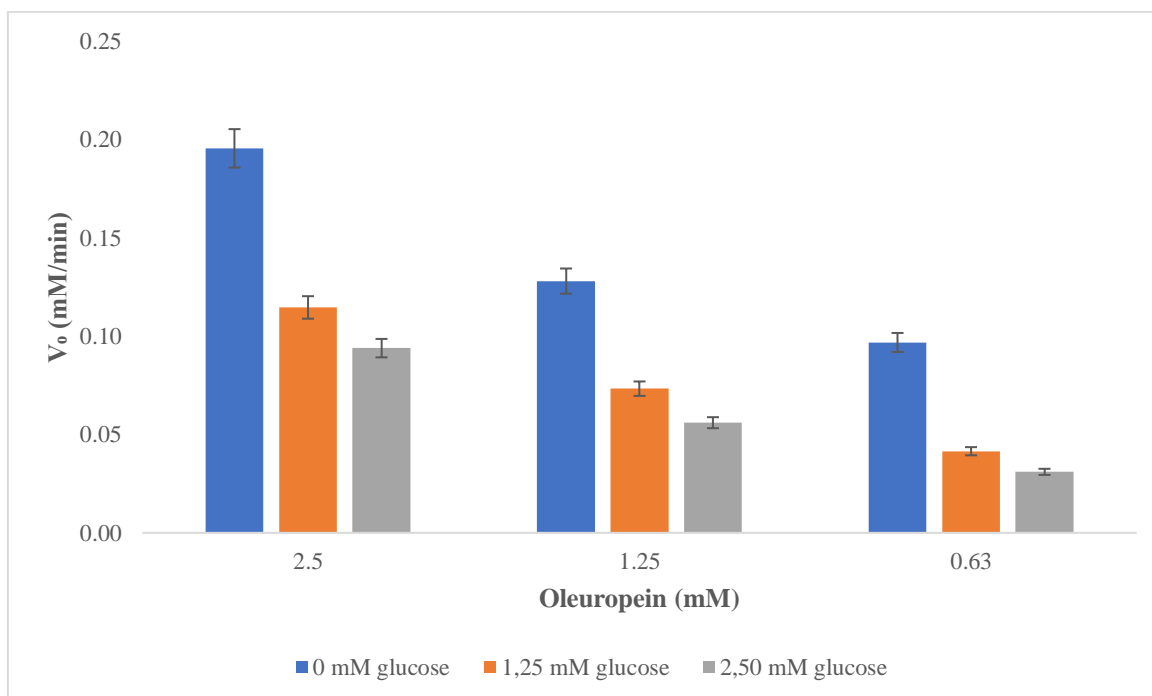


**Fig. 6.4.** Initial reaction rate ( $V_0$ ) as a function of initial substrate and inhibitor concentration.



As previously described,  $V_{max}$  and  $K_m$  were calculated from equations of straight lines obtained. Table 6.1 reports the resulting values of  $V_{max}$  and  $K_m$  in presence of inhibitor.

**Tab. 6.1.**  $V_{max}$  and  $K_m$  in presence of inhibitor

Glucose (mM)	$K_m$ (mM)	$V_{max}$ (mM/min)
0	1.97	0.3
1.25	$3.7 \cdot 10^{-3}$	0.3
2.50	$5.8 \cdot 10^{-3}$	0.3

By analyzing data reported in table 6.1 and by plotting the corresponding Lineweaver–Burk graph (Fig. 6.5) it was possible to establish the type of enzymatic inhibition.

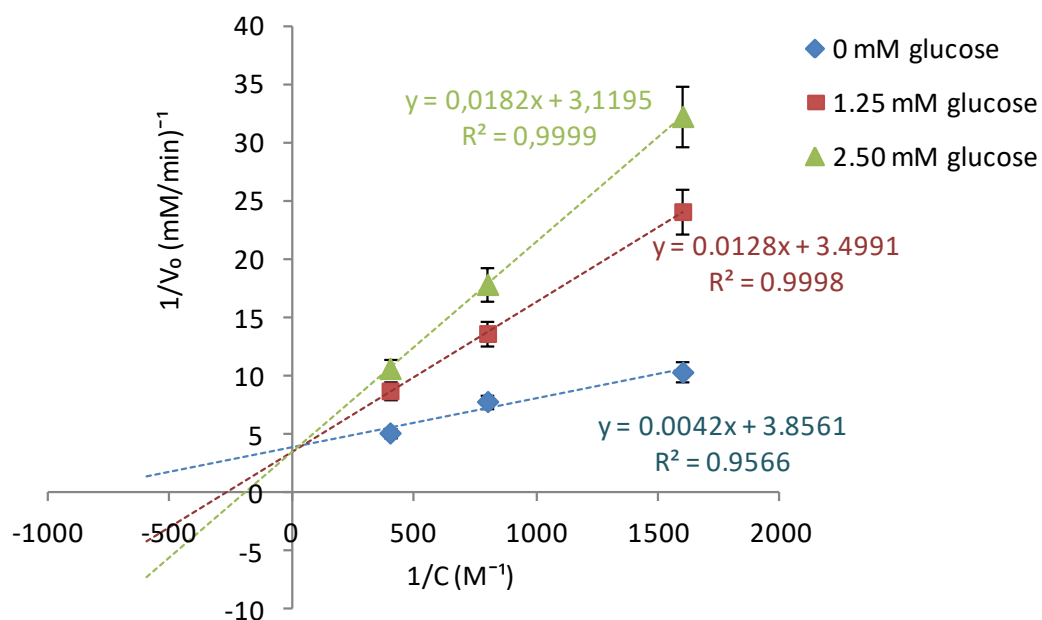


**Fig. 6.5.** Lineweaver-Burk graph with increased concentrations of inhibitor.

Graphic and resulting data define the typical profile belonging to a competitive enzyme inhibition (described in Chapter 2). In inhibited reaction, the true values of the  $K_m$  and  $V_{max}$  do not change. According the Michaelis-Menten assumptions, this behavior means a reduction of the enzyme affinity towards its substrate due to the presence of inhibitor. The measured values of  $K_m$  in the presence of the inhibitor are altered, and are called the apparent  $K_m$ . The apparent  $K_m$  varies depending on the inhibitor concentration involved. In fact, an increase of the apparent  $K_m$  occurs by increasing inhibitor concentration. In the same time,

the apparent  $V_{max}$  does not undergo variations because it is unaffected by a competitive inhibitor. This is because once substrate binds to the enzyme, the reaction proceeds normally, and therefore  $V_{max}$  depends only on the maximum possible [ES] complex concentration (and on the  $k_{cat}$ , but  $k_{cat}$  is unaffected by a competitive inhibitor), and the maximum ES concentration depends only on the total amount of enzyme present. Thus, inhibitor does not prevent catalysis in ES but is able to compete with the substrate for the active site.

Once confirmed the type of inhibition,  $K_i$  was derived from the slope of each straight line represented in Fig. 6.5. The slope corresponds to the value of  $\alpha \frac{K_m}{V_{max}}$  in the equation which describe a competitive inhibition ( $\frac{1}{v_0} = \alpha \frac{K_m}{V_{max}} \frac{1}{[S]} + \frac{1}{V_{max}}$ ). By considering that the minimum value of  $\alpha$  is 1 in the case of inhibitor absence, it was possible measure  $\alpha$  values in the case of 1.25 mM and 2.50 mM inhibitor concentration. Taking into account data reported in Fig. 6.5, it was possible to define the following kinetic parameters (Tab. 6.2).

**Tab. 6.2.** Kinetics parameters depending on inhibitor concentration

[I] (mM)	$\frac{K_m}{V_{max}}$	$\alpha$
0	$4.2^{-3}$	1
1.25	$1.23^{-2}$	2.93
2.50	$1.81^{-2}$	4.31

From the straight line obtained by reporting  $\alpha$  values as a function of the inhibitor concentration, it was possible establish the value of  $K_i$  (Figure 6.6).

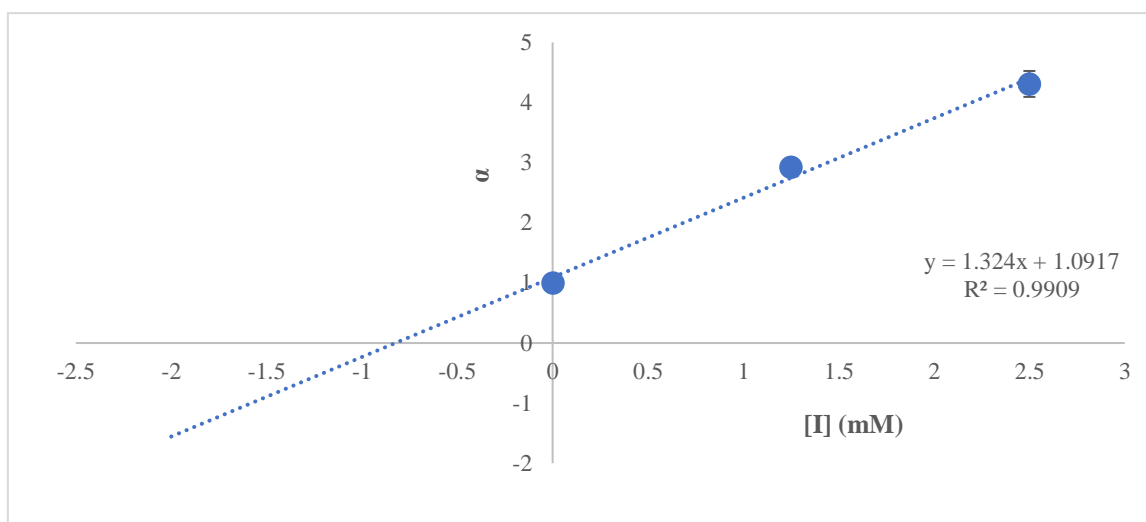


**Fig. 6.6.** Variation of  $\alpha$  parameter in function of inhibitor concentration.

In fact, by considering the equation of the represented straight line in Figure 6.6. ( $\alpha = 1 + \frac{[I]}{K_i}$ ), the value of resulting  $K_i$  was  $0.75 (\pm 0.07)$  mM. Thus, during the hydrolysis reaction of oleuropein by  $\beta$ -glucosidase, the co-product glucose acts as competitive inhibitor by negatively affecting the enzymatic performance if not removed from the reaction mixture. The stirred tank reactor does not allow to selectively recover the reaction products as soon as it is formed and an accumulation of the new formed inhibitor is unavoidable. On the contrary, in a biocatalytic membrane reactor, hydrolysis reaction takes place into the pores of biocatalytic membrane (where the enzyme is immobilized) and the new formed product is continuously removed from catalytic site by a convective flow. Thus, each pore works like a continuous stirred tank reactor where no accumulation of product occurs and immobilized enzyme does not undergo kinetic alteration due to the presence of inhibitor in the reaction environment. In this way, continuous operations with a constant enzymatic performance is possible. In the following paragraph, results about performance of immobilized  $\beta$ -glucosidase in such system will be reported and discussed.

### **6.2.2. Characterization of grafted alumina membranes surface**

Prior to enzyme immobilization, as explained in Materials and Methods section, blank experiments were carried out on native membranes to exclude immobilization given by enzyme adsorption or entrapment, since the aim is to bind the enzyme covalently. Also for the  $\beta$ -glucosidase, no adsorbed or entrapped enzyme was detected (as already obtained with the lipase, Chapter 5).

### 6.2.3. Covalent immobilization of $\beta$ -glucosidase

By analyzing results obtained from immobilization of lipase, discussed in the previous chapter, it can be seen that native hydroxyl groups of alumina support are sufficient to allow the immobilization of a considerable enzyme amount able to catalyze reaction in a BMR with a good yield. Therefore, it was considered appropriate to immobilize  $\beta$ -glucosidase by performing the surface functionalization of alumina fibers directly through silanization reagent, thus the hydroxylation process was not performed. In this way, a milder immobilization method was adopted by avoiding the use of very strong reagent (piranha solution) which requires several precautions. In this case the study of immobilization process was focused on the influence of the initial enzyme concentration on the amount of the immobilized enzyme by keeping constant both APTES (5%) and glutaraldehyde concentration (10%) during the functionalization process. By using initial concentration of enzyme of 0.05, 0.1, 0.2, 0.4 mg/ml, the amount of immobilized enzyme resulted 0.9, 2.2, 5, and 7.8 mg. The immobilized enzyme concentration was evaluated by measuring protein concentration in the initial, final, and washing solution through BCA test. Then, the amount of immobilized enzyme, is determined by mass balance according to equation 3.1 (see chapter 3). Experimental data were reported in the Figure 6.6, where the trend of immobilized enzyme amount as a function of different initial enzyme concentration is represented. It is clear that the amount of immobilized enzyme increases as the increase of the initial protein concentration. The slope of the obtained straight line allows to predict the desired immobilized enzyme amount depending on the concentration of enzymatic solution used during the immobilization process.

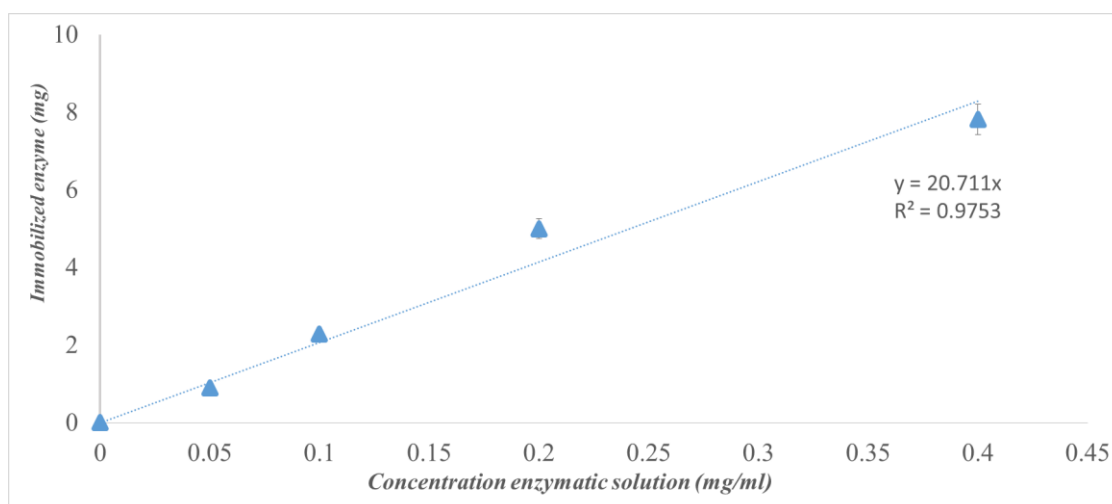


**Fig. 6.6.** Immobilized enzyme amount in function of enzymatic solution concentration

#### **6.2.4. $\beta$ -glucosidase activity measurements in a monophasic biocatalytic membrane reactor**

Hydrolysis reaction of oleuropein was performed by using the different biocatalytic membranes with different immobilized enzyme amount and by using both 2.5 mM pure oleuropein solution and olive leaves extract. Prior to perform the reaction, a characterization of olive leaves extracts belonging to different cultivar was carried out in order to evaluate the oleuropein concentration. Besides, a method for oleuropein extraction from olive leaves was developed.

##### **6.2.4.1. Extraction and characterization of olive leaves extracts**

A method for oleuropein extraction from olive leaves was developed. Briefly, 1 g of olive leaves were pulverized and then macerated in a mixture of ethanol/ultrapure water in a ratio of 80/20 under gentle stirring for 24 h and a temperature of 40 °C. After that, the mixture was centrifuged at 3000 rpm for 10 minutes and the obtained supernatant was filtrated by a filter paper. A schematic representation of the process is reported in the Figure 6.7.

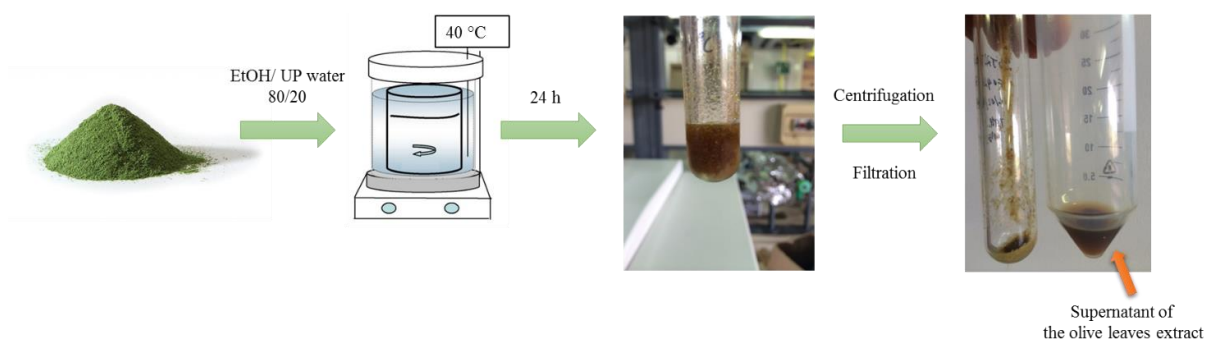


**Fig. 6.7.** Schematic representation of oleuropein extraction from olive leaves.

By analyzing through HPLC the extract obtained from the described process, a concentration of oleuropein of about 5.2 ( $\pm$  2.7) mg/ml was detected. This confirms that a significant oleuropein amount could be obtained from natural source such as olive leaves, which are commonly considered waste material of the oil industry. This approach could be a potential strategy to valorize industrial waste and natural source easily available.

Characterization of olive leaves extract obtained from olive leaves belonging to different cultivar was carried out by HPLC analysis. The higher oleuropein amount was detected in the cultivar “Ciciariello”, this was the reason why this extract was used as feed in the biocatalytic membrane reactor. In Fig. 6.8a, 8b, 8c, The HPLC chromatograms, related to the different analyzed cultivars are reported, from which it is possible to see that together the oleuropein other polyphenols are also present.

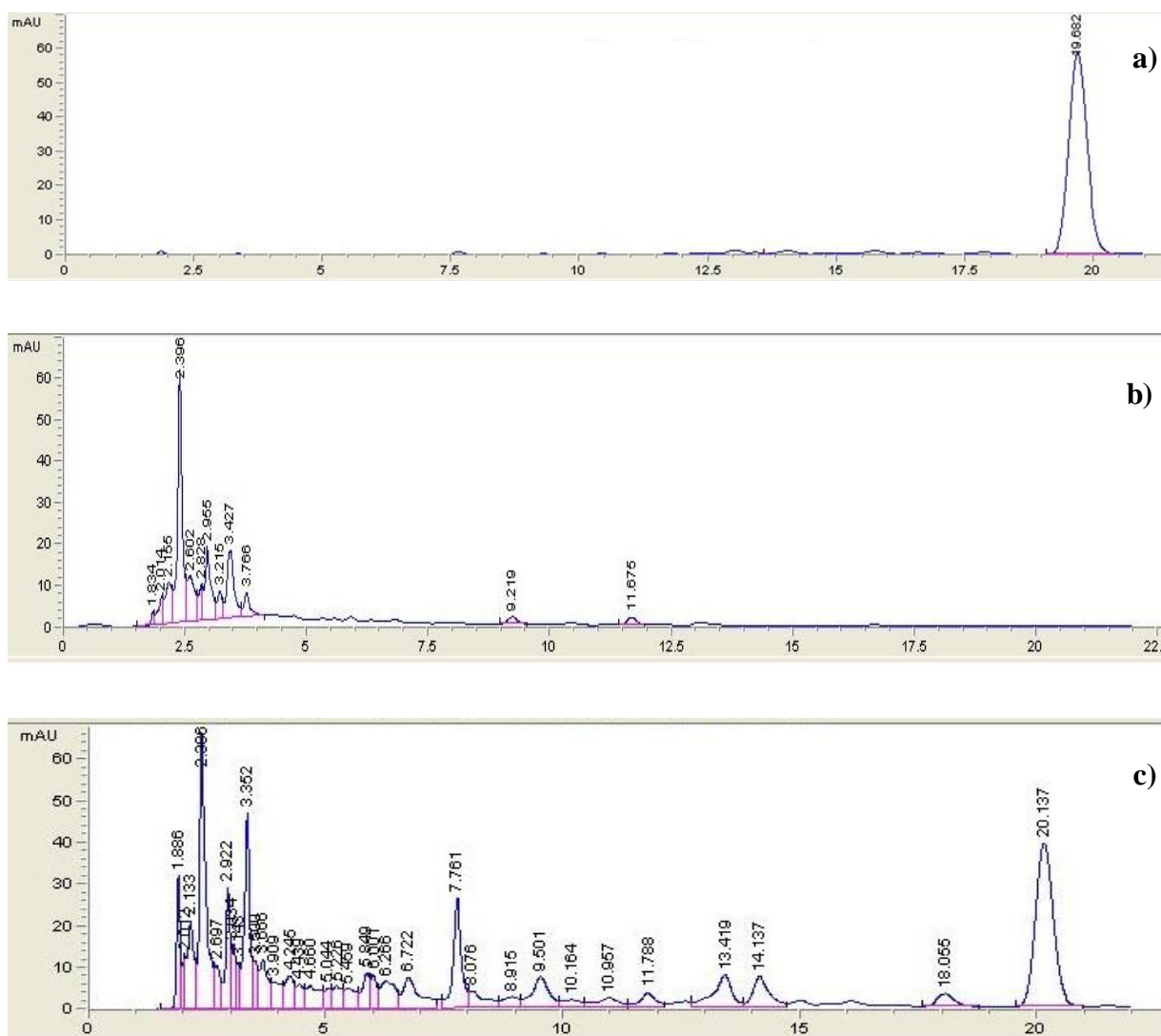


**Fig. 6.8.** Chromatogram of standard oleuropein (a), olive leaves extract belonging both to Ottobratica and Sinopolese cultivar (b) and Ciciariello cultivar (c).

In the table (Tab. 6.3) the corresponding oleuropein concentrations belonging to different cultivars are reported.

**Tab. 6.3.** Oleuropein concentration of olive leaves extracts belonging to different cultivar

<b>CULTIVAR</b>	<b>HARVESTIN PERIOD</b>	<b>OLEUROPEIN CONCENTRATION (mg/ml)</b>
Ottobratica	July 2014	0.04
Sinopolese	July 2014	0.02
Ciciariello	July 2014	2.85

#### ***6.2.5. Monophasic biocatalytic membrane reactor with immobilized $\beta$ -glucosidase by covalent binding***

In the Figure 6.9 is shown a schematic representation of the monophasic biocatalytic membrane reactor where  $\beta$ -glucosidase was immobilized by covalent binding according the method and operation conditions previously described in “materials and method” (Chapter 3). Oleuropein solution is forced to pass through the pores of membrane by a convective mass transport. Here, the substrate met the immobilized biocatalyst and hydrolysis reaction occurred. Aglycon, glucose (products of reaction) and unreacted oleuropein were recovered in the lumen circuit of the system. Hydrolysis reaction was performed as a function of time by using different biocatalytic membranes where the loaded-enzyme amount was 0.9, 2.2, 5, and 7.8 mg. Same operation mode and operative condition were then repeated by changing the feed of the reaction (olive leaves extract).

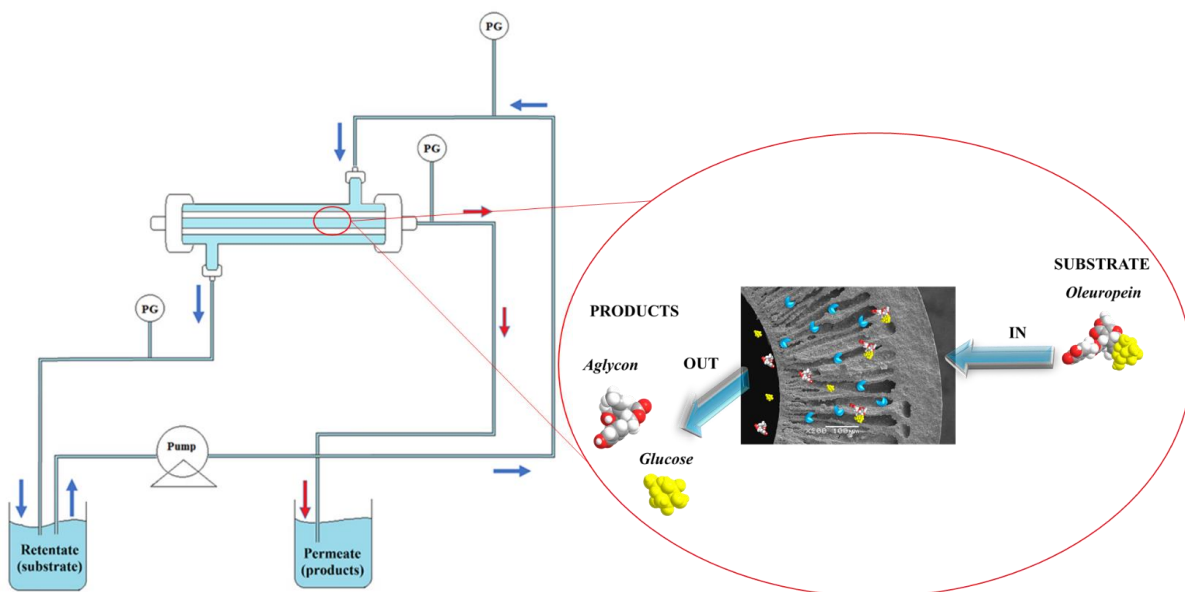


**Fig.6.9** Schematic representation of monophasic biocatalytic membrane reactor with immobilized  $\beta$ -glucosidase by covalent binding.

In the Figure below (Fig. 6.10) a typical reaction run profile in a monophasic biocatalytic membrane reactor (working in conditions of a continuous stirred tank reactor) is reported. In such system a constant concentration profile of oleuropein that enters into the biocatalytic membrane (IN) and a constant oleuropein (OUT) (as it occurs in the first hour) is a confirmation that the system works in a continuous mode, which means constant conversion when the steady state is reached.

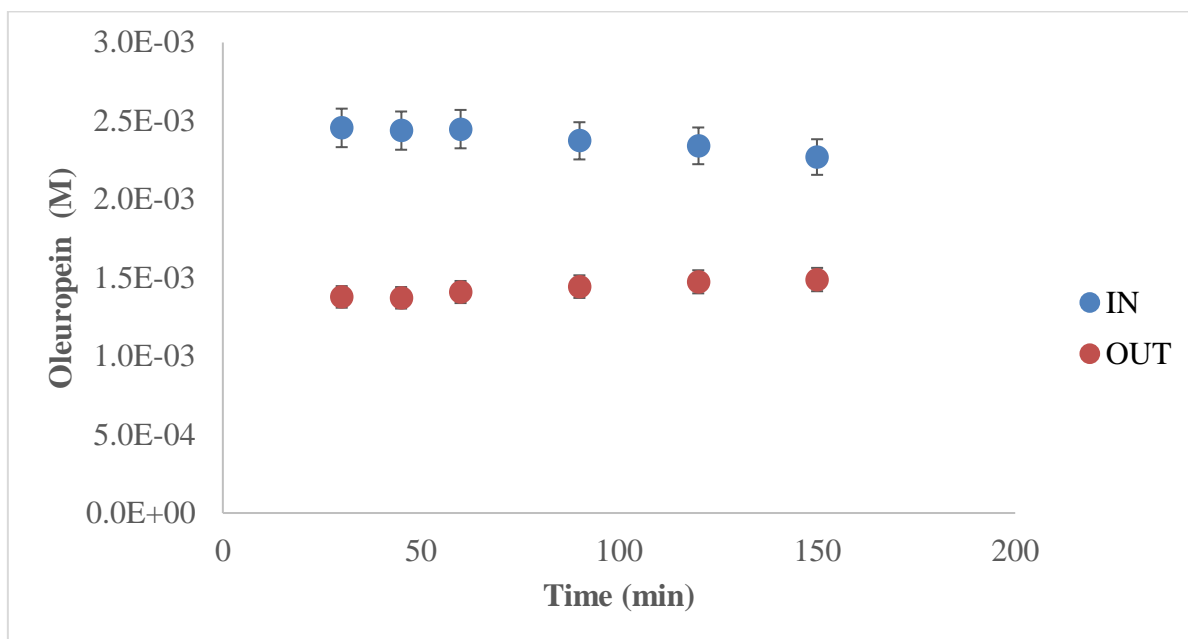


**Fig. 6.10.** Oleuropein concentration in a monophasic biocatalytic membrane reactor.



Instead, the following Figure (6.11) shows the trend of the enzymatic conversion as a function of immobilized enzyme amount, when the system was fed with both pure oleuropein (●) and the olive leaves extract (●).

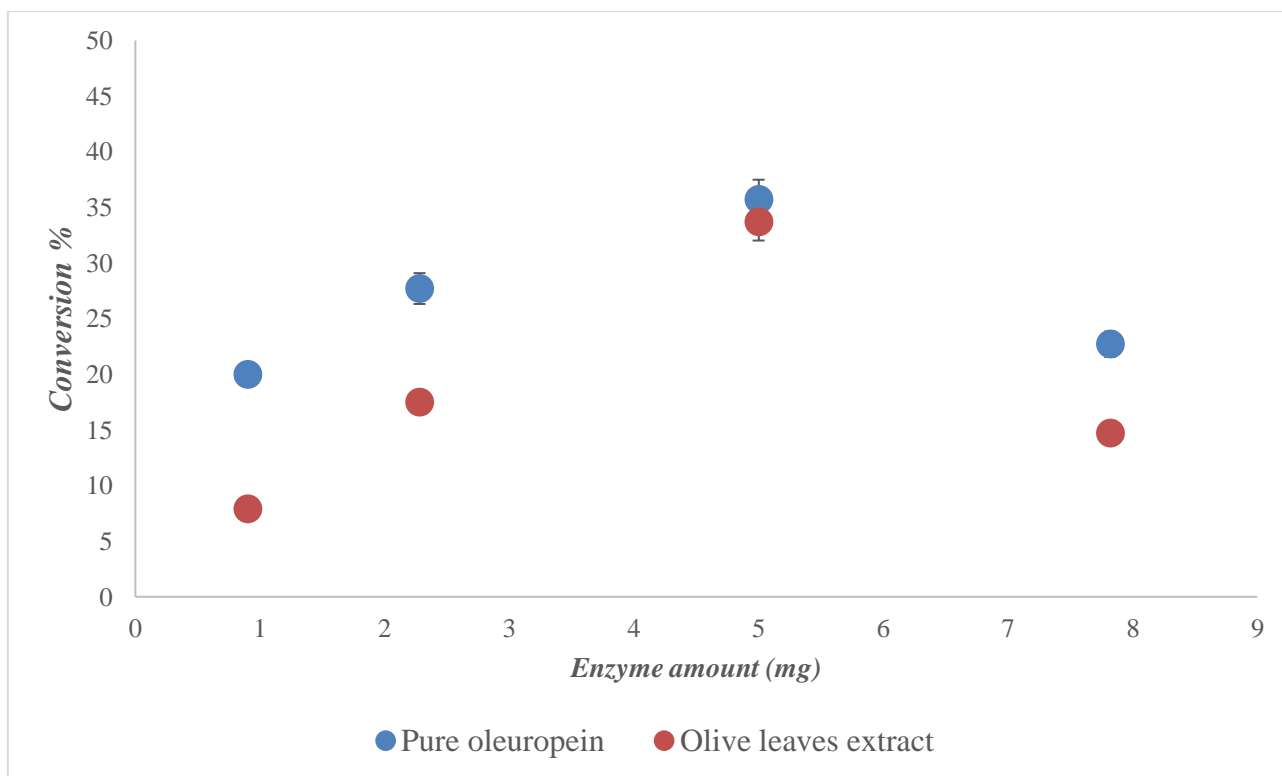


**Fig. 6.11.** Oleuropein Conversion as a function of covalently immobilized  $\beta$ -glucosidase amount.

As it can be seen, an increase of conversion degree is observed until an immobilized enzyme amount of about 5 mg was used. When a higher enzyme amount was used the conversion decreased from 36% to 22%. Also in this case, such as in the case of lipase, the crowding phenomenon occurs which negatively affects the enzymatic activity. In these conditions, the substrate is hindered to reach active site because of enzyme excess. The same behavior is observed by performing the reaction with leaves extract, although a lower conversion was observed, probably due slightly different optimal residence time. In fact, when 5 mg of enzyme are immobilized and a slightly higher residence time is used, similar conversions are obtained. Results related to the experiments carried out in the BMRs are summarized in table 6.4.

**Tab. 6.4.** Conversion degree related to different immobilized enzyme amount by using 2.5 mM of oleuropein as pure or present in olive leaves extracts.

Immobilized E (mg)	Substrate: pure oleuropein		Substrate: olive leaves extract	
	Conversion (%)	Residence time (sec)	Conversion (%)	Residence time (sec)
<b>0.9</b>	20% ( $\pm 1.3$ )	37 ( $\pm 3.2$ )	7.9% ( $\pm 0.4$ )	35 ( $\pm 1.1$ )
<b>2.28</b>	27.7% ( $\pm 0.5$ )	36 ( $\pm 1.7$ )	17.5% ( $\pm 0.5$ )	36 ( $\pm 1.6$ )
<b>5</b>	35.7% ( $\pm 1$ )	36 ( $\pm 1.1$ )	33.7% ( $\pm 1.8$ )	35 ( $\pm 1.1$ )
<b>7.8</b>	22.7% ( $\pm 1.1$ )	35 ( $\pm 1.1$ )	14.7% ( $\pm 0.5$ )	36 ( $\pm 1.3$ )

Hydrolysis reaction of oleuropein was monitored for about two weeks for a total time of about 60 hours. The behavior of immobilized enzyme is reported in the following graph (Figure 6.12).

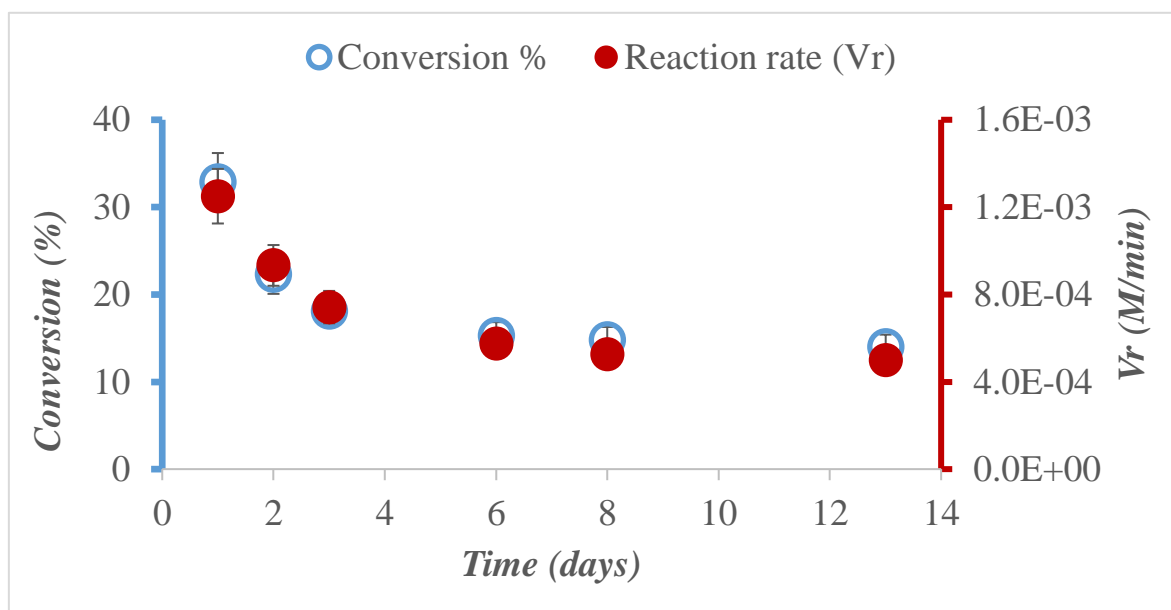


**Fig. 6.12.** Conversion degree and reaction rate of immobilized  $\beta$ -glucosidase for different reaction cycles in a range of about 14 days.

It is evident how both reaction rate and consequently conversion degree gradually decreased until a steady state reached after about 6 days. More precisely, a decrease of about 30% occurred after second day of operation which gradually stabilized until a loss of about 43% during the next days.

Anyway, by comparing results between the immobilized enzyme and the free one, conversion is quite similar. But it must be underlined that in the BMR 36 % of conversion was obtained at each passage through the biocatalytic membrane with a residence time of 0.6 minutes, while in the free batch system about same conversion was achieved in 300 minutes. In addition, in the second reactor there will be in any case the problem to separate reagents at the end of the process, not necessary in the BMR. Table 6.5 reports a comparison of performance between free and covalently immobilized  $\beta$ -glucosidase.

**Tab. 6.5.** Performance comparison between free and covalently immobilized  $\beta$ -glucosidase.

<i>Enzyme</i>	<i>Substrate conc. (mM)</i>	<i>Enzyme conc. (mg/ml)</i>	<i>Vr (mM/min)</i>	<i>Conversion degree (%)</i>	<i>Residence time (min)</i>
<i>Free</i>			$1.9 \cdot 10^{-4}$		
<i><math>\beta</math>-Glucosidase</i>	2.5	0.008	$(\pm 5 \cdot 10^{-6})$	34.3 ( $\pm 1.7$ )	300
<i>Covalently immobilized</i>			$7.9 \cdot 10^{-4}$		
<i><math>\beta</math>-Glucosidase</i>	2.5	27.7	$(\pm 1.2 \cdot 10^{-4})$	35.7 ( $\pm 4.6$ )	0.6

### 6.3. Monophasic BMR with entrapped $\beta$ -glucosidase

#### 6.3.1. Physical entrapment of $\beta$ -glucosidase into polymeric membrane

Ultrapure water permeability of PS membrane of prototype plant was about 300 L/hm<sup>2</sup>bar. Preliminary blank experiments were carried out before to entrapping  $\beta$ -glucosidase into the pores of polysulfone membranes of the pilot plant in order to verify that no substrate adsorption occurs and membranes properties do not undergo alterations. Results demonstrated that membranes are inert to olive leave extract and that oleuropein was not adsorbed. After ultrafiltration process, no significant variation about water permeability and

oleuropein concentration of extract were detected. In addition, as evident from the following graph (Figure 6.13), permeability of membranes remains unchanged after treatment with olive leaves extract, further demonstrating that any fouling phenomena occurs.

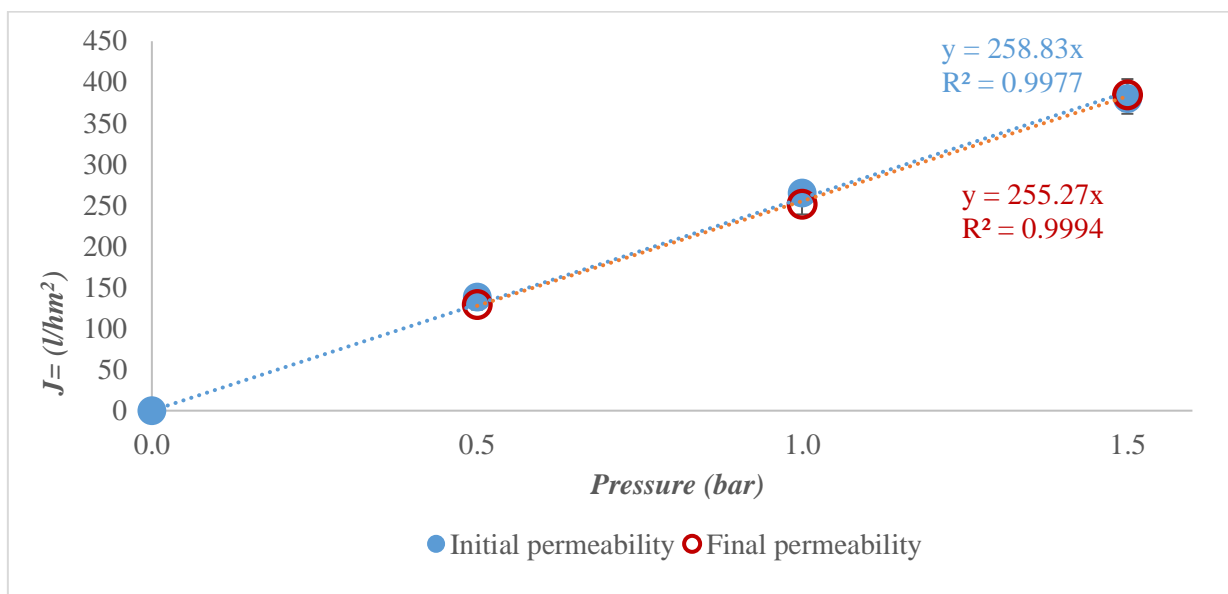


**Fig. 6.13.** Comparison between initial permeability of membranes and after ultrafiltration of olive leaves extract.

This means that results obtained from experiments are not compromised by any type of interferences and that any variation of oleuropein concentration during reaction is due only to oleuropein hydrolysis. Therefore, enzymatic entrapment was performed by ultrafiltering enzyme solution through the membranes from shell to lumen. Finally, the resulting immobilized enzyme amount was  $3.5 \text{ mg/cm}^3$

### 6.3.2. Activity measurements of entrapped $\beta$ -glucosidase

Performance of entrapped  $\beta$ -glucosidase into the pores of polysulfone membranes was studied in the prototype plant monophasic biocatalytic membrane reactor. The method used for the enzymatic entrapment was already described in chapter 3. In order to best reproduce the optimized operative conditions already studied by Mazzei et al [13], also in this study the performance of the entrapped enzyme was studied by considering a residence time of about 112 seconds. Reaction products and unreacted oleuropein was then collected in the permeate solution.

In the Figure 6.14 a schematic representation of monophasic biocatalytic membrane reactor with entrapped  $\beta$ -glucosidase into polysulfone membrane is reported. The picture of the prototype is reported in Figure 6.15.

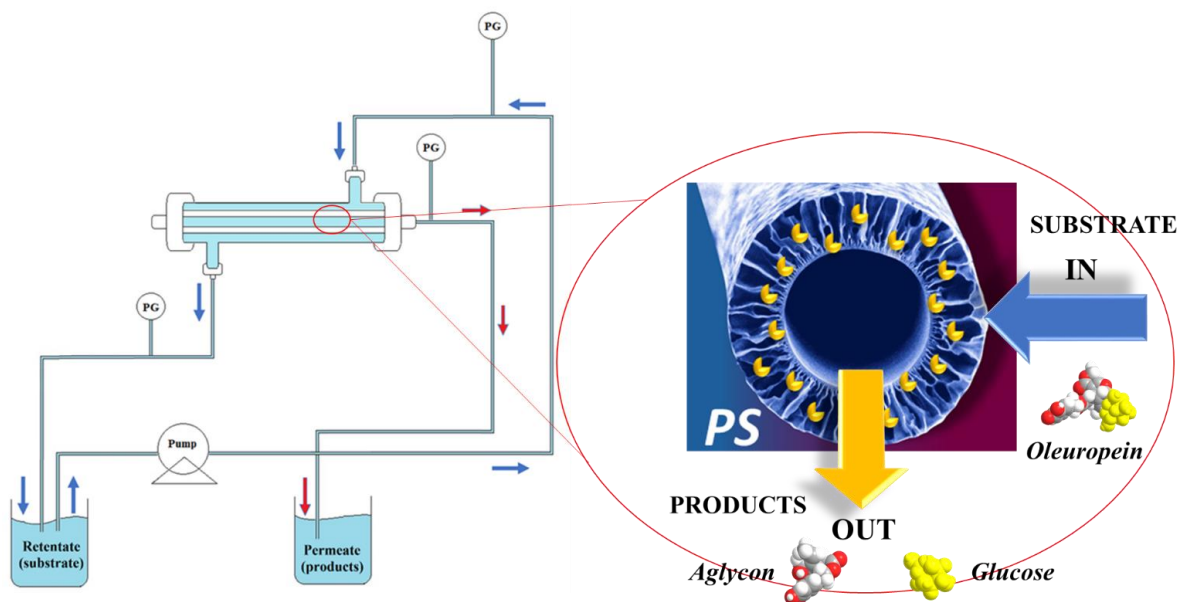


**Fig 6.14.** Schematic representation of monophasic biocatalytic membrane reactor with entrapped  $\beta$ -glucosidase into polysulfone membrane.

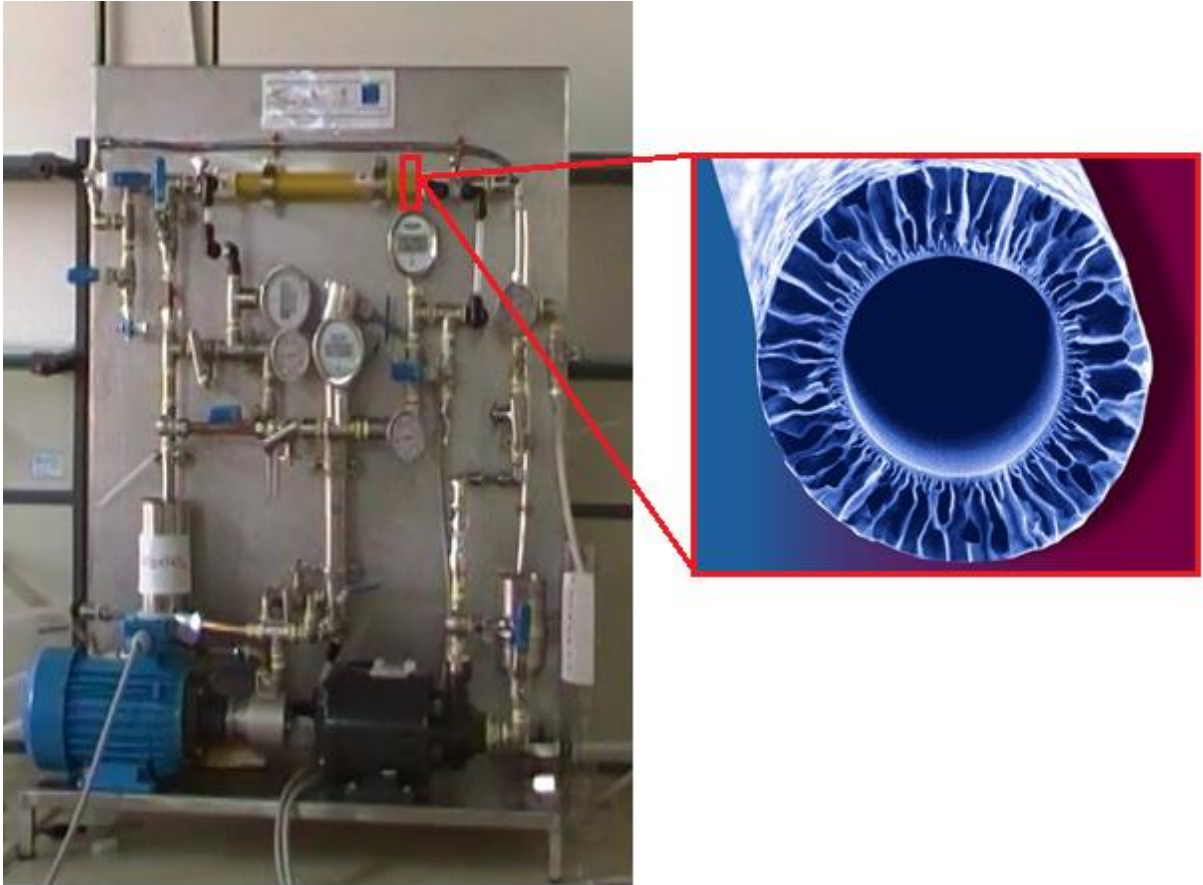


**Fig. 6.15.** Picture of the prototype plant of the biocatalytic membrane reactor with inset of the PS asymmetric membrane.

Figure 6.16 shows the conversion degree of commercial oleuropein at the steady state in the prototype plant biocatalytic membrane reactor. The system works constantly with a conversion of about 30% at each passage through the biocatalytic membrane.

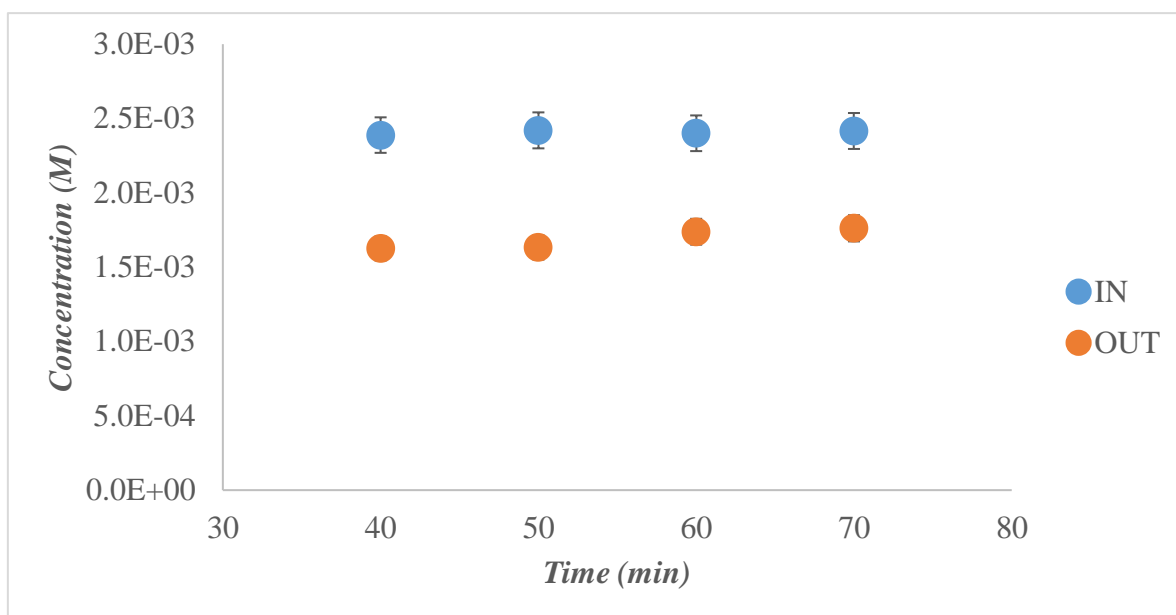


**Fig. 6.16.** Pure oleuropein hydrolysis reaction in the pilot plant biocatalytic membrane reactor

The lower value of conversion obtained in the present work compared to Mazzei et al. is due to the lower immobilized enzyme concentration ( $3.5 \text{ mg/cm}^3$ ) obtained in the present work compared to the one ( $4.67 \text{ mg/cm}^3$ ) previously obtained. The lower immobilized enzyme derived from high volume needed for the prototype that forced to use lower initial enzyme concentration due to its high cost for lab experiment.

#### 6.4. Conclusions

In this study kinetic parameters and inhibition constant of free  $\beta$ -glucosidase were determined. Monophasic biocatalytic membrane reactor was developed by immobilizing both  $\beta$ -glucosidase onto alumina membranes by covalent binding and onto polysulfone membranes by entrapment. Different amounts of  $\beta$ -glucosidase were covalently immobilized onto alumina membranes by varying the concentration of enzymatic solution. At the end, about 5 mg was the immobilized amount in which the enzyme showed the highest conversion. The enzyme activity is slightly reduced after the first reaction cycle until it stabilizes to a constant value with a total activity loss of about 43% after 13 days for a total time of reaction of 60 hours.

Since the polymeric membranes are commercially available in modules of about  $0.1 \text{ m}^2$ , the development of the biocatalytic system on large scale was carried out using these membrane

materials. In this system, about same performance was achieved in comparison with polymeric biocatalytic membrane developed on lab-scale. For both polymeric and inorganic biocatalytic membrane reactors pure oleuropein and olive leaves extract (containing oleuropein) were used as feed solution, demonstrating about same performance. This means that the presence of the other polyphenols does not alter the catalytic properties of the immobilized enzyme. By considering both the substantial cost of commercial oleuropein and the importance of its hydrolysis derivative, the industrial application of a biocatalytic membrane reactor could bring to a sustainable process development in which production of added value compound, such as oleuropein aglycon, can be performed starting from waste material.



## References

1. H.R. Tang, A.D. Covington, R.A. Hancock, *Biopolymers* 70 (2003) 403.
2. Y.F. Chu, J. Sun, X. Wu, R.H. Liu, *J. Agric. Food Chem.* 51 (2002) 6910.
3. M.M. Cowan, *Clin. Microbiol. Rev.* 12 (1999) 564.
4. J. Sun, Y.F. Chu, X. Wu, R.H. Liu, *J. Agric. Food Chem.* 50 (2002) 7449.
5. R. Bouhamidi, V. Prevost, A. Nouvelot, *Plant Biology and Pathology: Comptes Rendus de l'Academie des Sciences – Series III – Sciences de la Vie* 321(1998) 31.
6. R.H. Liu, *Am. J. Clin. Nutr.* 78 (3S) (2003) 517S.
7. R.H. Liu, *J. Nutr.* 134 (12S) (2004) 3479S.
8. D. Ryan, H. Lawrence, P.D. Prenzler, M. Antolovich, K. Robards, *Anal. Chim. Acta* 445 (2001) 67.
9. I.C.F.R. Ferreira, L. Barros, M.E. Soares, M.L. Bastos, J.A. Pereira, *Food Chem.* 103 (2007) 188.
10. O.B. Garcia, J. Castillo, J. Lorente, A. Ortuno, J.A. Del Rio, *Food Chem.* 68 (2000) 457.
11. C. Savournin, B. Baghdikian, R. Elias, F. Dargouth-Kesraoui, K. Boukef, G. Balansard, *J. Agric. Food Chem.* 49 (2001) 618.
12. E. Campeol, G. Flamini, P.L. Cioni, I. Morelli, R. Cremonini, L. Ceccarini, *J. Agric. Food Chem.* 51 (2003) 1994.
13. R. Mazzei, E. Drioli, L. Giorno, *Enzyme membrane reactor with heterogenized  $\beta$ -glucosidase to obtain phytotherapeutic compound: Optimization study*, *Journal of Membrane Science* 390–391 (2012) 121–129

## **CHAPTER 7**

### ***Multiphasic biocatalytic membrane reactor***

#### ***Abstract***

Ceramic membranes with an asymmetric structure were used to develop a multiphase hollow fiber membrane in order to overcome some limits of polymeric membrane related to both enzyme immobilization and reactor performance in multiphase membrane systems. The multiphase system has the aim of extracting reaction product into organic phase in order to stabilize it avoiding molecular rearrangement in water phase. The model system used was the enzyme/substrate  $\beta$ -glucosidase/oleuropein for the production of the isomer oleuropein aglycon 3,4-DiHydroxyPhenyl Ethanol–Elenolic acid (3,4-DHPEA-EA), an antioxidant low water-soluble compound. The enzyme was heterogenized by chemical attachment on ceramic hollow fiber membrane and the production/isolation of the poor water-soluble compound was studied in a multiphase biocatalytic membrane reactor. The multiphase system permits the hydrolysis of oleuropein in the biocatalytic membrane and the extraction of the isomer oleuropein aglycon on the other side of the membrane, where an organic phase is recirculated. Basing on membrane emulsification concept, an unstable water-in-oil emulsion is produced, which permits the compartmentalization of the product in the organic phase. The emulsion, once recovered, spontaneously separates and the two-different phases could be easily recovered. The technical aspects of the enzymatic conversion of oleuropein by  $\beta$ -glucosidase and the extraction of produced isomer oleuropein aglycon from aqueous phase into an organic solvent phase were investigated. Prior to perform the reaction, a screening of different organic solvents was carried out in order to select the best solvent in which the isomer of oleuropein aglycon is soluble. Finally, the degree of the aglycon extraction simultaneously to the hydrolysis reaction at the steady state of the integrated system was determined.

## 7.1. Introduction

Multiphase biocatalytic membrane reactors are systems in which a biocatalyst is immobilized in a membrane between two immiscible liquid streams. Thanks to membrane emulsification concept the water phase containing the substrate passes through the biocatalytic membrane where the reaction occurs, then the products and unconverted substrate pass on the other side of the membrane where the organic solvent is recirculated. Based on membrane emulsification concept, a water-in-oil-emulsion is produced, which spontaneously separates into the collected fractions, permitting the extraction of the compounds of interest into the solvent. In this way, bioconversion and simultaneous separation of reaction products as a function of its solubility and stability in water or in organic solvent can occur in a single operation step. The characteristics of organic solvent play an important role in a multiphase biocatalytic membrane reactor since they must permit the extraction of the compound of interest without damage to membrane structure. Polymeric membranes in hollow fibre configuration were the most commonly used in such application. Asymmetric hollow fiber membranes possess a number of special advantages among which a very large membrane surface area per unit volume and consequently a high available surface for enzyme immobilization. In addition, hollow fibre membranes, if made of polymeric matrix, are inexpensive and easily available in commerce. Although polymeric membranes are widely used for the development of biocatalytic membrane reactors, the organic nature of membrane matrix could be a limitation, in terms of stability, in case of contact with solvents, commonly used during membrane surface functionalization (for covalent enzyme immobilization) and for long time operation in multiphase system. In order to overcome these drawbacks, inorganic membranes could be employed to satisfy these specific requirements. In the present work, a multiphase biocatalytic membrane reactor was developed by immobilizing  $\beta$ -glucosidase onto asymmetric alumina hollow fibre membranes through covalent binding (the membrane preparation was already described in chapter 4). The aim of the study is the production and recovery of oleuropein aglycon deriving from the hydrolysis reaction of oleuropein catalyzed by immobilized  $\beta$ -glucosidase. The developed system is no more than a simulation of the compartmentalization of oleuropein and  $\beta$ -glucosidase which take place in the olive during fruit ripening or deterioration. In the *in vivo* compartmentalization the enzyme and the substrate are located in different places given by cellular membranes, the oil and water phases. Olive and leaf destruction permits compartments to break, and enzyme/substrate contact, with the production

of the water unstable compounds. The presence of the oil phase in olives will permit the extraction of the poor soluble water compounds in the oil phase. Although different studies have confirmed the presence of several phenolic compounds derivatives of oleuropein in virgin olive oil [1-3], the one which is arising major interest in recent years is 3,4-DiHydroxyPhenyl Ethanol– Elenolic acid (3,4-DHPEA-EA), an isomer of oleuropein aglycon, produced in the first reaction step of oleuropein hydrolysis. The molecular structure of 3,4-DHPEA-EA and its dialdehydic form 3,4-DiHydroxyPhenyl Ethanol – Elenolic acid Di-Aldehyde (3,4-DHPEA-EDA) are depicted in Figure 7.1.

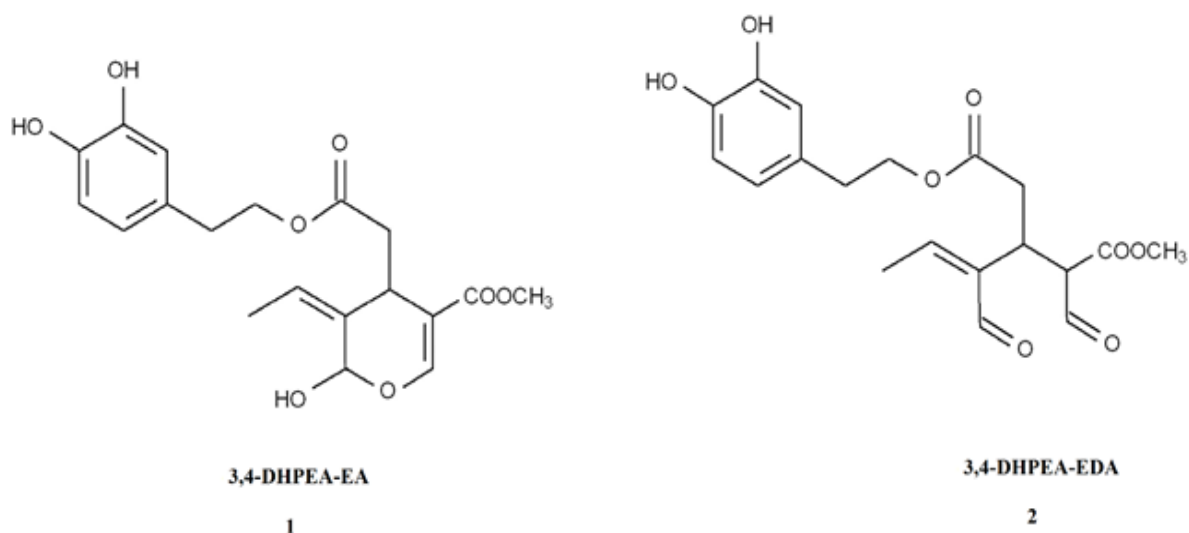


**Fig. 7.1.** Structures of (1) 3,4-DHPEA-EA (3,4-DiHydroxyPhenyl Ethanol – Elenolic acid) and (2) 3,4-DHPEA-EDA (3,4-DiHydroxyPhenyl Ethanol – Elenolic acid Di-Aldehyde).

This molecule is of particular importance because of its strong antioxidant activity. Due to its peculiar properties, it has been difficult to produce and it is not yet commercially available in pure form. The difficulty of isolating this compound is due to its low stability in water, so after its production in absence of an organic solvent, it is fastly rearranged into water soluble molecules. Different studies confirm the absence of 3,4-DHPEA-EA if the hydrolysis reaction is carried out in aqueous phase, since the rearrangement of the molecules will happen (Figure 7.2) [4].

Fig. 7.2 reports the compounds present where the reaction is carried out with the commercial enzyme from Almond [5]. There it is also reported the aglycon rearrangement into water stable compounds, elenolates.

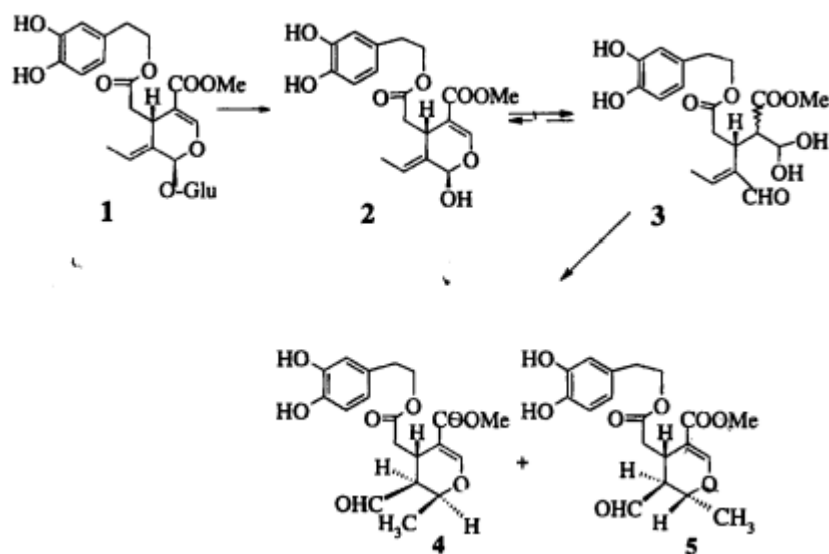


**Fig. 7.2.** Oleuropein hydrolysis pathway in water phase.

On the contrary, 3,4-DHPEA-EA and 3,4-DHPEA-EDA were detected by performing the reaction in a mixture of  $D_2O/CDCl_3$ . The presence of organic solvent in such system avoids the transformation of 3,4-DHPEA-EA and 3,4-DHPEA-EDA by allowing the recovery in their active form. Besides, the partition coefficient ( $K_p = C_{oil}/C_{water}$ ) between aqueous and organic phase of both 3,4-DHPEA-EDA ( $K_p = 0.189$ ) and in particular 3,4-DHPEA-EA ( $K_p = 1.49$ ) confirms their affinity towards organic phase in which their molecular structures are preserved [6]. In the Table 7.1 are summarized the partition coefficient ( $K_p = C_{oil}/C_{water}$ ) of oleuropein and its hydrolysis products (3,4-DHPEA, 3,4-DHPEA-EA, 3,4-DHPEA-EDA) between the olive oil and the water. In the same table were also reported the partition coefficient of the same compounds changing the organic phase with octanol [7].

**Tab.7.1.** Partition coefficients of oleuropein and its hydrolysis products

Antioxidant	Partition coefficient	
	oil/water	octanol/water
Oleuropein	0.0006	0.1300
3,4-DHPEA-EDA	0.1890	1.0900
3,4-DHPEA-EA	1.4900	1.3800

Basing on the 3,4-DHPEA-EA properties about solubility and its benefits in pharmaceutical and food field, in the present work a multiphase biocatalytic membrane reactor was designed and set-up in order to create best condition for the production and recovery of the compound. Thus, hydrolysis reaction of oleuropein in aqueous phase and simultaneous extraction of 3,4-DHPEA-EA in organic phase were performed in a system where different compartments coexist. In such system the properties of membrane component are of primary importance because it strongly affects process efficiency. Membranes have to provide the support for the biocatalyst immobilization and to create systems in which there is the contact between two different phases. In addition, due to the constant contact with organic solvent, membrane matrix has to possess a certain chemical resistance. Therefore, in this work asymmetric alumina hollow fibre membranes were used in order to overcome common limitations of polymeric membrane about stability to organic solvents. Finger-like voids, present in the lumen side of fibre, provided a high surface area available for enzyme location. Here hydrolysis reaction takes place and products immediately extracted and removed from the catalytic site.

## ***7.2. Results and discussion***

In the first part of this section the study related to the selection of the best solvent in which the aglycon was soluble will be presented. In the following second part the oleuropein hydrolysis in ceramic multiphase biocatalytic membrane reactor will be discussed.

### ***7.2.1. Selection of organic solvent***

Prior to perform hydrolysis reaction of oleuropein in a multiphase biocatalytic membrane reactor, it was necessary to carry out a screening of some organic solvents with specific requirements in order to select the most suitable to extract the oleuropein aglycon, produced during the first reaction step of oleuropein hydrolysis by the immobilized  $\beta$ -glucosidase. In addition to the capacity of oleuropein aglycon extraction, ideal organic solvent should be immiscible in water and should have low boiling temperature and low toxicity. Therefore, each organic solvent was mixed, with aqueous solution containing aglycon and stirred for 5 minutes in order to favor emulsion formation and extraction process

In the following table (Table 7.2) data concerning the organics solvents tested for the extraction of oleuropein aglycon are reported. Emulsions for the extraction process were produced by homogenizer.

**Tab. 7.2** Properties of organic solvent tested for the extraction of oleuropein aglycon.

Organic solvent	Solubility in water (%)	Aglycon extraction (%)	Boiling Temperature $T_b$ (°C)
CYCLOHEXANE	0.01	0	81
OCTANOL	0.03	47	188
ETHYL ACETATE	8	53	77.1
SQUALENE	Insoluble	0	275
TOLUENE	0.05	0	110.6
DICHLOROMETHANE	1.3	3	39.6

As shown, significant aglycon extraction occurs only in two organic solvents. About 47% of extraction was detected in the case of octanol, while about 53% by performing extraction into ethyl acetate. In the Figure 7.3 chromatograms of initial solution containing aglycon (Fig. 7.3 a) and same solution after extraction with ethyl acetate (Fig. 7.3 b) are illustrated.

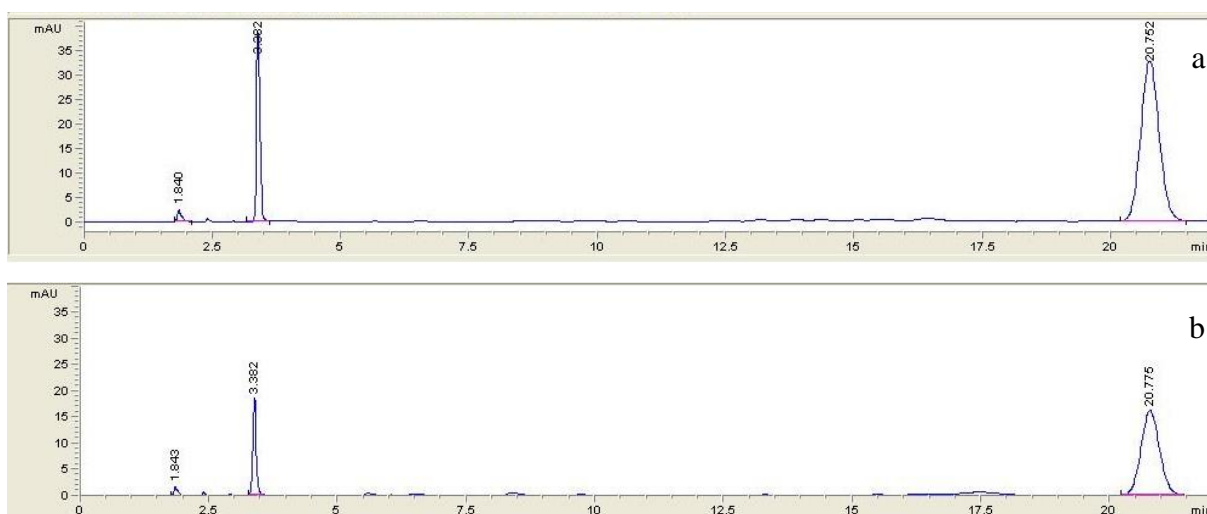


**Fig. 7.3.** a) Chromatogram of initial solution containing aglycon; b) Chromatogram of aglycon solution after extraction with ethyl acetate.

It is quite clear how the peak of aglycon (RT = 3.38 min) is halved. Because of its similar structure to aglycon, also a certain oleuropein amount is extracted in the solvent (peak at RT = 20.77 min). Although, the presence of oleuropein was not intended, it does not represent a problem as it is not a contaminant. The selection of organic solvent between octanol and ethyl acetate was determined also on the basis of solubility of the solvent in the aqueous phase and the boiling temperature. Although octanol has a lower solubility in water respect to ethyl acetate, it has a significant boiling temperature (188°C). Considering that the solvent has to be removed by evaporation after the extraction, in order to recover the solid residue, a lower boiling temperature, as in the case of ethyl acetate is better. This was the reason why it was selected as the organic phase to be used in the multiphasic system. Since this solvent shows a certain solubility in water phase, results were elaborated by taking into account that about 8% of solvent is dispersed in water. In this way results were normalized by considering a correction factor. Although the aim of this work was to recover powder of not commercially available antioxidant compounds, ethyl acetate is also well known for its non-toxic nature and already used in food field. This will permit its direct use, after enriching it of polyphenols, in food formulation production [8]. Once the organic solvent was identified, different emulsions with different aqueous phase/organic phase ratio were prepared in order to investigate about the best conditions in which the highest aglycon amount was extracted. In the Figure 7.4, it is reported the trend of extraction degree by increasing the organic/aqueous ratio.

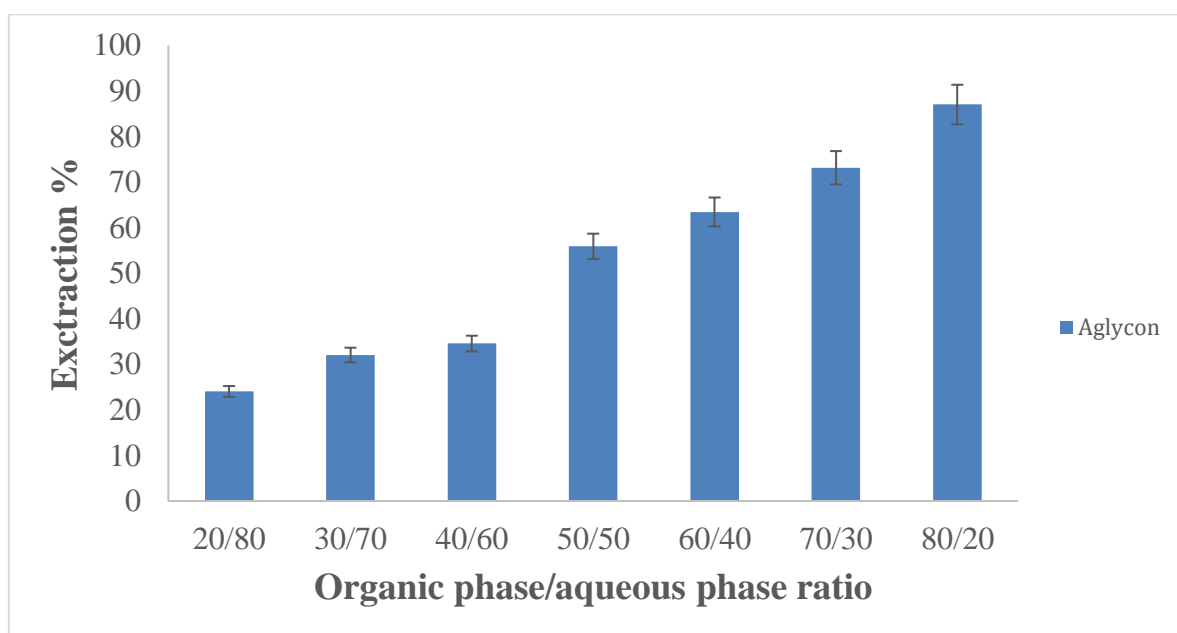


**Fig.7.4.** Extraction degree by increasing the organic phase respect to the aqueous phase.



As evident, the highest extraction degree of about 87% was obtained in conditions in which the amount of ethyl acetate is four times greater than aqueous solution containing aglycon. Therefore, in the multiphase biocatalytic membrane reactor the volume of the organic phase was chosen to work in conditions in which ethyl acetate is always in excess respect to the aqueous solution, in order to enhance the diffusive mass transfer until the maximum oleuropein aglycon solubility.

### 7.2.2. Study of oleuropein aglycon production/extraction in a multiphase biocatalytic membrane reactor

A scheme of the multiphase biocatalytic membrane process for the oleuropein hydrolysis is described in Figure 7.5. About 5 mg of  $\beta$ -glucosidase was covalently immobilized (immobilization procedure and conversion optimization were reported in chapter 6), an oleuropein concentration of 2.5 mM and a volume of ethyl acetate of about 50 ml was recirculated in the lumen of the ceramic hollow fiber membranes.

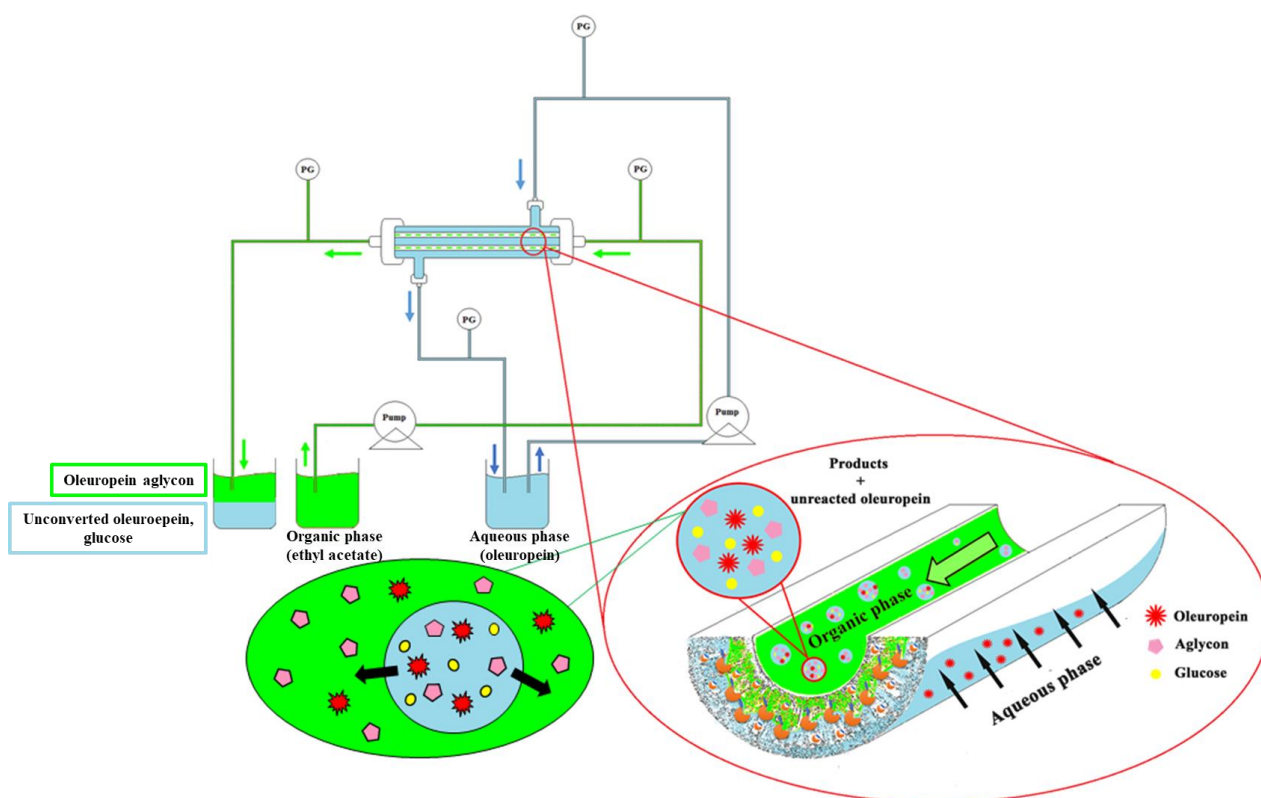


**Fig 7.5.** Schematic representation of multiphase biocatalytic membrane reactor.

The aqueous phase, containing the oleuropein was recirculated into the system at axial velocity of  $4.2 \cdot 10^{-3}$  m/sec, and passed through the biocatalytic membrane with a flow rate of

0.3 ml/min resulting in a residence time of about 36 seconds. After reaction, the aqueous phase containing unreacted oleuropein, isomer of oleuropein aglycon and the co-product glucose passes on the other side of the membrane where an ethyl acetate phase was continuously recirculated with an axial velocity of  $1.6^{-3}$  m/sec. Due to non-miscibility of the two phases, water droplets in continuous ethyl acetate phase are formed at the pore border, which are drag thanks to the axial velocity of the ethyl acetate phase. Therefore, basing on membrane emulsification mechanism, unstable emulsions are formed which spontaneously separate once collected in the tank. This configuration assured the hydrolysis reaction to take place in aqueous phase, the reaction product of interest to be extracted and stabilized in the organic phase, the co-product (glucose) to be removed from the reaction site preventing inhibition effect.

In order to evaluate the efficiency of the multiphasic biocatalytic membrane reactor, prior to recirculate the organic phase into the system, the performance of the immobilized  $\beta$ -glucosidase (in terms of reaction rate and conversion degree) was studied in a single phase condition. Reaction rate and conversion degree calculated in monophasic conditions of biocatalytic membrane reactor were  $8.63 \cdot 10^{-04} (\pm 7.1 \cdot 10^{-05})$  M/min and 35.7%, respectively, confirming data reported on chapter 6. After some time the steady state was reached, i.e. after 2 h, ethyl acetate was started to recirculate in the lumen circuit in order to promote the extraction of the compound of interest. In Figure 7.6 the concentration profile of oleuropein that enters the biocatalytic membrane (IN) and the unconverted one (OUT) recovered in the permeate is reported, either when the system works in monophasic that when it works in multiphase conditions. The arrow in the Figure highlights the moment when the system starts to work in multiphase conditions. From this moment, the oleuropein measured in the collected water after emulsion separation resulted lower, due to its partial solubility in ethyl acetate (in the Figure the measured value is named "observed" to underline that it is not the real one coming out from the biocatalytic membrane where the reaction occurs). Knowing its solubility in ethyl acetate, the value of oleuropein coming out of the reactor could be calculated and reported in Figure 7.6 as "out".

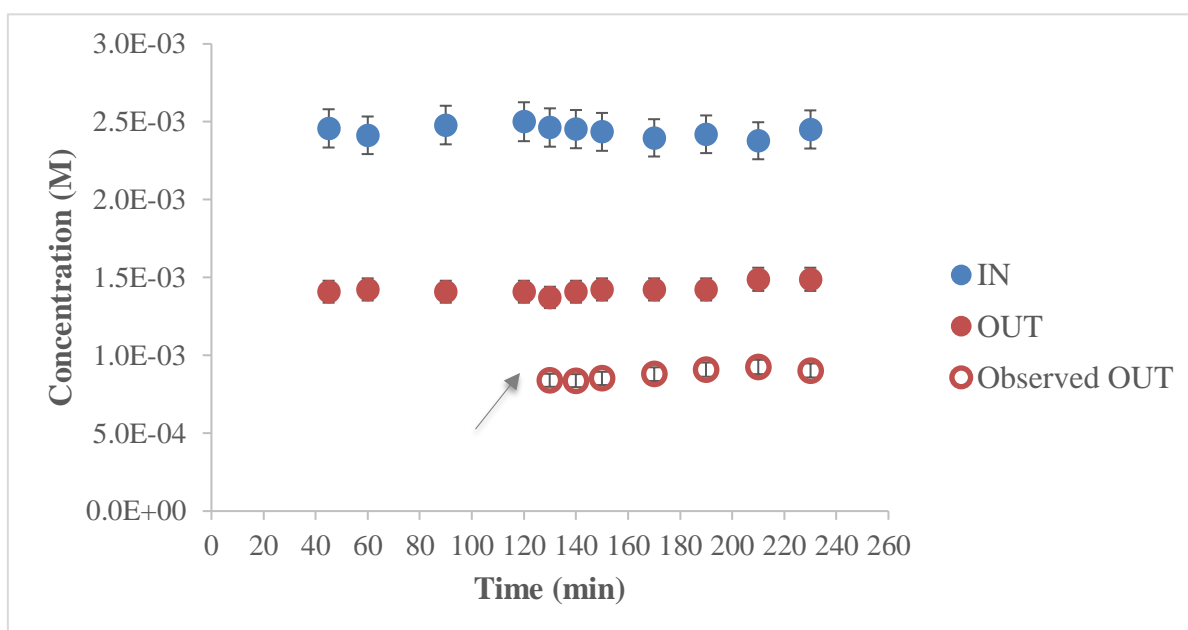


**Fig.7.6.** Concentration profile of oleuropein that enters in the biocatalytic membrane (IN) and collected in the aqueous phase after hydrolysis (OUT) in monophasic biocatalytic membrane reactor and in multiphasic biocatalytic membrane reactor (The arrow indicates when the system started to work in multiphasic configuration).

The degree of extracted aglycon was obtained in two ways. In one case it was calculated by the equation 7.1:

$$\frac{(\text{aglycon amount in aqueous phase of monophasic system} - \text{aglycon amount in aqueous phase of multifasic system})}{\text{aglycon amount in aqueous phase of monophasic system}} \cdot 100 \quad (7.1)$$

In another case, it was obtained by re-suspending the powder recovered from ethyl acetate evaporation in a known volume of water and measuring it by HPLC. Experimental data used to calculate aglycon extraction in the multiphasic biocatalytic membrane reactor are reported in the Table 7.3.

**Tab.7.3.** Experimental data about aglycon extraction in the multiphase biocatalytic membrane reactor.

Initial aglycon concentration (mg/ml)	Final aglycon concentration (mg/ml)	Aqueous phase volume (ml)	Aglycon amount before extraction (mg)	Aglycon amount after extraction (mg)	Aglycon extraction (%)
0.16	0.01	5.00	0.82	0.05	93.9

This result confirms that almost all produced aglycon can be extracted and collected in ethyl acetate simultaneously to the hydrolysis reaction. Samples of saturated ethyl acetate in which aglycon was extracted, were then subjected to evaporation process in order to recover the product in solid form. The solid powder remained after evaporation process was then suspended in 50 mM phosphate buffer pH 6.5. The HPLC analysis, confirmed the presence of the aglycon in the samples. The resulting peak from chromatogram corresponds to an aglycon amount of about 0.04 mg, that is the amount of aglycon given by the numerator in Eq. 7.1. The same aglycon amount found after extraction and evaporation, confirms the entire process as a valid approach for the recovery of the molecule. The chromatogram of the analysis of the powder suspended in buffer is represented in Figure 7.7, where it is evident the presence of the aglycon peak (RT = 3 min).

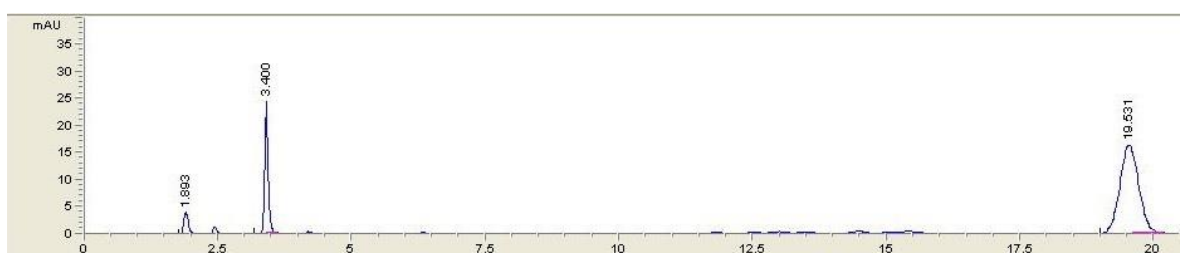


**Fig. 7.7.** Aqueous phase chromatograph after dissolution of residue obtained from evaporation of ethyl acetate used for the extraction process.

This result confirms the possibility to recover the aglycon in solid form through the development of an approach that involves its production starting from oleuropein hydrolysis, followed by a recovery procedure which consists in an extraction in ethyl acetate and subsequent concentration. The higher the conversion the higher the purity of extracted

aglycon. In this study it was simply used evaporation to demonstrate the concept, but less energy intensive processes can be applied, such as solvent resistant nanofiltration, membrane distillation.

### ***7.3. Conclusions***

Results showed that using a multiphase biocatalytic membrane reactor it is possible to perform hydrolysis reaction and extraction of product basing on membrane emulsification mechanism in a single step. The process evidenced the possibility to extract the non-commercially available oleuropein aglycon in a pure solvent, separating it from the other product (glucose). The possibility to produce and simultaneously recover a high added value compound in an organic solvent, already used in food industry (as ethyl acetate) makes the system developed an interesting innovation which could be applied in different sectors. The effort to obtain the aglycon in solid powder is due to the major versatility of solid compound respect to dissolved forms, which could be used in several formulations (e.g. emulsions) in many fields. In addition, the solid form promotes higher aglycon stability, since powders are generally less reactive in comparison with solutions.

The intensified reactor proposed well respond to the need to develop “green systems”, since it promotes both the valorization of renewable material (olive leaves), and the production/ extraction of not commercially available phytotherapics.

## References

1. M. Servili, S. Esposito, R. Fabiani, S. Urbani, A. Taticchi, F. Mariucci, R. Selvaggini, G.F. Montedoro, *Phenolic compounds in olive oil: antioxidant, health and organoleptic activities according to their chemical structure*, *Inflammopharmacology* (2009) 76–84.
2. A. Carrasco-Pancorbo, L. Cerretani, A. Bendini, A. Segura-Carretero, T. Gallina-Toschi, A. Fernandez-Gutierrez, *Determination of polyphenols in olive oils*, *J. Sep. Sci.* 28 (2005) 837–858.
3. A. Bendini, L. Cerretani, A. Carrasco-Pancorbo, A.M. Gómez-Caravaca, A. Segura-Carretero, A. Fernández-Gutierrez, G. Lercker, *Phenolic molecules in virgin olive oils: a survey of their sensory properties, health effects, antioxidant activity and analytical methods. An overview of the last decade*, *Molecules* 12 (2007) 1679–1719.
4. A.D. Bianco, A. Piperno, G. Romeo, N. Uccella, *NMR experiments of oleuropein biomimetic hydrolysis*, *J. Agric. Food Chem.* 47 (1999) 3665–3668 9- M. Guiso, C. Marra, *Highlights in oleuropein aglycon structure*, *Nat. Prod. Res.* 19 (2005) 105–109
5. Bianco A. D., Piperno A., Romeo G., Uccella N., *J. Agric. Food Chem.*, 47 (1999), 3665-3668.
6. P. S. Rodis, V. T. Karathanos, A. Mantzavinou, *Partitioning of Olive Oil Antioxidants between Oil and Water Phases*, *J. Agric. Food Chem.* 50 (2002) 596-601.
7. Paiva Martins F., Gordon M.H., *JAACS* 79, (2002) 571-576.
8. Claudine Manach, Augustin Scalbert, Christine Morand, Christian Rémésy, and Liliana Jimenez, *Polyphenols: food sources and bioavailability*, *Am J Clin Nutr* 2004;79:727–47. Printed in USA. © 2004 American Society for Clinical Nutrition.

## ***OVERALL CONCLUSIONS***

In this thesis advances on biocatalytic membrane reactors have been promoted. Different types of biocatalytic membrane reactors were developed by using different membrane support, biocatalyst and phases. Both ceramic and polymeric membranes were used. Ceramic membranes were used in order to overcome the limitations imposed from the common use of polymeric membranes, especially when operating with organic solvents. Although their high cost, ceramic membranes are an attractive alternative to polymeric membranes due to their high stability, chemical, thermal and mechanical resistance. Therefore, asymmetric alumina membranes in a hollow fibre configuration were prepared for biocatalytic membrane reactors. Membrane in such configuration offers a high surface area/volume ratio which promotes a better distribution of an increased loading of the enzyme and a higher oil/water interfacial surface preferred in a multiphasic system. Combination of phase inversion and sintering process was adopted for the preparation of alumina fibres. During preparation process, one single preparation parameters was varied (internal coagulant flow rate) in order to obtain different membrane microstructures. Finger-like voids region growth was observed in the cross section of the fibre with the increase of the internal coagulant flow rate. Thus, also an increase of membrane permeability was detected due to a thinner sponge layer. At the same time the mechanical resistance of membrane decreased. Finally, prepared membranes with intermediate properties were selected to use for the biocatalytic membrane reactor development. A functionalization method was proposed in order to create suitable functional groups for the enzyme immobilization on the surface of alumina membranes. Reactive amino groups suitable for biomolecules immobilization were grafted on the alumina surface using the silanization reagent (3-Aminopropyl) triethoxysilane (APTES). The amino groups were then activated for biomolecules immobilization by glutaraldehyde treatment. Both lipase from *Candida rugosa* and  $\beta$ -glucosidase from almond were covalently immobilized into the pores of alumina membrane and their performance was studied in different systems. Lipase was immobilized onto alumina fibre in order to develop a two-separate phase biocatalytic membrane reactor in which the membrane works as both catalytic and separation unit. Catalytic activity and stability of the immobilized lipase were investigated as a function of the amount of the immobilized biocatalyst. The performance of the biphasic enzymatic membrane reactor was evaluated based on the fatty acids extraction in the aqueous phase. Results showed that it is

possible to immobilize lipase on a ceramic membrane without altering its catalytic performance (initial residual specific activity 93%), which remains constant after 6 reaction cycles with a running period of about 18 days and without alteration of membrane matrix despite the long contact with organic phase.

$\beta$ -glucosidase was covalently immobilized into the pores of alumina membrane or by entrapment in polymeric membranes. It was used in aqueous monophasic system or aqueous/organic multiphase system. In the latter case the aim was to develop an intensified and integrated multiphase system for the simultaneous production and recovery of oleuropein aglycon, a high added value compound, derived from the oleuropein hydrolysis by the action of  $\beta$ -glucosidase.

Prior to perform the enzyme immobilization, reaction rate and conversion degree of free  $\beta$ -glucosidase was investigated in order to compare the performance with the immobilized one. Also kinetic and inhibition parameters were studied in order to determine the type of enzymatic inhibition by product. Covalent immobilization process on ceramic membrane was optimized by investigating the effect of the initial concentration of enzymatic solution on the immobilized enzyme amount. Reaction rate and conversion degree of immobilized enzyme were then investigated in order to establish the optimal immobilized amount. Commercial oleuropein and olive leaves extract were used as substrate to perform the reaction in a monophasic aqueous system. Results showed that by immobilizing about 27.7 mg/cm<sup>3</sup> of enzyme, a conversion degree of about 35.7 ( $\pm$ 1)% was obtained by using commercial oleuropein and about 33.7 ( $\pm$ 1)% by using natural feed as substrate. From comparison of conversion degree between free and immobilized  $\beta$ -glucosidase, it was observed that the immobilized enzyme converted about 35.7% of substrate in about 36 seconds respect the 33 % in 300 minutes by the free one in a stirred tank reactor. Besides, in the stirred tank reactor, the co-product (glucose) accumulated during the reaction showed a competitive inhibition of the enzyme. Stability of immobilized enzyme for long periods was also investigated. A loss of about 43% of the enzymatic activity was detected after 13 days.

The performance of  $\beta$ -glucosidase was also investigated in a lab-scale prototype biocatalytic membrane reactor where it was entrapped into the pores of asymmetric polysulfone membranes. Here polymeric membranes were used as the system operated in aqueous phase and the conversion degree of the enzyme immobilized in ceramic membranes was not significantly different. In this study the enzyme was immobilized by physical entrapment



and optimal operative conditions were adapted to the larger size system where a conversion degree of about 30% was obtained with 3.5 mg/cm<sup>3</sup> of entrapped  $\beta$ -glucosidase. Results confirmed that the biocatalytic membrane reactor could produce 3.6 g/day of aglycon in water phase.

An additional study using  $\beta$ -glucosidase immobilized in multiphase system was carried out in order to extract aglycon in an organic phase. In fact, due to the low water stability of oleuropein aglycon, it was necessary to adopt a suitable strategy in order to recover it from the aqueous phase as soon as it was produced. Alumina hollow fibre membrane, thanks to the properties of its material and configuration, offered the possibility to develop an advanced system, in which membrane serves both as separation and catalytic unit, where the reaction is performed within the membrane pore by introducing oleuropein from one side of membrane, under convective flow and the aglycon is recovered from the other side by extraction in an organic solvent, by forming water-in-oil emulsion basing on membrane emulsification mechanism. Results showed the possibility to produce and recover the oleuropein aglycon in a multiphase biocatalytic membrane reactor where the enzyme was covalently immobilized into the pores of alumina hollow fibre membranes, the hydrolysis reaction occurred and aglycon was simultaneously extracted by organic solvent recirculating in a separate compartment. Here, the membrane stability played an important role since, thanks to its chemical resistance, it permitted long operation time without undergoing damaging due to the presence of organic solvent. Ethyl acetate was selected as organic solvent thanks its excellent properties, such as ability to solubilize aglycon, the poor water solubility, the low boiling temperature and toxicity. Results obtained from multiphase membrane reactor confirmed the possibility to recover about 93% of freshly produced aglycon in the ethyl acetate collected in the permeate which easily separates from permeated aqueous phase, since the emulsion was not stabilized. Furthermore, thanks to the low boiling temperature of ethyl acetate, aglycon was obtained in solid form by performing solvent evaporation.

Considering the possibility to produce aglycon from industrial waste or natural abundant source, such as olive leaves, the multiphase biocatalytic membrane reactor proposed in this research work can be a potential strategy for industrial sustainable processes development. From an industrial point of view, an application of a such system could lead significant

advantages considering the cost reduction for the wastes disposal which will be instead the source of a production process as well as the reduction of environmental pollution.